The Serine Hydrolases of *Drosophila melanogaster:* Integrated Chemoproteomics and Genetics

ड्रोसोफिला मेलानोगास्टर का सेरीन हाइड्रोलेज़: एकीकृत कीमो-प्रोटिओमिक्स एवं आनुवंशिकी

विद्या वाचस्पति की उपाधि की अपेक्षाओं की आंशिक पूर्ति में प्रस्तुत शोध प्रबंध

A thesis submitted in partial fulfillment of the requirements of the degree of Doctor of Philosophy

द्वारा / By

कुन्दन कुमार/Kundan Kumar

पंजीकरण सं. / Registration No.:

२०१७२००१/20172001

शोध प्रबंध पर्यवेक्षक / Thesis Supervisor:

प्रोफेसर गिरीश रत्नपारखी / Professor Girish Ratnaparkhi

शोध प्रबंध सह-पर्यवेक्षक / Thesis Co-Supervisor:

प्रोफेसर सिद्धेश कामत / Professor Siddhesh Kamat

भारतीय विज्ञान शिक्षा एवं अनुसंधान संस्थान पुणे

२०२४

Indian Institute of Science Education and Research Pune,

2024

CERTIFICATE

Certified that the work incorporated in the thesis entitled “The Serine Hydrolases of *Drosophila melanogaster*: Integrated Chemoproteomics and Genetics”, submitted by Kundan Kumar was carried out by the candidate, under my supervision. The work presented here or any part of it has not been included in any other thesis submitted previously for the award of any degree or diploma from any other University or institution.

Prof. Girish Ratnaparkhi

Thesis Supervisor

Dr. Siddhesh Kamat

Thesis Co-Supervisor

Declaration by Student

Name of Student: **Kundan Kumar**

Reg. No.: **20172001**
Thesis Supervisor(s): **Prof. Girish Ratnaparkhi and Dr. Siddhesh Kamat**

Department: **Biology**
Date of joining program: **01/08/2017**

Date of Pre-Synopsis Seminar: **08.07/2024**

Title of Thesis: **The Serine Hydrolases of *Drosophila melanogaster*: Integrated Chemoproteomics and Genetics**

I declare that this written submission represents my idea in my own words and where others' ideas have been included; I have adequately cited and referenced the original sources. I declare that I have acknowledged collaborative work and discussions wherever such work has been included. I also declare that I have adhered to all principles of academic honesty and integrity and have not misrepresented or fabricated or falsified any idea/data/fact/source in my submission. I understand that violation of the above will be cause for disciplinary action by the Institute and can also evoke penal action from the sources which have thus not been properly cited or from whom proper permission has not been taken when needed.

The work reported in this thesis is the original work done by me under the guidance of

Dr./Prof. **Prof. Girish Ratnaparkhi and Dr. Siddhesh Kamat**
Date:16/10/2024

Signature of the student

Dedicated to my brother Awadhesh Kumar Prasad

Acknowledgements

My journey at IISER Pune has been a golden journey along with being a rollercoaster ride, and I owe it to many people for making precious.

First and foremost, I owe my deepest gratitude to my supervisors, Prof**. Girish Ratnaparkhi** and Prof. **Siddhesh Kamat**, for their invaluable guidance, support, and mentorship throughout my PhD journey. Their insightful feedback and unwavering encouragement have been instrumental in shaping both my scientific thinking and this thesis. I am deeply grateful for their patience and trust in allowing me the freedom to explore new ideas.

Since, every person have very specific bonding to mentor or I called it Guru Ji. Now, I will be thanking to supervisor one by one. I thank **Prof**. **Girish Ratnaparkhi** for understanding me and taking me his laboratory as PhD student. He has been approachable and liberal advisor throughout my PhD journey. He is always been attentive to idea and results for my exploratory experiments. He has been my first choice for all of the exploratory results, especially for fly biology. He is not giving person and owe my heart by making me to try genome engineering experiments (grass) multiple times and finally the grass became greener. He is instrumental in development in many aspects my scientific skills and temperaments. I started my project on Serine hydrolase (SH) in *Drosophila* which is possibly discussed and formulated before joining by the both supervisor Prof, Girish Ratnaparkhi and Dr. Siddhesh Kamat. Now, It is time for **Prof. Siddhesh Kamat**. I was growing my SH projects as child and Dr. Siddhesh nourished it to mature and publishable on time. During this nourishment learned the focus on maturing one and left others for future. His weekly one o one meeting make me focused exploratory research temperament development. He fastens my PhD journey. He pulled me from long distracted ideas and pushed me to focus and ripening research. He is also approachable and attentive my idea and results. I thank him for being instrumental in development of many aspects in my scientific skills and temperaments. Together, Prof. Girish and Prof. Siddesh act as scientific pot maker and nourished, shaped and built my scientific skills, approach and temperaments and lastly nurtured me to become resourceful human being. I thank both of them for being indulgent teacher.

I thank my research advisory committee members, Dr. Mrudula Nambiar and Dr. Krishanpal Karmodiya, Dr. Anuradha Ratnaparkhi for their comments and advice

throughout the course of my PhD. The RAC meetings were very fruitful and made the constant progress of thesis research.

I extend my gratitude to Dr. Anuradha Ratnaparkhi, Dr. Richa Rikhy, and Dr. Girish Deshpande for providing me valuable scientific inputs for my project. I am thankful to Biology department chairs Prof. Thomas Pucadyil and Prof Richa Rikhy for shaping the biology department at IISER Pune during my time. I am thankful to weekly student talks and the its committee for improvement in our skills.

I would like extend my gratitude to Dr Amol Mhetre and Dr Kavita Sharma for synthesizing chemical probes for chemoproteomics experiments.

I would like to acknowledge all GR lab (Dr. Bhagyashree Kaduskar, Dr. Kriti Chaplot, Dr. Prajna Nayak, Dr. Shweta Tendulkar, Dr. Amarendranath Soory, Dr. Sushmita Hegde, Dr. Aparna Thulsidharan, Lovleen Garg, Subhradip Das, Namrata Kulkarni, Amrita Roy, Alex vergese, Neena Dhiman, Neel Wagh, Jyothish Sudhakaran, Aarti Kejriwal, Anjana T, Mrunal Pazare, Shruti Pawar, Shivani Deshpande) and Kamat lab (Dr. Dhanashree Kelkar, Dr. Neha Khandelwal, Dr. Kavita Sharma, Dr. Jyotsna, Dr. Shubham Singh, Dr. Neelay Mahendale, Dr. Abinaya Rajendran, Dr. Minhaj Shaikh, Dr. Kaveri Vaidya, Karthik GS., Arnab Chakraborti, Sonali Gupta, Ojal Saharan, Aakash C, Abhishek Kumar, Niraj Kumar Yadav, Adithya Kallattu, Shrutika Raje, Alaumy Joshi, Rohith CS, Chaitanya Katkar, Archit Devranjan,) members for fruitful scientific discussion during lab meets, on tea breaks, lab outing and game nights. I would especially thank to Lovleen Garg, Namrata Kulkarni and Amrita Roy for helping me fly research work and Shubham Singh, Arnab Chakravarty, Aakash C and Ojal Saharan for help in biochemistry and mass spectrometry troubleshooting.

I would like to thank the academic office staff, especially, Tushar Kurulkar, Sayali Damle, and Swapnil Bhutkar for their help with the funding applications for my visit to the European *Drosophila* Research Conference in Lyon, France, 2023. I am thankful to the Infosys foundation and CSIR funding my visit to Lyon, France.

I thank the mass spectrometry facility (Saddam Shekh for running MS samples), microscopy facility (Dr. Santosh Poddar and Vijay Vittal) and National Facility For Gene Function In Health and Disease (Dr. Swapnil Bangar) for help with experiments for my thesis work. I want highlight Dr Swapnil Bangar along with his team for generous effort in generation of antibodies.

I would to thank fly facility as well as the biology office teams for their help throughout my PhD, notably, Snehal Patil, Yashwant Pawar, Ashwini, Mrinalini Virkar, Mahesh Rote, Kalpesh Thakare, Piyush Gadekar, Rupali, Hari Prasad, Sachin among others.
I would like to thank all the canteen workers. I am also thankful to all cleaning staff and security at IISER Pune campus.
I would like to thank Ojal Saharan, Namrata Kulkarni, Lovleen Garg, Amrita Roy and Priti Kumari and Km Babita for reading, reviewing and making suggestions of my chapters of thesis.
I would like thank members of different lab for sharing and teaching proper use instruments and helping and troubleshooting experiments. I would like mention the Dr. Madhusudan lab (Dr. Tejashree K, Dr. Sanjana, Guljar Singh for Summer lab training), Prof Gayathri lab (Saumyajit Dutta, for FPLC experiment), Dr. Sai lab (Aman, Akash)Dr. Thomas lab (Kirti, Uma, Krishnendu for sharing bacterial culture instrument and reagents), Dr Anjan lab (Mohit Mantri, RTqPCR experiments), Dr. Krishanpal lab (Bhagyashree), Dr Nagaraj lab (Prachi and Mayuresh), Dr Kundan Sengupta (Dr Ajay labade, Santhnam, Balaji), Dr. Sutirth Dey lab (Akshay). I want mention special thanks to B322 wing member for making lab area calm and working as team. Prof. Richa lab members has been integral for conducting both wet lab and fly lab experiments. I am grateful to friend cum mentor Dr. Bhavin Utterkar for teaching me dissection and fly genetics. Dr. Kalika lab (Akanksha), Dr. Chaitanya lab and Dr Mayurika lab (Benchamin) members also earn my gratitude to sharing instruments and help in conducting experiments.
I extend my gratitude to my official local guardian Prashant Kumar and his family.
I would like thank my school friends (Prashant Kumar, Manu Kumar, Ravi Prakash, Rupak Kumar, Antima Gupta and all others) and alumni (Kameshwar Mishra, Scientist ARDE Pune Guardian at Pune) form Jawahar Navodaya Vidyalaya Gopalganj for being supportive and fun and family. I would like to thank Krishna Pandey (PGT Biology) and Subhash Bhagata (PGT chemistry) for ignite my scientific thinking early in my life and providing all day access to lab for my idea and exploration at JNV Gopalganj. I would to thank JNV alumni family at IISER Pune especially, Dr. Krishanpal Karmodiya and his wife Dr. Anamika for their supports; Umashank, Muskan, Prabhat, Bhoj and Deepak for Navodaya meet at IISER. I also thank JNV Pune family and Principal B.R. Khedkar sir for his support.

I would like to thank Kho-Kho, Kabaddi and Cricket Players and at IISER Pune for sports.

I would like to thank my friends Saurabh Anand, Priti Kumari, Pranjal Vishwakarma, Manish Kumar, Manjeet, Aman, Akhilesh Singh, Umashankar, Vrinda, Bhumika, Hitendra Kumar, Aniket, Prashant Kumar, Pawan Kumar, Nikki Dutt, Kirti Tomar, Tumpa Mahto, and Ravishankar Yadav for through all the ups and downs over the years and during covid time (Bhavin Uttekar, Snehal, Prajna, Gitanjali, Alok).

I would like thank my sisters Kanti, Tanya, Aditi for their love and sending me wishes. My Parents Shree Ramjee Prasad and Smt. Sunaina Devi and my brothers Sanjay, Sunil, Suresh, Pawan, Sujit and Rupesh, for always lifting my spirits and pushing me for my education. I would like extend my gratitude to my wife Km Babita for being supportive and careful in ups and down during last couple of years. I would like thank my all families and friends.

Finally, I want to thank IISER Pune family for everything during this journey by quoting part of poem by Shivmangal Singh Suman.

"जीवन अस्थिर अनजाने ही, हो जाता पथ पर मेल कहीं,
सीमित पग-डग, लम्बी मंज़िल, तय कर लेना कुछ खेल नहीं।
दाएँ-बाएँ सुख-दुख चलते, **सम्मुख चलता पथ का प्रमाद**
जिस-जिस से पथ पर स्नेह मिला,
उस-उस राही को धन्यवाद।"

-Shivmangal Singh Suman

Table of Contents

LIST OF FIGURE ..... **VII**

LIST OF TABLES ..... **XII**

SYNOPSIS ..... **XIV**

CHAPTER 1 ..... **1**

SERINE HYDROLASES IN THE *DROSOPHILA MELANOGASTER* **1**

CHAPTER 1 2

SERINE HYDROLASES IN THE *DROSOPHILA MELANOGASTER* ..... **ERROR! BOOKMARK NOT DEFINED.**

ABSTRACT 2

GRAPHICAL ABSTRACT 2

INTRODUCTION 3

MATERIAL AND METHODS 6

Generation and Phylogenetic Characterization of a SH database for Drosophila melanogaster *6*

RESULTS 7

Bioinformatics analysis towards identification of SHs in Drosophila melanogaster *7*

MEROPS database-classification of Serine Hydrolases in the Drosophila melanogaster *11*

Serine Protease *12*

Metabolic SHs *13*

DISCUSSION AND CONCLUSIONS 14

REFERENCE 15

CHAPTER 2 ..... **19**

ACTIVITY ATLAS OF THE SERINE HYDROLASES SUPERFAMILY IN THE *DROSOPHILA MELANOGASTER* **19**

ABSTRACT 20

GRAPHICAL ABSTRACT 21

INTRODUCTION 22

MATERIAL AND METHODS 24
Gel-based ABPP Sample Preparation and Analysis 24
LC-MS/MS-based ABPP Sample Preparation and Analysis 25
Data Analysis 27
RESULTS 27
Identification of SH activities during different developmental phases in Drosophila melanogaster 27
Anatomical profiling of SH activities in adult Drosophila melanogaster 30
Sexual dimorphism of SH activities in adult Drosophila melanogaster 35
DISCUSSION AND CONCLUSIONS 37
REFERENCE 42

CHAPTER 3 46

***DROSOPHILA*'S SERINE HYDROLASES FUNCTION IN HOST DEFENSE AND BEYOND 46**

ABSTRACT 47
GRAPHICAL ABSTRACT 48
INTRODUCTION 49
LITERATURE SURVEY, GENERAL TRENDS AND INTERPRETATIONS 51
SHS UPON IMMUNE CHALLENGE 57
SHs in organ-specific immunity 58
PATHWAYS AFFECTING SH EXPRESSION IN DROSOPHILA'S IMMUNITY 61
DISCUSSION AND CONCLUSION 64
REFERENCE 67

CHAPTER 4 73

ACTIVITY BASED PROTEIN PROFILING (ABPP) AS A TOOL TO MAP 'ACTIVE' SERINE HYDROLASES INVOLVED IN THE *DROSOPHILA* INNATE IMMUNE RESPONSE 73

ABSTRACT 74
GRAPHICAL ABSTRACT 75
INTRODUCTION 76
MATERIAL AND METHODS 80
Fly Experimentation 80

Systemic wounding *80*
Gel-based ABPP *80*
LC-MS/MS Based ABPP *80*
RESULTS 83
Gel-based ABPP in wildtype (w^{1118}) upon injury and/or Infection (SWR) *83*
Role of NF-κB pathway (Toll and ImD) in SHs activity upon infection *86*
LC-MS/MS (Redime) based ABPP in wildtype (w^{1118}) upon infection *89*
DISCUSSION AND CONCLUSION 93
REFERENCE 96

CHAPTER 5 103

DROSOPHILA CG17192 IS A PHOSPHOLIPASE C THAT IS SECRETED IN THE GUT LUMEN IN RESPONSE TO INFECTION 103

COVER ART: CHEMOPROTEOMICS AND LIPIDOMIC APPROACH FOR CG17192 CHARACTERIZATION 104
ABSTRACT 105
GRAPHICAL ABSTRACT 106
INTRODUCTION 107
MATERIAL AND METHODS 108
Fly Experimentation *108*
Real Time qPCR (RT-qPCR) *109*
Untargeted Lipidomics *109*
Overexpression of CG17192 in Insect Cells *111*
Substrate assays *112*
Bacterial clearance test and life span *114*
RESULTS 115
Lipidomics characterization in the adult gut upon CG17192 knockdown *115*
Expression of CG17192 in S2 cells *118*
Phospholipase activity of CG17192. ..... *120*
Effect of CG17192 activity on PI and DAG levels in the adult gut upon infection *123*
CG17192 knockdown favor the host to clear infecting bacteria *127*
DISCUSSION AND CONCLUSION 128
REFERENCES 131

CHAPTER 6 136

***DROSOPHILA* CG10038 IS UBIQUITOUSLY EXPRESSED, SHOW DEACETYLASE ACTIVITY 136**

ABSTRACT 137
GRAPHICAL ABSTRACT 138
INTRODUCTION 139
MATERIAL AND METHODS 141
Fly Experimentation 141
Systemic wounding 142
Gel-based and LC-MS/MS ABPP 142
Overexpression of CG10038 in Bacteria 142
pNp hydrolysis: Calorimetric assay 143
Overexpression of CG10038 in Insect Cells 143
Real Time qPCR (RT-qPCR) 144
Immunoprecipitation 144
In-gel LC-MS/MS 144
Data Plotting and Analysis 145
RESULTS 145
Validating CG10038 as active SH using Competitive LC-MS/MS-based ABPP 146
Bacterial expression and purification of Drosophila CG10038 147
Biochemical properties of CG10038 148
Cellular localization of CG10038 151
Characterization of BL-91433 fly line 152
DISCUSSION AND CONCLUSION 160
REFERENCE 161

ANNEXURE 1 169

A SYSTEMATIC APPROACH FOR GENERATION OF GENETIC AND BIOCHEMICAL REAGENTS TO ANNOTATE ORPHAN SERINE HYDROLASES 169

AIM 170
RATIONALE 170

OBJECTIVES 171
OBJECTIVE 1 172
OBJECTIVE 2 173
Material and methods *173*
Cloning and expression *173*
FPLC Purification of CG11309 ..... *173*
RESULTS 174
Purification of CG11309 ..... *174*
FPLC cleanup of CG11309 ..... *175*
OBJECTIVE 3 176
Material and methods *176*
RESULTS 177
OBJECTIVE 4 178
MATERIAL AND METHOD 178
RESULTS 179
OBJECTIVE 5 182
MATERIAL AND METHOD 182
pUASp AttB fly lines/strains *182*
RESULTS 183

ANNEXURE 2 188

PROTOCOL FOR 'ACTIVE' SERINE HYDROLASES STAINING IN *DROSOPHILA*'S EMBRYO USING ACTIVITY BASED PROBES (ABPS) 188

ABSTRACT 189
INTRODUCTION 190
MATERIALS 191
PROCEDURE 192
EXPECTED RESULTS 194
Titration of FP-Rh with in-vivo activity of SHs of Drosophila embryo *194*
Reaction of tailored ABPs (WHP01) with active SHs in the Drosophila embryo *195*
Summary *196*
REFERENCES 196

ANNEXURE 3 198

MODULATION OF PHOSPHATIDYLINOSITOL UPON *WUNEN* AND *SAC1* KNOCKDOWN 198

AIM 199

RATIONALE 199

MATERIAL AND METHODS 199

RESULTS 200

REFERENCE 203

ANNEXURE 4 205

DATABASE OF SERINE HYDROLASE 205

ANNEXURE 5 235

ACTIVITY ATLAS OF SERINE HYDROLASE IN *DROSOPHILA MELANOGASTER* 235

ANNEXURE 6 264

LITERATURE SURVEY OF SERINE HYDROLASE IN *DROSOPHILA'S* IMMUNE RESPONSE 264

List of Figure

FIGURE 1.1 CONSENSUS CATALYTIC MECHANISM OF THE ENZYMES FROM THE SH SUPERFAMILY. 4

FIGURE 1.2. SCHEMATIC SHOWING FUNCTION OF SHS IN VARIOUS PATHOPHYSIOLOGICAL PROCESSES. 5

FIGURE 1.3. MEROP DATABASE-BASED CLASSIFICATION OF SERINE HYDROLASE SUPERFAMILY. 6

FIGURE 1.4. BIOINFORMATICS ANALYSIS IN BUILDING A SH DATABASE FOR *D. MELANOGASTER*. (A) VENN DIAGRAM REPRESENTING THE NUMBER OF UNIQUE SHS IDENTIFIED AND THE EXTENT OF THEIR REDUNDANCIES FROM FOUR PUBLICLY AVAILABLE DATABASES. (B) CATEGORIZATION OF THE SHS INTO “SERINE PROTEASES” AND “METABOLIC SERINE HYDROLASES” ALONG WITH AN ANALYSIS OF KNOWN FUNCTIONS WITHIN THESE CATEGORIES. (C) LIST OF KNOWN FUNCTIONS AND/OR CLANS WITH THE “SERINE PROTEASES” AND “METABOLIC SERINE HYDROLASES” CATEGORIES. 10

FIGURE 2.1. THE MECHANISM OF ACTIVITY-BASED PROTEIN PROFILING. ... 23

FIGURE 2.2. ABPP ANALYSIS ON LYSATES FROM DIFFERENT STAGES OF FLY DEVELOPMENT 29

FIGURE 2.3. GEL-BASED ABPP ANALYSIS ON FLY TISSUE LYSATES. 31

FIGURE 2.4. DETERMINING THE FULL COMPLEMENT OF ACTIVE SHS IN ADULT FLIES. 33

FIGURE 2.5. MAPPING SH ACTIVITIES DURING FLY DEVELOPMENT. 35

FIGURE 2.6. A CHEMOPROTEOMIC ATLAS OF SH ACTIVITIES IN *DROSOPHILA MELANOGASTER*. 41

FIGURE 2.S.1. COOMASSIE STAINING OF GEL SHOWN IN FIGURE 3A, SHOWING EQUAL LOADING OF ACTIVE (A) AND DENATURED (D) SOLUBLE (LEFT GEL) AND MEMBRANE (RIGHT GEL) LYSATES FOR RESPECTIVE DEVELOPMENTAL STAGES IN FLIES. 44

FIGURE 2.S.2. COOMASSIE STAINING OF GEL SHOWN IN FIGURE 4, SHOWING EQUAL LOADING OF ACTIVE (A) AND DENATURED (D) LYSATES FROM DIFFERENT TISSUES AND/OR ANATOMICAL COMPONENTS IN ADULT MALE AND FEMALE FLIES. 45

FIGURE 3.1. LITERATURE SURVEY FOR MULTI-OMIC STUDY ON DROSOPHILA INNATE IMMUNE RESPONSE. 52

FIGURE 3.2. STATUS OF EXPRESSION OF SHS UPON IMMUNE CHALLENGE. 57

FIGURE 3.3. MODULATION OF SHS IN GUT UPON GUT IMMUNITY. 59

FIGURE 3.4. MODULATION OF SHS IN PLASMATOCYTES UPON SEPTIC OR CLEAN INJURY. 61

FIGURE 3.5. PATHWAYS AFFECTING SH EXPRESSION IN DROSOPHILA'S IMMUNITY. 62

FIGURE 4.1. SCHEMATIC REPRESENTATION OF TOLL AND MELANISATION PATHWAY OF *DROSOPHILA* 79

FIGURE 4.2. PROCEDURE FOR ABPP. 82

FIGURE 4.3. MAPPING SHS ACTIVITY IN WILDTYPE UPON INJURY-INFECTION. 86

FIGURE 4.4. SHS ACTIVITY USING GEL-BASED ABPP IN MUTANTS OF TOLL AND IMD PATHWAYS. 88

FIGURE 4.5. MAPPING SH ACTIVITIES IN ADULT WILDTYPE FLIES DURING INFECTION BY ABPP 91

FIGURE 4.6. CG17192 ACTIVITIES IN PPO1 AND HAYAN MUTANT AS WILDTYPE DURING INFECTION BY ABPP. 93

FIGURE 5.1. EXPRESSION OF CG17192 IN DIFFERENT FLY TISSUES. 115

FIGURE 5.2. WORKFLOW OF THE CROSSES TOWARDS GENERATING THE WT AND CG17192-KD ADULT FLY LINES USED IN THIS STUDY. 116

FIGURE 5.3. UNTARGETED LIPIDOMICS ANALYSIS ON THE ADULT GUTS OF THE CG17192-KD FLY LINE. 118

FIGURE 5.4. ASSESSING EXPRESSION AND ACTIVITY OF CG17192 IN S2 CELLS. 120

FIGURE 5.5. PHOSPHOLIPASE ACTIVITY OF CG17192. 122

FIGURE 5.6. RELATIVE PI AND DAG LEVELS IN THE WT ADULT FLY GUT UPON INFECTION. 124

FIGURE 5.7. RELATIVE PHOSPHOLIPID LEVELS IN THE WT ADULT FLY GUT UPON INFECTION. 125

FIGURE 5.8. PI AND DAG LEVELS IN THE GUTS OF ADULT WT AND *CG17192-KD* FLIES DURING AN INFECTION. 127

FIGURE 5.9. CG17192 SHOW SEXUALLY DIMORPHIC HOST-DEFENCE ROLE IN THE DROSOPHILA GUT. 128

FIGURE 10. REACTION CATALYZED BY CG17192. 129

FIGURE 6.1. MULTIPLE SEQUENCE ANALYSIS (MSA) OF CG10038. 141

FIGURE 6.2. COMPETITIVE LC-MS/MS-BASED ABPP 146

FIGURE 6.3. EXPRESSION AND PURIFICATION OF CG10038 IN BACTERIA (BL21-DE3). 148

FIGURE 6.4. S222A MUTANT OF HUMAN ABHD14B THAT IS PARTIALLY CATALYTICALLY ACTIVE. 149

FIGURE 6.5. CG10038 PREFERS HYDROLYSIS OF THE ACETYL GROUP FROM DIFFERENT PNP ANALOGUES, THAT IS, SUBSTRATES HAVING VARYING ACYL CHAIN LENGTHS, (C2, C4, C8, C10, C12 AND C16). 151

FIGURE 6.6. CG10038 IS A SOLUBLE CYTOPLASMIC SH 152

FIGURE 6.7. CHARACTERIZATION OF BL-91433 FLY LINE AS CG10038 LOSS OF FUNCTION AND UBIQUITOUS GAL4 ALLELE. 154

FIGURE 6.8. CG10038 IS PROTEIN DEACETYLASE. 156

FIGURE 6.9. REPRESENTATIVE SNAPSHOT OF ACETYLATED PEPTIDES OF CG10038 AND ARC1 PROTEINS FROM PROTEINPILOT (SCIEX) LC-MS/MS ANALYSIS SOFTWARE. 157

FIGURE 6.10. CG10038^{LOF} IS SUSCEPTIBLE TO INFECTION. 159

FIGURE ANNEXURE1.1. SCHEMATIC FOR GENETIC AND BIOCHEMICAL APPROACH FOR THE GLOBAL ANALYSIS OF AN ENZYME FUNCTION. 171

FIGURE ANNEXURE1. 2. NI-NTA BASED AFFINITY PURIFICATION OF THE CG11309. 174

FIGURE ANNEXURE1.3 CHROMATOGRAM OF CG11309 PROTEIN. THE CHROMATOGRAM SHOWS THAT CG11309 GET ELUTED JUST AFTER VOID VOLUME I.E 7 TO 19 MINUTES ON SUPERDEX-75 ANALYTICAL COLUMN. ... 175

FIGURE ANNEXURE1.4. VALIDATION OF IN HOUSE GENERATED RABBIT POLYCLONAL ANTIBODY AGAINST (A AND A') CG10038 AND (B, B', C AND C') CG11309 FULL LENGTH PROTEIN USING WESTERN BLOT TECHNIQUE. 177

FIGURE ANNEXURE1.5. *DROSOPHILA* CROSSES FOR EXCISION OF THE SHS GENES LOCUS TO GENERATE NULL FLY LINE OF SHS. 179

FIGURE ANNEXURE1.6. PCR BASED SCREENING OF CG17192 KNOCKOUT USING CRISPR/CAS9 GENOME ENGINEERING. 180

FIGURE ANNEXURE1.7. PCR BASED SCREENING OF CG11309 KNOCKOUT USING CRISPR/CAS9 GENOME ENGINEERING. 181

FIGURE ANNEXURE1.8. PCR BASED SCREENING OF CG4757 KNOCKOUT USING CRISPR/CAS9 GENOME ENGINEERING. 182

FIGURE ANNEXURE1.9. THE VARIOUS PROTEOMIC FRACTIONS (MEMBRANE, SOLUBLE AND SECRETED MEDIA) OF S2 CELLS TRANSFECTED WITH MOCK, PUASP WT AND S179A CG17192 AS DESCRIBED IN METHOD, WERE ASSESSED USING GEL-BASED ABPP (TOP PANEL) AND PONCEAU S STAINING (BOTTOM PANEL). THE RED ASTERISK CORRESPONDS TO THE ACTIVITY (TOP PANEL) OR EXPRESSION (MIDDLE PANEL) OF CG10038. 184

FIGURE ANNEXURE1.10. REPRESENTATIVE IMAGE OF TRANSGENIC FLIES. SELECTION OF MINI-WHITE SELECTION MARKER BASED TRANSGENIC FLIES FOR WT AND S222A UAS-CG17192. 185

FIGURE ANNEXURE2.1. WORK SCHEME FOR HIGH-RESOLUTION IMAGING OF THE ACTIVE SERINE HYDROLASES. 194

FIGURE ANNEXURE2.2. TITRATION OF FP-RH WITH ACTIVE OF SHS IN DROSOPHILA EMBRYO IN-VIVO. 195

FIGURE ANNEXURE2.3. IMAGE OF TAILORED ABPS (WHP01) REACTION WITH ACTIVE SHS IN THE DROSOPHILA EMBRYO. 196

FIGURE ANNEXURE 3.1. UNTARGETED LIPIDOMICS EXPERIMENT ON THE WUN-KD EMBRYO. 201

FIGURE ANNEXURE 3.2. UNTARGETED LIPIDOMICS EXPERIMENT ON THE SAC1-KD EMBRYO. 202

FIGURE ANNEXURE 3.3. EXPRESSION OF WUN AND SAC1 PROTEIN IN *DROSOPHILA* EMBRYO. 203

List of Tables

TABLE 1.1. CLASSIFICATION OF SHS IN THE DROSOPHILA MELANOGASTER BASED ON MEROPS AND HMMER DATABASE 11

TABLE 2.1. LIST OF SHS SHOWING SEXUAL DIMORPHISM IN ACTIVITIES IN ADULT FLY. 36

TABLE 3.1: SUMMARY OF INFECTION-BASED EXPERIMENTS CARRIED OUT IN *DROSOPHILA*. 53

TABLE 3.2: MOST CITED DIFFERENTIALLY EXPRESSED SHS 65

TABLE 4.2. SH IDENTIFIED FROM THE LC-MS/MS BASED ABPP EXPERIMENT SHOWN IN FIGURE 4.5. 99

TABLE 4.3. SH IDENTIFIED FROM THE LC-MS/MS BASED ABPP EXPERIMENT SHOWN IN FIGURE 4.6.A. 100

TABLE 4.4. SH IDENTIFIED FROM THE LC-MS/MS BASED ABPP EXPERIMENT SHOWN IN FIGURE 4.6.B. 101

TABLE 4.5. SH IDENTIFIED FROM THE LC-MS/MS BASED ABPP EXPERIMENT SHOWN IN FIGURE 4.6.C. 102

TABLE 5.1. PRIMERS USED IN THIS STUDY. 112

TABLE 6.1. PRIMERS USED IN THIS STUDY. 145

TABLE 6.2: SH IDENTIFIED FROM THE LC-MS/MS BASED ABPP EXPERIMENT SHOWN IN FIGURE 6.2 164

TABLE 6.3. CG10038 INTERACTING PROTEIN IDENTIFIED COMMON TO WT AND S222A I.P PROTEOME (FIGURE 6.8). 165

TABLE 6.4. CG10038 INTERACTING PROTEIN IDENTIFIED UNIQUE TO WT (FIGURE 6.8). 166

TABLE 6.5. CG10038 INTERACTING PROTEIN IDENTIFIED UNIQUE TO S222A (FIGURE 6.8). 168

TABLE ANNEXURE1.1: BIODATA OF CANDIDATE GENES. 172

TABLE ANNEXURE1.2: SUMMARY OF TARGET SHS GENE CLONING 174

TABLE ANNEXURE1.3: PLAN OF IN-HOUSE GENERATION OF ANTIBODY AGAINST CG10038 AND CG11309 176

TABLE ANNEXURE 1.1: LIST OF PRIMERS 185

TABLE ANNEXURE 5.1:SERINE PROTEASE IN DEVELOPMENT 236

TABLE ANNEXURE 5.2:METABOLIC SERINE HYDROLASE IN DEVELOPMENT 238

TABLE ANNEXURE 5.3:SERINE PROTEASE IN ADULT ORGANS 240

TABLE ANNEXURE 5.4:METABOLIC SERINE HYDROLASE IN ADULT ORGANS 243

TABLE ANNEXURE 5.5:SHS IDENTIFIED 249

Synopsis

The serine hydrolase (SH) superfamily is one of the largest functional enzyme classes in all forms of life and catalyzes hydrolysis reaction at electron-deficient carbon of substrates using nucleophilic serine at its active site.

In chapter 1, *Drosophila'*s SHs genes were collated from various databases and literature and further classified into families and classes based on protein structure, motifs and molecular functions. The analysis focused on compiling a list of serine hydrolase genes in *Drosophila melanogaster* using four databases: FLYBASE, NCBI, MEROPS, and HMMER. 354 non-redundant SH genes were identified, comprising about 2.5% of the fly's total proteome (13,968 genes). The SH superfamily is classified into two main categories: serine proteases (210 members) and metabolic SHs (144 members). However, only a small subset of these proteins had experimentally validated functions, with 84% remaining uncharacterized. Further classification revealed specific subtypes within both categories, such as clip proteases and trypsin-like proteases among the serine proteases and carboxylesterase-like and phospholipases among metabolic SHs. This collation and classification will be critical to the systemic study of SH function in subsequent chapters.

The SH superfamily has played a pivotal role as a classical prototype in developing multiple platforms within the chemical proteomics field, specifically the activity-based protein profiling (ABPP) technique. These platforms have been essential for conducting comprehensive investigations into the functions of the various members of this superfamily across a diverse range of native yet complex biological contexts. While ABPP-based proteome-wide activity atlas for SH activities is accessible in

numerous organisms, including humans, such an analysis has been notably absent in any insect model.

In chapter 2, Activities of the SH superfamily throughout various identify and globally map developmental stages in various adult tissues of *Drosophila* using the ABPP chemoproteomic tool. Using this ABPP approach, we found a total of 136 non-redundant active SHs with a superfamily-wide coverage of 38.4%, of which 61 were serine proteases (29% coverage for this category), while 75 belonged to the metabolic SH category (52% coverage for this category). The Activity of SHs is distinct in the different developmental stages. Also, sexual dimorphism is present in SH activities across distinct tissues in adult *Drosophila melanogaster*. Looking ahead to the prospective future, chapter 2 will constitute the second foundational step in the discovery and functional annotation of SH proteins in the *Drosophila* innate immune response.

In chapter 3, Intending to enumerate the novel SHs involved in the innate immune response, we have undertaken a literature survey of SHs involved in the host defence. We find that 252 SH genes are modulated in response to infection. 99 and 101 genes are uniquely up or downregulated, while 51 are context-dependent. Based on published multi-omics and genetic studies, we assigned SHs to the three major signalling cascades: the Toll, Immune Deficient, and JNK pathways. Literature points out that each immune pathway regulates specific sets of SHs expression.

Our literature survey in this chapter highlights that over half of SHs modulate during infection paradigms. The extent of modulation of SHs Depends on the immunogenicity of the pathogen and organ of the fly. This chapter will make the foundation of literature

to the biochemical characterization of unannotated SHs that are involved in the *Drosophila*'s immunity.

Yet, despite significant advances, the utility of ABPP platforms in fly models still needs to be explored. Realizing this knowledge gap, leveraging complementary ABPP platforms, in Chapter 2, we mapped the full array of SH activities during various stages of development and in different adult tissues in the fruit fly (*Drosophila melanogaster*). In chapter 4, using ABPP, we mapped SH activities in adult fruit flies in multiple infection models. Our studies also suggest the existence of sexual dimorphism in SHs activities upon infection. Furthermore, leveraging loss-of-function mutant lines in the canonical Toll/NFkB and Imd/NFkB pathways reveals novel immune-responsive SHs, particularly CG17192, which is not previously implicated in these signal transduction pathways. Given the conservation of many genes and proteins involved in immune responses between flies and mammals, it is anticipated that orthologous SH genes may play similar roles in human host defence

In chapter 4, We mapped the SHs activity during different infection models of the *Drosophila* and identify CG17192 as a potential target to charterisation. In this chapter, to assign a biological function to CG17192 as-of-yet uncharacterized lipase, we performed an untargeted lipidomics analysis and found that phosphatidylinositols were significantly elevated when *CG17192* was knocked down in the adult fruit fly gut. Next, we overexpressed this putative lipase in insect cells and using biochemical assays, we show that CG17192 is a secreted enzyme that has phospholipase-C (PLC) type activity with phosphatidylinositol being a preferred substrate. Finally, we show during infection, that heightened CG17192 regulates phosphatidylinositol levels, and by doing so, likely modulates signaling pathways in the adult fruit fly gut that might be involved in the resolution of this pathophysiological condition. This chapter, with

CG17192, we demonstrate the complementary use of ABPP platforms, lipidomic and biochemical assays in assigning functions to enzymes in different physiological contexts.

As we discussed, only a small fraction of the enzymes have been biochemically characterized and/or have correct biological functions. Many enzymes involved in human diseases and metastasis are awaiting to be characterized for their biochemical functions. Realizing this, we found in Chapter 1 and Chapter 2 that CG10038 is a novel SH enzyme and orthologous to mammalian FAM172A protein, which interacts with NF-κB factor control apoptosis in hepatocellular carcinoma. However, FAM172A is also biochemically uncharacterized. Hence, in the Chapter 6, we chose CG10038 as a potential target to identify its biochemical function in the *Drosophila* model organism. To assign a biological function to this as-of-yet uncharacterized SH, we confirm the CG10038 is cytoplasmic and soluble SH using chemoproteomics and expression in S2 cells. Then, we expressed and purified CG10038 and found that it is a small molecule hydrolase using *p*-Np substrates hydrolysis assays. Following this, we characterize the BL-91433 fly line as a hypomorphic allele using RTqPCR and chemoproteomics. Next, we hypothesized and showed that CG10038 as deacetylase by performing lysine acetated western blotting (adult fly proteome using hypomorphic allele) and immuno-precipitation of CG10038 (S2 cell proteome) followed by in-gel LC-MS. Since CG10038 is a deacetylase, it may regulate the function of its immune-responsive partner proteins by deacetylation.

In annexure 1, we generated reagents using cloning, protein expression antibody generation, CRISPR/cas9 based knockouts flies for the annotation of each target.

List of Publication

1. **Kundan, Kumar**, Amol Mhetre, Girish Ratnaparkhi, Siddhesh Kamat. (2021). A Superfamily-wide Activity Atlas of Serine Hydrolases in Drosophila melanogaster. Biochemistry 60(16):1312--1324. DOI:10.1021/acs.biochem.1c00171

2. **Kundan, Kumar**, Mrunal Pazare, Girish Ratnaparkhi, Siddhesh Kamat. (2024). CG17192 is a phospholipase that regulates signaling lipids in the Drosophila gut upon infection. Biochemistry 19;63(22):3000-3010**.** Doi:10.1021/acs.biochem.4c00579.

3. Arnab Chakraborty, Archit Devarajan, **Kundan Kumar**, Rohith C. S., M. S. Madhusudhan, Girish S. Ratnaparkhi, Siddhesh S. Kamat. Bioinformatics analysis identifies sequence determinants of enzymatic activity for the PHARC associated lipase ABHD12. Manuscript under submission.

Chapter 1

Serine Hydrolases in the *Drosophila melanogaster*

Chapter 1

Database of Serine Hydrolases in *Drosophila melanogaster*

Abstract

The serine hydrolase superfamily is one of the largest functional enzyme classes in all forms of life and catalyzes hydrolysis reaction at electron-deficient carbon of substrates using nucleophilic serine at its active site. Serine hydrolases are involved in most cellular and physiological processes, such as body axis patterning, digestion, blood coagulation, stress and humoral immune response. *Drosophila melanogaster* is a popular model organism for studying gene function. However, a Superfamily-wide study of SHs is lacking in *Drosophila melanogaster*. Thus, the listing of the SH genes is the primary foundation for the study of SHs function in *Drosophila melanogaster.* In this chapter, *Drosophila*'s SHs genes were collated from various databases and literature and further classified into families and classes based on protein structure, motifs and molecular functions. A total of 354 non-redundant SH genes were identified, comprising about 2.5% of the fly's total proteome (13,968 genes). The SH family was classified into two main categories: serine proteases (210 members) and metabolic SHs (144 members). The collation and classification will be key to the systemic study of SH function in subsequent chapters.

Graphical abstract

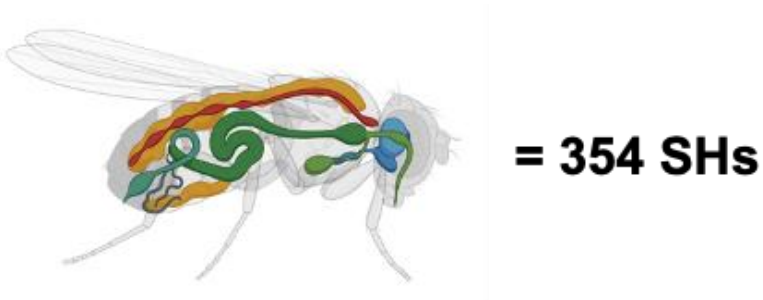

Image generated using Biorender

Keywords: Serine Hydrolase, Serine Protease, Metabolic Serine hydrolase, Catalytic triad, *Drosophila melanogaster*

Introduction

The serine hydrolase (SH) superfamily consists of enzymes that catalyze physiologically important hydrolytic reactions at electron-deficient carbon (or phosphorus) centres at amide, ester or thioester functionalities and consists of proteases, peptidases, esterases, lipases, amidases, and transacylases as prototypical members [1–4]. This enzyme superfamily is known to be present in both prokaryotes and eukaryotes and constitutes 1 – 3 % of the total cellular proteome, thus making them, one of the largest functional enzyme classes across all forms of life. All members of this superfamily, without any exceptions known to date, contain a catalytically competent, conserved nucleophilic serine residue in the active site to perform the aforementioned hydrolytic-type reactions via a consensus two-step ping pong mechanism involving a covalent enzyme intermediate (**Figure 1.1**), thus, leading to the “serine hydrolase” moniker for this superfamily[1–4]. This invariant catalytic serine residue is part of the famous catalytic triad[3,4] (which is the hallmark of this superfamily), and is activated by an active site base (generally a histidine residue) to initiate the enzyme catalytic cycle (**Figure 1.1**). The catalytic triad residues form hydrogen bonds with each other. The hydrogen bonds facilitate the pooling of proton from serine residue, The lone pair electron of serine’s oxygen atom attack on the carbonyl carbon of the substrate and forms a tetrahedral intermediate. The carbonyl carbon of the substrate forms easter bond with the enzyme and this intermediate is known as acyl-enzyme intermediate. Glycine residue in the vicinity stabilises the negative charge of carbonyl oxygen of the substrate that comprises the “oxyanion hole”. The protonated histidine transfers its proton to leaving first product of the hydrolysis. Then, hydrogen of a water molecule forms a hydrogen bond with histidine and the lone pair electron of

water's oxygen attack the carbonyl carbon of the acyl-enzyme and thus, the second product leaves (**Figure 1.1**).

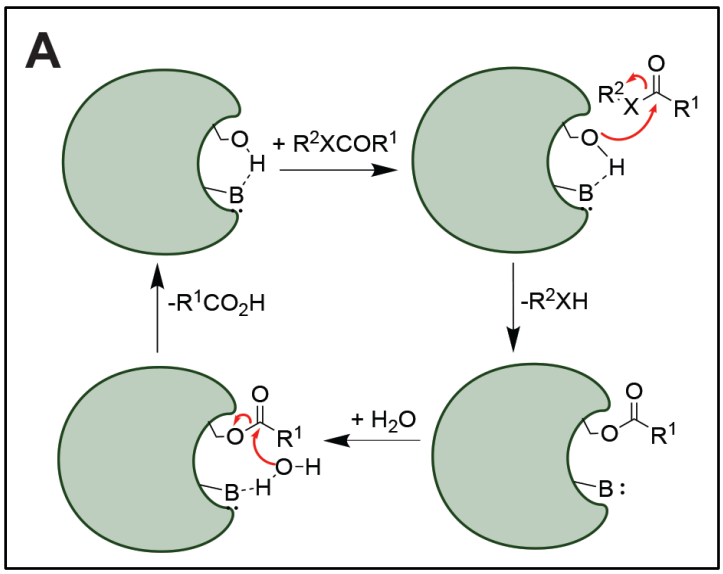

Figure 1.1 Consensus catalytic mechanism of the enzymes from the SH superfamily.

Typically, this catalytic serine residue is part of a canonical GxSxG motif (x = any amino acid), although, exceptions to this motif have been found in all organisms[1,2]. SHs play fundamental roles in the various organismal and cellular processes such as peptide/protein processing, digestion, blood coagulation, immune response, fertilisation and embryonic development, neuronal plasticity, and neurotransmitter catabolism (**Figure 1.2**.)[5–9]. SH activity regulates many pathways that cause disease and disorders. From a biological standpoint, deregulation in the activities of different SH enzymes has been linked to detrimental pathophysiological consequences in several organisms and is often associated with various metabolic and/or autoimmune diseases in humans[1]. SHs can be the target for treating various pathologies like obesity, microbial infection, cancer, neurodegenerative disorders etc.

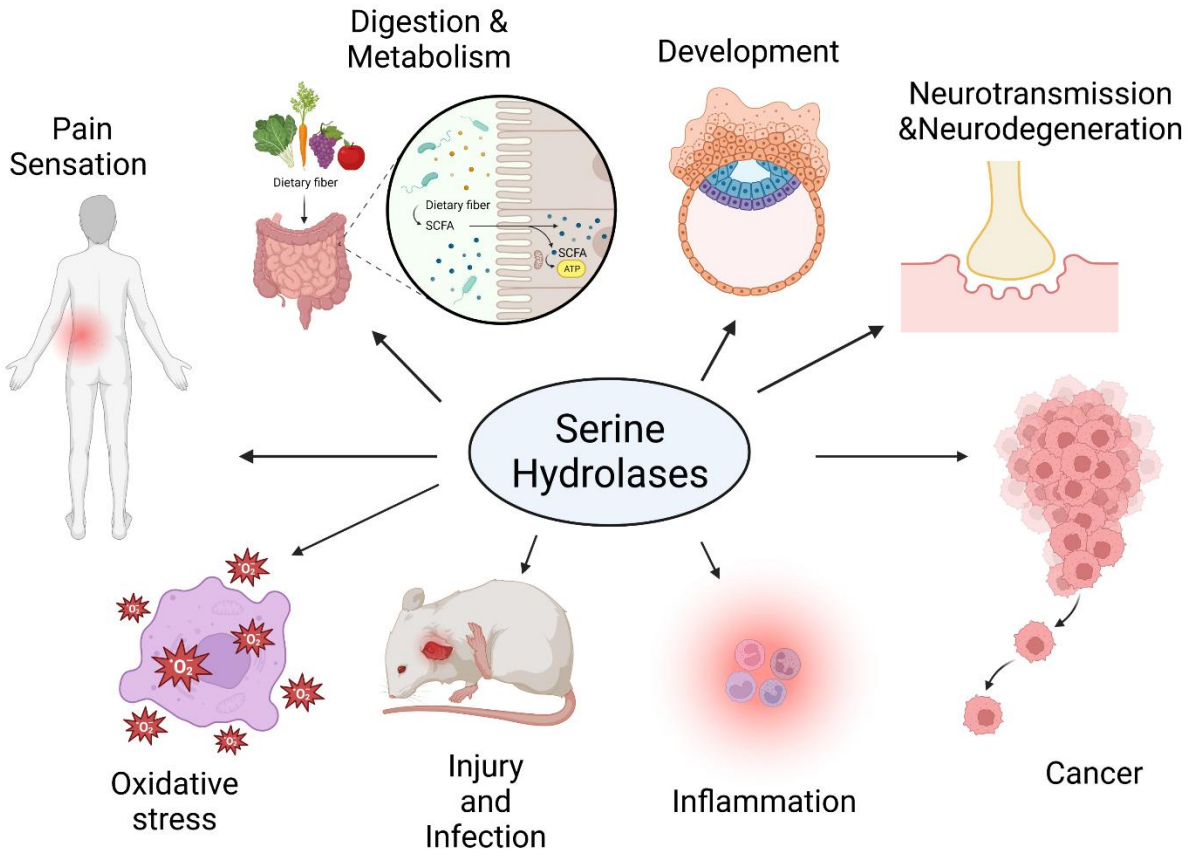

Figure 1.2. Schematic showing Function of SHs in various Pathophysiological processes.

Many attempts have been made to compile and classify the SHs gene for fruit fly in the past two decades [6,7,10–12]. MEROPS and Flybase databases classify SH superfamily into various clans and sub-divided into families based on structural similarity and catalytic mechanisms (**Figure 1.3**) [13]. This superfamily is classified into 15 clans based on order of catalytic traid order or amino acid residue composition. Alternatively, SHs have been classified based on substrate specificity, as Serine Proteases (SPs) or metabolic serine hydrolases (mSHs) [1]. Serine Proteases hydrolyse the amide bond in peptides and Proteins. Metabolic SHs hydrolyse ester, thioester, amide and epoxide bonds in the small molecules, peptides or proteins [1].

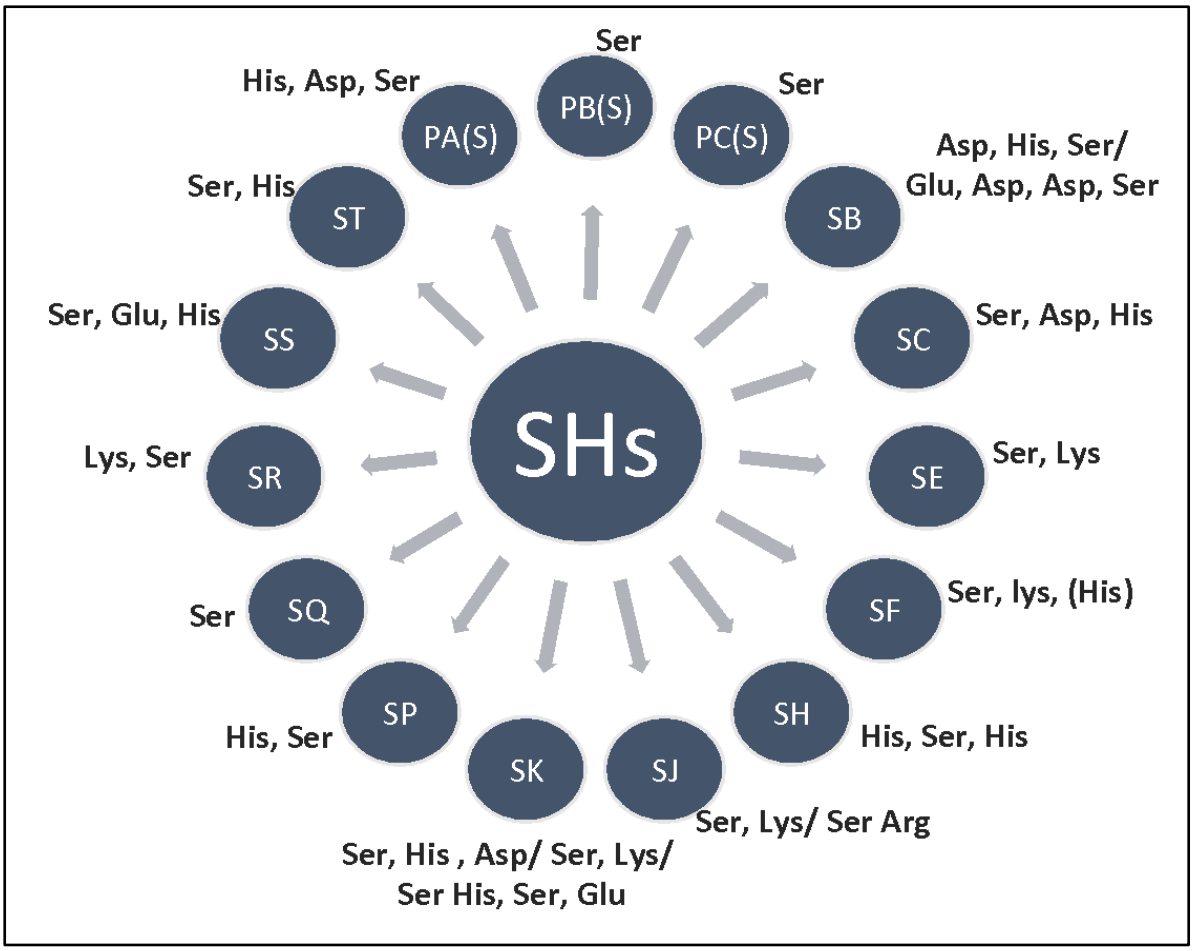

Figure 1.3. MEROP database-based classification of Serine Hydrolase superfamily.

Material and Methods

Generation and Phylogenetic Characterization of a SH database for *Drosophila melanogaster*

Genes encoding proteins predicted to be SHs were filtered and collated from four publicly available databases namely: (i) FLYBASE[2-8], (ii) NCBI database (Release 6 plus ISO1 MT, GCF_000001215.4, last modified: 2020-04-24) (SH_motif search), (iii) MEROPS[9-12], and (iv) HMMER[13-15]. Within the HMMER database, the filtered fasta sequence of each SH was further analyzed for a Pfam motif using HmmerWeb version 2.41.1. The command for this analysis was 'hmmscan --cut_ga --hmmdb pfam' against the Pfam version 32.0 database. The Pfam protein domain, catalytic residue order and Pfam family identity number were retrieved, and the SHs having the same protein motif

and catalytic order were grouped together. The SH genes whose catalytic residue were not predicted by the aforementioned HMMER searches were retrieved using multiple sequence alignments from sequences collated from the other three databases. Proteins with an active SH motif i.e. GxSxGG, GxSxG, GxSxxG (where x is any amino acid) were filtered using a Python code on a local computer. The final enzyme list from all the published databases was manually curated to ensure they fit with the SH superfamily and split into two categories: serine proteases or metabolic SHs, based on sequence alignments to known enzyme activities within this superfamily. Towards generating a phylogenetic tree for the serine proteases and metabolic SHs, multiple sequence alignments for enzymes of each category were performed using the MUSCLE program (MEGA-X) with default software-defined parameters. The phylogenetic tree was generated by the MEGA-X software using the "Neighbor-Joining" method[18, 19], and visualized using the FigTree (version 1.4.4) software.

Results

Bioinformatics analysis towards identification of SHs in *Drosophila melanogaster*

Towards collating this list, four publicly available databases: (i) FLYBASE (a database specific to *Drosophila* genes and genomes)[14–17], (ii) NCBI database (Release 6 plus ISO1 MT, GCF_000001215.4, last modified: 2020-04-24) (with a SH_motif search), (iii) MEROPS (the peptidase/protease database)[18–20], and (iv) HMMER (the biosequence search and analysis tool)[21–23] were choosed. The curated number of SH-like genes in MEROPS and FlyBase are 434 and 486, respectively. SHs gene were collated from the Flybase, MEROPS and literature and examined them for the

presence of the catalytic serine motif (GXSXGG, where x is any natural amino acid) from the protein sequence. Then, Gene has a serine motif subjected to protein motif analysis using HMMER that builds more confidence. Thus, the SHs gene list was generated. The SHs list has improved as compared with the previous analysis. The FLYBASE and HMMER databases yielded the most non-redundant SH protein sequences, with 346 and 342 respectively, with a significant overlap (339 common sequences between both databases), while the NCBI and MEROPS databases together provided unique non-redundant SH protein sequences that were not found (or missed in searches) in the FLYBASE or HMMER databases (**Figure 1.3.A**, **Annexure 4**). Together, 354 non-redundant SHs in *Drosophila melanogasterwere* identified, which were further manually curated to ensure that they possessed the conserved catalytic serine residue and/or the catalytic triad (**Annexure 4**). Our bioinformatics analysis thus shows that the SH enzyme family in *Drosophila melanogaster* comprises of ~ 2.5 % of the total proteome (354 gene-coded serine hydrolase enzymes from a total of 13968 gene-coded proteins in *Drosophila melanogaster*).

Consistent with previous classifications of this superfamily in other organisms[1], The member SHs superfamily is broadly categorize as (i) serine proteases, and (ii) metabolic SHs. Using the inbuilt multiple protein alignment algorithms/tools in HMMER database, and correlating them to known/validated enzyme activities reported in both the FLYBASE and Uniprot databases, 210 protein sequences could be categorized as serine proteases, while 144 protein sequences were classified as metabolic SHs (**Figure 1.4.B, Annexure 4**). Next, upon manually searching these protein sequences for validated functions in Uniprot, only a small number of the serine proteases (30 members), and metabolic SHs (26 members) had been experimentally validated, with

functions and/or associations to established biological activities (**Figure 1.4.B, Annexure 4**). Functional annotation analysis using Flybase and literature survey further showed that approximately 84% of members of the SH superfamily (86% of serine proteases, and 82% of metabolic SHs) remain uncharacterized (**Figure 1.4.B**).

Finally, in an attempt to broadly map the extent of possible putative enzymatic activities within the two categories of this superfamily in *Drosophila melanogaster*, 354 protein sequences analysed across the FlyBase and MEROPS databases in search of possible clans or sub-families. Based on predicted molecular functions from the protein sequences from all the databases, further sub-classified the 210 serine proteases as putative clip proteases (33 members), trypsin/chymotrypsin-like proteases (159 members), rhomboid proteases (5 members), and subtilisin-like proteases (6 members) (**Figure 1.4.C, Annexure 4**). Rest 7 serine proteases could not classified as any of the above, and hence were classified as other proteases within this category (**Figure 1.4.C, Annexure 4**). A similar analysis for the metabolic SH category revealed a greater diversity in putative enzymatic activities and a more even spread across its members (**Figure 1.4.C, Annexure 4**). Here, the 144 metabolic SH enzymes sub-classified as carboxylesterase-like (31 members), neutral or sterol lipase (32 members), phospholipases (34 members), acyltransferases (10 members) and peptidases (18 members) (**Figure 1.4.C, Annexure 4**)[24]. Like the serine proteases, 19 members of the metabolic SH category did not have enough sequence homology to the sub-category members listed above and were therefore grouped together as “Others/Unknown” members (**Figure 1.4.C, Annexure 4**).

A

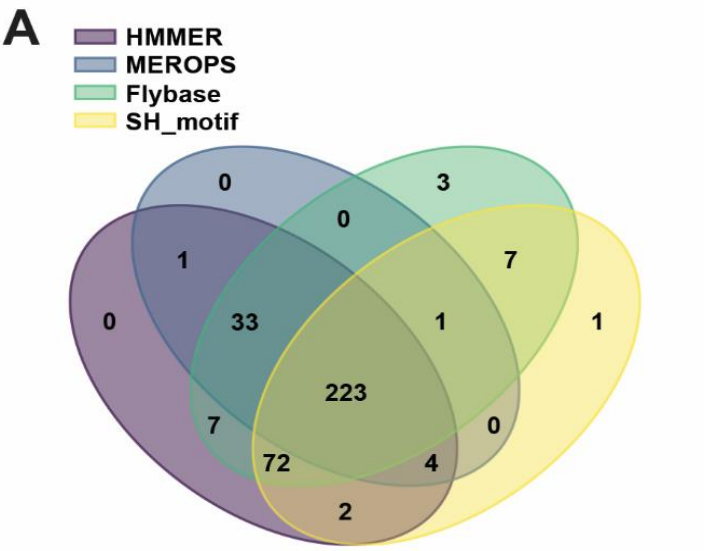

B

Category	Number	Validated Functions	% Unknown
Serine Proteases	210	30	86
Metabolic Serine Hydrolases	144	26	82
Total	354	56	84

C

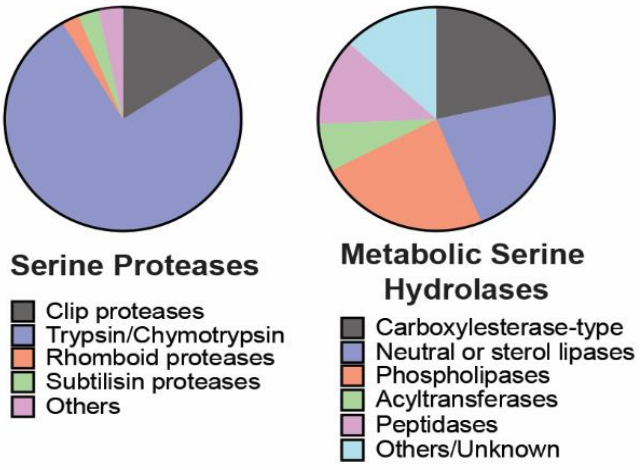

Figure 1.4. Bioinformatics analysis in building a SH database for *D. melanogaster*. (A) Venn diagram representing the number of unique SHs identified and the extent of their redundancies from four publicly available databases. (B) Categorization of the SHs into "serine proteases" and "metabolic serine hydrolases" along with an analysis of known functions within these categories. (C) List of known functions and/or clans with the "serine proteases" and "metabolic serine hydrolases" categories.

MEROPS database-classification of Serine Hydrolases in the *Drosophila melanogaster*

According to MEROPS enzyme classification, SHs superfamily in *Drosophila* can also be systematically classified into nine clans and clans further categorised into 15 families depending on structural homology and order of the catalytic residues (**Figure 3. And Table.1**)[18,19].

Table 1.1. Classification of SHs in the *Drosophila melanogaster* based on MEROPS and HMMER database

S.No.	Category	Clan	MEROPS Family	HMMER Family	Count	Example
1	SP	PA	S1	CL0124	190	Hayan, Jon99Cii, modSP
2		PA	S1	CL0155	2	teq, Cda5
3		PC	S51	CL0014	1	CG2200
4		SB	S8	Undefined	5	amon, Fur1, TppII
5		SF	S26	CL0299	3	CG11110; CG9240, twr
6		SJ	S16	CL0329	1	Lon
7		SK	S14	CL0127	1	ClpP
8		ST	S54	CL0207	6	ru; rho; stet
9		SP	S59	CL0661	1	CG10198
10	mSH	SC	S9A	CL0028	27	Ace; alpha-Est1; CG4757
11		SC	S33	CL0028	17	CG5377, CG5707, kraken
12		SC	S28	CL0028	6	CG9953, CG3739
13		SC	S10	CL0028	5	hiro, CG4572, CG32483
14		Other	ABHD	CL0028	60	MESK2, Ppt1, CG17192
15		S-	S81	CL0037	2	CG14823, CG6435
16		SC	S15	CL0186	1	CG3744
17		SC	S9B	CL0186	5	ome, CG11319
18		Other	mSH		21	iPLA2-VIA, CG10038
				Total SH	354	

Serine Protease

Serine protease is classified into 8 clans (Table 1). Each clan with their family members are described below[12].

Clan PA and family S1 consist of trypsin-like SPs with catalytic order His, Asp and Ser (Veillard et al. 2017, cao et al. 2018). 190 SPs of the S1 family categorised into trypsin(114), chymotrypsin (61), and elastase(15) [6,20]. 33 SP contains the regulatory CLIP domain, which is subclassified as clip protease in the Serine protease class[6].

PC clan, family S51 contain exopeptidase that hydrolyses alpha-aspartyl bonds and has a single member i.e. CG2200, in the fruit fly[25]. The catalytic residue order is Ser, Asp, His. The tertiary structure of CG2200 is similar to class I glutamine amidotransferase-like protein[20].

Clan SB, family S8 consists of Subtilase group of peptidases with Asp, His, His, Ser catalytic residue[26]. Sp1, Fur1, Fur2, amon and TppII are serine-type endopeptidases and express across all stages of the Drosophila life cycle[27–29]. Proteomics data suggest that TppII undergoes post-translational modification with SUMO[30]. All members of the clan SB are not well studied in the fruitfly except amon. amon show peptidase activity and localizes to the extracellular region, involved in several biological processes such as R8 cell fate specification; hatching behavior; and larval wandering behavior[31–33].

Clan SF, family S26 consists of membrane-bound endopeptidase with Ser, and Lys as catalytic residue[26]. The S26 family is involved in the signal peptide processing peptidase[20]. CG11110 and CG9240 are mitochondrial inner membrane proteases and share high sequence similarity as compared to Twr, which is an endomembrane protease[26,34]. CG11110 and CG9240 process the protein targeting mitochondria[35]. Twr's homologue cleaves the signal sequence of the target proteins in the endomembrane system[36].

CLAN SJ, Family S16 has a single member, the Lon protease with Ser, Lys catalytic residue[20]. Lon protease hexamerises into a ring with a central cavity[20]. LON protease is annotated to several cellular processes such as stress-dependent protein catabolic process, protein quality control for misfolded or truncated protein, chaperon mediated protein assembly[37–39].

SK clan, family S14 contain endopeptidase Clp with a single member ClpP in the fruit fly[20]. ClpP exhibits ATP-dependent serine endopeptidase activity and mediates protein quality control through selective degradation of polypeptides in the mitochondrial matrix for misfolded or incompletely synthesized proteins [40].

Clan ST, family S54 consists of intramembrane rhomboid proteases[20]. Serine and Histidine are the catalytic residues and have six or seven repeats of the transmembrane domain[21,22]. S54 SPs are expressed in a spatio-temporal manner and activate the EGFR ligand spitz by its cleavage. For instance, rhomboid1 is involved in the EGFR ligand maturation, wing, larval salivary gland morphogenesis, leg disc proximal and distal pattern formation, Malpighian tubules formation[41–43]. Rhomboid 2 is required for the germ cell differential via EGFR signalling from follicular somatic cells [44,45].

Clan SP, family S59 consist of the single member Nucleoporin 98-96 kD[20]. It consists of multiple repeats of the phenylalanine-glycine (F-G repeats), Nucleoporin autopeptidase and nup96 domains[22,23]. Serine (1029) is predicted as only a catalytic residue[22,23]. The Nup98-96 is homologous to *Saccharomyces cerevisiae*'s Nup145[12].

Metabolic SHs

Metabolic SHs are classified into SC clan, other ABHD and other mSH[20,22]. In the Clan SC catalytic residue order is Ser, Asp, His or Ser, Glu, His or Ser[20,22,23]. Members of

the SC clan share the 'alpha-beta hydrolase' protein fold in which the beta-sheet has eight strands in order of 12345678, and strand 2 is antiparallel to the rest[18–20]. Clan SC includes carboxylesterase, neutral or sterol lipase, phospholipase, acyltransferase, peptidase and others. The SC clan of mSHs are structurally alpha-beta hydrolase and classified into families S9, S33, S28, S10, S51, and S15[12]. The members of the fruit fly's SC clan are orphans Except for Kynurenine formamidase (KFase), and Acetylcholinesterase (Ace), Fatty acid synthases[11]. KFase expresses in all stages of the life cycle and exhibits N-formyl-L-kynurenine to L-kynurenine catalysis and assists the toxic metabolite elimination from the system[27,29,46]. Ace is well studied in *Drosophila melanogaster*[47], [48], [49]. Ace catalyzes the hydrolysis of the neurotransmitter acetylcholine to acetate and choline[50]. Fatty acid synthase (FASN) family consists of three members FASN1, FASN2 and FASN3[11]. The catalytic residue is C199; S619; H721; D1062;; S2249; H24216 in the Beta-ketoacyl synthase, N-terminal; Beta-ketoacyl synthase, C-terminal; Acyl transferase domain; Polyketide synthase dehydratase, Polyketide synthase dehydratase respectively. FASN is involved in glycogen metabolism and triglyceride biosynthesis in many biological processes [51–53]

Other mSH needs to be categorised into clans and families based on the protein tertiary structure and catalytic residue order.

Discussion and conclusions

SH enzyme superfamily remains poorly explored in flies. To address this problem, using bioinformatics, we first collated a list of all the known non-redundant SHs in *Drosophila melanogaster* from various publicly available databases/sources and found that flies genetically encode 354 of them (**Figure 1.3, Annexure 1**). Consistent with

previous classifications done for this superfamily in other organisms, we classified based on sequence homology to known molecular functions these 354 non-redundant SHs into serine proteases and metabolic SHs, and found that the two categories contained 210 and 144 members, respectively, of which a significant fraction lacked known physiological function **Figure 1.3, Annexure 1**). Also, We classified SPs into PA, PC, SB, SF, SJ, SK, ST SP clans (**Table.1.1**). PA clan contain the largest fraction (192 of 210) of SPs (**Table.1.1**). Also, the PA clan contain regulatory clip proteases. The mSHs contain only SC clans with 123 members. The members of SC clan shared alpha beta hydrolase domain (ABHD) and grouped into 8 families i.e. S9A, S9B, S33, S28, S10, S81, S15, and other ABHD (**Table.1.1**) .

Acknowledgments

We thank Gulzar Singh (MS Madhusudhan lab, IISER Pune) for technical help with python.

References

1. Long, J. Z. & Cravatt, B. F. The metabolic serine hydrolases and their functions in mammalian physiology and disease. *Chem. Rev.* **111**, 6022–6063 (2011).
2. Simon, G. M. & Cravatt, B. F. Activity-based proteomics of enzyme superfamilies: serine hydrolases as a case study. *J. Biol. Chem.* **285**, 11051–11055 (2010).
3. Dodson, G. & Wlodawer, A. Catalytic triads and their relatives. *Trends Biochem. Sci.* **23**, 347–352 (1998).
4. Carter, P. & Wells, J. A. Dissecting the catalytic triad of a serine protease. *Nature* **332**, 564–568 (1988).
5. Yoshida, S. & Shiosaka, S. Plasticity-related serine proteases in the brain (review). *Int. J. Mol. Med.* **3**, 405–409 (1999).
6. Cao, X. & Jiang, H. Building a platform for predicting functions of serine protease-related proteins in *Drosophila melanogaster* and other insects. *Insect Biochem. Mol. Biol.* **103**, 53–69 (2018).
7. Ross, J., Jiang, H., Kanost, M. R. & Wang, Y. Serine proteases and their homologs in the *Drosophila melanogaster* genome: an initial analysis of sequence conservation and phylogenetic relationships. *Gene* **304**, 117–131 (2003).
8. Valanne, S., Wang, J.-H. & Rämet, M. The *Drosophila* Toll Signaling Pathway. *The Journal of Immunology* vol. 186 649–656 Preprint at

https://doi.org/10.4049/jimmunol.1002302 (2011).
9. Cravatt, B. F. *et al.* Molecular characterization of an enzyme that degrades neuromodulatory fatty-acid amides. *Nature* **384**, 83–87 (1996).
10. Drysdale, R. & FlyBase Consortium. FlyBase : a database for the *Drosophila* research community. *Methods Mol. Biol.* **420**, 45–59 (2008).
11. Attrill, H. *et al. FlyBase: establishing a Gene Group resource for Drosophila melanogaster*. *Nucleic Acids Research* vol. 44 D786–D792 Preprint at https://doi.org/10.1093/nar/gkv1046 (2016).
12. Rawlings, N. & Barrett, A. The MEROPS Database. *Nature Precedings* Preprint at https://doi.org/10.1038/npre.2009.3103.1 (2009).
13. Hedstrom, L. Serine protease mechanism and specificity. *Chem. Rev.* **102**, 4501–4524 (2002).
14. Larkin, A. *et al.* FlyBase: updates to the *Drosophila melanogaster* knowledge base. *Nucleic Acids Res.* **49**, D899–D907 (2021).
15. Thurmond, J. *et al.* FlyBase 2.0: the next generation. *Nucleic Acids Res.* **47**, D759–D765 (2019).
16. Rey, A. J., Attrill, H., Marygold, S. J. & FlyBase Consortium. Using FlyBase to Find Functionally Related *Drosophila* Genes. *Methods Mol. Biol.* **1757**, 493–512 (2018).
17. Marygold, S. J., Crosby, M. A., Goodman, J. L. & FlyBase Consortium. Using FlyBase, a Database of *Drosophila* Genes and Genomes. *Methods Mol. Biol.* **1478**, 1–31 (2016).
18. Rawlings, N. D. & Bateman, A. How to use the MEROPS database and website to help understand peptidase specificity. *Protein Sci.* **30**, 83–92 (2021).
19. Rawlings, N. D. *et al.* The MEROPS database of proteolytic enzymes, their substrates and inhibitors in 2017 and a comparison with peptidases in the PANTHER database. *Nucleic Acids Res.* **46**, D624–D632 (2018).
20. Rawlings, N. D. & Barrett, A. J. MEROPS: the peptidase database. *Nucleic Acids Res.* **28**, 323–325 (2000).
21. Potter, S. C. *et al.* HMMER web server: 2018 update. *Nucleic Acids Res.* **46**, W200–W204 (2018).
22. Prakash, A., Jeffryes, M., Bateman, A. & Finn, R. D. The HMMER Web Server for Protein Sequence Similarity Search. *Curr. Protoc. Bioinformatics* **60**, 3.15.1–3.15.23 (2017).
23. Finn, R. D., Clements, J. & Eddy, S. R. HMMER web server: interactive sequence similarity searching. *Nucleic Acids Res.* **39**, W29–37 (2011).
24. Horne, I., Haritos, V. S. & Oakeshott, J. G. Comparative and functional genomics of lipases in holometabolous insects. *Insect Biochem. Mol. Biol.* **39**, 547–567 (2009).
25. Lassy, R. A. & Miller, C. G. Peptidase E, a peptidase specific for N-terminal aspartic dipeptides, is a serine hydrolase. *J. Bacteriol.* **182**, 2536–2543 (2000).
26. Rawlings, N. D. & Barrett, A. J. Introduction: aspartic peptidases and their clans. *Handbook of Proteolytic Enzymes* 3–12 Preprint at https://doi.org/10.1016/b978-0-12-079611-3.50009-4 (2004).

27. Casas-Vila, N. *et al.* The developmental proteome of. *Genome Res.* **27**, 1273–1285 (2017).
28. Graveley, B. R. *et al.* The developmental transcriptome of *Drosophila* melanogaster. *Nature* **471**, 473–479 (2011).
29. Matthews, B. B. *et al.* Gene Model Annotations for *Drosophila melanogaster: Impact of High-Throughput Data. G3* **5**, 1721–1736 (2015).
30. Nie, M., Xie, Y., Loo, J. A. & Courey, A. J. Genetic and proteomic evidence for roles of *Drosophila* SUMO in cell cycle control, Ras signaling, and early pattern formation. *PLoS One* **4**, e5905 (2009).
31. Rayburn, L. Y. M., Rhea, J., Jocoy, S. R. & Bender, M. The proprotein convertase amontillado (amon) is required during *Drosophila* pupal development. *Dev. Biol.* **333**, 48–56 (2009).
32. Rhea, J. M., Wegener, C. & Bender, M. The proprotein convertase encoded by amontillado (amon) is required in *Drosophila* corpora cardiaca endocrine cells producing the glucose regulatory hormone AKH. *PLoS Genet.* **6**, e1000967 (2010).
33. Siekhaus, D. E. & Fuller, R. S. A Role for amontillado, the *Drosophila* Homolog of the Neuropeptide Precursor Processing Protease PC2, in Triggering Hatching Behavior. *The Journal of Neuroscience* vol. 19 6942–6954 Preprint at https://doi.org/10.1523/jneurosci.19-16-06942.1999 (1999).
34. InterPro. http://www.ebi.ac.uk/interpro/entry/InterPro/IPR037730/.
35. InterPro. http://www.ebi.ac.uk/interpro/entry/InterPro/IPR037730/.
36. Guan, J. *et al.* Analysis of the functions of the signal peptidase complex in the midgut of Tribolium castaneum. *Arch. Insect Biochem. Physiol.* **97**, (2018).
37. D'Arrigo, P. *et al.* The splicing FK506-binding protein-51 isoform plays a role in glioblastoma resistance through programmed cell death ligand-1 expression regulation. *Cell Death Discov* **5**, 137 (2019).
38. Matsushima, Y., Goto, Y.-I. & Kaguni, L. S. Mitochondrial Lon protease regulates mitochondrial DNA copy number and transcription by selective degradation of mitochondrial transcription factor A (TFAM). *Proc. Natl. Acad. Sci. U. S. A.* **107**, 18410–18415 (2010).
39. Pomatto, L. C. D. *et al.* The Mitochondrial Lon Protease Is Required for Age-Specific and Sex-Specific Adaptation to Oxidative Stress. *Curr. Biol.* **27**, 1–15 (2017).
40. Matsushima, Y. *et al. Drosophila* protease ClpXP specifically degrades DmLRPPRC1 controlling mitochondrial mRNA and translation. *Sci. Rep.* **7**, 8315 (2017).
41. Ip, Y. T., Park, R. E., Kosman, D., Bier, E. & Levine, M. The dorsal gradient morphogen regulates stripes of rhomboid expression in the presumptive neuroectoderm of the *Drosophila* embryo. *Genes Dev.* **6**, 1728–1739 (1992).
42. Guichard, A. *et al.* rhomboid and Star interact synergistically to promote EGFR/MAPK signaling during *Drosophila* wing vein development. *Development* vol. 126 2663–2676 Preprint at https://doi.org/10.1242/dev.126.12.2663 (1999).
43. Lanoue, B. R. & Roger Jacobs, J. rhomboid function in the midline of the

Drosophila CNS. *Developmental Genetics* vol. 25 321–330 Preprint at https://doi.org/10.1002/(sici)1520-6408(1999)25:4<321::aid-dvg6>3.0.co;2-y (1999).
44. Schulz, C., Wood, C. G., Leanne Jones, D., Tazuke, S. I. & Fuller, M. T. Signaling from germ cells mediated by the rhomboid homolog stet organizes encapsulation by somatic support cells. *Development* vol. 129 4523–4534 Preprint at https://doi.org/10.1242/dev.129.19.4523 (2002).
45. Guichard, A., Roark, M., Ronshaugen, M. & Bier, E. brother of rhomboid, a rhomboid-related gene expressed during early *Drosophila* oogenesis, promotes EGF-R/MAPK signaling. *Dev. Biol.* **226**, 255–266 (2000).
46. Rhea- Annotated reactions database. https://www.rhea-db.org/rhea/13009.
47. Buchner, E. Genes expressed in the adult brain of *Drosophila* and effects of their mutations on behavior: a survey of transmitter- and second messenger-related genes. *J. Neurogenet.* **7**, 153–192 (1991).
48. Greenspan, R. J., Finn, J. A., Jr & Hall, J. C. Acetylcholinesterase mutants in *Drosophila* and their effects on the structure and function of the central nervous system. *J. Comp. Neurol.* **189**, 741–774 (1980).
49. Mutero, A., Pralavorio, M., Simeon, V. & Fournier, D. Catalytic properties of cholinesterases: importance of tyrosine 109 in *Drosophila* protein. *Neuroreport* **3**, 39–42 (1992).
50. Tougu, V. Acetylcholinesterase: Mechanism of Catalysis and Inhibition. *Current Medicinal Chemistry-Central Nervous System Agents* vol. 1 155–170 Preprint at https://doi.org/10.2174/1568015013358536 (2001).
51. Garrido, D. *et al.* Fatty acid synthase cooperates with glyoxalase 1 to protect against sugar toxicity. *PLoS Genet.* **11**, e1004995 (2015).
52. Lim, H. S., Kim, J. S., Park, Y. B., Gwon, G. H. & Cho, Y. Crystal structure of the Mre11-Rad50-ATPγS complex: understanding the interplay between Mre11 and Rad50. *Genes Dev.* **25**, 1091–1104 (2011).
53. Parvy, J.-P. *et al. Drosophila* melanogaster Acetyl-CoA-carboxylase sustains a fatty acid-dependent remote signal to waterproof the respiratory system. *PLoS Genet.* **8**, e1002925 (2012).

Chapter 2

Activity atlas of the Serine Hydrolase superfamily in the *Drosophila melanogaster*

Chapter 2
Activity atlas of the Serine Hydrolase superfamily in the *Drosophila melanogaster*

ABSTRACT

The SH superfamily has played a pivotal role as a classical prototype in the development of multiple platforms within the chemical proteomics field, specifically the activity-based protein profiling (ABPP) technique. These platforms have been essential for conducting comprehensive investigations into the functions of the various members of this superfamily across a diverse range of native yet complex biological contexts. While ABPP-based proteome-wide activity atlas for SH activities is accessible in numerous organisms, including humans, such an analysis has been notably absent in any insect model.

In Chapter 1, An extensive bioinformatics analysis was done to identify and categorise non-redundant SHs within *Drosophila melanogaster*. In this chapter, Activities of the SH superfamily throughout various identify and globally map developmental stages in various adult tissues of *Drosophila* using the ABPP chemoproteomic tool. The Activity of SHs is distinct in the different developmental stages. Also, There is the presence of sexual dimorphism in SH activities across distinct tissues in adult *Drosophila melanogaster*. Looking ahead to the prospective future, Chapter 2 will constitute the second foundational step in the discovery and functional annotation of SH proteins in the *Drosophila* innate immune response.

Graphical abstract

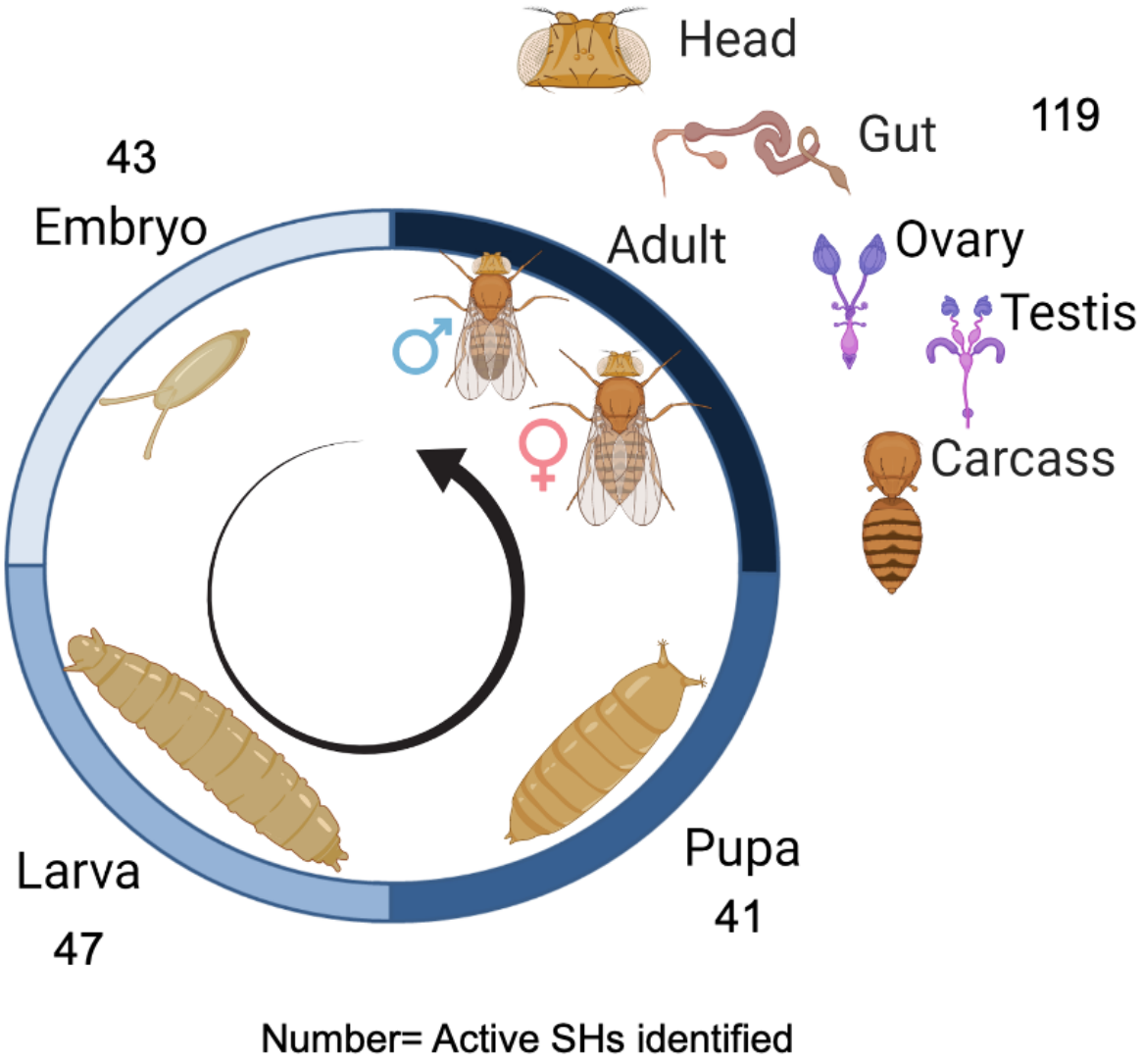

Keyword: Activity Based Protein Profiling (ABPP), Activity Atlas, Serine Hydrolase, Sexual Dimorphism, *Drosophila melanogaster*

Introduction

The examination of gene transcription and translation through genomic and proteomic methods provides only partial and indirect means of investigating enzyme functionality. Cravatt and his colleagues pioneered the enhancement of the traditional chemical proteomic method known as "activity-based protein profiling" (ABPP) by utilizing the conserved catalytic mechanism of serine hydrolases as a means to directly assess enzyme activity[1–5]. ABPP is a functional proteomics technique that utilizes a biorthogonal “activity” probe with a reactive chemical group (often referred to as a “reactive warhead”) (**Figure 2.1A**), which reacts with enzymes (or even proteins) that are mechanistically (or sometimes even functionally) related, typically from the same enzyme superfamily and allows for their detection, enrichment and quantitative identification via a reporter tag at a proteome-wide scale from complex biological samples like cells or tissues[1–5]. The fluorophosphonate (FP) moiety in particular, has served as an excellent reactive chemical group (reactive warhead) for the SHs, and has been an integral part of most ABPP probes used for profiling enzymes of this superfamily[1–5] (**Figure 2.1B**).

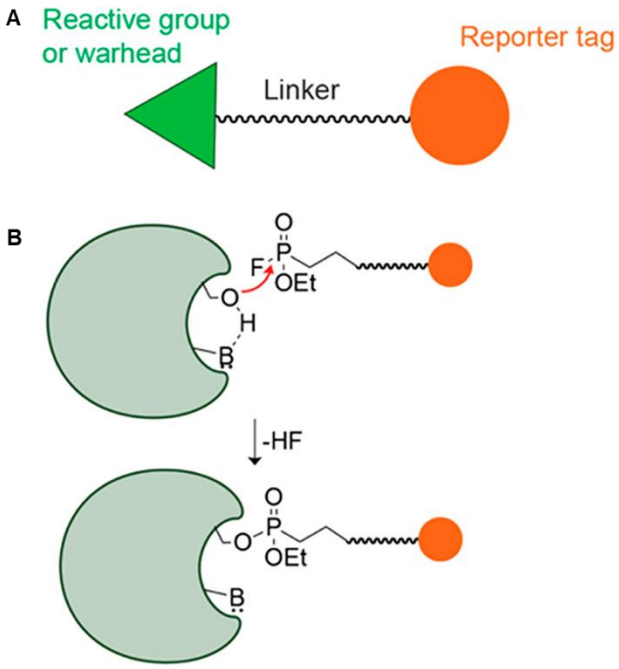

Figure 2.1. The mechanism of activity-Based Protein Profiling.
(A) Generic structure of an activity-based probe, having three components, i.e. the reactive group or warhead, a linker and a reporter tag. (B) Reaction of a SH enzyme with a fluorophosphonate (FP) activity probe, leading to the formation of an irreversible covalent adduct, thus showing the utility of FP-probes towards ABPP applications (Image adapted from kumar et al. 2021).

ABPP has two popular platforms for assessing superfamily-wide enzyme activities: (i) an in-gel fluorescence readout using SDS-PAGE analysis, also known as the "gel-based ABPP" platform, which is a medium throughout qualitative (or semi-quantitative) method, used for studying previously known enzymes and their activities in more physiological settings; and (ii) a liquid chromatography coupled to an advanced mass spectrometry (LC-MS/MS) readout, popularly known as "ABPP-MudPIT" (MudPIT = Multidimensional Protein Identification Technology), which is relatively low throughput, but an exhaustive discovery-based and/or quantitative method used towards identification and quantification of previously unknown enzyme activities from complex biological settings[1–6]. Traditionally, the activity probes used for gel-based ABPP experiments have various fluorophores (like fluorescein, rhodamines, BODIPYs, and their variants) as reporter tags, while biotin (leveraging avidin-based enrichment) has almost exclusively been used as a reporter tag for the activity probes used in the corresponding LC-MS/MS ABPP experiments.

Given their physiological importance, the enzymes from the SH family have been extensively investigated across all forms of life, and leveraging complementary ABPP platforms, superfamily-wide activity maps for this superfamily are available for numerous biological systems (e.g. cell lines, cancers cells)[11-13] and/or model organisms (e.g. rodents, worms)[7–14]. Surprisingly, to the best of our knowledge, such an organismal level superfamily-wide activity map for the SHs (or any enzyme family

for that matter) has not been described in the literature for *Drosophila melanogaster* (fruit fly), a popular model organism used extensively for mechanistic discovery using its powerful genetic toolkit[15–19]. Not surprisingly, our current understanding of SH functions in *Drosophila* is mostly based on genetic experiments that have uncovered critical roles of SHs, particularly the serine proteases[21], to be important in physiological processes related to immune responses,[20–22] embryonic development and patterning[23,24].

Chapter 2 presents chemoproteomics-aided superfamily-wide activity atlas for the SH family in the very well-studied fly model, *Drosophila melanogaster*. Superfamily-wide activity status of SHs activity was assayed across the various stages during its developmental life cycle (embryo, larva, pupa, and adult) and also in different tissues of adult flies. This study shows interesting new insights into the differential activities of SHs in various developmental life forms in flies and also suggests sexual dimorphism in their activities. Given the immense value of chemoproteomics and its lack of utilization in fly models, the superfamily-wide activity atlas will be an invaluable resource to the fly community and will provide new research directions towards connecting enzyme activities (particularly the SHs), to genetic phenotypes in different physiological processes and settings.

Material and Methods

Gel-based ABPP Sample Preparation and Analysis

All the gel-based ABPP experiments were done using established protocols previously reported by us[20, 21]. Briefly, each sample [fly developmental stages (embryo, larva, pupa or adult), or tissue (head, gut) that was fractionated] was suspended in 500 µL of cold, sterile 1x PBS (pH 7.4) and homogenized using a tissue homogenizer (Bullet Blender24, Next Advance) with one scoop of glass beads (0.5-

mm diameter; Next Advance) at a speed setting of 10 for 5 min at 4 °C. Thereafter, an additional 500 µL of cold sterile 1x PBS was added, mixed by pipetting, and centrifuged at 1000g for 5 min at 4 °C to separate the tissue debris. The resulting supernatant (700 µL) was collected and centrifuged at 21,000g for 90 min at 4 °C. Following this high speed centrifugation step, the resulting supernatant (soluble proteome) and pellet (membrane proteome) were collected in different tubes. The pellet (membrane proteome) was washed 3x with cold sterile 1x PBS and re-suspended in 500 µL of cold sterile 1x PBS by pipetting. For tissues not needing fractionation (carcass, hemolymph, and reproductive organs) in soluble/membrane proteomes, all steps remained the same, except that the high-speed centrifugation step was excluded, and the resulting lysate was used as whole tissue lysate. The protein concentration of each sample lysate was estimated using BCA protein assay kit (Pierce). For the gel-based ABPP assays, 50 µg of each lysate (50 µL of 1 mg/mL concentration) was treated with FP-rhodamine (2 µM, 60 min, 37 °C, with shaking). The reaction was quenched with 12.5 µL of 5X loading buffer and was followed by boiling the samples (95 °C, 10 min). The fluorescently labelled proteomes were resolved on 12% SDS–PAGE gel and visualized using a Syngene G-Box Chemi-XRQ gel documentation system.

LC-MS/MS-based ABPP Sample Preparation and Analysis

For the proteomic preparations for the LC-MS/MS-based ABPP assays, 1 mg of each lysate (1 mg/mL in 1x PBS (pH = 7.4)) was labelled with FP-biotin (200 µM, 60 min, 37 °C, with shaking). After labelling, the proteomes were denatured, reductively alkylated using iodoacetamide, and subsequently digested with trypsin as described earlier using a protocol previously reported by us[21]. The tryptic peptides were desalted and cleaned using the StageTip protocol[22]. All LC–MS/MS analysis was performed on

a Sciex TripleTOF6600 mass spectrometer interfaced with an Eksigent nano-LC 425. Tryptic peptides (~ 1 µg) were loaded onto an Eksigent C18 trap column (5 µg capacity) and subsequently eluted on an Eksigent C18 analytical column (15 cm × 75-µm internal diameter) with a linear acetonitrile gradient. A typical LC run consisted of 360 min post-loading onto the trap at a constant flow rate of 300 nL/min with solvent A consisting of water + 0.1% formic acid and solvent B consisting of acetonitrile. The gradient schedule for the LC run was 5% (v/v) B for 1 min, a linear gradient of B from 0% to 30% (v/v) over 330 min, 90% (v/v) B for 20 min and equilibration with 5% (v/v) B for 10 min. For all proteomics samples, data were acquired in information-dependent acquisition (IDA) mode over a mass range of 200–2,000 m/z. Each full MS survey scan was followed by MS/MS of the 15 most intense peptides. Dynamic exclusion was enabled for all experiments (repeat count 2; exclusion duration 6 s). Peptide identification were carried out using the Protein Pilot (version 2.0.1, Sciex) using Pro Group™ and Paragon™ algorithms against the RefSeq protein database of the *Drosophila melanogaster* (Release 6). While searching the peptides, iodoacetamide alkylation of cysteine was defined as a static modification, while the oxidation of methionine and N-terminal acetylation were defined as variable modifications. During the peptide searches, the precursor ion and MS/MS mass tolerance were set at 20 and 50 ppm respectively. The Protein Pilot software[23] defined “Peptide Count” parameter was used for quantifying the extent of activity of a SH enzyme, and only those SHs that were identified in at least two biological replicates were considered for further analysis with Peptide Counts ≥ 1. Precursor ions and MS/MS fragmentations were viewed using the PeakView software (Sciex).

Data Analysis

All heat map plots presented in this study (Figure 3 & 5) represent mean of three biological replicates, and were made using the Prism 9 (version 9.0.2) for macOS (GraphPad) software.

Results

Identification of SH activities during different developmental phases in *Drosophila melanogaster*

After finalizing the updated database of Serine Hydrolases (SHs) in *Drosophila melanogaster*, the next step was evaluating the activity levels of SHs across various stages of the *Drosophila* life cycle, namely the embryo, larva, pupa, and adult stages. In the case of the adult stage, male and female were profiled separately to investigate potential sexual dimorphism in the enzymatic activities of SHs. Henceforth, the distinct life stages of flies were fractionated into soluble and membrane proteomes using establish protocol and and performed a gel-based ABPP analysis to confirm activity-based labeling of SHs using the FP-rhodamine probe (2 µM, 50 µg proteome in 50 µl, 45 mins, 37 ^{o}C, with constant shaking). To inactivate SHs, the respective proteom were heat denatured proteom and used for control gel based ABPP experiment. Consistent with similar studies using FP probes from other systems, both the soluble and membrane proteomes from the different stages (embryo, larva, pupa and adult) displayed activity-dependent labeling of SHs, as evident in the active lysates, but not in the denatured lysates (**Figure 2.2.A**). Equal loading of respective lysates confirmed by Coomassie Blue staining of the gel (**Figure 2.S.1**). As expected, gel based ABPP unveiled distinct activity patterns between the soluble and membrane proteomes, implying that different SHs exhibit activity during different developmental stages in *Drosophila* (as depicted in Figure 3A).

After gel based activity atlas of SHs, the next aim was to identify and enrich various SHs enzyme during various developmental stages of *Drosophila*. To achieve this, LC-MS/MS ABPP experiments were performed on the soluble and membrane proteomes from the different stages (embryo, larva, pupa and adult) using the FP-biotin probe using established protocol (see material and mathods). From this LC-MS/MS ABPP experiment, a total of 89 SH enzymes were identified, of which 35 were serine proteases (**Figure 2.2.B, Annexure 5, Table 1**), while 54 belonged to the metabolic SH category (**Figure 2.2.C, Annexure 5, Table 1**). Consistent with previous reports from mammalian systems showing FP-probes being better suited at enriching metabolic SHs, we found from our LC-MS/MS ABPP experiments, that, of the total SH enzymes enriched and identified (25.1%, 89 out of 354) using the FP-biotin probe in *Drosophila melanogaster*, there were substantially more metabolic SH enzymes (37.5%, 54 out of 144) (**Figure 2.2.C**) than serine proteases (16.7%, 35 out of 210) (**Figure 2.2.B**). Concomitant with the gel-based ABPP experiments, the LC-MS/MS ABPP experiments also identified differential SH activity profiles and showed that certain SHs were exclusively present in only one developmental stage, pointing to a critical and possibly indispensable role for that enzyme in that phase of development in flies (**Figure 2.2.B, 2.2C**).

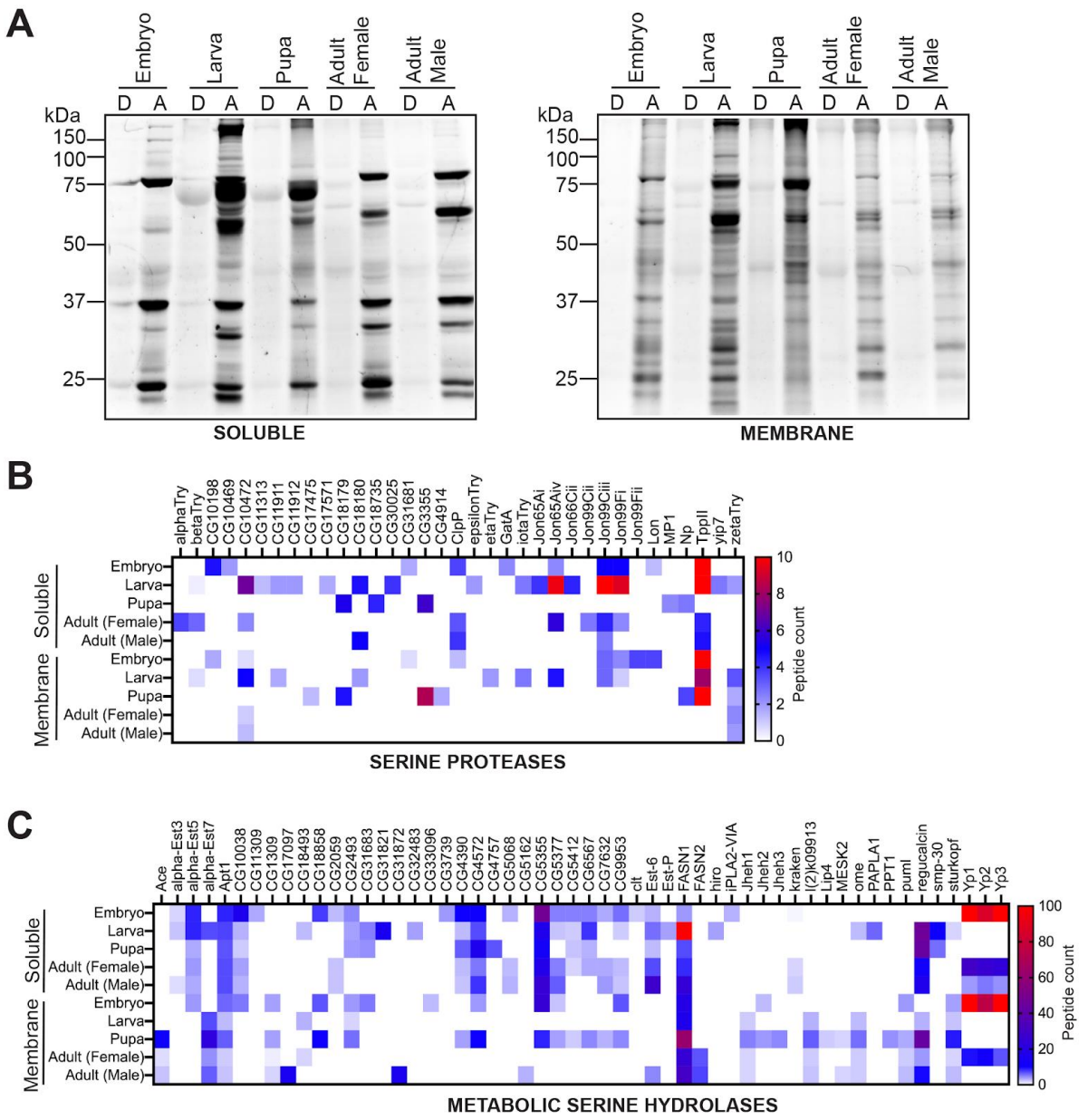

Figure 2.2. ABPP analysis on lysates from different stages of fly development. (**A**) Gel-based ABPP analysis on soluble and membrane proteomes from different developmental stages of *Drosophila* labeled with the SH-directed FP-rhodamine probe, and analyzed by SDS-PAGE analysis and in-gel fluorescence scanning. This gel-based ABPP experiment clearly shows that active (A), but not denatured (D) proteomes, have distinct SH activity profiles during different stages of *Drosophila* development. This gel-based ABPP experiment was done thrice with reproducible results each time. (**B, C**) Heat map plots for (**B**) *Serine Proteases*, and (**C**) *Metabolic Serine Hydrolases*, showing SH activity signals identified from a LC-MS/MS based ABPP experiment using the SH-directed FP-biotin probe during various stages of

Drosophila development. Data in the heat maps are represented as average peptide counts from three independent biological replicates, and peptide counts above 10 & 100 for the serine proteases and metabolic SHs respectively are coloured red.

Anatomical profiling of SH activities in adult *Drosophila melanogaster*

Having profiled and identified unique active SHs during the different developmental stages in *Drosophila melanogaster*, next, we wanted to increase the superfamily-wide coverage for them in flies. Toward this, we decided to isolate different tissues and/or anatomical components in an adult fly (male and female done separately) and perform tandem gel-based and LC-MS/MS based ABPP experiments to enrich and identify active SHs in their lysates. Here, we isolated the head, gut, reproductive organs (testis for males, and ovaries for females), hemolymph, and the remaining carcass from adult male and female flies separately for a chemoproteomics analysis. Since some tissues (reproductive organs, hemolymph, and the carcass) were difficult to get in sufficient amounts from adult flies, we decided to profile them as whole tissue lysates, while, more abundantly available tissues (head and gut) were fractionated into soluble and membrane proteomes. First, leveraging established gel-based ABPP protocols[25,26], using the FP-rhodamine probe (2 µM, 50 µg proteome in 50 µl, 45 mins, 37 ^{o}C, with constant shaking), we found that all the tissues showed activity-dependent labeling of SHs in the tissue lysates, but not in the corresponding denatured lysate controls (**Figure 2.3.A**). We confirmed the equal loading of respective corresponding active and denatured lysates by Coomassie Blue staining of the gel after in-gel fluorescence imaging for SH activity (**Figure 2.3.B**). Analogous to results from the various developmental stages, not surprisingly again, we found distinct activity profiles for SHs in the different tissues and/or anatomical components, suggesting that specific SHs

have distinct spatiotemporal expression and are functionally active in different tissues of flies (**Figure 4**).

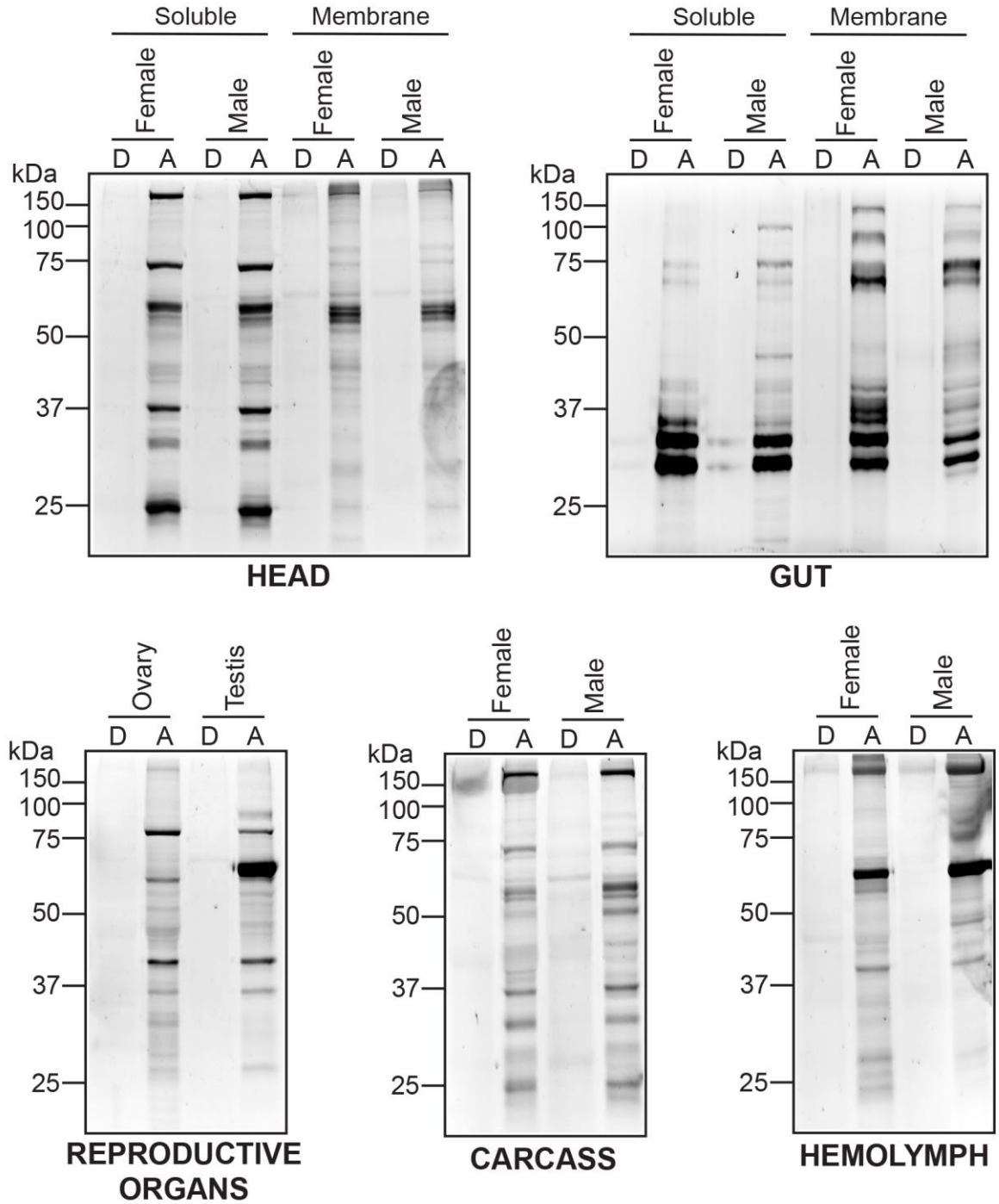

Figure 2.3. Gel-based ABPP analysis on fly tissue lysates.

(A) A panel of *Drosophila melanogaster* tissue and/or anatomical component proteomes labelled with the SH-directed FP-rhodamine probe and analyzed by SDS-PAGE and in-gel fluorescence scanning. This gel-based ABPP experiment clearly shows that active (A), but not denatured (D) lysates, have distinct SH activity profiles

in different *Drosophila* tissues and/or anatomical components. This gel-based ABPP experiment was done thrice with reproducible results each time. **(B)**. Coomassie staining of gel shown in ***Figure 4***, showing equal loading of active (A) and denatured (D) lysates from different tissues and/or anatomical components in adult male and female flies.

Having confirmed efficient activity-dependent labeling of SHs by a FP-probe in adult fly tissue lysates by gel-based ABPP experiments, next, we wanted to enrich and identify the SHs that were active in the aforementioned tissues using LC-MS/MS based ABPP experiments. Here, using an established protocol described earlier[26], with the FP-biotin probe (200 µM, 1 mg proteome in 1 mL, 60 mins, 37 ^{o}C, with constant shaking), we enriched SHs, and identified them by established LC-MS/MS analysis. From this LC-MS/MS based ABPP experiment in the different adult fly tissues, we identified 118 unique SHs, of which 50 and 68 belonged to serine proteases and metabolic SHs categories respectively (**Figure 2.4, Annexure 5, Table 2**). Consistent with the gel-based ABPP experiments (**Figure 2.4**), we found several SHs were uniquely enriched in certain tissues in adult flies, and possibly suggests an important role for these SHs activities in regulating this tissue's physiology. Not surprisingly, we found amongst all the tissues and/or anatomical components, that a large fraction of active SHs (both serine proteases and metabolic SHs) were present in the adult fly gut (both male and female), consistent with the role of this organ in digestion of food, and its metabolism.

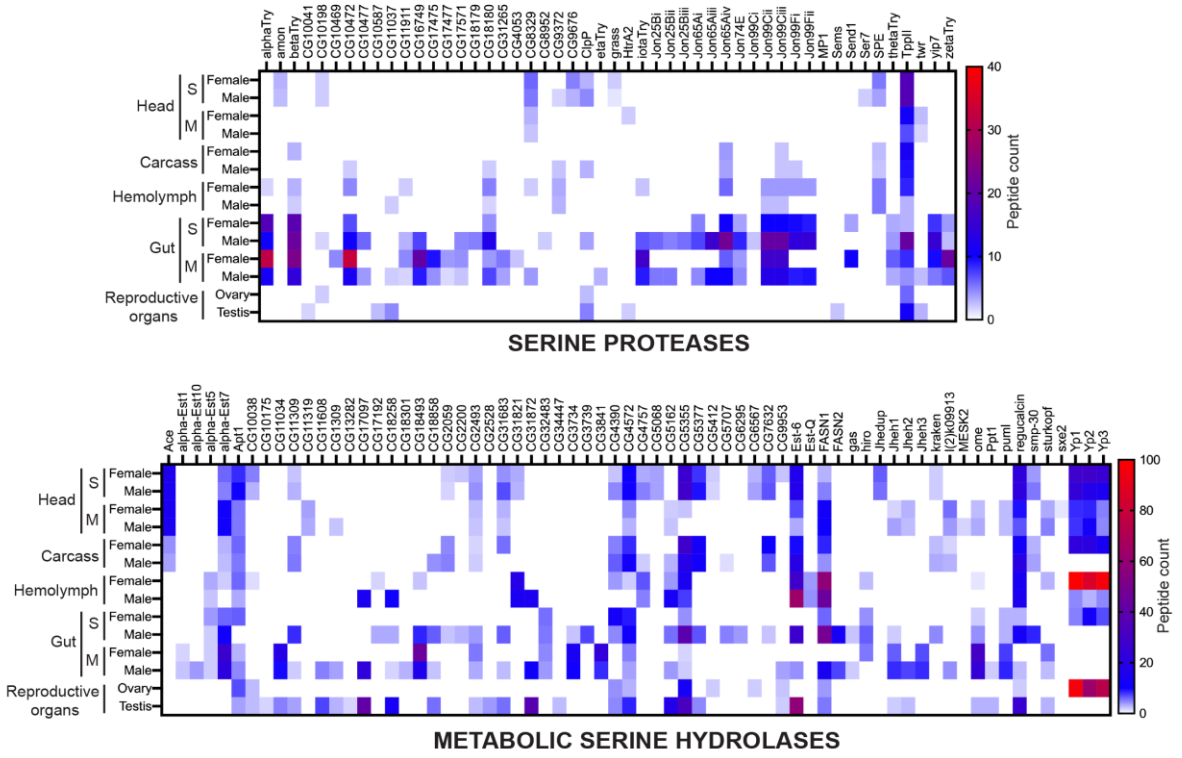

Figure 2.4. Determining the full complement of active SHs in adult flies.
Heat map plots for the '*Serine Proteases*', and '*Metabolic Serine Hydrolases*', showing SH activity signals identified from a LC-MS/MS based ABPP experiment using the SH-directed FP-biotin probe from various tissues and/or anatomical components from adult male and female flies. Data in the heat maps are represented as average peptide counts from three independent biological replicates, and peptide counts above 40 & 100 for the serine proteases and metabolic SHs respectively are colored red.

Of note, this LC-MS/MS based ABPP experiment led to a significant increase in the overall number of non-redundant active SHs identified in adult flies. Specifically, we identified an additional 40 and 34 serine proteases and metabolic SHs respectively (**Figure 2.4**), from this tissue-based anatomical profiling in adult flies, relative to previous whole adult fly profiling (**Figure 2.3**), which had identified only 10 and 35 serine proteases and metabolic SHs respectively. Next, upon collating all the tissue profiling data together with the SHs identified from LC-MS/MS based ABPP

experiments on the different developmental life forms, in total, we have now identified 136 non-redundant active SHs in flies, thus reaching a coverage of 38.4% (136 out of 354) for the SH superfamily with a single FP-biotin probe (**Figure 2.5**). Upon further categorization, we find amongst the total non-redundant active SHs identified, that 61 are serine proteases (29%, 61 out of 210 total serine proteases), while 75 are metabolic SHs (52%, 75 out of 144 total metabolic SHs) (**Figure 2.5, Annexure5, Table 2.1**). Interestingly, our chemoproteomics profiling data further shows that only a small portion of SHs (11 out of 61 serine proteases, and 6 out of 75 metabolic SHs) are actually exclusively unique and active in early developmental stages (embryo or larva or pupa) in flies, relative to those found exclusively unique and active in adults (30 out of 61 serine proteases, and 26 out of 75 metabolic SHs) (**Figure 2.5, Annexure5, Table 2.1**). Not surprisingly, several of the identified non-redundant active SHs were present in at least 1 early developmental stage (embryo or larva or pupa) and also in adult flies (20 out of 61 serine proteases, and 43 out of 75 metabolic SHs) (**Figure 2.5, Annexure5, Table 2.1**).

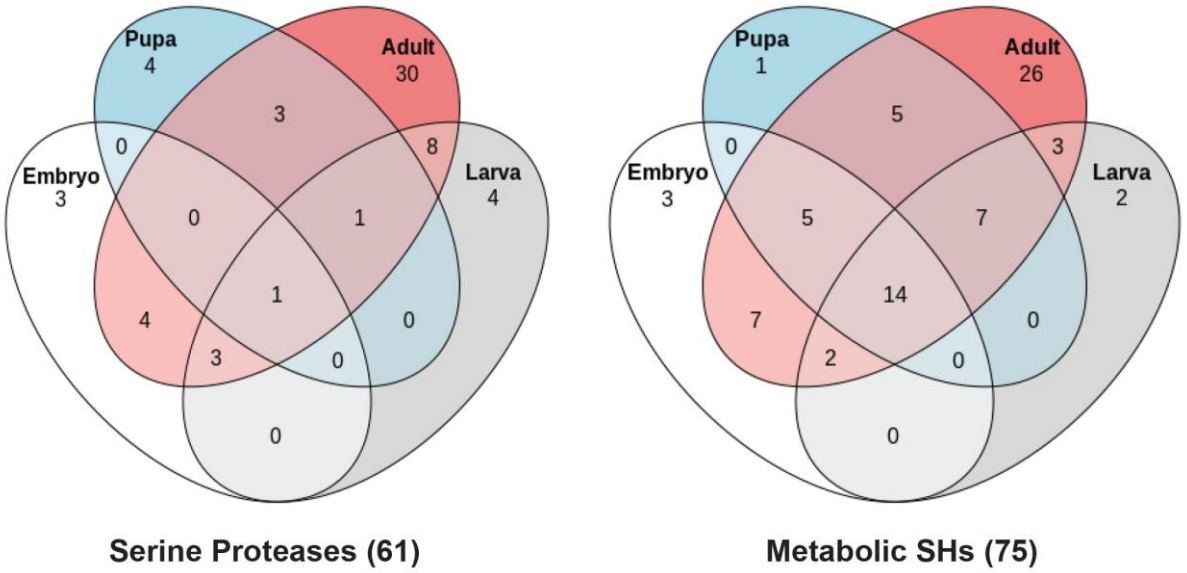

Serine Proteases (61) **Metabolic SHs (75)**

Figure 2.5. Mapping SH activities during fly development.
A Venn diagram analysis showing the complete distribution of the full complement of active SHs identified by us using a LC-MS/MS based ABPP approach, during various life stages of *Drosophila* development.

Sexual dimorphism of SH activities in adult *Drosophila melanogaster*

Having mapped the non-redundant active SHs, as a proof of concept of the utility of such a superfamily-wide activity atlas, next, we wanted to assess whether there exists any sexual dimorphism in SH activities in the different tissues and/or anatomical components between adult males and female flies. To collate a list of such SHs, we looked at tissues and/or anatomical components (head, gut, carcass and hemolymph) other than the reproductive organs, and filtered those SHs that were present only in either adult males or females and had average peptide counts ≥ 2 from 3 biological replicates. Additionally, we also looked for SHs in these same tissues that had average peptide counts ≥ 2 from 3 biological replicates and were enriched ≥ 5-fold in one gender over the other. Based on this criteria for selection, we found that 16 serine proteases, and 19 metabolic SHs, in adult flies displayed sexual dimorphism in their activities (**Table 2.1**). Not surprisingly, a large fraction of the differentially active SHs identified, were found in the gut, given this organ's role in metabolism and digestion (**Table 2.1**). Interestingly, a significant majority of the identified serine proteases (11 out of 16), and metabolic SHs (16 out of 19) were present in adult male flies (**Table 2.1**). Amongst the metabolic SHs, the enrichment of Yp1, Yp2 and Yp3 in females was expected, as these SHs are needed for necessary for egg formation. However, the enrichment of all other metabolic SHs displaying sexual dimorphism in activities in males was surprising, and raises intriguing new possibilities of hormonal regulation of enzymatic activities in flies, as most of these metabolic SHs lack proper functional annotation experimentally, despite having predicted molecular functions (**Table 2.1**).

Table 2.1. List of SHs showing sexual dimorphism in activities in adult fly.

Gene ID	Predicted Molecular Function	Gender	Tissue(s)
Serine Proteases			
CG10469	Serine-type endopeptidase	Female	Gut
Send1	Serine-type endopeptidase	Female	Gut
CG4053	Serine-type endopeptidase	Female	Gut
Jon65Aiii	Serine-type endopeptidase	Female	Gut
HtrA2	Serine-type endopeptidase	Female	Head
CG17477	Serine-type endopeptidase	Male	Gut
CG8952	Serine-type endopeptidase	Male	Gut
Jon99Ci	Serine-type endopeptidase	Male	Gut
etaTry	Serine-type endopeptidase	Male	Gut
CG18179	Serine-type endopeptidase	Male	Gut
Jon25Biii	Serine-type endopeptidase	Male	Gut
CG10477	Serine-type endopeptidase	Male	Gut
Jon25Bii	Serine-type endopeptidase	Male	Gut
Jon25Bi	Serine-type endopeptidase	Male	Gut
Ser7	Serine-type endopeptidase	Male	Head
CG11037	Serine-type endopeptidase	Male	Hemolymph
Metabolic SHs			
Yp1	Carboxylic ester hydrolase	Female	Hemolymph
Yp2	Carboxylic ester hydrolase	Female	Hemolymph
Yp3	Carboxylic ester hydrolase	Female	Hemolymph
CG31872	Sterol esterase	Male	Hemolymph, Gut
CG17097	Sterol esterase	Male	Hemolymph, Gut
CG18258	Carboxylic ester hydrolase	Male	Hemolymph, Gut
Est-Q	Unknown hydrolase	Male	Hemolymph
FASN2	Fatty acid synthesis	Male	Gut
CG3739	Serine-type peptidase	Male	Gut
CG5707	Unknown hydrolase	Male	Gut
Alpha-Est10	Carboxylic ester hydrolase	Male	Gut
Gas	Unknown hydrolase	Male	Gut
CG11608	Triglyceride lipase	Male	Gut
CG18301	Triglyceride lipase	Male	Gut
CG6295	Phospholipase	Male	Gut
Ppt1	Palmitoyl-(protein) hydrolase	Male	Gut
CG18858	O-acyltransferase	Male	Gut, Carcass
MESK2	Unknown hydrolase	Male	Head
CG1309	Phospholipase	Male	Head

Discussion and conclusions

From its early beginnings as a model organism for genetics in the Columbia “fly room” in 1910, *Drosophila* continues to be a powerful experimental tool in the fields of genetics, cell biology, developmental biology, neurobiology, and evolutionary biology[15–18]; [16,19]. Many fundamental discoveries have been based on work done in *Drosophila*, and this has led to six Nobel prizes, in diverse fields of biology. Its continued popularity is a consequence of the sustained upgradation of its genetic toolkit, with quantum improvements seen every decade. Increasingly, the fly model is seen as a translational tool for improving human health, with a focus on understanding human genetic diseases[15–19]. Chemoproteomics has proved to be an invaluable and powerful tool in assigning functions to proteins,[27,28] particularly enzymes, in the postgenomic era, yet to the best of our knowledge, there are no reports describing its utility in *D. melanogaster*, despite the fly being such a popular biological model. The functional proteomics strategy, also popularly called ABPP, developed initially by Cravatt and co-workers, has been extensively used to study the SH superfamily[1–3,5,9]. SHs are known to function as metabolic lynchpins and regulate several physiologically important processes, and their deregulation is often associated with detrimental effects in all forms of life[29]. However, despite their biological importance, the SH superfamily remains poorly explored in flies (Figure 7).

Next, leveraging gel-based and LC-MS/MS based chemoproteomics approaches, we profiled and identified active SHs in various stages of fly development (**Figure 2.2, Annexure 5, Table 2.1**) and in different tissues and/or anatomical components in male and female adult flies (**Figure 2.2-4, Annexure 5, Table 2.1**) in an attempt to develop the first superfamily wide activity atlas for the SHs in *Drosophila melanogaster*. Using this ABPP approach, we found a total of 136 non-redundant active SHs with a

superfamily wide coverage of 38.4%, of which 61 were serine proteases (29% coverage for this category), while 75 belonged to the metabolic SH category (52% coverage for this category) (**Figure 2.6**). Upon further inspection of the data, we found that of the total identified SHs, several of them were present exclusively in the adult life form, and perhaps suggest an important (and perhaps conserved) role for these enzymes in metabolism of adults (**Figure 2.5, Annexure 5, Table 2.1.**) During the course of our ABPP studies of the adult life form, we purposefully decided to profile males and females separately. Interestingly, we found in adult flies that several SHs display sexual dimorphism in their enzyme activities, and most of them have unknown physiological and/or molecular functions (**Table 1**). Overall, our studies reported here, to the best of knowledge, describe the first chemoproteomics enabled superfamily wide activity atlas for any enzyme family in *Drosophila melanogaster*.

Moving ahead, we anticipate that this study will lead to chemoproteomics being more extensively used in fly models, and more ABPP enabled superfamily-wide activity atlas' for different well studied enzyme families in *Drosophila melanogaster* will emerge, towards understanding endogenous function of unannotated enzymes, and uncovering of new biological pathways. Here, we show that a large fraction of the SH superfamily, particularly metabolic SHs, lack defined and/or experimentally validated physiological functions, but are amenable to labelling/enrichment using FP-probes. Therefore, following up on this study, assigning the endogenous function to such SHs, and mapping the biological pathways they regulate in flies, should now be more tractable using the rich array of established pharmacological tools and chemical genetic screening methods used for members of this superfamily in other organisms[11,30]. Next, we also report several candidate SHs that show sexual dimorphism in their activity in adult flies, and characterizing the basis of this differential

activity, will certainly provide new biological insights and advanced our understanding of gender-based regulation of enzymatic activities. Further, we acknowledge that a large portion of the SHs (> 60%) are still not covered using the FP-probes and the ABPP approaches we describe here. We attribute this to two major factors: (i) We profiled adult male and female flies between 5 – 10 days of age, under normal conditions and environment, and we posit that several SHs display age and/or context (e.g. exposure to infection, inflammatory stimuli, stress etc.) dependent expression and in turn activity; and (ii) Previous reports from mammalian systems have shown that several SHs (particularly serine proteases) don't react with FP-probes[11,30], and therefore tailored activity probes (e.g., HT01, WHP01, and MB064)[31–34] for such SHs may need to be developed to increase the chemoproteomic coverage of members of this family. Lastly, as more ABPP profiling studies in flies with FP-probes emerge, it will be interesting to also determine whether non-SH enzymes (e.g. threonine hydrolases) are also active and FP reactive, and if such enzyme classes indeed exist in flies[31–35].

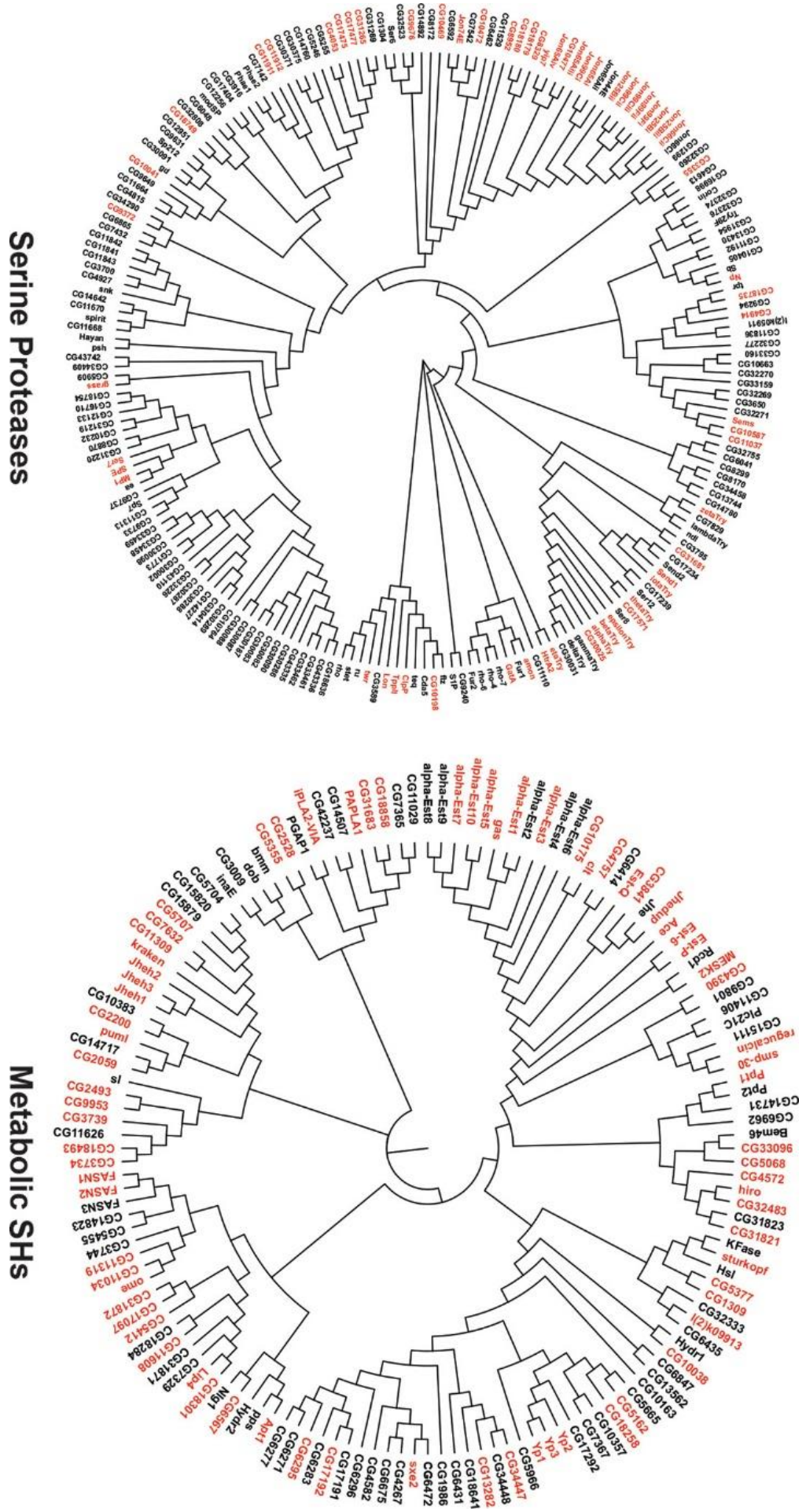
Serine Proteases
Metabolic SHs

Figure 2.6. A chemoproteomic atlas of SH activity in *Drosophila melanogaster*. A dendrogram analysis of all the predicted serine proteases and metabolic SHs in *Drosophila melanogaster*, in which, the red and black coloring represents enzymes that were enriched and not enriched respectively in the LC-MS/MS based ABPP experiments using the SH-directed FP-biotin probe. All protein sequences of the respective category (serine proteases and metabolic SHs) were aligned using the MUSCLE program of the MEGA-X software by the neighbor joining method, where the branch length denotes relatedness between protein sequences.

The rapid progress in genome sequencing technologies have made a large number of protein sequences available for numerous organisms, and assigning function to these proteins represents a major challenge for researchers in the post-genomic era[36]. Over the past decade, the chemoproteomics technique ABPP has emerged as a powerful and popular tool in bridging this knowledge gap, and has greatly facilitated the functional annotation of enzymes from diverse enzyme families[2,3]. The SHs catalyze a large number of physiologically important hydrolysis reactions, and this superfamily remains the most investigated enzyme class using ABPP[1–3,9]. While ABPP aided superfamily-wide activity atlas' are available for SHs in various organisms, both ABPP and the SH superfamily remain largely unexplored in the fly model, *Drosophila melanogaster*. Here, using gel-based and LC-MS/MS based ABPP platforms, we build an activity atlas map of SHs in flies, and report the activity profiles of enzymes from this superfamily during various stages of development and in different adult tissues. Our studies also suggest sexual dimorphism in SH activities, and the resource we provide here, will greatly facilitate the use of ABPP, and aid functional annotation of hitherto unknown SHs in various fly models.

Contribution

Dr Amol Mhetre for synthesis of FP-biotin probe which used in the study of this chapter.

Acknowledgments

We thank Saddam Shaikh for technical assistance in MS samples run.

Reference

1. Liu, Y., Patricelli, M. P. & Cravatt, B. F. Activity-based protein profiling: the serine hydrolases. *Proc. Natl. Acad. Sci. U. S. A.* **96**, 14694–14699 (1999).
2. Cravatt, B. F., Wright, A. T. & Kozarich, J. W. Activity-based protein profiling: from enzyme chemistry to proteomic chemistry. *Annu. Rev. Biochem.* **77**, 383–414 (2008).
3. Niphakis, M. J. & Cravatt, B. F. Enzyme inhibitor discovery by activity-based protein profiling. *Annu. Rev. Biochem.* **83**, 341–377 (2014).
4. Jessani, N. *et al.* Class assignment of sequence-unrelated members of enzyme superfamilies by activity-based protein profiling. *Angew. Chem. Int. Ed Engl.* **44**, 2400–2403 (2005).
5. Jessani, N. & Cravatt, B. F. The development and application of methods for activity-based protein profiling. *Curr. Opin. Chem. Biol.* **8**, 54–59 (2004).
6. Jessani, N. *et al.* A streamlined platform for high-content functional proteomics of primary human specimens. *Nat. Methods* **2**, 691–697 (2005).
7. Nomura, D. K., Dix, M. M. & Cravatt, B. F. Activity-based protein profiling for biochemical pathway discovery in cancer. *Nat. Rev. Cancer* **10**, 630–638 (2010).
8. Jessani, N. *et al.* Carcinoma and stromal enzyme activity profiles associated with breast tumor growth in vivo. *Proc. Natl. Acad. Sci. U. S. A.* **101**, 13756–13761 (2004).
9. Jessani, N., Liu, Y., Humphrey, M. & Cravatt, B. F. Enzyme activity profiles of the secreted and membrane proteome that depict cancer cell invasiveness. *Proc. Natl. Acad. Sci. U. S. A.* **99**, 10335–10340 (2002).
10. Keller, L. J. *et al.* Characterization of Serine Hydrolases Across Clinical Isolates of Commensal Skin Bacteria Using Activity-Based Protein Profiling. *ACS Infect Dis* **6**, 930–938 (2020).
11. Bachovchin, D. A. *et al.* Superfamily-wide portrait of serine hydrolase inhibition achieved by library-versus-library screening. *Proc. Natl. Acad. Sci. U. S. A.* **107**, 20941–20946 (2010).
12. Chen, A. L. *et al.* Pharmacological convergence reveals a lipid pathway that regulates C. elegans lifespan. *Nat. Chem. Biol.* **15**, 453–462 (2019).
13. Yoo, E. *et al.* The Antimalarial Natural Product Salinipostin A Identifies Essential α/β Serine Hydrolases Involved in Lipid Metabolism in P. falciparum Parasites. *Cell Chem Biol* **27**, 143–157.e5 (2020).
14. Lentz, C. S. *et al.* Identification of a S. aureus virulence factor by activity-based protein profiling (ABPP). *Nat. Chem. Biol.* **14**, 609–617 (2018).
15. Hales, K. G., Korey, C. A., Larracuente, A. M. & Roberts, D. M. Genetics on the Fly: A Primer on the Drosophila Model System. *Genetics* **201**, 815–842 (2015).
16. Rajan, A. & Perrimon, N. Of flies and men: insights on organismal metabolism

from fruit flies. *BMC Biol.* **11**, 38 (2013).
17. Jennings, B. H. Drosophila – a versatile model in biology & medicine. *Mater. Today* **14**, 190–195 (2011).
18. Bier, E. Drosophila, the golden bug, emerges as a tool for human genetics. *Nat. Rev. Genet.* **6**, 9–23 (2005).
19. Bilder, D. & Irvine, K. D. Taking Stock of the Research Ecosystem. *Genetics* **206**, 1227–1236 (2017).
20. Cho, Y. S., Stevens, L. M., Sieverman, K. J., Nguyen, J. & Stein, D. A ventrally localized protease in the Drosophila egg controls embryo dorsoventral polarity. *Curr. Biol.* **22**, 1013–1018 (2012).
21. Misra, S., Hecht, P., Maeda, R. & Anderson, K. V. Positive and negative regulation of Easter, a member of the serine protease family that controls dorsal-ventral patterning in the Drosophila embryo. *Development* vol. 125 1261–1267 Preprint at https://doi.org/10.1242/dev.125.7.1261 (1998).
22. Morisato, D. & Anderson, K. V. Signaling pathways that establish the dorsal-ventral pattern of the Drosophila embryo. *Annu. Rev. Genet.* **29**, 371–399 (1995).
23. Cao, X. & Jiang, H. Building a platform for predicting functions of serine protease-related proteins in Drosophila melanogaster and other insects. *Insect Biochem. Mol. Biol.* **103**, 53–69 (2018).
24. Levashina, E. A. *et al.* Constitutive activation of toll-mediated antifungal defense in serpin-deficient Drosophila. *Science* **285**, 1917–1919 (1999).
25. Rajendran, A., Vaidya, K., Mendoza, J., Bridwell-Rabb, J. & Kamat, S. S. Functional Annotation of ABHD14B, an Orphan Serine Hydrolase Enzyme. *Biochemistry* **59**, 183–196 (2020).
26. Kelkar, D. S. *et al.* A chemical-genetic screen identifies ABHD12 as an oxidized-phosphatidylserine lipase. *Nat. Chem. Biol.* **15**, 169–178 (2019).
27. Saghatelian, A. & Cravatt, B. F. Assignment of protein function in the postgenomic era. *Nat. Chem. Biol.* **1**, 130–142 (2005).
28. Saghatelian, A. & Cravatt, B. F. Global strategies to integrate the proteome and metabolome. *Curr. Opin. Chem. Biol.* **9**, 62–68 (2005).
29. Long, J. Z. & Cravatt, B. F. The metabolic serine hydrolases and their functions in mammalian physiology and disease. *Chem. Rev.* **111**, 6022–6063 (2011).
30. Bachovchin, D. A. & Cravatt, B. F. The pharmacological landscape and therapeutic potential of serine hydrolases. *Nat. Rev. Drug Discov.* **11**, 52–68 (2012).
31. Kamat, S. S. *et al.* Immunomodulatory lysophosphatidylserines are regulated by ABHD16A and ABHD12 interplay. *Nat. Chem. Biol.* **11**, 164–171 (2015).
32. Hsu, K.-L. *et al.* DAGLβ inhibition perturbs a lipid network involved in macrophage inflammatory responses. *Nat. Chem. Biol.* **8**, 999–1007 (2012).
33. Baggelaar, M. P. *et al.* ABHD2 Inhibitor Identified by Activity-Based Protein Profiling Reduces Acrosome Reaction. *ACS Chem. Biol.* **14**, 2295–2304 (2019).
34. Janssen, A. P. A. *et al.* Development of a Multiplexed Activity-Based Protein Profiling Assay to Evaluate Activity of Endocannabinoid Hydrolase Inhibitors. *ACS Chem. Biol.* **13**, 2406–2413 (2018).
35. Parsons, W. H. *et al.* AIG1 and ADTRP are atypical integral membrane hydrolases that degrade bioactive FAHFAs. *Nat. Chem. Biol.* **12**, 367–372 (2016).
36. Gerlt, J. A. *et al.* The Enzyme Function Initiative. *Biochemistry* **50**, 9950–9962 (2011).

Supplementry Figures

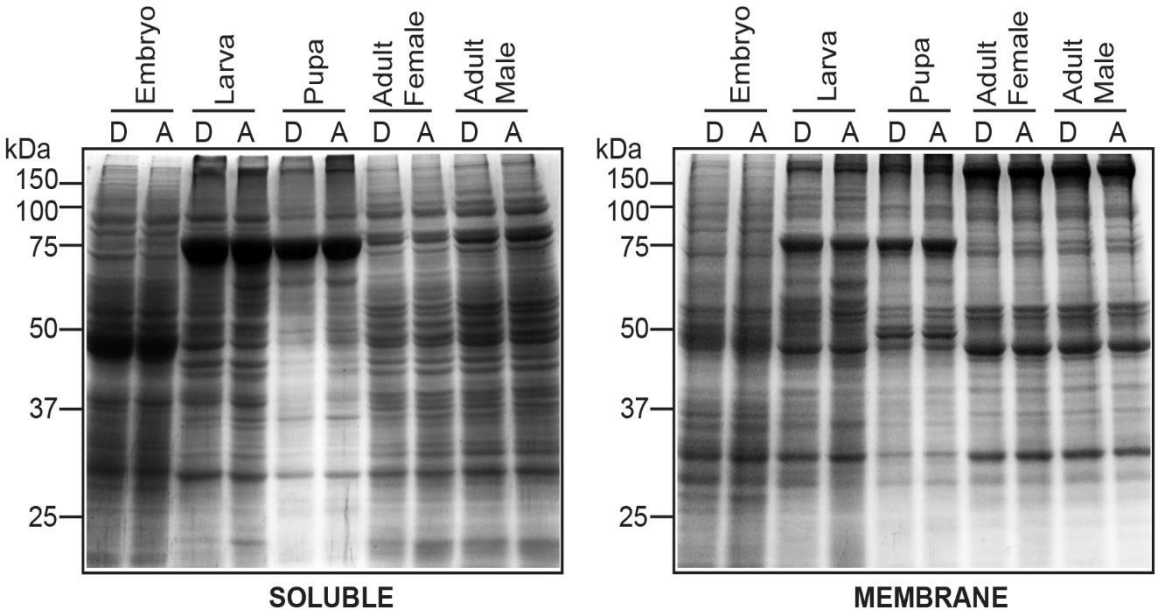

Figure 2.S.1. Coomassie staining of gel shown in Figure 3A, showing equal loading of active (A) and denatured (D) soluble (left gel) and membrane (right gel) lysates for respective developmental stages in flies.

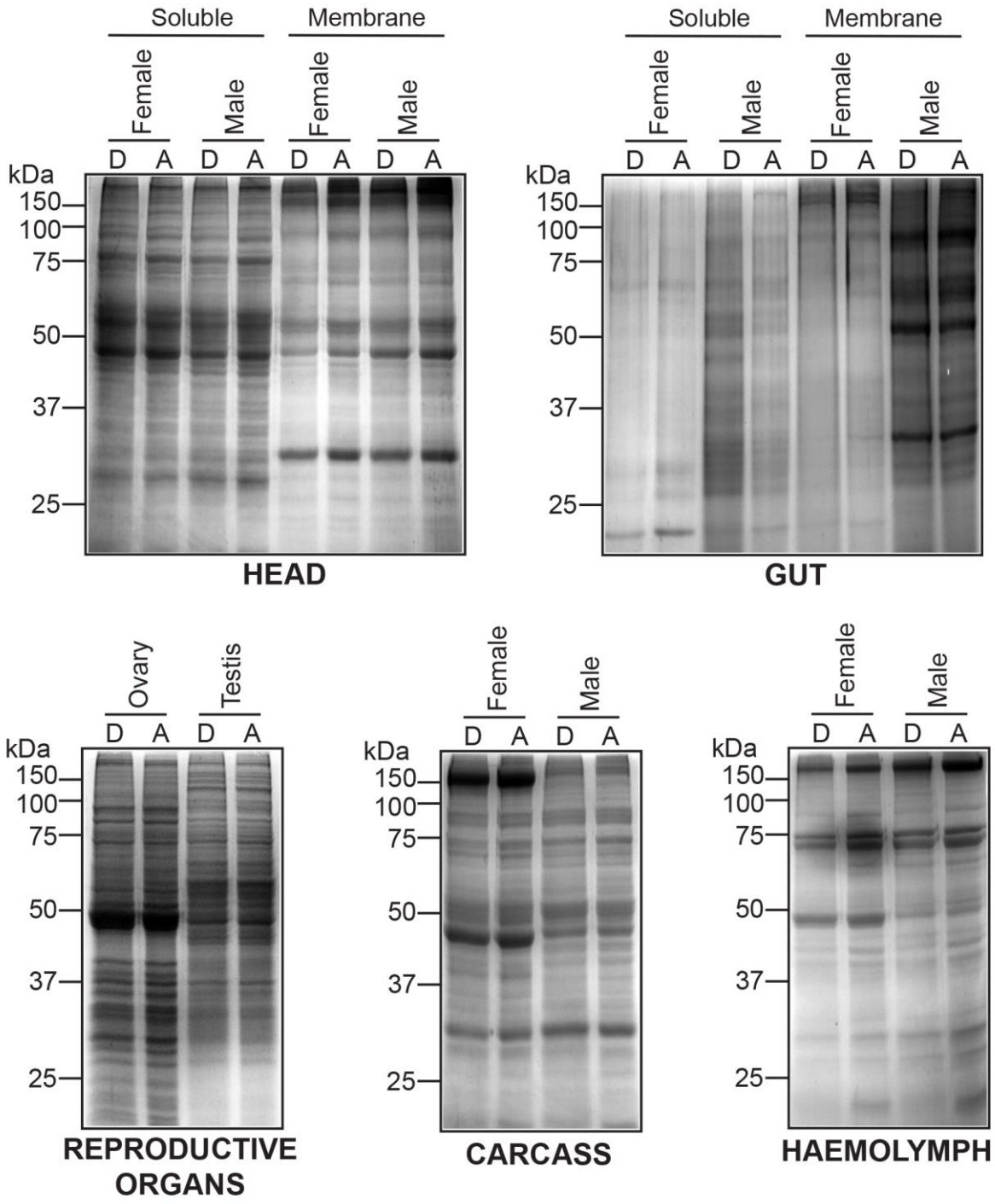

Figure 2.S.2. Coomassie staining of gel shown in Figure 4, showing equal loading of active (A) and denatured (D) lysates from different tissues and/or anatomical components in adult male and female flies.

Chapter 3

Drosophila Serine Hydrolases in host defense

Chapter 3

Drosophila Serine Hydrolases in host defense

Abstract

In *Drosophila*, the Serine Hydrolase (SH) superfamily consists of 354 members (Kumar et al., Biochemistry, 2021, 60:1312). A small number of SHs, specifically Serine proteases, have been studied as part of proteolytic cascades, both in embryonic axis determination (Schupbach T, 2009, Current Biology, 19:R548), and also in immune response signaling.

Quantitative RNA sequencing and proteomics comprise the bulk of data available. These techniques have proven to tool for discovery for genes that are either up or downregulated in response to infection. They are the efficient reliable methods for discovering genes depending on their expression patterns in response to infection. Intending to enumerate the novel SHs involved in the innate immune response, we have undertaken a literature survey of SHs involved in the host defense. We find that 252 SH genes are modulated in response to infection. 99 and 101 genes are uniquely up or downregulated, while 51 are context-dependent. Based on published multi-omics and genetic studies, we have assigned SHs to the three major signaling cascades, the Toll, Immune Deficient, and JNK pathways. Literature pin point that each immune pathways regulates specific sets of SHs expression.

Our literature survey in this chapter highlights that more than half of SHs modulates during infections paradigms. The extent of modulation of SHs Depends on the immunogenicity of pathogen and organ of the fly. This chapter will make foundation of literature to biochemical characterization of unannotated SHs that involved in the *Drosophila*'s immunity.

Graphical abstract

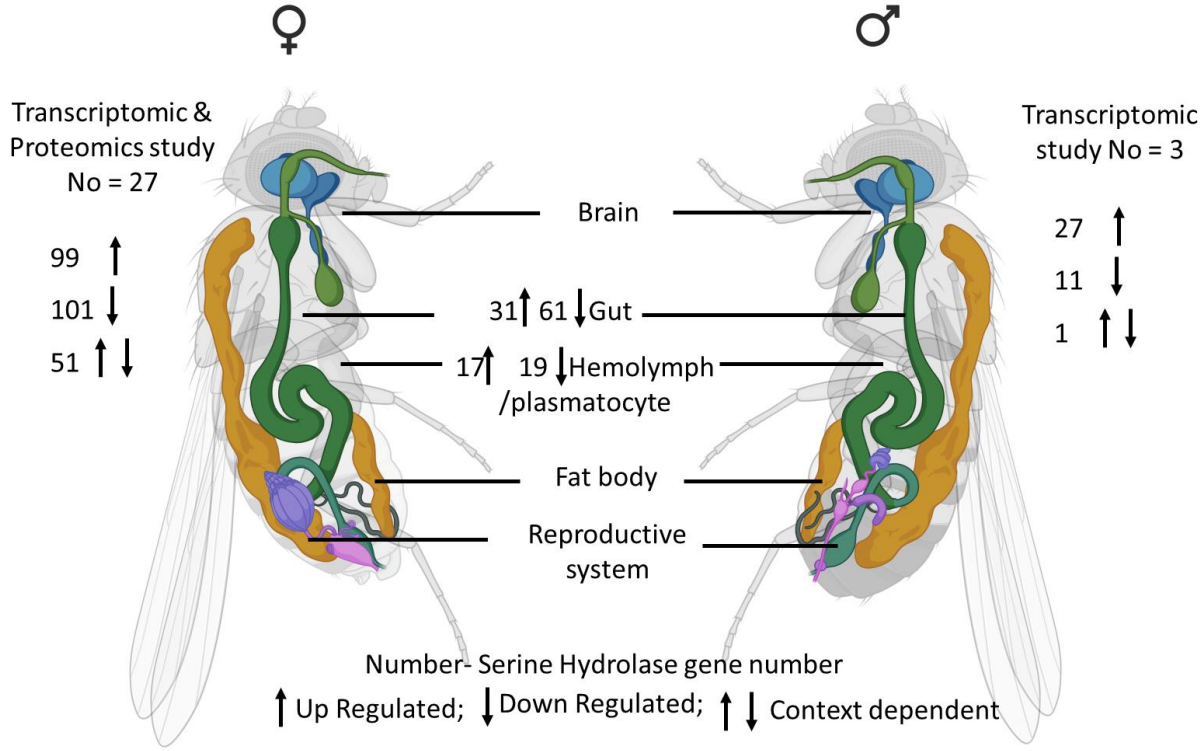

Image generated using Biorender

Keywords: *Drosophila melanogaster*, Innate Immunity, Serine Hydrolases, Transcriptomics, Proteomics, Review

Introduction

The serine hydrolase (SH) superfamily consists of 354 enzymes in *Drosophila melanogaster*.[1] SHs, by definition uses nucleophilic serine at an active site for the hydrolysis of amide, ester, and thioester bonds in protein and small molecule (metabolite) substrates.[2] The involvement of the catalytic triad activates the catalytic serine residue (e.g., His-Asp-Ser or Ser-Asp/Glu-His) and diad (e.g. Ser, Lys). It catalyzes the reaction via a two-step ping-pong mechanism; the first step involves the formation of the intermediate covalent acyl-enzyme adduct and is followed by water-induced hydrolysis, which leads to the regeneration of the active serine residue for the next cycle reaction. All species encode SH genes, from bacteria to mammals but differ in the numbers. Differences arise because the independent gene duplication event that occurs in the ancestry of the species and gets diverse in function. Serine hydrolases are involved in most pathophysiological processes in the fruit fly, such as development, growth, metamorphosis, digestion, inflammation, metabolism, oxidative stress, and bacterial infection. Further, SHs are classified into two subfamilies serine proteases and metabolic SHs. Serine proteases have gained attention in fly due to their involvement in the Toll signalling and transduced extracellular signalling in the cascade.[3,4] First, During *Drosophila*'s early development, Pipe Protein activates the cascade of Nudel-Gastrulation defective-snake-Easter.[5] The terminal SP, Easter, processes the Pro-Spätzle into Spätzle, a Toll receptor-ligand.[6] Second, During Gram-positive bacterial and fungal infection, pathogen recognition receptor PGRP-SA, GNBP1 and GNBP3 activate the downstream modSP-Grass-Hayan/Psh-SPE cascade.[4] SPE cleaves Pro-Spätzle into Spätzle, which binds to the Toll receptor and transduces the downstream signalling.[7] Despite the above fact, 86 and 84 percent of

the SPs and mSHs are not characterised yet,.[2] There is a differential regulation of SHs expression during the immune challenge in quantitative transcriptomics and proteomics in the literature.[8–11] Furthermore, *Drosophila melanogaster* has a primary level of resistance and tolerance against pathogens or immune elicitors.[12] The fly's natural immune response includes physical and chemical barriers along with primary immune signaling cascades such as Toll (TLR, Human homolog), Imd (TNF, Human homolog) that share homology with mammalian innate immune response.[8,10,13] Fly has been used to study the effects of various pathogens like bacteria, fungi, nematodes, viruses, etc[14,15]. The two significant pathways which act as a line of defence against immune challenges are the Toll and Imd (Immune Deficiency) pathways.[16,17] Apart from these pathways, other mechanisms exist, including the JAK/STAT pathway and the RNA interface[13,18,19]. Melanization is a reaction where melanin deposits around wounds and foreign objects (Fig 1).[9,20] There has been a rapid surge in high throughput data upon immune challenge in the *Drosophila melanogaster*. For detecting Differential Expressed Genes (DEGs) upon immune challenge, the general procedure is to infect the fly with a bacterium or a virus or a fungus or a nematode through pricking, microinjection or gut feeding, followed by a full transcriptomic and proteomic profiling to identify genes up/down-regulated at the transcriptional and translational level respectively. Antimicrobial peptides (AMPs) are produced upon infection and gain the most focus for monitoring immune responses. Apart from the immunity signature gene, the various families of the gene, such as receptors, complement, encapsulation, cytoskeleton, the component of the signalling pathways, coagulation, hematopoiesis, AMPs, ROS, and serine hydrolases genes, are strongly induced or found in different studies as a function of the immune response. In this review, We have explored the quantitative transcriptomics and proteomic literature to

identify and validate immune-related SHs and classify them as positive or negative regulators in pathophysiology and disease. The intersection of these two data sets serves as validation for the differential expression of those particular genes. At the same time, discrepancies between the two indicate regulatory mechanisms acting differently at RNA and protein levels. Nevertheless, both could serve as the reverse genetic screens in identifying target genes for deeper Spatio-temporal analyses using individual genetic studies.

Literature Survey, General Trends and Interpretations

Quantitative RNA sequencing and proteomics studies are widely accepted to predict and study the function of genes. Henceforth, we first performed a literature survey using the permutations and combinations of relevant keywords (*Drosophila*, Innate Immunity, Transcriptomics, Proteomics, Serine Hydrolases and Serine Proteases) at the Pubmed database. We identified 452 individual articles, of which only 92 are directly related to *Drosophila melanogaster* as of June 2021; The rest are associated with other species. Then we further classified all relevant papers based on the method employed to document the genes. The categories they were segregated into were Microarray/RNAseq (25), proteomics (11), non-omics (34) and review (21) articles, respectively (**Figure 3.1**). We analyzed 26 transcriptome and 11 proteomic papers to summarise pathogen used for infection, mode of infection, and differentially regulated genes (DRGs) for all genes (**Figure 3.1.A and Table 3.1**).[21–60] Pathogenic bacteria are the most commonly administered pathogens, followed by certain fungal species (examples) and viruses. Second, We collated SHs from all 37 studies (transcriptomics and proteomics) and grouped them under up-regulated and down-regulated. Then,

SHs are assigned to immune pathways based on pathway-specific mutant analysis (**Figure 3.1.B**).

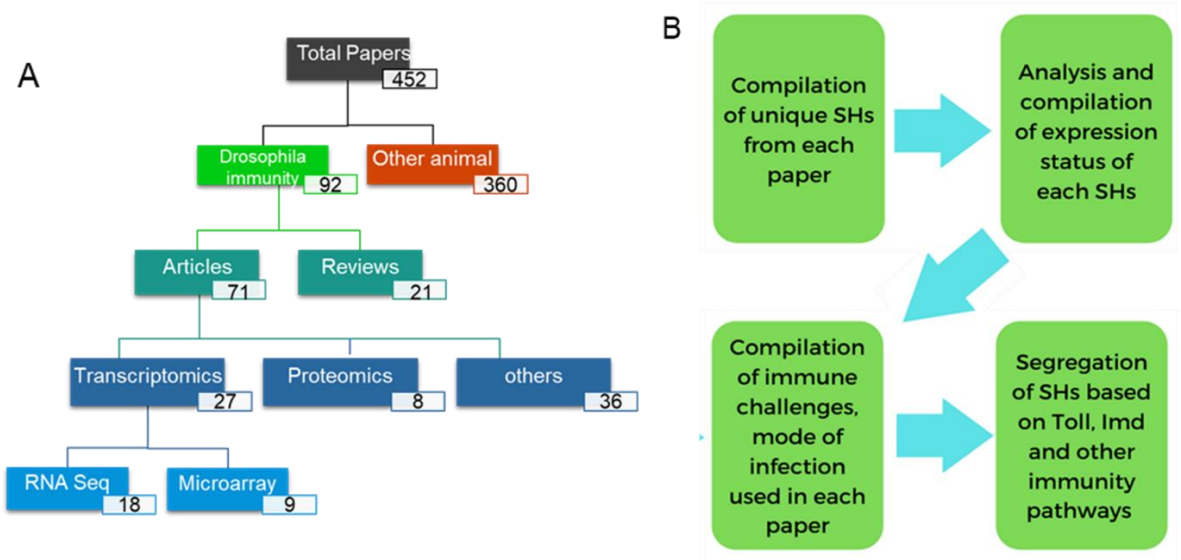

Figure 3.1. Literature Survey for multi-omic study on *Drosophila* innate immune response.

The output of the transcriptomic and proteomic study query on Pubmed resulted in 452 papers. Out of 452, 92 were directly related to *Drosophila melanogaster* and 71 and 21 were research and review articles respectively. The research articles further classified into transcriptomic, proteomics for global study and others for individual gene study. (B). Fours step procedure to fetch SHs. Firsrt Compile unique SHs from paper along with differential expression which provided in the data Second, Compile of expression status from respective paper. Third, fetch the mode of infection, type of pathogens, tissue used for study and genotype of animal. Fourth, Depending upon mutant used to study particular pathway, assign the pathway which regulate SHs depnding on context.

Table 3.1: Summary of infection-based experiments carried out in *Drosophila*.

SHs form a sub-category amongst genes/proteins that are up **(↑)** or downregulated **(↓).** These SHs, tabulated below, based on the context of the infection, represent 1-15% of the total SH genes coded by the *Drosophila* genome. The data is sorted in ascending order of date of publication of the manuscript.

S. No.	Method	Immune challenge	Mode of Infection	Genes (↑/↓)	SHs (↑/↓)	Reference
1	Microarray	*E. coli and M. luteus*	Septic injury	108/26	17/13	(De Gregorio *et al.* 2001)
2	Microarray	*E. coli and M. luteus*	Septic injury	101/37	14/13	(De Gregorio *et al.* 2002)
3	Proteomics	*B. bassiana*	Septic injury	26/11	2/0	(Levy *et al.* 2004a)
4	Proteomics	*B. bassiana*	Septic injury	11/2	3/0	(Levy *et al.* 2004b)
5	Proteomics	*M. luteus/ S. cerevisiae/ LPS*	Septic injury	20/3	3/0	(Vierstraete *et al.* 2004)
6	Microarray	*DCV, Serratia, Beauveria, Octosporea*	Gut Feeding	400/0	41/0	(Roxstrom-Lindquist *et al.* 2004)
7	Proteomics	*D. pneumoniae, N. catarrhalis, S. aureus, K. pneumoniae, H. influenza, S. pyogenes*	Gut feeding	39/25	2/0	(de Morais Guedes *et al.* 2005)
8	Microarray	*E. coli/Crude LPS*	mbn cell line	387/539	15/0	(Johansson *et al.* 2005)
9	Proteomics	*FHV*	Viral inoculation	150/66	1/1	(Go *et al.* 2006)
10	Microarray	*E. coli, Micrococcus luteus*	Septic injury	504/179	11/24	(Brun *et al.* 2006)
11	Microarray	*Ecc15*	Gut feeding	576/414	12/15	(Buchon *et al.* 2009a; Buchon *et al.* 2009b)
12	RNA seq	*Mixed bacterial culture of Serratia marcescens and Enterococcus faecalis*	Septic injury	483/2	9/0	(Sackton *et al.* 2010)
13	RNA seq	*P. entomophila, Ecc15*	Gut feeding	559/395	16/60	(Chakrabarti *et al.* 2012)

14	RNA seq	*Heterorhabditis bacteriophora*	Gut Feeding	517/124	6/8	(AREFIN *et al.* 2014)
15	Microarray	*Providencia rettgeri*	Septic injury	103/21	7/3	(SHORT AND LAZZARO 2013)
16	Microarray	*S2 cell, C virus*	S2 cell, C virus	273/442	2/13	(ZHU *et al.* 2013)
17	RNA seq	*Penicillium*	Rearing on fungal medium	94/5	1/0	(SETO AND TAMURA 2013)
18	Microarray	*Ecc15*	Larval feeding	105/119	3/5	(GENDRIN *et al.* 2013)
19	RNA seq	*Ecdysone*	Hormonal induction	744/1213	21/13	(REGAN *et al.* 2013)
20	Transcriptome	*L. plantarum, L. brevis, C. intestini, A. pomorum*	Gut feeding	105	30	(ERKOSAR *et al.* 2014)
21	Proteomics	*Wolbachia*	Wolbachia symbiont infection	78/59	10/1	(YUAN *et al.* 2015)
22	RNA seq	*Heterorhabditis bacteriophora*	Injection and Gut Feeding	13/179	6/2	(CASTILLO *et al.* 2015)
23	RNA seq	*DCV and CrPV*	S2 cell, Virus	31;71/14;64	15/1	(MERKLING *et al.* 2015a; MERKLING *et al.* 2015b)
24	Proteomics	*Wolbachia*	Gut feeding	1247	19	(CHRISTENSEN *et al.* 2016)
25	RNA seq	*M. luteus*	Pricking	1505	93	(WEI *et al.* 2018)
26	RNA seq	*Pseudomonas entomophila*	Septic injury	659/948	63/24	(RAGHEB *et al.* 2017)
27	RNA seq	*M. luteus, E.coli, S. mar, Ecc15, P. rett, E. fae, S.aureus, P. sneebia, S.mar, P.ento,*	Septic injury	166/86	9/11	(TROHA *et al.* 2018)
28	RNA seq	*Clean injury, E. coli septic injury, S. aureus septic injury*	Septic injury	2443/4039	17/22	(RAMOND *et al.* 2020)
29	Transcriptome	*A. flavus*	Inoculation	75/108	5/1	(RAMIREZ-CAMEJO AND BAYMAN 2020)
30	RNA seq	*G. queenslandicus*	Gut feeding	1373	32	(BENOIT *et al.* 2020)

31	RNA Seq	*Prion infection*	Feeding	2975/1582	1/0	(THACKRAY *et al.* 2020)
32	RNA seq	*Wasp infection*	Wasp oviposition	3214/6385	46/32	(HIGAREDA ALVEAR *et al.* 2021)
33	Proteomics	*Spiroplasma*	Septic injury	171/36	13/1	(MASSON *et al.* 2021)
34	RNA seq	*E. coli derived crude LPS*	Septic injury	951	66	(SCHLAMP *et al.* 2021)
35	RNA seq	*P. entomophila*	Gut feeding	592/580	12/41	(SOORY AND RATNAPARKHI 2022)

When collated, the number of SHs that are modulated (Table 1) come to a total of 251 SHs, of which 80 are Metabolic SHs and 120 are Serine proteases (***Annexure 6***).

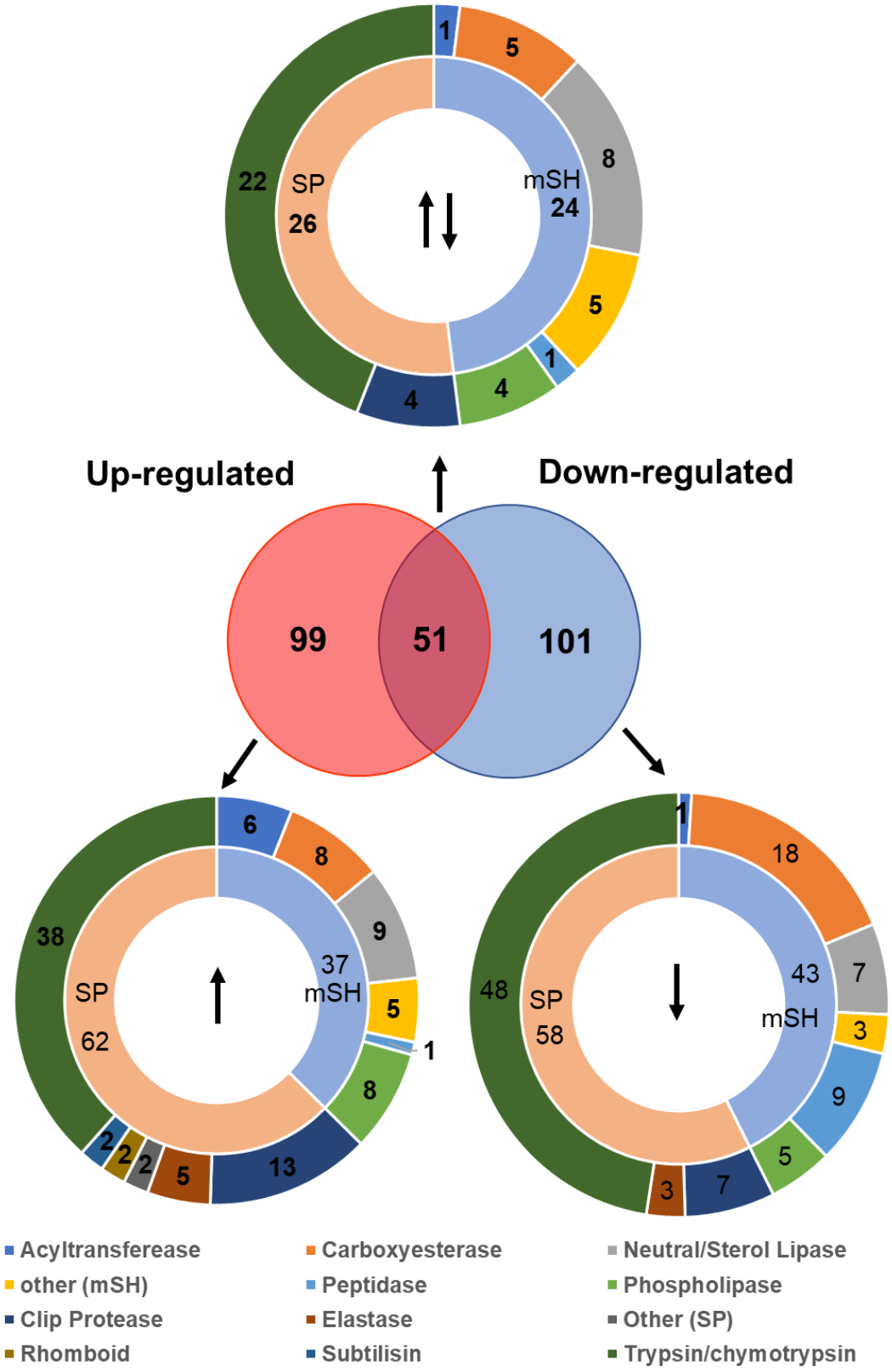

SHs upon Immune Challenge

When collated, the number of SHs that are modulated comes to a total of 251 SHs, of which 104 are Metabolic SHs and 147 are Serine proteases (*Suppl. Table 1*). Out of the 251 genes documented, 99 were solely up-regulated, 101 were down-regulated and 51 are/were context dependent (**Figure 3.2., *Annexure 6***). Out of 99 up-regulated SHs, 62 are SPs and 37 are mSHs. Out of 101 down-regulated SHs, 58 SPs and 43 mSHs are downregulated (**Figure 3.2., *Annexure 6***). The SHs classes like Trypsin/Chymotrypsin (38/48), Clip protease (13/7), Rhomboid (5/3), Acetyltransferase (6/1), Carboxylesterase (8/18), Phospholipase (8/5), Neutral/sterol lipase (9/7) and peptidase (1/9) subclasses get modulated [up(↑**)**/downregulated (↓**)**] upon infection (**Figure 3.2., *Annexure 6***).

Figure 3.2. Status of Expression of SHs upon Immune Challenge.
The differentially regulated gene upon immune challenge were compiled from all literature and extracted the SHs genes. A total of 251 SHs modulated and 80 were Metabolic SHs, 120 were Serine proteases. Also, 99 and 101 SHs up-regulated and down-regulated respectively, and 51 SHs were context-dependent. The pie chart shows class of SHs gets modulated in response to infection. Notation- up-regulation (↑) and down-regulation (↓).

SHs in organ-specific immunity

The organ system of flies is analogous to the higher model system to investigate the innate immune mechanism. Fly organs-like the Brain, Gut, Fatbody, Malpighian tubes, Ovary and Testis mount an immune response against pathogens.

Brain harbours cellular and humoral immune mechanisms and mounts immune response to neurodegenerative diseases. No multi-omics study has been done on the fly brain upon infection. Physical injury to fly head leads to the induction of a plethora of immune-responsive genes like antimicrobial peptides, including serine hydrolases. The physical injury leads to a change in mental ability and sleep for a few days and also causes a shorter life span. The fly brain may serve as an injury and infection model to study.

Gut harbors the expression of more than 750 enzymes for food digestion, assimilation, and host and commensal microbiota-interaction.[1,61] Enzymes are expressed either for digestive function or in response to infection, or to sustain gut-associated microbes[44,58,61]. Nearly all SPs and half of the mSHs are expressed in the gut at basal metabolism with trypsin, chymotrypsin, Janah Proteases, esterases, Carboxyl ester hydrolases, Serine-type carboxypeptidases and lysophospholipase family members[44,61] being observed predominantly. Activation of toll, Imd and Jnk pathways is common to intestinal injury and infection[44,58,61]. SHs are enriched predominantly in addition to AMPs. Time lapsed infection study has been carry out to demonstrate the immune response in the gut[44,58]. For simplification of analysis, we have considered 4 hours post-infection time point. A total of 92 SHs get modulated upon post 4 hours of gut feeding, and 30-up-regulated, 61-down-regulated and 1 SHs are context-dependent, respectively (**Figure 3.3.A**). The following subfamily of SHs is modulate (Upregulated/downregulated) in gut upon infection i.e. Peptidase (0/8), Clip protease (1/2), Elastase (1/0), Rhomboid protease (2/0) and trypsin/chymotrypsin (30/9)

subclass (**Figure 3.3.B**)**.** The modulation of SHs expression is dependent on the potency of bacterial infection. The *pseudomonas entomophilia* cause severe infection than ECC15. P. entomophilia infection leads to down-regulation of 55 SHs, whereas ECC15 infection down regulates 18 SHs, with 12 SHs being common. SImilarly, *Pseudomonas entemophila* infection leads to the up-regulation of 26 SHs, whereas ECC15 up-regulates 10 SHs with 6 common SHs (**Figure 3.3.A, *Annexure 6***).

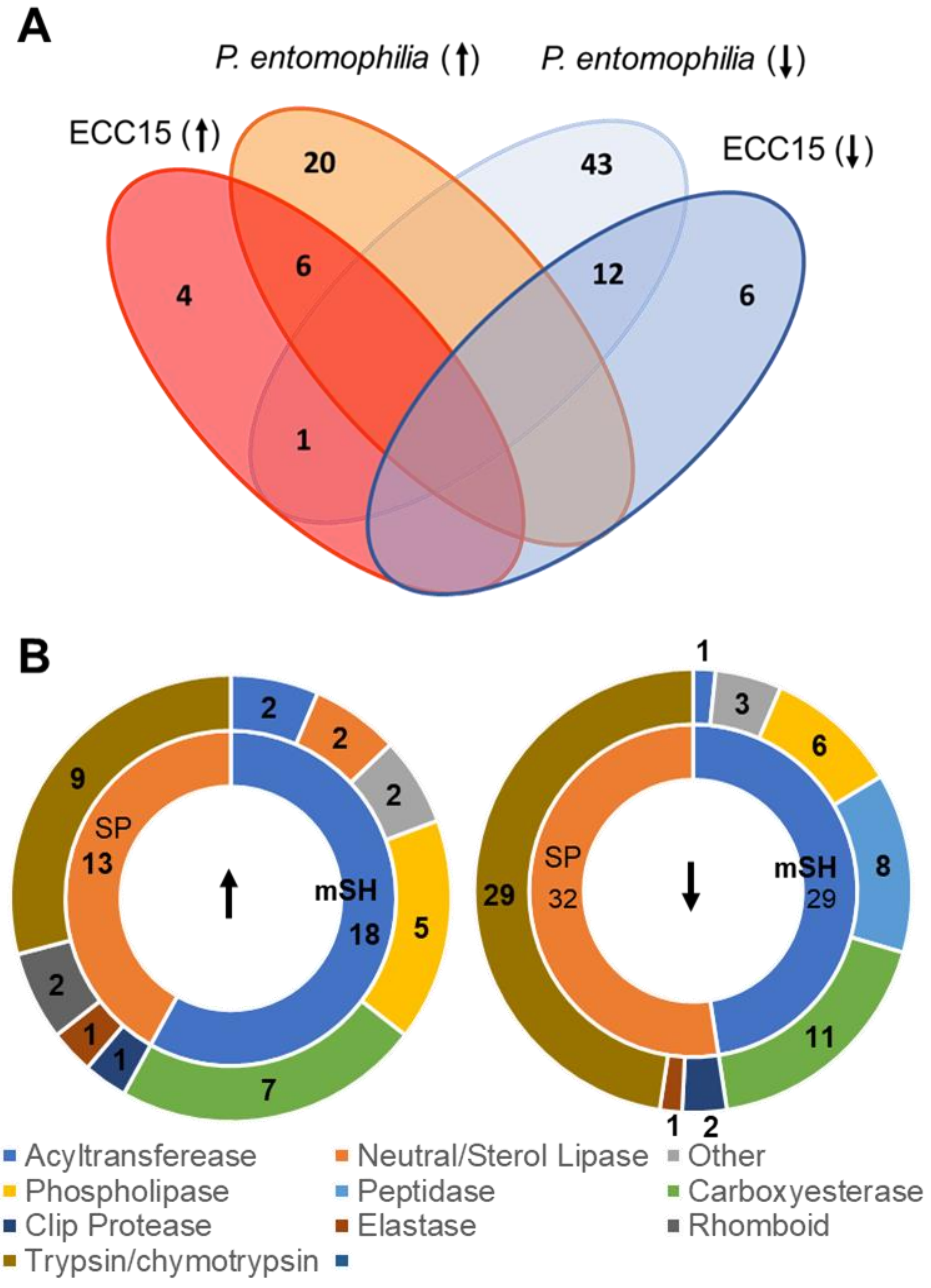

Figure 3.3. Modulation of SHs in gut upon gut immunity.

(A). Differential modulation of SHs depending upon immunogenic potency of gram-negative bacteria. 20SHs were upregulated by *P. entomophilia,* 4SHs by ECC15 and 6SHs by both pathogens in the gut immunity*.* 43SHs were downregulated by *P. entomophilia,* 6SHs by ECC15 and 12SHs by both pathogens*.* **(B).** Pie chart represent the subfamilies od SHs that gets upregulated and down regulated during gut infection. Notation- up-regulation (↑) and down-regulation (↓).

Hemolymph is the blood equivalent fluid in insects and circulates in the body cavity. Levy et al, 2004 have shown that MP1, SPE and CG9372 protein level get upregulated using 2D SDS-PAGE-based mass spectrometry[36]. Masson et al., 2021 have shown that Ser7, CG4757, MP1, CG5162, CG3700, CG9372, Est-Q, CG16749, CG5246, SPE, grass, CG11841, CG11842, CG30002 are upregulated and *CG16749* down-regulated upon *Spiroplasma infection* in the hemolymph using mass spectrometry[30].

Fatbody MP1, Hayan, spirit, psh, Sp7, SPE, grass, modSP, Ace, Jheh1, Try29F, CG5355, CG10041, CG17239 are up regulated and CG10038, CG30098 are down regulated.[56]

Trachea CG4757, CG10383 and CG5255 are up regulated and l(2)k05911, CG32808, CG319554 and Est-Q are down regulated.[48]

Plasmaocyte: Ramond et al. 2020 have shown that 37 SHs are differentially regulated in the plasmatocytes using RNAseq upon clean injury and septic injury (**Figure 3.4., *Annexure 6***).[21] The SHs modulation is distinct for clean and septic injury except CG6277, CG6283 and Jon66Ci, which are upregulated upon clean injury and downregulated upon septic injury. The Imd signalling components like PGRP-LB, PGRP-LF, and Relish are upregulated in the plasmatocyte upon septic injury. It may be possible that Imd signaling regulates the induction of defense gene in the plasmatocytes. Since *Grass* and *SPE* gene expression do not get modulated at the transcript level in the plasmatocytes. But at the protein level, Grass and SPE

upregulated the hemolymph. Also, the expression of *Hayan, psh, Sp7, grass* and *SPE* are upregulated in fatbody. Thus, the activated toll extracellular cascade in hemolymph transduce toll signaling in fatbody and in response, fatbody generate the effector molecules like antimicrobial peptides opsonization factors, stress factors, and enzymes of the melanisation cascade.

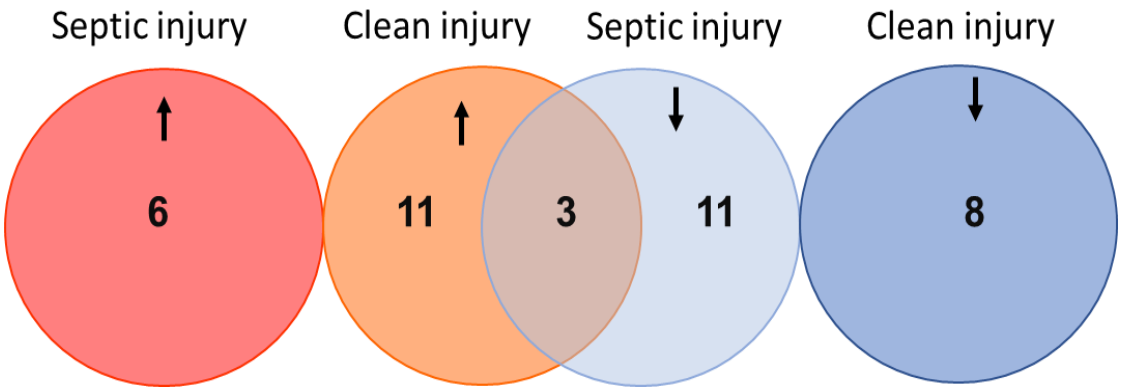

Figure 3.4. Modulation of SHs in plasmatocytes upon Septic or clean injury. Distinct sets of SHs up or down regulated during clean and septic injury and 3SHs were context depended. Notation- up-regulation (↑) and down-regulation (↓).

Overy: No SHs are differentially regulated upon Wolbachia infection in *Drosophila melanogaster*. But Yp1, and Yp2 get upregulated and TppII is down-regulated in *D. simulan* upon Wolbachia infection.[33]

Spermathecae and seminal receptacles: CG11307, CG31872, and CG17097 get up-regulated whereas Smp-30 get down-regulated in Spermathecae and seminal receptacles of female mated with Wolbachia-infected male fly in comparison to female mated with uninfected male.[38]

Pathways Affecting SH expression in *Drosophila*'s immunity

Toll, Imd and Jnk signaling are canonical signalling pathways that are activated by pathogen recognition.[17] The Toll and Imd mediate differential expression of AMP-

encoding genes via distinct NF-κB-like transcription factors *dorsal/dif* and *relish* respectively(**Figure 3.5.A**)[17]. The Toll and Imd together regulate almost 80% of genes that induce upon infection.[17] The imd and Jnk pathways primarily involved in gut infection. p38b/MAPK and JAK/STAT are stress pathways and are also implicated in the immune response (**Figure 3.5.A**). Toll, Imd, Jnk and p38b/MAPK pathways

A

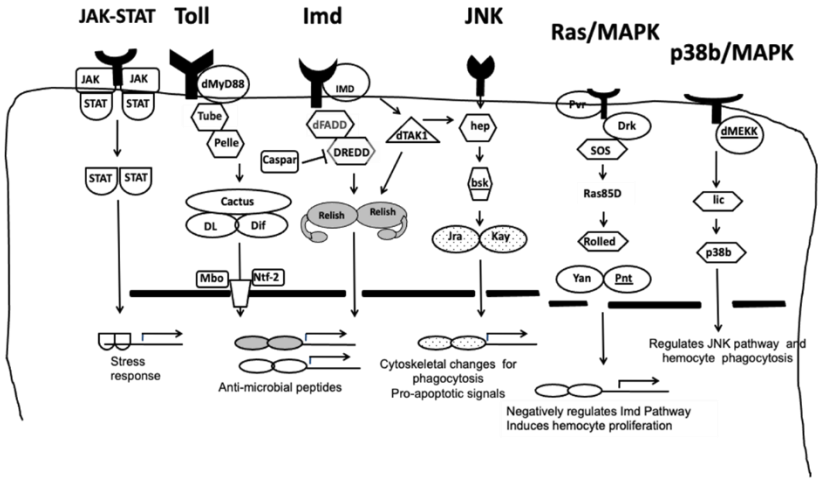

B

Toll/NFκB
CG17571, CG4757, CG9631, deltaTry, ea, grass, Jon99Fi, modSP, psh, snk, Sp7, SPE,

IMD/NFκB
alpha-Est5, alpha-Est8, alpha-Est9, CG1304, CG9733, CG11313, CG11668, CG11836, CG16749, CG17477, CG18179, CG18180, CG30090, CG3739, CG5355, CG6283, Jon25Bii, Jon25Biii, Jon65Aii, Jon66Cii, rho, S1P, Ser6, Ser8, smp-30, Try29F, Yp1, Yp2, Yp3

p38b/MAPK
CG10232, CG1299, CG1304, CG14892, CG16710, CG4267, kraken, tpr, Sp7, SPE, Yp3

Toll & IMD
CG11842, CG17192, CG4267, CG5909, CG6296, Hayan, Jon66Ci, spirit
CrebA: CG10472, CG17097, CG17571, CG18258, CG18493, CG30083, CG30289, CG31872, CG3700, CG5162, Est-Q

JNK
alpha-Est10, alpha-Est5, alpha-Est8, alpha-Est9, alpha-Est7, CG10175, CG10469, CG11911, CG1304, CG14507, , CG17192, CG17475, CG17571, CG18180, CG4053, CG4572, CG5246, CG5455, CG5704, CG6048, CG6271,CG6277, CG6295, Gas, Hiro, Hydra, inaE1, Jon25Bi, Jon25Bi, Jon25Bii, Jon65Aii, Jon65Aiv, Jon65Aiv, Jon99Ciii, lambdaTry, Nup98-96, PAPLA1, Ppt2, Rcd1, Ser6, Ser8, zetaTry, Yp3

regulate the induction of SHs in response to infection (**Figure 3.5.A and Figure 3.5.B**)[41,44–46,58]. Toll and Imd pathways have been shown to regulate 12 and 29 SHs gene expression, respectively, and together 8 SHs (**Figure 3.5.B**). Also, Toll and Imd regulated 12 SHs through *KrebA*. Jnk regulates 43 SHs and 12 are also regulated by Imd (**Figure 3.5.B**).

Figure 3.5. Pathways Affecting SH expression in *Drosophila*'s immunity.

(A). Multiple pathways like, Toll, Imd, JNK, JAK-STAT, p38b/MAPK and Ras/MAPK regulated the innate immune response to *Drosophila*. **(B).** List of SHs modulated by immune pathways. SHs genes in the Red font regulated by more than one pathways.

Discussion and conclusion

The review delves into quantitative transcriptomics and proteomics literature to identify and validate immune-related SHs, classifying them as positive or negative regulators in pathophysiology. The intersection of these data sets serves as validation for differential gene expression, while discrepancies may indicate regulatory mechanisms acting differently at the RNA and protein levels. Both sets of data can be used for reverse genetic screens to identify target genes for further spatio-temporal analyses through individual genetic studies. In the insights derived from transcriptomic and proteomic analyses, a literature survey identified 92 relevant articles, categorized into Microarray/RNAseq, proteomics, non-omics, and review articles. A comprehensive analysis of transcriptome and proteome studies highlighted the pathogens used for infection, modes of infection, and differentially regulated genes (DRGs). The study also grouped SHs from these studies based on their up-regulation or down-regulation and assigned them to immune pathways through pathway-specific mutant analysis. When considering the compiled data, a total of 251 SHs were found to be modulated, comprising 104 Metabolic SHs and 147 Serine Proteases (SPs) (**Annexure 6**). This extensive modulation highlights the significance of SHs in orchestrating responses to various immune challenges. Breaking down the modulated SHs, it is observed that 99 genes are exclusively up-regulated, 101 genes are down-regulated, and 51 genes exhibit context-dependent regulation (**Figure 3.2**). This diversity in regulation emphasizes the dynamic nature of SH responses to various immune stimuli. Further classification of the up-regulated SHs reveals that 62 belong to the Serine Protease (SP) category, while 37 are Metabolic SHs (mSHs). On the other hand, out of the 101 down-regulated SHs, 58 are SPs, and 43 are mSHs, indicating a complex interplay between these subclasses in the context of immune challenges (**Figure 3.2**).

Examining specific SH classes, various subclasses exhibit modulation in response to infection. Classes such as Trypsin/Chymotrypsin, Clip Protease, Rhomboid, Acetyltransferase, Carboxylesterase, Phospholipase, Neutral/Sterol Lipase, and Peptidase show both up-regulation (↑) and down-regulation (↓) patterns upon infection (**Figure 3.2**). This detailed classification underscores the functional diversity within the SH superfamily and their specific roles in immune responses. Also, We have listed the most cited modulated SHs from our analysis. I have characterized CG17192, a Metabolic Serine Hydrolases (**Table 3.2**).

Table 3.2: Most Cited Differentially Expressed SHs

UP-Regulated	Down-Regulated
Yp1, Hydr2, CG6048, PAPLA1, sturkopf, CG10175, CG6296, Apt1, FASN2, CG30371, modSP, CG31821, CG33226, pps, CG43110, Phae2, ndl, iPLA2-VIA, CG7142, CG11313, CG17097, CG9649, CG9649, CG30083 *teq, CG11911, CG11841, CG5162, CG11842, CG30091, CG33462, CG4267, Jon65Aiv, CG5246, Ser7, spirit, CG6675, Jon74E, CG9733, CG5909, Sp212, CG11912, CG9372, CG10472, alpha-Est8, CG30287, Jon65Aiii, CG5966, CG10383, CG4757, MP1*	*gd, rho, Ser8, CG18301, CG2493, CG8299, CG4914, CG11668, CG30414, CG33096, CG34447, twr, CG17192, Est-P, Est-P, Jheh2, CG15820, sxe2, Jon65Ai, Jon25Biii, yip7, CG18179, CG18754, CG5707, Jon25Bii, CG4927, Jon65Ai, CG6295, lambdaTry, Jheh1, CG30088, Jon99Ci, CG16749, CG3739, CG18180.*

The organ-specific immunity of *Drosophila melanogaster*, shedding light on the intricate roles of serine hydrolases (SHs) across various tissues. The fly's organs, including the Brain, Gut, Fatbody, Malpighian Tubes, Ovary, and Testis, exhibit distinct immune responses against pathogens. In the Brain, both cellular and humoral immune

mechanisms are at play, responding not only to infections but also neurodegenerative diseases. Despite a lack of multi-omics studies on the fly brain upon infection, physical injury to the head triggers a robust immune response, with numerous immune-responsive genes, including antimicrobial peptides and serine hydrolases, being induced. Such injuries lead to altered mental abilities, sleep patterns, and a shortened lifespan, making the fly brain a potential model for studying both injury and infection. The Gut, a crucial organ for digestion and microbiota interaction, expresses a myriad of enzymes under basal conditions. Upon infection, the time-lapsed studies reveals the modulation of 92 SHs post 4 hours of gut feeding, with 36 SHs-upregulated, 62 SHs-downregulated, and 1SHs being context-dependent (**Figure 3.3**).[44,58] The differential regulation of SHs in response to varying bacterial infections emphasizes the gut organ role as a frontline defense(**Figure 3.3**). Hemolymph, the insect's blood equivalent fluid, shows alterations in SH protein levels upon infection. Surprigingly, distinct SHs exhibit differential regulation in response to Spiroplasma infection, offering insights into the dynamic immune responses in circulation(**Figure 3.4**). The Fatbody, Trachea, and Plasmaocyte also display unique patterns of SH modulation in response to infections and injuries. The up-regulation of specific SHs in the Fatbody, along with the activation of Toll extracellular cascades, underscores the intricate interplay between different immune components. Moreover, we have explored SH expression in the Ovary, Spermathecae, and Seminal Receptacles, highlighting specific SHs that are up-regulated or down-regulated upon Wolbachia infection. The canonical Toll, Imd, and Jnk signaling pathways emerge as key regulators of SH expression in *Drosophila*'s immunity[7,58,62]. These pathways, activated by pathogen recognition, govern the differential expression of AMP-encoding genes and regulate a substantial portion of genes induced upon infection. Toll and Imd pathways, in particular, play

pivotal roles in the regulation of SHs, both independently and collaboratively. Additionally, stress pathways, such as p38b/MAPK and JAK/STAT, are implicated in the immune response, further expanding the regulatory landscape of SHs in *Drosophila*'s immunity(**Figure 3.5**). In conclusion, the organ-specific immune responses and pathway regulations provide a comprehensive understanding of the SHs in *Drosophila melanogaster*'s immunity. The findings pave the way for future investigations into the molecular intricacies of these responses and their implications for overall host defense mechanisms.

Contributions

Parth Anand Ankam (BS-MS IISER TVM) and Shruti Pawar (BS-MS IISER Pune) contributed to the analysis for this Chapter.

References

1. Kumar, K., Mhetre, A., Ratnaparkhi, G. S. & Kamat, S. S. A Superfamily-wide Activity Atlas of Serine Hydrolases in *Drosophila melanogaster*. *Biochemistry* vol. 60 1312–1324 Preprint at https://doi.org/10.1021/acs.biochem.1c00171 (2021).
2. Kumar, K., Mhetre, A., Ratnaparkhi, G. S. & Kamat, S. S. A Superfamily-wide Activity Atlas of Serine Hydrolases in. *Biochemistry* **60**, 1312–1324 (2021).
3. Gilbert, S. F. Developmental Biology. (2000).
4. More Than Black or White: Melanization and Toll Share Regulatory Serine Proteases in *Drosophila*. *Cell Rep.* **27**, 1050–1061.e3 (2019).
5. Cho, Y. S., Stevens, L. M. & Stein, D. Pipe-dependent ventral processing of Easter by Snake is the defining step in *Drosophila* embryo DV axis formation. *Curr. Biol.* **20**, 1133–1137 (2010).
6. DeLotto, Y. & DeLotto, R. Proteolytic processing of the *Drosophila* Spätzle protein by Easter generates a dimeric NGF-like molecule with ventralising activity. *Mech. Dev.* **72**, 141–148 (1998).
7. Jang, I.-H. *et al.* A Spätzle-processing enzyme required for toll signaling activation in *Drosophila* innate immunity. *Dev. Cell* **10**, 45–55 (2006).

8. Hoffmann, J. A. The immune response of *Drosophila*. *Nature* **426**, 33–38 (2003).
9. Dudzic, J. P., Hanson, M. A., Latsenko, I., Kondo, S. & Lemaitre, B. More than black and white: complex relationships involving serine proteases regulate the Toll pathway and the melanization response in *Drosophila*. Preprint at https://doi.org/10.1101/383257.
10. Hultmark, D. *Drosophila* immunity: paths and patterns. *Curr. Opin. Immunol.* **15**, 12–19 (2003).
11. Veillard, F., Troxler, L. & Reichhart, J.-M. *Drosophila* melanogaster clip-domain serine proteases: Structure, function and regulation. *Biochimie* **122**, 255–269 (2016).
12. Ayres, J. S. & Schneider, D. S. A signaling protease required for melanization in *Drosophila* affects resistance and tolerance of infections. *PLoS Biol.* **6**, 2764–2773 (2008).
13. Mussabekova, A., Daeffler, L. & Imler, J.-L. Innate and intrinsic antiviral immunity in *Drosophila*. *Cell. Mol. Life Sci.* **74**, 2039–2054 (2017).
14. Troha, K. & Buchon, N. Methods for the study of innate immunity in *Drosophila* melanogaster. *Wiley Interdiscip. Rev. Dev. Biol.* **8**, e344 (2019).
15. Neyen, C., Bretscher, A. J., Binggeli, O. & Lemaitre, B. Methods to study *Drosophila* immunity. *Methods* **68**, 116–128 (2014).
16. Govind, S. Innate immunity in *Drosophila*: Pathogens and pathways. *Insect Sci.* **15**, 29–43 (2008).
17. Lemaitre, B. & Hoffmann, J. The host defense of *Drosophila* melanogaster. *Annu. Rev. Immunol.* **25**, 697–743 (2007).
18. Tafesh-Edwards, G. & Eleftherianos, I. *Drosophila* immunity against natural and nonnatural viral pathogens. *Virology* **540**, 165–171 (2020).
19. Sabin, L. R., Hanna, S. L. & Cherry, S. Innate antiviral immunity in *Drosophila*. *Curr. Opin. Immunol.* **22**, 4–9 (2010).
20. Tang, H. Regulation and function of the melanization reaction in *Drosophila*. *Fly* **3**, 105–111 (2009).
21. Ramond, E., Dudzic, J. P. & Lemaitre, B. Comparative RNA-Seq analyses of *Drosophila* plasmatocytes reveal gene specific signatures in response to clean injury and septic injury. *PLoS One* **15**, e0235294 (2020).
22. Cho, B. *et al.* Single-cell transcriptome maps of myeloid blood cell lineages in*Drosophila*. Preprint at https://doi.org/10.1101/2020.01.15.908350.

23. Castillo, J. C. *et al. Drosophila* anti-nematode and antibacterial immune regulators revealed by RNA-Seq. *BMC Genomics* **16**, 519 (2015).
24. Benoit, J. B., Bose, J., Bailey, S. T. & Polak, M. Interactions with ectoparasitic mites induce host metabolic and immune responses in flies at the expense of reproduction-associated factors. *Parasitology* **147**, 1196–1205 (2020).
25. Alvear, V. M. H., Mateos, M., Cortez, D., Tamborindeguy, C. & Martinez-Romero, E. Differential gene expression in a tripartite interaction:*Drosophila*,*Spiroplasma*and parasitic wasps. *PeerJ* vol. 9 e11020 Preprint at https://doi.org/10.7717/peerj.11020 (2021).
26. Wei, G. *et al.* Dynamic miRNA-mRNA regulations are essential for maintaining *Drosophila* immune homeostasis during Micrococcus luteus infection. *Dev. Comp. Immunol.* **81**, 210–224 (2018).
27. Thackray, A. M., Lam, B., Razak, A. S. B., Yeo, G. & Bujdoso, R. Transcriptional signature of prion-induced neurotoxicity in a *Drosophila* model of transmissible mammalian prion disease. *Biochemical Journal* vol. 477 833–852 Preprint at https://doi.org/10.1042/bcj20190872 (2020).
28. Schlamp, F. *et al.* Dense time-course gene expression profiling of the *Drosophila* melanogaster innate immune response. *BMC Genomics* **22**, 304 (2021).
29. de Morais Guedes, S. *et al.* Proteomics of immune-challenged *Drosophila* melanogaster larvae hemolymph. *Biochem. Biophys. Res. Commun.* **328**, 106–115 (2005).
30. Masson, F., Rommelaere, S., Marra, A., Schüpfer, F. & Lemaitre, B. Dual proteomics of *Drosophila* melanogaster hemolymph infected with the heritable endosymbiont Spiroplasma poulsonii. *PLOS ONE* vol. 16 e0250524 Preprint at https://doi.org/10.1371/journal.pone.0250524 (2021).
31. Vierstraete, E. *et al.* Proteomics in *Drosophila* melanogaster: first 2D database of larval hemolymph proteins. *Biochemical and Biophysical Research Communications* vol. 304 831–838 Preprint at https://doi.org/10.1016/s0006-291x(03)00683-1 (2003).
32. Go, E. P. *et al.* Mass spectrometry reveals specific and global molecular transformations during viral infection. *J. Proteome Res.* **5**, 2405–2416 (2006).
33. Christensen, S. *et al.* Wolbachia Endosymbionts Modify *Drosophila* Ovary Protein Levels in a Context-Dependent Manner. *Applied and Environmental Microbiology* vol. 82 5354–5363 Preprint at https://doi.org/10.1128/aem.01255-16 (2016).

34. Vierstraete, E., Verleyen, P., De Loof, A. & Schoofs, L. Differential proteomics for studying *Drosophila* immunity. *Ann. N. Y. Acad. Sci.* **1040**, 504–507 (2005).
35. Vierstraete, E. *et al.* A proteomic approach for the analysis of instantly released wound and immune proteins in *Drosophila* melanogaster hemolymph. *Proc. Natl. Acad. Sci. U. S. A.* **101**, 470–475 (2004).
36. Levy, F., Bulet, P. & Ehret-Sabatier, L. Proteomic analysis of the systemic immune response of *Drosophila*. *Mol. Cell. Proteomics* **3**, 156–166 (2004).
37. Levy, F. *et al.* Peptidomic and proteomic analyses of the systemic immune response of *Drosophila*. *Biochimie* **86**, 607–616 (2004).
38. Yuan, L.-L. *et al.* Quantitative Proteomic Analyses of Molecular Mechanisms Associated with Cytoplasmic Incompatibility in *Drosophila* melanogaster Induced by Wolbachia. *J. Proteome Res.* **14**, 3835–3847 (2015).
39. Loseva, O. & Engström, Y. Analysis of signal-dependent changes in the proteome of *Drosophila* blood cells during an immune response. *Mol. Cell. Proteomics* **3**, 796–808 (2004).
40. Arefin, B. *et al.* Genome-Wide Transcriptional Analysis of *Drosophila* Larvae Infected by Entomopathogenic Nematodes Shows Involvement of Complement, Recognition and Extracellular Matrix Proteins. *Journal of Innate Immunity* vol. 6 192–204 Preprint at https://doi.org/10.1159/000353734 (2014).
41. Brun, S. *et al.* The MAPKKK Mekk1 regulates the expression of Turandot stress genes in response to septic injury in *Drosophila*. *Genes to Cells* vol. 11 397–407 Preprint at https://doi.org/10.1111/j.1365-2443.2006.00953.x (2006).
42. Buchon, N., Broderick, N. A., Chakrabarti, S. & Lemaitre, B. Invasive and indigenous microbiota impact intestinal stem cell activity through multiple pathways in *Drosophila*. *Genes & Development* vol. 23 2333–2344 Preprint at https://doi.org/10.1101/gad.1827009 (2009).
43. Buchon, N., Broderick, N. A., Poidevin, M., Pradervand, S. & Lemaitre, B. *Drosophila* Intestinal Response to Bacterial Infection: Activation of Host Defense and Stem Cell Proliferation. *Cell Host & Microbe* vol. 5 200–211 Preprint at https://doi.org/10.1016/j.chom.2009.01.003 (2009).
44. Chakrabarti, S., Liehl, P., Buchon, N. & Lemaitre, B. Infection-Induced Host Translational Blockage Inhibits Immune Responses and Epithelial Renewal in the *Drosophila* Gut. *Cell Host & Microbe* vol. 12 60–70 Preprint at https://doi.org/10.1016/j.chom.2012.06.001 (2012).

45. Gregorio, E. D. *et al.* An Immune-Responsive Serpin Regulates the Melanization Cascade in *Drosophila*. *Developmental Cell* vol. 3 581–592 Preprint at https://doi.org/10.1016/s1534-5807(02)00267-8 (2002).
46. Gregorio, E. D., De Gregorio, E., Spellman, P. T., Rubin, G. M. & Lemaitre, B. Genome-wide analysis of the *Drosophila* immune response by using oligonucleotide microarrays. *Proceedings of the National Academy of Sciences* vol. 98 12590–12595 Preprint at https://doi.org/10.1073/pnas.221458698 (2001).
47. Combe, B. E. *et al. Drosophila* Microbiota Modulates Host Metabolic Gene Expression via IMD/NF-κB Signaling. *PLoS ONE* vol. 9 e94729 Preprint at https://doi.org/10.1371/journal.pone.0094729 (2014).
48. Gendrin, M. *et al.* Functional Analysis of PGRP-LA in *Drosophila* Immunity. *PLoS ONE* vol. 8 e69742 Preprint at https://doi.org/10.1371/journal.pone.0069742 (2013).
49. Johansson, K., Metzendorf, C. & Soderhall, K. Microarray analysis of immune challenged hemocytes. *Experimental Cell Research* vol. 305 145–155 Preprint at https://doi.org/10.1016/j.yexcr.2004.12.018 (2005).
50. Merkling, S. H. *et al.* The Epigenetic Regulator G9a Mediates Tolerance to RNA Virus Infection in *Drosophila*. *PLOS Pathogens* vol. 11 e1004692 Preprint at https://doi.org/10.1371/journal.ppat.1004692 (2015).
51. Merkling, S. H. *et al.* The heat shock response restricts virus infection in *Drosophila*. *Scientific Reports* vol. 5 Preprint at https://doi.org/10.1038/srep12758 (2015).
52. Ramírez-Camejo, L. A. & Bayman, P. Gene expression on the fly: A transcriptome-level view of *Drosophila*'s immune response to the opportunistic fungal pathogen Aspergillus flavus. *Infection, Genetics and Evolution* vol. 82 104308 Preprint at https://doi.org/10.1016/j.meegid.2020.104308 (2020).
53. Regan, J. C. *et al.* Steroid Hormone Signaling Is Essential to Regulate Innate Immune Cells and Fight Bacterial Infection in *Drosophila*. *PLoS Pathogens* vol. 9 e1003720 Preprint at https://doi.org/10.1371/journal.ppat.1003720 (2013).
54. Roxström-Lindquist, K., Terenius, O. & Faye, I. Parasite-specific immune response in adult *Drosophila melanogaster:* a genomic study. *EMBO reports* vol. 5 207–212 Preprint at https://doi.org/10.1038/sj.embor.7400073 (2004).
55. Sackton, T. B., Lazzaro, B. P. & Clark, A. G. Genotype and Gene Expression Associations with Immune Function in *Drosophila*. *PLoS Genetics* vol. 6

e1000797 Preprint at https://doi.org/10.1371/journal.pgen.1000797 (2010).

56. Seto, Y. & Tamura, K. Extensive Differences in Antifungal Immune Response in Two *Drosophila*Species Revealed by Comparative Transcriptome Analysis. *International Journal of Genomics* vol. 2013 1–15 Preprint at https://doi.org/10.1155/2013/542139 (2013).
57. Short, S. M. & Lazzaro, B. P. Reproductive Status Alters Transcriptomic Response to Infection in Female*Drosophila melanogaster*. *G3 Genes|Genomes|Genetics* vol. 3 827–840 Preprint at https://doi.org/10.1534/g3.112.005306 (2013).
58. Soory, A. & Ratnaparkhi, G. S. SUMOylation of Jun fine-tunes the *Drosophila* gut immune response. *PLOS Pathogens* vol. 18 e1010356 Preprint at https://doi.org/10.1371/journal.ppat.1010356 (2022).
59. Troha, K., Im, J. H., Revah, J., Lazzaro, B. P. & Buchon, N. Comparative transcriptomics reveals CrebA as a novel regulator of infection tolerance in D. melanogaster. *PLOS Pathogens* vol. 14 e1006847 Preprint at https://doi.org/10.1371/journal.ppat.1006847 (2018).
60. Zhu, F., Ding, H. & Zhu, B. Transcriptional profiling of *Drosophila* S2 cells in early response to *Drosophila* C virus. *Virology Journal* vol. 10 Preprint at https://doi.org/10.1186/1743-422x-10-210 (2013).
61. Lemaitre, B. & Miguel-Aliaga, I. The Digestive Tract of *Drosophila melanogaster*. *Annual Review of Genetics* vol. 47 377–404 Preprint at https://doi.org/10.1146/annurev-genet-111212-133343 (2013).
62. De Gregorio, E., Spellman, P. T., Tzou, P., Rubin, G. M. & Lemaitre, B. The Toll and Imd pathways are the major regulators of the immune response in *Drosophila*. *EMBO J.* **21**, 2568–2579 (2002).

63. Trudi Schüpbach, Developmental Biology: Pipe's Smoking Guns, Current Biology, Volume 19, Issue 14, 2009, Pages R548-R550,

Chapter 4

Activity Based Protein Profiling (ABPP) as a tool to map ‘active’ Serine Hydrolases involved in the *Drosophila* innate immune response

Chapter 4

Activity Based Protein Profiling (ABPP) as a tool to map 'active' Serine Hydrolases involved in the *Drosophila* innate immune response

Abstract

The chemical proteomics technique, activity-based protein profiling (ABPP), has proved to be an invaluable tool in assigning function to enzymes in the post-genomic era. The serine hydrolase (SH) enzyme superfamily in particular, has served as an excellent example in displaying the versatility of various ABPP platforms, and has resulted in a comprehensive cataloging of the biochemical activities associated within this enzyme superfamily especially in mammals. Besides SHs, several other enzyme classes in mammals have now been thoroughly investigated using ABPP platforms. Yet, despite significant advances, the utility of ABPP platforms in fly models remains under-explored. Realizing this knowledge gap, leveraging complementary ABPP platforms, in chapter 2, we mapped the full array of SH activities during various stages of development and in different adult tissues in the fruit fly (*Drosophila melanogaster*). In this chapter, using ABPP, we mapped SH activities in adult fruit flies in multiple infection models. Ours studies also suggest existence of sexual dimorphism in SHs activities upon infection. Furthermore, leveraging loss-of-function mutant lines in the canonical Toll/NFκB and Imd/NFκB pathways reveals novel immune-responsive SHs, particularly, CG17192 which is not previously implicated in these signal transduction pathways. Given the conservation of many genes and proteins involved in immune responses between flies and mammals, it is anticipated that orthologous SH genes may play similar roles in human host defense.

Graphical abstract

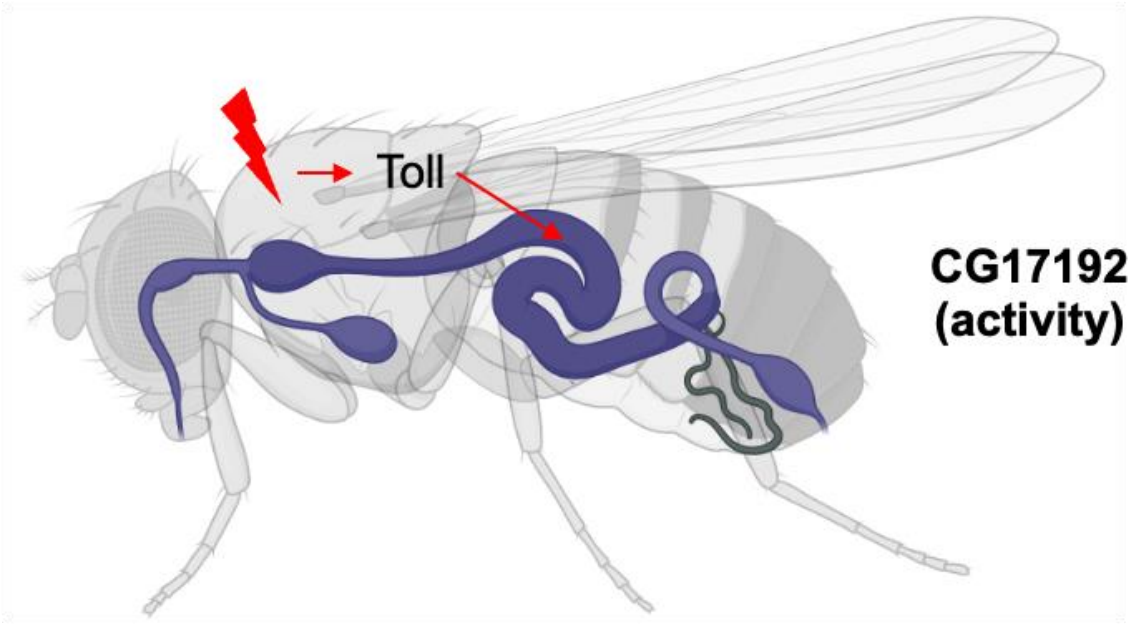

Keyword: ABPP, Chemoproteomics, Serine hydrolase, Immunity, Toll signalling, Melanisation reaction, *Drosophila melanogaster*

Introduction

The chemical proteomics strategy, activity-based protein profiling (ABPP) has significantly expanded our ability to study numerous enzyme families and assign biological functions to uncharacterized members within them, under diverse physiological conditions[1–11]. Briefly, ABPP is a functional proteomic strategy which uses tailored chemical probes (also known as activity-based probes[2–4]) that react with enzyme active sites based on their biochemical activities (or enzymatic mechanisms), and by doing so, allows detecting and quantifying "active" enzymes from native biological settings (e.g. cells, tissues) (for detail- refers to chapter 2). Specifically, over the past two decades, ABPP has been exhaustively used to assign biochemical functions to several unannotated members of the metabolic serine hydrolase (SH) family of enzymes, and this enzyme superfamily in turn, has served as an excellent testing ground for developing diverse ABPP platforms[3,4,12–14]. In mammals, the metabolic SH family comprises of numerous physiological important enzymes such as esterases, lipases, acyltransferases, peptidases, and dysregulation in their biochemical activities is causally linked to pathophysiology and disease in humans[15]. While both ABPP and the metabolic SH enzyme family have been extensively studied in different mammalian systems, till date, they remain somewhat underexplored in other animal model systems.

Over the years, the fruit fly (*Drosophila melanogaster*) has become a popular animal model system owing to its powerful genetic toolkit, and hence, has been used by biologists for discerning various universally conserved physiological mechanisms[16–20]. Yet, in our survey of literature, the use of ABPP in fly models has been sparse. Hence, it is also not surprising, that very little remains known in terms of the diversity in biochemical functions within the metabolic SH family in flies, despite genetic studies

showing a critical role for various serine proteases in important physiological processes[21], such as immune responses[22], and development[23]. Realizing this, using established ABPP platforms, we recently mapped the full array of SH activities (both serine proteases and metabolic SHs) in flies during different stages of development and in various anatomical regions in an adult fly (chapter 2)[24]. Our ABPP studies show despite being “active” at specific developmental stages and in adult tissues, a significant portion (> 80%) of the SH enzyme family in flies remains uncharacterized in terms of a biochemical activity, and in turn, a physiological function (chapter 1)[24]. Following up on our ABPP efforts in cataloguing the active SH enzymes, in this and next chapters, we were specifically interested in assigning biochemical functions to unannotated metabolic SHs that showed differential activity during an immune response (e.g. injury or infection) in flies.

Our literature survey in chapter 3 highlights that SHs get regulated upon infection and more than 30 SHs is known to regulated by immune pathways such as Toll signaling (detailed in chapter 3). Briefly, The Toll pathway involves the activation of pathogen recognition receptors (PRRs) by pathogen-derived immunogens, leading to the activation of a cascade of serine proteases (SPs). Microbial proteases have been shown to directly cleave the proenzyme Psh, leading to the activation of SPE, followed by the activation of Spz. The active Toll receptor recruits Myd88, kinase Pelle, and Tube, which phosphorylate the dorsal inhibitor 'cactus,' causing its degradation. The active Toll pathway activates NF-κB transcription factors Dorsal and Dif, which translocate into the nucleus and regulate the transcription of immune-related genes like antimicrobial peptides (AMPs). However, regulation SHs activity, especially metabolic serine hydrolases by toll signaling upon an immune paradigm is remains to understand.

To this end, in this chapter, using established ABPP platforms[24], we mapped the activity of different SHs in adult flies during multiple injury/infection paradigms. Female flies showed the increased in the SHs activity post infection and A parallel investigation in male flies exhibited no noticeable change in SHs, highlighting a distinct sexual dimorphism during both infection and basal conditions (chapter 2). To understand the signaling cascade which regulated activity of SHs, we tested the mutant models of Toll and melanisation cascade (Figure 4.1)[25,26]. We tested the mutants of *PPO1, modSP, Hayan, psh, dorsal and found* reduced SHs activities compared to wildtype female flies during infection.

From these experiments, we found that the activity of a putative gut-resident lipase from the metabolic SH family, CG17192, significantly increased upon injury/infection in the adult wildtype fly. Further, activity of CG17192 decreased in PPO1 and Hayan mutants which indicated that CG17192 genetically regulated via toll and melanisation

cascade. CG17192 yet to biochemically characterized and determine its role in immune response.

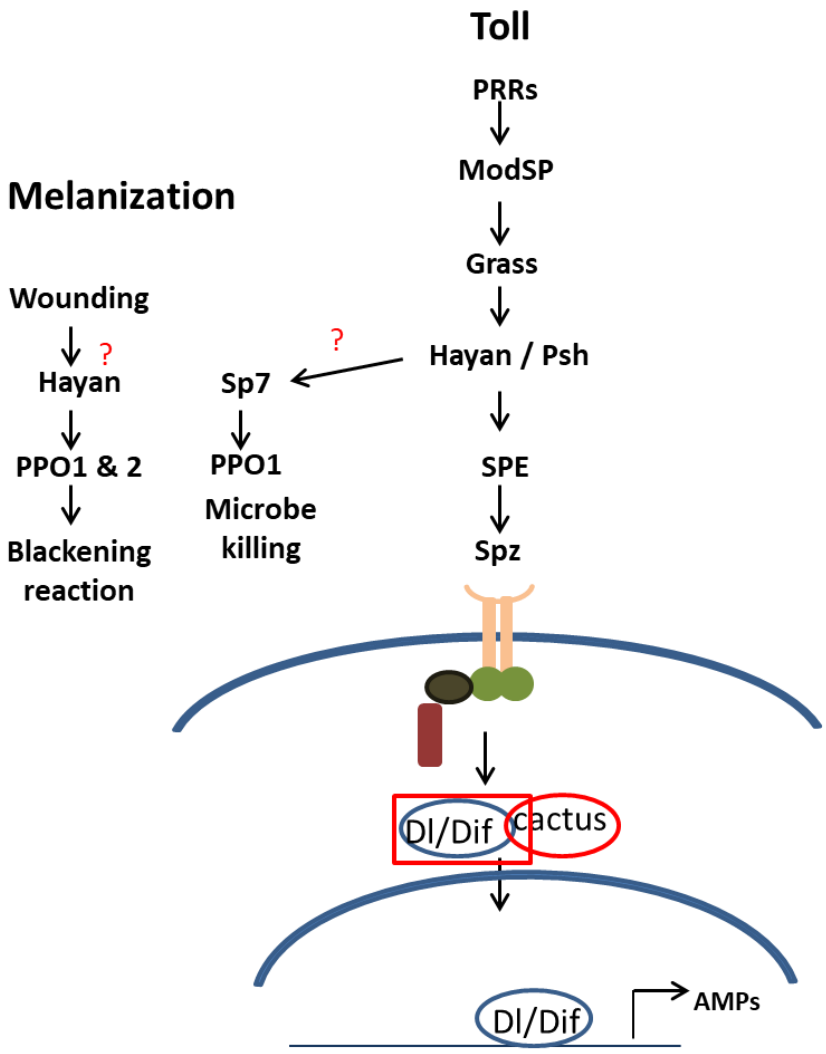

Figure 4.1. Schematic representation of Toll and melanisation pathway of *Drosophila*

(Adapted from (Dudzic et al. 2019).

Material and Methods

Fly Experimentation

The *Drosophila melanogaster* lines, w^{1118}, $PPO1^{BC}$, $Hayan^{34}$, $modSP^{1}$ $Hayanpsh^{def}$ and dl^{1} was grown on standard cornmeal agar medium at 25 °C.

Systemic wounding

For Septic wounding five days old male and female flies were pricked separately on thorax with a needle previously dipped into LPS (10µg/ml)[27], culture of M. luteus (OD-1) and *S. saprophyticus* (OD- 0.5)[28] and incubated in medial containing vials as per experiments.

Gel-based ABPP

All gel-based ABPP experiments were performed using protocols previously reported by us[24]. For all the gel-based ABPP assays, 50 µg of each lysate was incubated with FP-rhodamine (2 µM, 45 min, 37 °C) with constant shaking, following which, the reaction was quenched as reported earlier[24]. All gel-based ABPP samples were resolved on a 12% SDS-PAGE gel, and enzyme activities were visualized by in-gel fluorescence on an iBright1500 (Invitrogen) gel documentation system (**Figure 4.2.A**).

LC-MS/MS Based ABPP

All the proteomics sample preparations for LC-MS/MS based ABPP experiments were performed using established protocols previously reported by us[24,29]. Briefly, in these proteomics assays, 1 mg of lysate was incubated with FP-biotin (20 µM, 60 min, 37 °C with constant shaking), following which, the proteomes were denatured, reductively alkylated using iodoacetamide, and active SHs were enriched using avidin chromatography (**Figure 4.2.B**)[24,29]. Peptides were obtained after on-bead trypsin digestion, and labeled using a reductive demethylation (ReDiMe) protocol reported by

us for quantitative estimation of SH activities(**Figure 4.2.C)**[29,30]. All LC-MS/MS analysis was performed on a Sciex TripleTOF6600 mass spectrometer fitted with a front-end Eksigent nano-LC 425. All columns, LC solvents, LC run conditions and data acquisition parameters were identical to those previously reported by us in detail[24]. All LC-MS/MS proteomics data was searched using the Protein Pilot software (Sciex, version 2.0.1), and ReDiMe labeling (post-tryptic peptide labeling) was used as a criterion in the software for quantification of relative SH activities in these proteomics experiments. Only SH enzymes that were identified and subsequently quantified were filtered for this study.

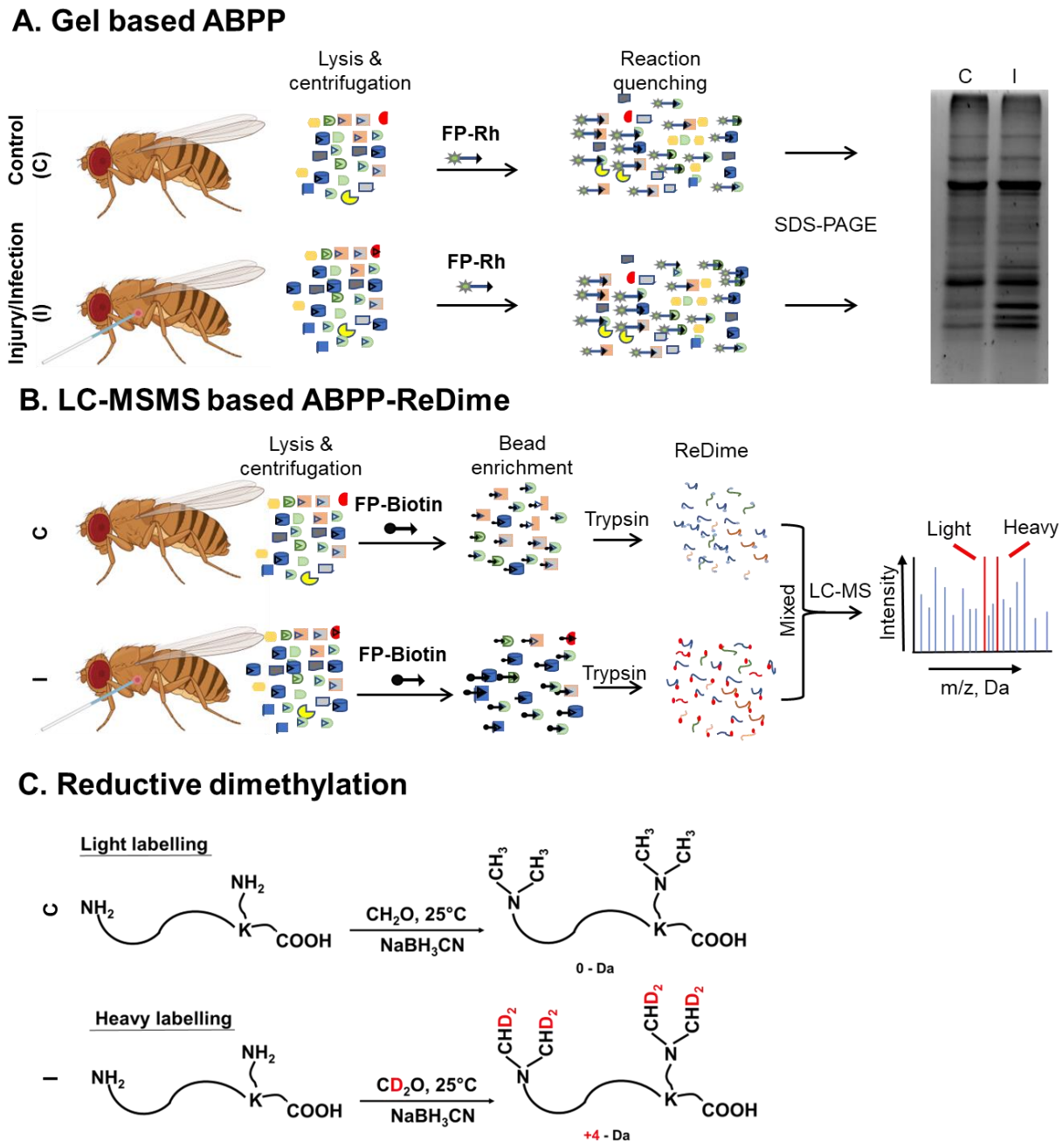

Figure 4.2. Procedure for ABPP.

A general workflow of the LC-MS/MS based quantitative ABPP platform for identifying an quantifying SHs in adult fly lysates from control or LPS-injury groups (A). Gel based ABBPP (B). LC-MSMS based ABPP (C). Chemistry for Reductive dimethylation labelling of tryptic digested peptide

Results

Gel-based ABPP in wildtype (w^{1118}) upon injury and/or Infection (SWR)

We have previously (in chapter 2) reported the use of established gel-based and LC-MS/MS based ABPP platforms to study SH activities in adult flies[34]. Leveraging the aforementioned ABPP platforms, in this study, we wanted to assess if the activity of any SH enzymes changes upon systemic infection in an adult fly. To investigate this, adult female and male flies were injured in the thorax with LPS, *Micrococcus luteus* (a mild pathogen) and *Staphylococcus saprophyticus* (a strong pathogen), and the animal harvested at different time points post-infection. Next, we prepared whole body proteomic lysates of the post-infection harvested adult female and male flies (at different time points), treated these lysates with FP-rhodamine, and using established gel-based ABPP protocols[34, 40], visualized the SH activities in them by in-gel fluorescence (**Figure 4.3**). From this gel-based ABPP experiments, we found that adult female flies showed a significant increase in the activities of a few SH enzymes at 45 min post-infection with LPS (**Figure 4.3.A**). In contrast, adult male flies did not show any discernable change in SH activities upon infection (**Figure 4.3.B**).

Given the heightened immunogenicity of live bacteria compared to LPS, the study was extended to explore sexual dimorphism in SHs activity during SWR with *Micrococcus luteus* and *Staphylococcus saprophyticus*. Five days old male and female flies were injured with *M. luteus* (OD-1) cultures, with unchallenged and sterile-wounded flies as controls. Samples from infected and sterile-wounded male and female flies were collected at 45, 120, and 360 min post-infection or injury. Gel-based ABPP analysis revealed that SHs activity in males remained unchanged post-infection with *M. luteus* (**Figure 4.3.C**) and female flies showed a significant increased SHs activity during infection at 180 min post-infection (**Figure 4.3.D**). Gel-based ABPP on the soluble

fraction of M. luteus lysate indicated negligible bacterial SHs contribution, with bacterial SHs levels much lower than those in the flies (last lane of **Figure 4.3.C and Figure 4.3.D, from left**).

Finally, five days old male and female flies were wounded with a fresh culture of *S. saprophyticus* (OD-0.5). Samples were collected at 0, 120, 180 and 360 min post-infection. Gel-based ABPP analysis demonstrated the disappearance of the active SHs band (30 kDa) in males at 180 and 360 minutes post-SWR compared to the control. As anticipated, females exhibited a robust response to infection with S. saprophyticus at 120 and 180 minutes, with SHs activity returning to normal at 360 minutes post-infection (Figure 4.3.E).

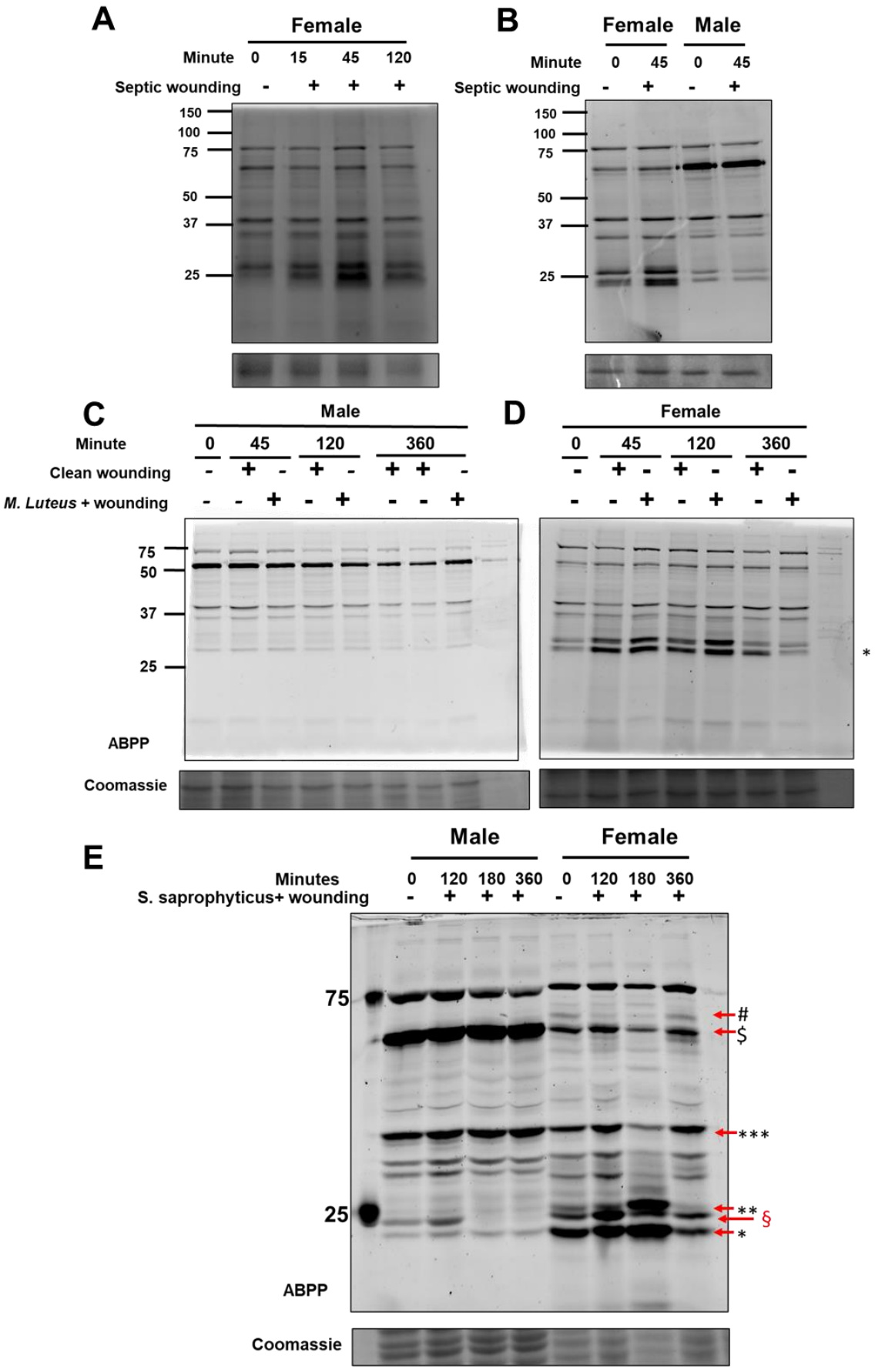
A
Female
Minute 0 15 45 120
Septic wounding - + + +
150
100
75
50
37
25
B
Female Male
Minute 0 45 0 45
Septic wounding - + - +
150
100
75
50
37
25
C
Male
Minute 0 45 120 360
Clean wounding - + - + - + + -
M. Luteus + wounding - - + - + - - +
75
50
37
25
ABPP
Coomassie
D
Female
0 45 120 360
- + - + - + -
- - + - + - +
*
E
Male Female
Minutes 0 120 180 360 0 120 180 360
S. saprophyticus+ wounding - + + + - + + +
75
25
#
$
***
**
§
*
ABPP
Coomassie

Figure 4.3. Mapping SHs activity in wildtype upon injury-infection.
(A). Gel-based ABPP analysis of female soluble lysate post 15, 45, and 105 minutes of systemic wounding with crude LPS extract, indicated as '**+**'. The intensity of 25 kDa activity bands increased post 15 and 45 minutes of septic wounding and decreased at 105 minutes. **(B).** Gel-based ABPP analysis of female and male soluble lysate post 45 minutes of systemic wounding. As expected, the female shows an increase in the intensity of 25 kDa band. But. Surprisingly, males do not show any change SHs activity. (**C** [Male] and **D** [Female]). Gel-based ABPP of male and female fly soluble lysates post 45, 120 and 360 minutes post systemic wounding with *M. luteus* (OD=1). Clean wounding was taken as wound control. Surprisingly, SHs activity intensity remained similar in both systemic wounding and clean wounding in male fly. On the other hand, females responded to systemic as well as clean wound responses for 25kDa SHs activity post 45 and 120 minutes. **(E)** Gel-based ABPP of male and female fly soluble lysates post 120, 180 and 360 minutes post systemic wounding with *S. saprophyticus* (OD=0.5). With more surprise, 25kDa SHs activity in males gets downregulated post 180 and 360 minutes of SWR. As an expected female, Females show an upswing in SHs activity post 120 and 180 of SWR and the intensity of SHs activity back to normal at 360 minutes. Zero minutes is unwounded control, indicated as '**-**', and Coomassie images represents loading control for all images. Gel-based ABPP experiments were done thrice with reproducible results.

Role of NF-κB pathway (Toll and ImD) in SHs activity upon infection

To elucidate the toll pathway regulating serine hydrolase (SH) activity during infection, various mutants associated with Toll pathways were examined for SH activity following infection with LPS. *Hayan*^{34}*, and PPO1*^{BC} the mutant of Toll and melanisation pathway respectively, were examined to understand the regulation of SH activity during LPS infection. *Hayan, and PPO1* null flies were tested for SHs upon LPS-injury. Gel-based ABPP assays revealed that Hayan, and PPO1 null mutants have declined SHs activity compared to wildtype flies during systemic wounding (**Figure 4.4.A**). Thus, extracellular Toll and the melanization cascade were implicated in the regulation of SH

activity during infection in females. Further, investigations were involved testing gram-positive bacteria *M. luteus* and *S. saprophyticus* against Toll mutants to understand their role in regulating SH activity. Male wildtype and dorsal null flies did not exhibit regulation of SH activity upon M. luteus-infection in gel-based ABPP (**Figure 4.4.B**). Whereas, in female, SH activity was not upregulated in dorsal null compared to wildtype during *M. luteus*-infection (**Figure 4.4.C,** marked as '⋆' and '⋆⋆'**)**. However, higher molecular weight SH activity was upregulated during infection in the dorsal null (**Figure 4.4.C,** marked as '⋆⋆⋆' and $). Notably, the strong pathogen *S. saprophyticus* induced increased in SH activity (marked as '⋆') during infection in Toll pathway mutants (i.e. *PPO1, modSP, Hayan, Hayan-psh* and *dorsal* nulls) as similar to wildtype (**Figure 4.4.E**). Also, the higher molecular SHs activity (marked as $) is upregulated in Toll mutants as compared to wildtype (**Figure 4.4.E**). However, male mutant flies do not show any change in SHs activity as expected (**Figure 4.4.D**). In summary, Toll pathway mutants were implicated in the regulation of SH activity during SWR in females exclusively, both with LPS and gram-positive (*M. luteus and S. saprophyticus*) bacterial challenges. Toll pathway activates low molecular weight SHs and suppresses high molecular weight SHs both in the wildtype flies (**Figure 4.4**).

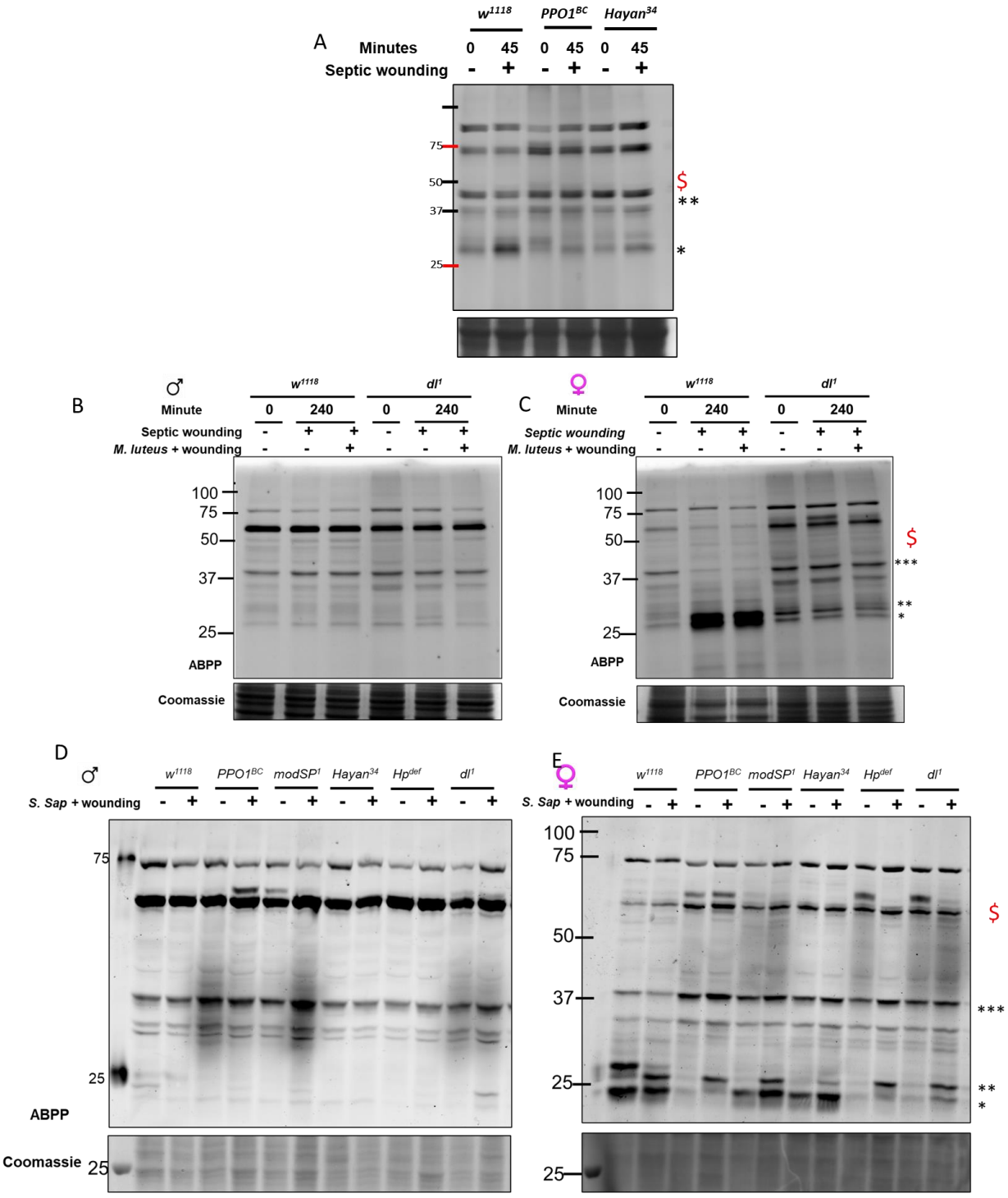

Figure 4.4. SHs activity using gel-based ABPP in mutants of Toll and IMD pathways.

Gel based ABPP analysis of female fly lysates of **(A)** *Hayan*^{34} *and PPO1*^{BC} mutant post 45 minutes of systemic wounding with crude LPS **(B).** On the other hand, gel-based analysis for *Hayan*^{34} *and PPO1*^{BC} mutant female fly revealed that 25kDa SH band (indicated as 'red star') disappeared in the unwounded fly compared to wildtype

unwounded control. Also, 25kda SH activity intensity is downregulated in *Hayan^{34} and PPO1^{BC}* mutant fly post 45 minutes of systemic wounding. Surprisingly, 37kDa (indicated as '**') and 70kDa (indicated as '$') SH activity intensity upregulated in unwounded control *of Hayan^{34} and PPO1^{BC}* mutant fly as compared to wildtype. Gel-based ABPP on w^{1118} female fly post 45 minutes of SWR and unwounded were taken as a control for each experiment. **(C and D)** Gel-based ABPP analysis of male and female fly for *dl^{1}* mutant upon SWR with *M.luteus*. **(C)** SHs activity in male fly remains similar upon SWR in male *dl^{1}* mutant as compared male *w^{1118}.* **(D)** Similar to the result of Hayan34 and dl1, females show down-regulation of 25kDa SHs activity (indicated as '*' and '**') compared to *w^{1118}* upon SWR. Also, 37kDa (indicated as '***') and 70kDa (indicated as '$') SH activity intensity upregulated in unwounded control *of dl^{1}* mutant fly as compared to wildtype. Gel-based ABPP on w^{1118} female fly post 240 minutes of SWR and unwounded were taken as control for each experiment. **(E and F)** Gel-based ABPP analysis of male and female fly for *PPO1^{BC}, modSP^{1}, Hayn^{34}, Hayan-psh^{def} (*abbreviated as *Hp^{def}) and dl^{1}* mutants upon SWR with *S. saprophyticus*. **(E)** SH activity in male fly remains similar upon SWR in male mutants as compared male *w^{1118}.* **(F)** Similar to result of *SWR with M. Luteus*, *PPO1^{BC}, modSP^{1}, Hayn^{34}, Hayan-psh^{def} (*abbreviated as *Hp^{def}) and dl^{1}* mutant female show down-regulation of ~25kDa SHs activity (indicated as '*') as compared to *w^{1118}* upon SWR. Surprisingly, All mutants shows the increase in SHs activity (indicated as '**') as similar to *w^{1118}* upon SWR with S. Saprophyticus except *Hayan^{34}*. Also, 37kDa (indicated as '***') and 70kDa (indicated as '$') SHs activity intensity upregulated in unwounded control *of dl^{1}* mutant fly as compared to wildtype. Gel based ABPP on w^{1118} female fly post 180 minutes of SWR and unwounded were taken as a control for each experiment. Additionally, Coomassie images represents loading control for all images. All Gel-based ABPP experiments were done thrice with reproducible results.

LC-MS/MS (Redime) based ABPP in wildtype (*w^{1118}*) upon infection

For the quantitative identification of serine hydrolases (SHs) regulated during infection in both wildtype and PPO1 and Hayna null flies, the lysates from control and test samples (**Table 4.1**) were subjected to LC-MS/MS (ReDiMe)-based ABPP analysis, following the procedure outlined in the materials and methods. Since we observed the

highest increase in SH activities 45 mins post-infection in wildtype, based on gel-based ABPP experiments, we chose this time point (post-infection) in adult female flies to identify the SHs that may have altered activities during this systemic infection paradigm using LC-MS/MS based ABPP experiment[24,29]. Here, 45 mins post-infection, we harvested the adult female flies, prepared proteomic lysates, treated these lysates with FP-biotin, and prepared samples for quantitative proteomics analysis using established protocols reported earlier (**Figure 4.2**)[24,29,30]. From this LC-MS/MS based ABPP experiment, we identified 32 unique SHs, that were present and quantified in both experimental replicates (**Figure 4.5**). For an enzyme from the SH family to be classified as having increased activity in our experiment, we set a threshold of 1.5 on mean enrichment (heavy/light) ratio from the ReDiMe labeling obtained from both replicates in the LPS treated versus control samples. Based on this filtering criteria, we found that only 5 SH enzymes could be classified as having increased activity from this LC-MS/MS based ABPP analysis, and no SH enzyme showed any decrease in activity (**Figure 4.5, Table 4.2**). Amongst the 5 SHs showing increased activity during the thoracic injury, 4 were serine protease [α-trypsin (A-TRY), CG18493, Jon99Ciii, and CG18180], and only 1 was a metabolic SH [CG17192] (**Figure 4.5, Table 4.2**). Given our long-standing interests in assigning functions to hitherto functionally unannotated enzymes from the metabolic SH family, we decided to biochemically characterize CG17192 further.

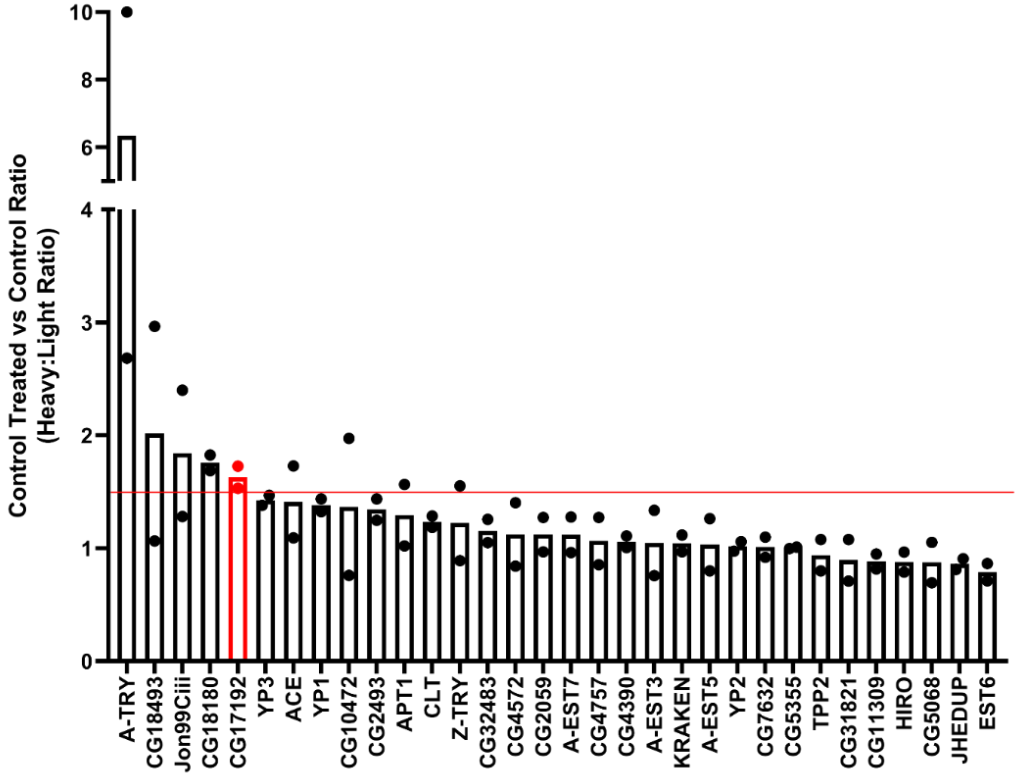

Figure 4.5. Mapping SH activities in adult wildtype flies during infection by ABPP.

LC-MS/MS based ABPP analysis coupled with the established post-tryptic ReDiMe labeling strategy[34, 40, 41] for quantifying SH activities from whole body lysates obtained from adult female flies after injury with LPS (10 µg/mL) or control (PBS) for 45 mins. Data represents mean from two independent proteomics experiments, where each replicate corresponds to the median of the enrichment ratio (heavy/light; heavy for LPS treatment; light for control treatment) for total quantified peptides for each SH. Enrichment ratio from the individual replicate per SH can be found in **Table 2.**

Next, we have observed gel-based ABPP, PPO1 and Hayan null flies showed decrease in activity of SHs at basal or upon LPS-injury (**Figure 4.4.A**). We choose PPO1 and Hayan null flies to identify the SHs that may have altered activities during the systemic infection paradigm using LC-MS/MS based ABPP experiments. In PPO1 and Hayan null LPS-injured flies, the SHs activity CG17192 is decreased by half fold as compared to wildtype LPS-injured fly. (**Figure 4.6.A, Table 4.3** and **Figure 4.6.B,**

Table 4.4). **Also,** CG17192 activity is not seen in Hayan null flies (**Figure 4.6.C, Table 4.5**).

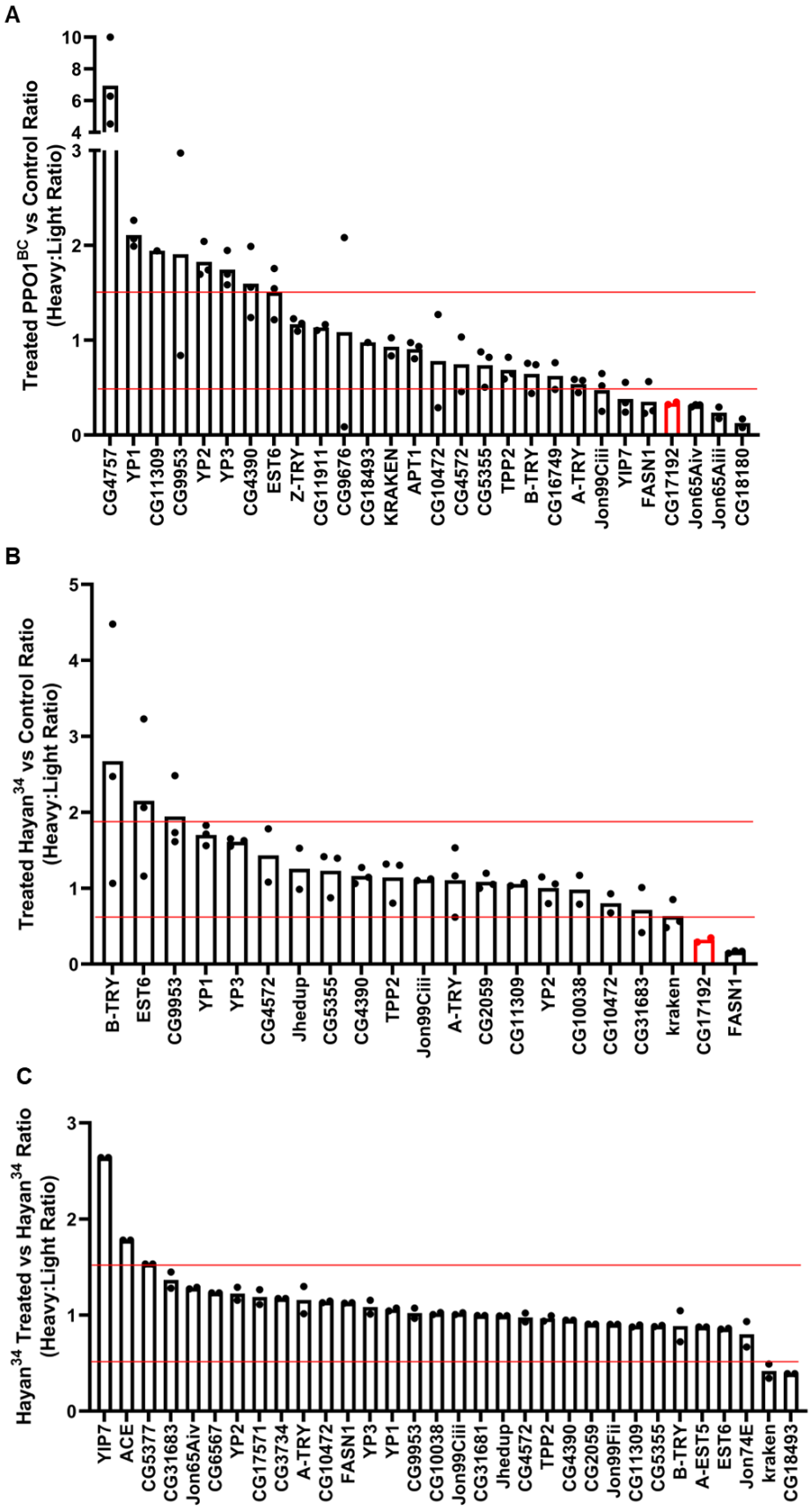

Figure 4.6. CG17192 activities in PPO1 and Hayan mutant as wildtype during infection by ABPP.

(A) Treated $PPO1^{BC}$ vs Control Ratio. (B) Treated $Hayan^{34}$ vs Control Ratio. (C) $Hayan^{34}$ Treated vs $Hayan^{34}$ Ratio**.** Data represents mean from three independent proteomics experiments, where each replicate corresponds to the median of the enrichment ratio (heavy/light; heavy for PPO1 or Hayan mutant; light for wildtype, both were LPS treated) for total quantified peptides for each SH. Enrichment ratio from the individual replicate per SH can be found in **Table 3, Table 4 and Table 5.**

Discussion and conclusion

All organisms produce robust immune responses under various diverse physiological stress conditions (e.g. injury, infection) to achieve a state of homeostasis[31,32]. For invertebrates like fruit flies, during an infection (or injury), the innate immune system works to destroy and/or clear the infective pathogen (or decaying tissue), and in doing so, elicits a response that can be local or systemic, depending on the site, intensity, and type of insult[33–35]. In fact, recent work shows that systemic responses by an organism during infections include alteration in activities of enzymes that induce large-scale changes in physiology and metabolism[36]. Amongst enzymes regulating metabolism, the members of the SH family are known to serve as metabolic lynchpins, and have important physiological roles to play during immune response[15].

Given our interests in assigning functions to hitherto uncharacterized metabolic SHs in *Drosophila melanogaster* (fruit fly), especially during an infection or injury, we performed an ABPP experiment to identify such candidate SH enzymes during a thoracic injury paradigm (Figure 4.3). We have used five days old adults flies, both male and female, to investigate the SHs activities upon systemic wound response in this chapter. This study involves a comprehensive exploration of serine hydrolase (SHs) activity in five days old female *Drosophila* flies subjected LPS-injury (**Figure 4.3.A**). The experimental timeline included incubation periods at 15, 45, and 105

minutes, revealing heightened SHs activity in females at 15 and 45 minutes, returned to baseline levels by 105 minutes post-infection (**Figure 4.3.A**). A parallel investigation in male flies exhibited no noticeable change in SHs activity at 45 minutes post-SWR, highlighting a distinct sexual dimorphism during both SWR and basal conditions (**Figure 4.3.B**). The study extended to explore SHs activity during SWR with *Micrococcus luteus* (a mild pathogen) and *Staphylococcus saprophyticus* (a strong pathogen). Gel-based ABPP analysis on male flies showed unchanged in SHs activity post- infection with *M. luteus (***Figure 4.3.C***)*, whereas, in females, SHs activity increased during infection and returning to normal at 360 minutes post-infection with *M. luteus (***Figure 4.3.D***)*. Lastly, in the case of *S. saprophyticus infection,* male flies exhibited a disappearance of the active SHs band at 180 and 360 minutes post-infection (**Figure 4.3.E**), while females displayed a robust response at 120 and 180 minutes, with SHs activity returning to normal at 360 minutes post-infection (**Figure 4.3.F**). In summary, this chapter, wildtype flies demonstrated a nuanced temporal and sexual dimorphism in SHs activity in response to infection with LPS and pathogenic challenges in *Drosophila*. Depending on pathogenicity, female flies show temporal increased in activity of SHs, as pathogenicity increases, longer periods of the increased SHs activity.

Next, in this chapter, we aimed to unravel the toll pathway governing serine hydrolase (SH) activity during infection by examining various mutants of aforementioned pathway. In modSP, Hayan, and PPO1 null flies, SH activity is decreased compared to wildtype flies during LPS-infection (**Figure 4.4.A**). Also, Further investigations that involved testing the SHs activity in response to gram-positive bacteria *M. luteus* and *S. saprophyticus*, in male wildtype and dorsal null flies, no modulation of SH activity were observed upon infection (**Figure 4.4.B and Figure 4.4.D**). However, in females,

SH activity was not upregulated in dorsal null (dl1) compared to wildtype during infection with M. Luteus, but higher molecular weight SH activity increased (**Figure 4.4.C**). *S. saprophyticus* induced increased in SHs activity during infection in Toll pathway mutants also, similar to wildtype, and higher molecular weight SHs were upregulated in toll mutants compared to wildtype (**Figure 4.4.E**).

Our chemical proteomics screen led us to a gut-resident lipase on unknown function, CG17192 (**Figure 4.5**)[52]. In PPO1 and Hayan null flies, CG17192 activity reduced by half fold compared to wildtype upon infection (**Figure 4.6.A and Figure 4.6.B**). Collectively, these results suggest that CG17192 activity is upregulated during infection and the Toll pathway regu.

This Chapter The chemical proteomics study in this chapter unveiled the temporal modulation and sexual dimorphism in SHs activity in response to LPS and bacterial infection in *Drosophila*. The proteomics study identifies A-TRY, CG18493, Jon99Cii, CG18180, CG17192 as immune responsive SHs. In *PPO1* null flies, A-TRY, Jon99Ciii, CG18180, CG17192 was decrease by more than half fold compared to wildtype in response to infection in both genotypes. In *Hayan* null flies, CG17192 and FASN1 activity was decrease by more than half fold compared to wildtype in response to infection in both genotypes. Thus, CG17192 activity regulated by both melanisation and Toll component. Therefore, CG17192 is taken as candidate immune responsive gene to further characterization in next chapter 5.

Contribution

Dr Kavita Sharma for synthesis of FP-biotin probe.

Acknowledgments

We thank Saddam Shekh for technical assistance with mass spectrometry.

Reference

(1) Serwa, R.; Tate, E. W. Activity-Based Profiling for Drug Discovery. *Chem. Biol.* **2011**, *18* (4), 407–409. https://doi.org/10.1016/j.chembiol.2011.04.002.
(2) Heal, W. P.; Dang, T. H. T.; Tate, E. W. Activity-Based Probes: Discovering New Biology and New Drug Targets. *Chem. Soc. Rev.* **2011**, *40* (1), 246–257. https://doi.org/10.1039/c0cs00004c.
(3) Cravatt, B. F.; Wright, A. T.; Kozarich, J. W. Activity-Based Protein Profiling: From Enzyme Chemistry to Proteomic Chemistry. *Annu. Rev. Biochem.* **2008**, *77* (1), 383–414. https://doi.org/10.1146/annurev.biochem.75.101304.124125.
(4) Niphakis, M. J.; Cravatt, B. F. Enzyme Inhibitor Discovery by Activity-Based Protein Profiling. *Annu. Rev. Biochem.* **2014**, *83* (Volume 83, 2014), 341–377. https://doi.org/10.1146/annurev-biochem-060713-035708.
(5) Willems, L. I.; Overkleeft, H. S.; van Kasteren, S. I. Current Developments in Activity-Based Protein Profiling. *Bioconjug. Chem.* **2014**, *25* (7), 1181–1191. https://doi.org/10.1021/bc500208y.
(6) Willems, L. I.; van der Linden, W. A.; Li, N.; Li, K.-Y.; Liu, N.; Hoogendoorn, S.; van der Marel, G. A.; Florea, B. I.; Overkleeft, H. S. Bioorthogonal Chemistry: Applications in Activity-Based Protein Profiling. *Acc. Chem. Res.* **2011**, *44* (9), 718–729. https://doi.org/10.1021/ar200125k.
(7) Jeffery, D. A.; Bogyo, M. Chemical Proteomics and Its Application to Drug Discovery. *Curr. Opin. Biotechnol.* **2003**, *14* (1), 87–95. https://doi.org/10.1016/s0958-1669(02)00010-1.
(8) Greenbaum, D.; Baruch, A.; Hayrapetian, L.; Darula, Z.; Burlingame, A.; Medzihradszky, K. F.; Bogyo, M. Chemical Approaches for Functionally Probing the Proteome. *Mol. Cell. Proteomics MCP* **2002**, *1* (1), 60–68. https://doi.org/10.1074/mcp.t100003-mcp200.
(9) Cravatt, B. F. Activity-Based Protein Profiling – Finding General Solutions to Specific Problems. *Isr. J. Chem.* **2023**, *63* (3–4), e202300029. https://doi.org/10.1002/ijch.202300029.
(10) Jessani, N.; Young, J. A.; Diaz, S. L.; Patricelli, M. P.; Varki, A.; Cravatt, B. F. Class Assignment of Sequence-Unrelated Members of Enzyme Superfamilies by Activity-Based Protein Profiling. *Angew. Chem. Int. Ed Engl.* **2005**, *44* (16), 2400–2403. https://doi.org/10.1002/anie.200463098.
(11) Jessani, N.; Cravatt, B. F. The Development and Application of Methods for Activity-Based Protein Profiling. *Curr. Opin. Chem. Biol.* **2004**, *8* (1), 54–59. https://doi.org/10.1016/j.cbpa.2003.11.004.
(12) Liu, Y.; Patricelli, M. P.; Cravatt, B. F. Activity-Based Protein Profiling: The Serine Hydrolases. *Proc. Natl. Acad. Sci. U. S. A.* **1999**, *96* (26), 14694–14699. https://doi.org/10.1073/pnas.96.26.14694.
(13) Bachovchin, D. A.; Cravatt, B. F. The Pharmacological Landscape and Therapeutic Potential of Serine Hydrolases. *Nat. Rev. Drug Discov.* **2012**, *11* (1), 52–68. https://doi.org/10.1038/nrd3620.
(14) Simon, G. M.; Cravatt, B. F. Activity-Based Proteomics of Enzyme Superfamilies: Serine Hydrolases as a Case Study*. *J. Biol. Chem.* **2010**, *285* (15), 11051–11055. https://doi.org/10.1074/jbc.R109.097600.
(15) Long, J. Z.; Cravatt, B. F. The Metabolic Serine Hydrolases and Their Functions in Mammalian Physiology and Disease. *Chem. Rev.* **2011**, *111* (10), 6022–6063. https://doi.org/10.1021/cr200075y.

(16) Hales, K. G.; Korey, C. A.; Larracuente, A. M.; Roberts, D. M. Genetics on the Fly: A Primer on the *Drosophila* Model System. *Genetics* **2015**, *201* (3), 815–842. https://doi.org/10.1534/genetics.115.183392.
(17) Rajan, A.; Perrimon, N. Of Flies and Men: Insights on Organismal Metabolism from Fruit Flies. *BMC Biol.* **2013**, *11* (1), 38. https://doi.org/10.1186/1741-7007-11-38.
(18) Bier, E. *Drosophila*, the Golden Bug, Emerges as a Tool for Human Genetics. *Nat. Rev. Genet.* **2005**, *6* (1), 9–23. https://doi.org/10.1038/nrg1503.
(19) Bilder, D.; Irvine, K. D. Taking Stock of the *Drosophila* Research Ecosystem. *Genetics* **2017**, *206* (3), 1227–1236. https://doi.org/10.1534/genetics.117.202390.
(20) Jennings, B. H. *Drosophila* – a Versatile Model in Biology & Medicine. *Mater. Today* **2011**, *14* (5), 190–195. https://doi.org/10.1016/S1369-7021(11)70113-4.
(21) Cao, X.; Jiang, H. Building a Platform for Predicting Functions of Serine Protease-Related Proteins in *Drosophila* Melanogaster and Other Insects. *Insect Biochem. Mol. Biol.* **2018**, *103*, 53–69. https://doi.org/10.1016/j.ibmb.2018.10.006.
(22) Levashina, E. A.; Langley, E.; Green, C.; Gubb, D.; Ashburner, M.; Hoffmann, J. A.; Reichhart, J.-M. Constitutive Activation of Toll-Mediated Antifungal Defense in Serpin-Deficient *Drosophila*. *Science* **1999**, *285* (5435), 1917–1919. https://doi.org/10.1126/science.285.5435.1917.
(23) Cho, Y. S.; Stevens, L. M.; Sieverman, K. J.; Nguyen, J.; Stein, D. A Ventrally Localized Protease in the *Drosophila* Egg Controls Embryo Dorsoventral Polarity. *Curr. Biol.* **2012**, *22* (11), 1013–1018. https://doi.org/10.1016/j.cub.2012.03.065.
(24) Kumar, K.; Mhetre, A.; Ratnaparkhi, G. S.; Kamat, S. S. A Superfamily-Wide Activity Atlas of Serine Hydrolases in *Drosophila* Melanogaster. *Biochemistry* **2021**, *60* (16), 1312–1324. https://doi.org/10.1021/acs.biochem.1c00171.
(25) Chakrabarti, S.; Liehl, P.; Buchon, N.; Lemaitre, B. Infection-Induced Host Translational Blockage Inhibits Immune Responses and Epithelial Renewal in the *Drosophila* Gut. *Cell Host Microbe* **2012**, *12* (1), 60–70. https://doi.org/10.1016/j.chom.2012.06.001.
(26) Buchon, N.; Broderick, N. A.; Poidevin, M.; Pradervand, S.; Lemaitre, B. *Drosophila* Intestinal Response to Bacterial Infection: Activation of Host Defense and Stem Cell Proliferation. *Cell Host Microbe* **2009**, *5* (2), 200–211. https://doi.org/10.1016/j.chom.2009.01.003.
(27) Imler, J. L.; Tauszig, S.; Jouanguy, E.; Forestier, C.; Hoffmann, J. A. LPS-Induced Immune Response in *Drosophila*. *J. Endotoxin Res.* **2000**, *6* (6), 459–462.
(28) Hegde, S.; Sreejan, A.; Gadgil, C. J.; Ratnaparkhi, G. S. SUMOylation of Dorsal Attenuates Toll/NF-κB Signaling. *Genetics* **2022**, *221* (3), iyac081. https://doi.org/10.1093/genetics/iyac081.
(29) Kelkar, D. S.; Ravikumar, G.; Mehendale, N.; Singh, S.; Joshi, A.; Sharma, A. K.; Mhetre, A.; Rajendran, A.; Chakrapani, H.; Kamat, S. S. A Chemical-Genetic Screen Identifies ABHD12 as an Oxidized-Phosphatidylserine Lipase. *Nat. Chem. Biol.* **2019**, *15* (2), 169–178. https://doi.org/10.1038/s41589-018-0195-0.
(30) Kamat, S. S.; Camara, K.; Parsons, W. H.; Chen, D.-H.; Dix, M. M.; Bird, T. D.; Howell, A. R.; Cravatt, B. F. Immunomodulatory Lysophosphatidylserines Are Regulated by ABHD16A and ABHD12 Interplay. *Nat. Chem. Biol.* **2015**, *11* (2), 164–171. https://doi.org/10.1038/nchembio.1721.
(31) Lemaitre, B.; Hoffmann, J. The Host Defense of *Drosophila* Melanogaster. *Annu. Rev. Immunol.* **2007**, *25* (Volume 25, 2007), 697–743. https://doi.org/10.1146/annurev.immunol.25.022106.141615.

(32) Saharan, O.; Kamat, S. S. Mapping Lipid Pathways during Phagocytosis. *Biochem. Soc. Trans.* **2023**, *51* (3), 1279–1287. https://doi.org/10.1042/BST20221424.
(33) Buchon, N.; Silverman, N.; Cherry, S. Immunity in *Drosophila* Melanogaster--from Microbial Recognition to Whole-Organism Physiology. *Nat. Rev. Immunol.* **2014**, *14* (12), 796–810. https://doi.org/10.1038/nri3763.
(34) Hoffmann, J. A. The Immune Response of *Drosophila*. *Nature* **2003**, *426* (6962), 33–38. https://doi.org/10.1038/nature02021.
(35) Ferrandon, D.; Imler, J.-L.; Hetru, C.; Hoffmann, J. A. The *Drosophila* Systemic Immune Response: Sensing and Signalling during Bacterial and Fungal Infections. *Nat. Rev. Immunol.* **2007**, *7* (11), 862–874. https://doi.org/10.1038/nri2194.
(36) Troha, K.; Ayres, J. S. Metabolic Adaptations to Infections at the Organismal Level. *Trends Immunol.* **2020**, *41* (2), 113–125. https://doi.org/10.1016/j.it.2019.12.001.

Supplementry Tables

Table 4.2. SH identified from the LC-MS/MS based ABPP experiment shown in Figure 4.5.

FlyBase ID	Gene Symbol	Treated vs Control Ratio (Heavy:Light Ratio)	
		Replicate 1	Replicate 2
FBgn0003863	A-TRY	2.68431592	10
FBgn0038701	CG18493	1.06433296	2.96634698
FBgn0003357	Jon99Ciii	1.28148699	2.40127993
FBgn0036024	CG18180	1.68840301	1.82662702
FBgn0039472	**CG17192**	**1.53188801**	**1.727386**
FBgn0004047	YP3	1.46932399	1.38030303
FBgn0000024	ACE	1.72917104	1.09210205
FBgn0004045	YP1	1.43784905	1.32329905
FBgn0035670	CG10472	0.76027638	1.97358501
FBgn0032864	CG2493	1.43749404	1.24838996
FBgn0042138	APT1	1.56620598	1.021631
FBgn0000326	CLT	1.28546202	1.18587804
FBgn0011556	Z-TRY	0.89109367	1.55386996
FBgn0052483	CG32483	1.05016601	1.25726998
FBgn0038738	CG4572	1.40285206	0.84209919
FBgn0029942	CG2059	1.27358306	0.96855801
FBgn0015575	A-EST7	0.96157849	1.27836096
FBgn0027584	CG4757	1.27292001	0.85550648
FBgn0038771	CG4390	1.10878801	1.006006
FBgn0015571	A-EST3	1.33571994	0.75755292
FBgn0020545	KRAKEN	1.117203	0.96939868
FBgn0261393	A-EST5	1.26317596	0.79973447
FBgn0005391	YP2	0.97485203	1.059762
FBgn0037071	CG7632	0.92083597	1.09983206
FBgn0032242	CG5355	1.01056004	0.99878222
FBgn0020370	TPP2	1.07734799	0.80014098
FBgn0051821	CG31821	0.71042693	1.07834005
FBgn0037070	CG11309	0.81800032	0.95025039
FBgn0035154	HIRO	0.79068828	0.96662641
FBgn0035951	CG5068	1.05156398	0.69505793
FBgn0034076	JHEDUP	0.90777922	0.81277257

FBgn0000592	EST6	0.86480349	0.71187317

Table 4.3. SH identified from the LC-MS/MS based ABPP experiment shown in Figure 4.6.A.

Flybase ID	Gene Symbol	Treated PPO1^{BC}vs Control Ratio (Heavy:Light Ratio)		
		Replicate 1	**Replicate 2**	**Replicate 3**
FBgn0027584	CG4757	6.28381777	10	4.534293175
FBgn0004045	YP1	2.26386499	1.990427971	2.069669962
FBgn0037070	CG11309	1.94202197		
FBgn0005391	YP2	1.69390905	1.740743995	2.041670084
FBgn0004047	YP3	1.947685	1.584897041	1.697613001
FBgn0038771	CG4390	1.23856199	1.56014204	1.98843205
FBgn0000592	EST6	1.75533497	1.543949008	1.215284944
FBgn0035726	CG9953	2.9734149		0.839494526
FBgn0011556	Z-TRY	1.22744	1.178915977	1.095918059
FBgn0042138	APT1	0.93405253	0.974433422	0.805367827
FBgn0031249	CG11911	1.10321403		1.164932013
FBgn0032242	CG5355	0.87829107	0.505838513	0.820911229
FBgn0030773	CG9676	2.08251309		0.087957323
FBgn0020370	TPP2	0.82063371	0.592619121	0.646095514
FBgn0010357	B-TRY	0.43870771	0.756840408	0.741574585
FBgn0020545	KRAKEN	1.02517903		0.835606813
FBgn0003863	A-TRY	0.57602799	0.448823392	0.586875618
FBgn0035670	CG10472	1.27233303		0.289155603
FBgn0038738	CG4572	1.03320706		0.45849359
FBgn0003357	Jon99Ciii	0.64917833	0.251327813	0.519350529
FBgn0037678	CG16749	0.76397967		0.481499702
FBgn0040060	YIP7	0.2421874	0.556613803	0.342115015
FBgn0283427	FASN1	0.25675899	0.229680106	0.563760281
FBgn0038701	CG18493	0.97757733		
FBgn0250815	Jon65Aiv	0.2967501	0.320512205	0.318880588
FBgn0039472	**CG17192**	**0.3227098**		**0.348707914**
FBgn0035665	Jon65Aiii	0.29616451	0.174202696	
FBgn0036024	CG18180	0.17099001		0.079793379

Table 4.4. SH identified from the LC-MS/MS based ABPP experiment shown in Figure 4.6.B.

Flybase ID	Gene Symbol	Treated Hayan^{34} vs Control Ratio (Heavy:Light Ratio)		
		Replicate 1	Replicate 2	Replicate 3
FBgn0010357	B-TRY	4.479047775	2.473011017	1.06407702
FBgn0000592	EST6	2.063946962	3.230360031	1.160030007
FBgn0035726	CG9953	1.614653945	1.733387947	2.482947111
FBgn0004045	Yp1	1.715327978	1.828287005	1.56160295
FBgn0004047	Yp3	1.628088951	1.650702	1.55240798
FBgn0038738	CG4572		1.784544945	1.079923034
FBgn0034076	Jhedup	0.985892773	1.525985003	
FBgn0032242	CG5355	1.396389961	1.41582799	0.875817776
FBgn0038771	CG4390	1.062000036	1.145594954	1.272706032
FBgn0020370	TppII	1.318534017	1.303038001	0.803012788
FBgn0003357	Jon99Ciii	1.102651	1.124047995	
FBgn0003863	A-TRY	1.162327051	1.533125043	0.619577289
FBgn0029942	CG2059	1.197710991	0.99808228	1.053089976
FBgn0037070	CG11309	1.072232008		1.034502983
FBgn0005391	Yp2	1.150876045	1.057890058	0.799037576
FBgn0038013	CG10038	0.790609777		1.170649052
FBgn0035670	CG10472	0.677426279	0.92729032	
FBgn0051683	CG31683	1.01075995	0.415912509	
FBgn0020545	kraken	0.852658093	0.563602209	0.482775688
FBgn0039472	CG17192		0.348194093	0.290863693
FBgn0283427	FASN1	0.175313801	0.170974195	0.1449368

Table 4.5. SH identified from the LC-MS/MS based ABPP experiment shown in Figure 4.6.C.

Flybase ID	Gene Symbol	Hayan[34] Treated vs Hayan[34] Ratio (Heavy:Light Ratio)	
		Replicate 1	Replicate 2
FBgn0040060	yip7	2.640119672	2.640119672
FBgn0000024	ACE	1.779885232	1.779885232
FBgn0038974	CG5377	1.531805905	1.531805905
FBgn0051683	CG31683	1.28051554	1.448871981
FBgn0250815	Jon65Aiv	1.289986937	1.274067952
FBgn0037842	CG6567	1.231262947	1.231262947
FBgn0005391	YP2	1.155507773	1.290098878
FBgn0259998	CG17571	1.111228559	1.264824175
FBgn0038700	CG3734	1.173784305	1.173784306
FBgn0003863	A-TRY	1.299195325	1.01591706
FBgn0035670	CG10472	1.145450899	1.130352481
FBgn0283427	FASN1	1.129786806	1.126340899
FBgn0004047	YP3	1.011779844	1.155531569
FBgn0004045	YP1	1.044825143	1.074392648
FBgn0035726	CG9953	0.967910658	1.073956478
FBgn0038013	CG10038	1.027890664	1.006089531
FBgn0003357	Jon99Ciii	1.006296062	1.025697121
FBgn0051681	CG31681	0.995244694	0.995244693
FBgn0034076	Jhedup	0.992851996	0.993152269
FBgn0038738	CG4572	0.929973591	1.021569719
FBgn0020370	TPP2	0.937969258	0.993370197
FBgn0038771	CG4390	0.94763381	0.94763381
FBgn0029942	CG2059	0.905646135	0.905646135
FBgn0039777	Jon99Fii	0.903875576	0.903875576
FBgn0037070	CG11309	0.876815742	0.898822315
FBgn0032242	CG5355	0.881037474	0.894526371
FBgn0010357	B-TRY	1.046648466	0.723179802
FBgn0261393	A-EST5	0.878249959	0.878249959
FBgn0000592	EST6	0.861690869	0.855077952
FBgn0023197	Jon74E	0.932844382	0.668629314
FBgn0020545	kraken	0.491392886	0.343587596
FBgn0038701	CG18493	0.391765708	0.391765708

Chapter 5

Drosophila CG17192 is a phospholipase C that is secreted in the gut lumen in response to infection

Cover Art: Chemoproteomics and lipidomic approach for CG17192 characterization

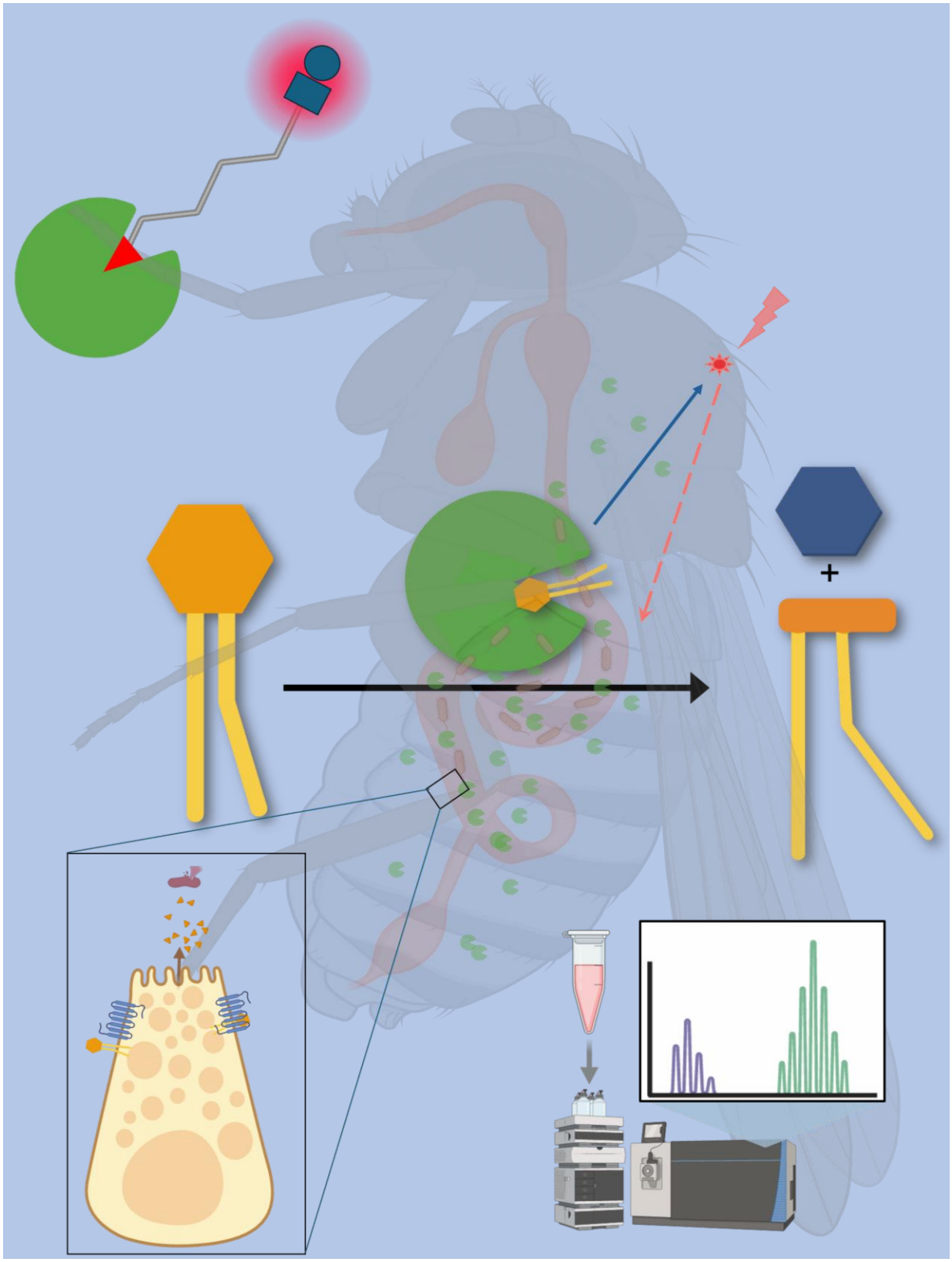

Chapter 5

Drosophila CG17192 is a phospholipase C that is secreted in the gut lumen in response to infection

Abstract

Assigning functions to enzymes in the post-genomic era has really benefitted from the emergence of LC-MS/MS based technologies like chemical proteomics and metabolomics/lipidomics. While the fruit fly (*Drosophila melanogaster*) has proved to be an invaluable tool in the field of genetics, both the aforementioned LC-MS/MS technologies have had very sparse use in the animal model system, especially towards finding functions to enzymes. Realising this research gap, in chapter 1 and 2, We first, generated the Serine hydrolase database and catalogue the SHs activity in various developmental stage and adult organs. In chapter 4, We mapped the SHs activity during different infection models of the *Drosophila* and identify CG17192 as a potential target to charterisation. In this chapter, to assign a biological function to CG17192 as-of-yet uncharacterized lipase, we performed an untargeted lipidomics analysis and found that phosphatidylinositols were significantly elevated when *CG17192* was knocked down in the adult fruit fly gut. Next, we overexpressed this putative lipase in insect cells and using biochemical assays, we show that CG17192 is a secreted enzyme that has phospholipase-C (PLC) type activity with phosphatidylinositol being a preferred substrate. Finally, we show during infection, that heightened CG17192 regulates phosphatidylinositol levels, and by doing so, likely modulates signaling pathways in the adult fruit fly gut that might be involved in the resolution of this pathophysiological condition. This chapter, with CG17192, we

demonstrate the complementary use of ABPP platforms, lipidomic and biochemical assays in assigning functions to enzymes in different physiological contexts.

Graphical Abstract

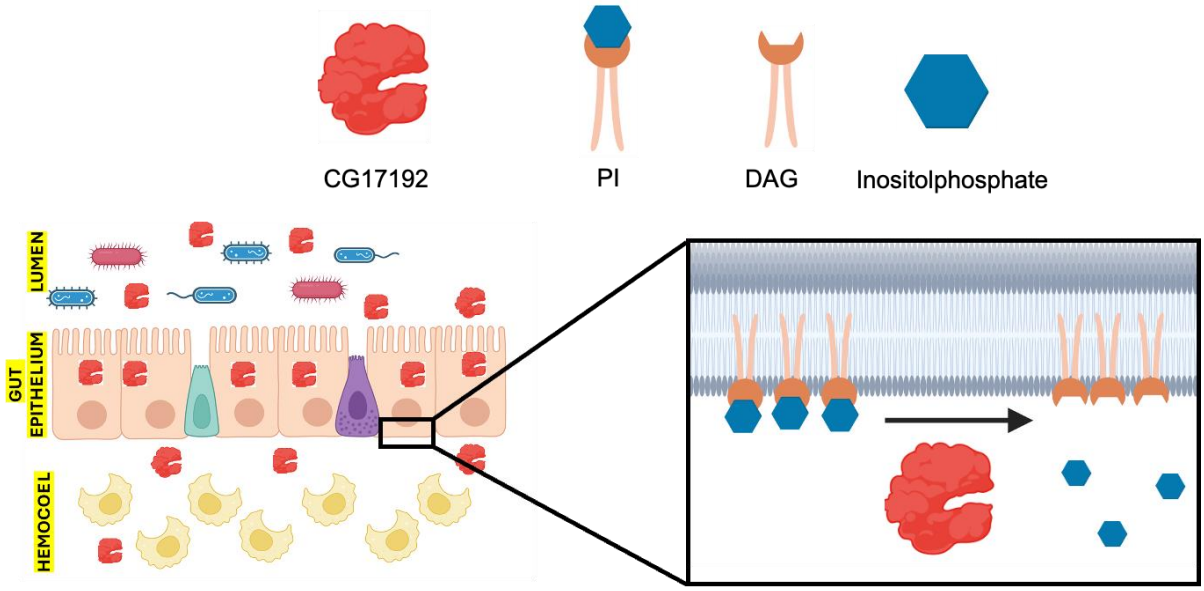

Keywords: *Drosophila melanogaster*; Serine Hydrolases; ABPP; infection; CG17192; Secretory enzyme; Phospholipase C; Lipid metabolism; Phosphatidylinositol

Introduction

Advances in DNA sequencing technologies over the past three decades have resulted in an explosion in the number of available unique protein sequences across different organisms[1]. Yet, various reported estimates and databases suggest that only a small fraction of the total available proteins have been biochemically characterized and/or have correctly assigned biological functions[2,3]. Of note, the extent of mis-annotations in publicly available databases is perhaps the highest for enzymes, given the diversity in their biochemical activities[3,4]. Thus, based on this knowledge gap, assigning functions to proteins, especially enzymes, still remains a major challenge for modern biochemists and chemical biologists in the post-genomic era. Realizing this, the past few years has seen the development of numerous bioinformatics tools, and artificial intelligence driven efforts towards assigning functions to enzymes[5–10]. While these computational tools and bioinformatics approaches have certainly helped facilitate efforts in curating mis-annotations across public databases, the development and application of high-throughput experimental biochemical strategies continue to remain the holy grail in identifying and functionally characterizing hitherto unannotated enzymes performing as-of-yet unknown biological reactions.

To this end, we build the SHs database in *Drosophila melanogaster* and bioinformatically group into various categories based on protein sequence and predicted protein structure (Chapter 1)[11]. To functionally annotate SHs, we generated the full array of SHs activity (Activity atlas of SHs) during fly development and various adult organs (Chapter 2)[11]. We particulary interested in the characterizing metabolic SHs that involved in the *Drosophila*'s immune response. In chapter 3, our literature survey enumerated the novel SHs that involved in the *Drosophila* immune response. Follow-up of literature foundation of SHs that involves in the immunity, in chapter 4,

using ABPP platforms, we mapped the activity of various SHs in adult flies subjected multiple infection models. This analysis revealed that the activity of CG17192, a likely gut-associated lipase from the metabolic SH family, showed a significant increase in activity in response to in the adult flies. Further, we show that CG17192 activity is epistatic regulated by Toll pathway component upon infection in the adult fly.

To complement the ABPP study, in this chapter 5, we generated a fly line, where CG17192 activity was depleted in the adult gut. Next, using an untargeted lipidomics approach, we show that phosphatidylinositol (PI) metabolism is dysregulated in the guts of adult flies that have diminished CG17192 activity. Further, by ABPP and biochemical assays using recombinant CG17192, we show that this as-of-yet unannotated metabolic SH has phospholipase C (PLC) type activity with PI being the best substrate for this lipase. Finally, we show that in the context of a gut-specific infection, CG17192 modulates PI metabolism, and by doing so, presumably plays in important role in regulating levels of bioactive lipids that are known to be central to signaling pathways in all organisms.

Material and Methods

Fly Experimentation

The following *Drosophila melanogaster* lines, *UAS-CG17192^{RNAi}* (BDSC 56042)*, UAS-mCherry^{RNAi}* (BDSC 35785), *NP1-GAL4^{ts}* (*Myo31DF-Gal4*;*UAS-GFP;tub*-Gal80^{ts})[12,13] were used in this study. The RNAi lines were procured from the Bloomington *Drosophila* Stock Center (BDSC), and grown on standard cornmeal agar medium in a 12-hour light-dark cycle. *UAS-CG17192^{RNAi}* is a Valium20 line generated at the Harvard Medical School as part of the transgenic RNAi project[14]. The *CG17192* mRNA was reduced in the adult gut enterocytes by crossing *UAS-CG17192^{RNAi}* to *NP1-Gal4^{ts}*,

with mock expression of *UAS-mCherry*^{RNAi} as a control. The Gal4/Gal80^{ts} system allows temporal regulation of Gal4. The crosses were set up at 20 ^{o}C, where the Gal80^{ts} effectively suppressed Gal4 activity. Post-eclosion, the animals were shifted to 29 ^{o}C, which increased Gal4 activation, and 5-6 days old flies were used for all experiments reported here. The well-established *Pseudomonas entomophilia* oral infection paradigm was used for the gut infection studies, as reported previously[15].

Real Time qPCR (RT-qPCR)

The guts from adult flies were dissected surgically, and RNA was extracted from them using the RNAiso Plus extraction reagent (TaKaRa, Catalog No.: 9108) as per manufacturer's instructions. The extracted RNA was air-dried, re-suspended in nuclear free water, and treated with TURBO^{TM} DNase (ThermoFisher Scientific, Catalog No.: AM2238) as per manufacturer's instructions to get rid of any contaminant DNA from the RNA preparation. The RNA concentration was measured using a nano-drop spectrometer (ThermoFisher Scientific, Catalog No.: ND-2000c), and 1 μg of isolated RNA was used for first-strand cDNA synthesis using the High-Capacity cDNA Reverse Transcription Kit (ThermoFisher Scientific, Catalog No.: 4374966) as per manufacturer's protocols. Next, all real time quantitative PCR (RT-qPCR) experiments were performed using the iTaq Universal SYBR Green Supermix Kit (Bio-Rad, Catalog No.: 1725124) on a CFX96 Touch Real-Time PCR Detection System (Bio-Rad) using standard RT-qPCR protocols. Fold inductions in transcript levels were determined using the ΔΔCt method, and all transcript levels were normalized to *rp49*. The complete list of primers used in this RT-qPCR experiment are listed in **Table 5.1**.

Untargeted Lipidomics

All untargeted lipidomics studies were performed on the guts of adult flies, where 1 biological replicate comprised of guts pooled from 20 adult flies. The pooled adult fly

guts were lysed in 0.5 mL of cold sterile PBS using a Bullet Blender (Next Advance) at an instrument setting of 10 for 5 mins, following which, a 20 μL aliquot of the resulting lysate was kept aside for determination of protein concentration using the BCA Protein Determination Kit (ThermoFisher Scientific, Catalog No.: 23225). The remaining lysate was transferred to a glass vial, and vigorously mixed with 1.5 mL of 2:1 chloroform ($CHCl_3$): methanol (MeOH) containing an internal standard mix [1 nmol each of pentadecanoic acid (Sigma-Aldrich, Catalog No.: P6125, for negative ion mode analysis) and C17:0/20:4 phosphatidylcholine (Avanti Polar Lipids, Catalog No.: LM-1002, for positive ion mode analysis)]. The resulting mixture was centrifuged at 1500g for 15 mins to separate the aqueous (top) and organic (bottom) layers, and the organic layer (bottom) was gently pipetted into a new glass vial. To enrich the extraction of phospholipids, the aqueous layer was acidified using 50 μL formic acid (Merck, Catalog No.: 5.33002), and further vigorously mixed with 1 mL of $CHCl_3$. The resulting mixture was again separated by centrifugation at 1500g for 15 min, and the organic layer (bottom) was separated and pooled with the organic extract from the previous extraction. The pooled organic phase was dried under a stream of nitrogen gas, re-solubilized with 500 μL of $CHCl_3$, and transferred to another glass vial, to remove any trace aqueous contamination. The organic layer was dried again under a stream of nitrogen gas, re-solubilized in 200 μL of 2:1 $CHCl_3$: MeOH, and 10 μL of this was injected into an Agilent 6545 Quadrupole Time-of-Flight (QTOF) LC-MS/MS instrument for untargeted lipidomics measurements in each ion mode (positive and negative). A standard untargeted lipidomics run in the positive or negative ion mode consisted of 60 mins, and the LC columns, solvents and solvent gradients were identical to those previously reported by us[16–19]. All LC-MS/MS experiments were performed using an electrospray ionization (ESI) source with the following parameters:

drying and sheath gas temperature = 320 ^{o}C; drying and sheath gas flow rate = 10 L/min; fragmentor voltage = 150 V; capillary voltage = 4 kV; nebulizer pressure = 45 psi; nozzle voltage = 1 kV. For the analysis of different lipids from the adult fly guts, a Personal Compound Database Library (PCDL) curated for lipids was generated, and peaks corresponding to lipids were verified based on relative retention times, mass error threshold (20 ppm or less at MS1), and MS/MS fragments obtained. All lipid species were quantified by measuring the area under the curve relative to the respective internal standard, and then normalizing this to the protein concentration of the respective sample.

Overexpression of CG17192 in Insect Cells

The *CG17192* gene (encoding CG17192) was amplified from a laboratory generated cDNA[20] library of the adult fly, and cloned into the *pRmHa3* vector[21,22] with a C-terminal FLAG epitope. Using site directed mutagenesis techniques, the catalytic serine (S179) was mutated to an alanine, to yield the S179A variant of CG17192 in the same *pRmHa3* vector. All primers used for generating the constructs are listed in **Table 5.1**. To study the biochemical functions of CG17192, we decided to overexpress this protein in Schneider 2 (S2) insect cells. For our experiments, S2 cells were cultured in Gibco Schneider's *Drosophila* medium (ThermoFisher Scientific, Catalog No.: 21720024) supplemented with 10% (v/v) heat-inactivated fetal bovine serum (FBS) (ThermoFisher Scientific, Catalog No.: 10082147) at 25 ^{o}C, and transfected with 1 μg of plasmid per mL of cells (at 30% confluence) in 12 well plates using TransIT-Insect transfection reagent (Mirus Bio, Catalog No.: 6100) as per manufacturer's instructions. 2 hours after transfection, the expression of *CG17192* was induced by adding 500 μM $CuSO_4$ to the same medium, and allowing the cells to grow for another 48 hours, at which point, the cells and secreted media were harvested. The secreted media was

separated from the cells by centrifugation of the culture at 500g for 15 mins at 18 ^{o}C. The resulting cell pellet was washed with cold sterile 1x-phosphate buffered saline (PBS) (2 times), re-suspended in 1 mL cold sterile PBS, lysed by sonication and separated in the membrane and soluble proteomic fractions as reported earlier[11]. Expression of CG17192 in the membrane, soluble and secreted media proteomic fractions was confirmed by gel-based ABPP (reported earlier in this section) and Western blot analysis using previously reported protocols[20,23,24], with Ponceau S staining (Sigma-Aldrich, Catalog No.: A40000279) used to confirm equal protein loading. Mouse anti-FLAG (Sigma-Aldrich, Catalog No.: F1804) and anti-Mouse conjugated to horseradish peroxidase (HRP) (ThermoFisher Scientific, Catalog No.: 31430) were used as the primary and secondary antibodies respectively for this Western blot analysis. The Western blots were developed with the Immobilon western chemiluminescent HRP substrate (Merck Millipore, Catalog No.: WBKLS0500), and imaged on a Syngene G-Box Chemi-XRQ gel documentation system.

Table 5.1. Primers used in this study.

S. No.	Primer Sequence (5' to 3')	Primer Description
1	TGCAGGAACTTGTTCCCATG	Primer pair for RT-qPCR amplification of CG17192
2	GAGCCTCACTGTTTACAGGC	
3	GACGCTTCAAGGGACAGTATCTG	Primer pair for RT-qPCR amplification of rp49
4	AAACGCGGTTCTGCATGAG	
5	GAATTCGAGCTCGGTACCATGAGGGAGTTATTTTTTCTAGCAGC	Primers for amplification of CG17192 from cloning into the pRmHa3 vector
6	TCACTTATCATCATCATCCTTGTAATCCTTCTTATTCGCTCGCTGTTC	
7	CAGGTCGACTCTAGAGGATCCCTACTTATCATCATCATCCTTGTAATC	
8	TGATTGGACATGCCTTGGGTGCCCATGTG	Primer pair for generating the S179A mutant
9	TGGGCACCCAAGGCATGTCCAATCACCTC	

Substrate assays

The sample preparation for substrate assays (lipase activity) was similar to that previously reported by us[16,23,25,26]. Briefly, 20 µg of the secreted media was incubated with 100 µM of the phospholipid substrate [C18:0/18:0 phosphatidylcholine (PC) (Avanti Polar Lipids, Catalog No.: 850365); C16:0/18:1 phosphatidylethanolamine

(PE) (Avanti Polar Lipids, Catalog No.: 850757); C18:0/18:1 phosphatidylserine (PS) (Avanti Polar Lipids, Catalog No.: 840039); and C17:0/20:4 phosphatidylinositol (PI) (Avanti Polar Lipids, Catalog No.: LM1502)] in sterile PBS to a final volume of 120 µL at 37 °C with constant shaking in a 1.5 mL glass vial (Eppendorf, Thermo Mixer C). After letting the reaction proceed to 45 mins, it was quenched with 360 µL of 2:1 $CHCl_3$: MeOH. The mixture was vortexed vigorously and centrifuged at 2300g to separate the aqueous (top) and organic (bottom) phases. The organic phase was gently separated by pipetting into another glass vial and dried under a stream of nitrogen gas. The dried organic extracts from the lipase reactions were resolubilized in 150 µL of 2:1 $CHCl_3$: MeOH for LC-MS/MS analysis. This reconstituted organic extract was injected into an Agilent G6125B single quadrupole LC/MSD and analyzed using an electrospray ionization (ESI) source in both the positive and negative ion mode (10 µL used in each mode). The LC separation was performed using a Gemini 5U C-18 column (Phenomenex) coupled with a Gemini guard column (Phenomenex, 4x3 mm, Phenomenex security cartridge). The solvents used were buffer A: 95:5 = Water: MeOH; and buffer B = 60:35:5 = Isopropanol: MeOH: water. For better ionization, 0.1% (v/v) formic acid + 10 mM ammonium formate was used in the solvents for the positive ion mode analysis, while 0.1% (v/v) ammonium hydroxide was used in the solvents for the negative ion mode analysis. All runs were 15 mins, starting with 0.3 mL/min 100% buffer A for 1.5 mins, 0.5 mL/min linear gradient to 100% buffer B over 5 mins, 0.5 mL/min 100% buffer B for 5.5 mins, and equilibration with 0.5 mL/min 100% buffer A for 3 mins. The following MS parameters were used for all the substrate assays: drying gas flow = 10 L/min, nebulizer pressure = 45 psi, drying gas temperature = 250 °C, capillary voltage = 4 kV. The product release was quantified by measuring the area under the curve for the respective analyte and normalizing this to the mock controls.

The substrate hydrolysis rate was further corrected by subtracting the non-enzymatic rate of hydrolysis, which was obtained by using heat-denatured (15 min at 95 °C) control proteomes as reported earlier[16,26,27]. In these substrate assays, PLA1 or PLA2-type phospholipase activity was determined by measuring free fatty acid release, while PLD-type activity was determined by measuring phosphatidic acid release from the different phospholipid substrates tested in the negative ion mode. On the other hand, PLC-type phospholipase activity was determined by measuring diacylglycerol (DAG) release from the different phospholipid substrates tested in the positive ion mode.

Bacterial clearance test and life span

Bacterial clearance test was performed using previous protocol[13,15]. Briefly, Five days old flies starved for two hours and then fed sugar solution of *P. entemophila* (OD-200) for two hours. For bacterial load, two hours fed flies were lysed in sterile 1XPBS and plated on LA plate contain appropriate antibiotics in serial dilution. For bacterial clearance, Two hours fed flies transferred to fresh media contain vial and incubated for 6 hours and then, flies were assayed for bacterial load.

Results

Lipidomics characterization in the adult gut upon CG17192 knockdown

To date, CG17192 remains an uncharacterized member of the metabolic SH family of enzymes. Both UniProt[28] (ID: Q9VB92) and FlyBase[29] (DmeI/CG17192) broadly classify CG17192 as a lipase, based on sequence homology to known lipases from other organisms. In addition, both publicly available large-scale gene expression analysis[30,31] (**Figure 5.1**) and our previously reported SH activity atlas[11] for the different tissues in adult flies suggest that *CG17192* has highest expression and enzymatic activity in the adult fly gut respectively.

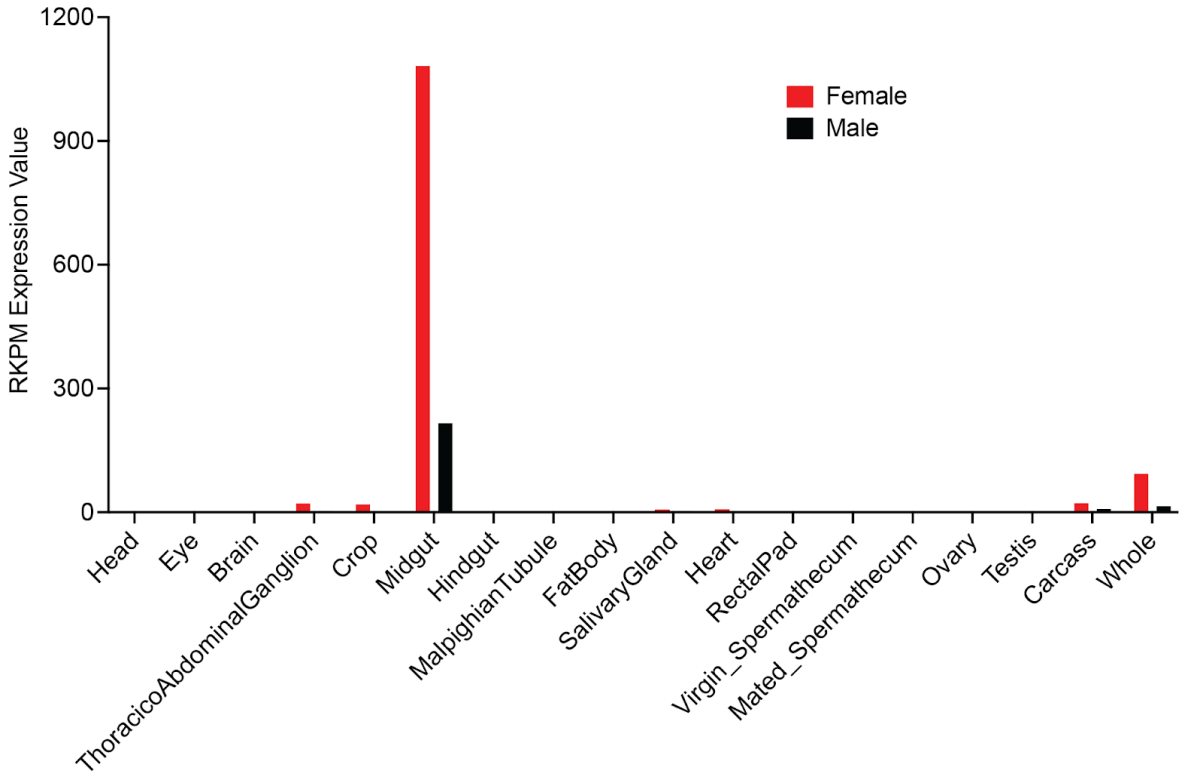

Figure 5.1. Expression of CG17192 in different fly tissues.
The mRNA levels of CG17192 in different anatomical regions of the adult female and male fly as per publicly available transcriptomics data from the FlyBase database.

Given this specific anatomical localization and enzymatic activity, we decided to knockdown *CG17192* in the guts of adult flies (both female and male) by crossing UAS-*CG17192*^{RNAi} with *NP1-Gal4*^{ts} to generate the *CG17192*^{RNAi}/*NP1-Gal4*^{ts} fly line (referred to as *CG17192-KD* fly line from here on). The control experiment had the genotype *NP1-Gal4*^{ts}/+; *UAS-mCherry*^{RNAi}/+ (referred to as WT from here on) (**Figure 5.2**).

FLY STOCKS

1. CG17192 RNAi Genotype (from BDSC, Valium20): *y1, sc*, v1, sev21; P{TRiP.HMC04350}attP40*

2. mCherry RNAi (from BDSC, Valium20)*: y1, sc*, v1, sev21*P{y[+t7.7] *v[+t1.8]=VALIUM20-mCherry.RNAi}attP2*

3. *NP-Gal4*^{ts}: *w*; *Myo31DF-Gal4*, *UAS-GFP*, *tub-gal80*^{ts}

CROSSES

I. Knockdown of *CG17192* mRNA in Gut enterocytes (referred to as ***CG17192-KD***):

Parents: *w; NP1-Gal4*^{ts} X *v*^{1}*; UAS-CG17192*^{RNAi}

↓

F1: *w*/*v*^{1}; *NP1-Gal4*^{ts}/*UAS-CG17192*^{RNAi}

II. Knockdown of *mCherry* mRNA in Gut enterocytes (Mock Control, referred to as ***WT***):

Parents: *NP1-Gal4*^{ts} *X UAS-mCherry*^{RNAi}

↓

F1: *NP1-Gal4*^{ts}/+; *UAS-mCherry*^{RNAi}/+

Figure 5.2. Workflow of the crosses towards generating the WT and CG17192-KD adult fly lines used in this study.

To assess the extent of reduction in the expression of this putative lipase in the adult fly guts, we harvested guts from adult flies of WT and *CG17192-KD* genotype, and assessed the relative expression of *CG17192* by standard RT-qPCR analysis (**Figure 5.3.A**). Based on this experiment, we found that relative to the WT fly line, CG17192 had substantially reduced expression (> 90%) in the guts of the *CG17192*-KD fly line (**Figure 5.3.A**). Having established the depletion of *CG17192* expression in the guts of the *CG17192-KD* fly line, next we wanted to assess the lipid pathways influenced by this putative lipase in the guts of adult flies. For this, we again harvested guts from adult flies of WT and *CG17192-KD* genotype (from both female and male), extracted lipids from these tissues using established protocols[16,19,23,27], and used these gut lipidomic extracts to perform an untargeted LC-MS/MS based lipidomics experiment. For any lipid species to be considered significantly changing (or altered) following reduction of *CG17192* in this LC-MS/MS based lipidomics analysis, relative to the WT group, it must have > 2-fold change (increased or decreased) with a stringent *p*-value cut-off < 0.01. Our untargeted lipidomics experiments led to the identification and quantification of > 150 unique lipid species spanning almost all lipid classes (e.g. neutral lipids, phospholipids, sterols, sphingolipids) (**Figure 5.3.B**). Quite strikingly, the only lipid class that showed consistent increase in the guts of both female and male adult flies upon *CG17192* depletion was phosphatidylinositol (PI), with long chain fatty acid variants (e.g. C32 C34, C36) showing the highest accumulation (**Figure 5.3.B**). This untargeted lipidomics experiment thus strongly suggested that CG17192 might possibly function as a phospholipase with PI being the possible substrate in the adult fly gut.

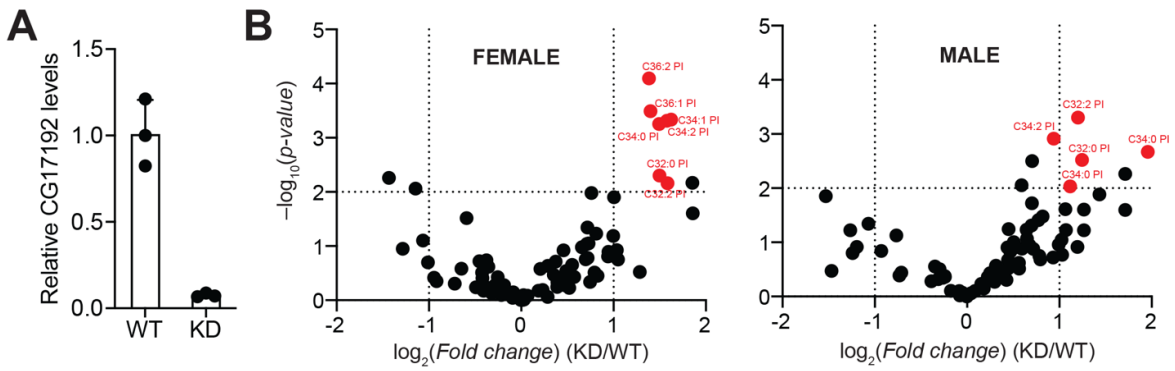

Figure 5.3. Untargeted lipidomics analysis on the adult guts of the CG17192-KD fly line.

(**A**) RT-qPCR analysis to check relative CG17192 expression in the guts of adult female flies from WT or the *CG17192-KD* (KD) fly line. The bar data represents mean ± standard deviation from three biological replicates per genotype. (B) Volcano plots (*left*, female; *right*, male) showing differentially changing lipids in the guts of adult flies from the *CG17192-KD* (KD) fly line relative to the WT fly line (KD/WT) as determined by LC-MS/MS analysis. Each data point represents mean value from three independent biological replicates. The dashed line parallel to the x-axis denotes a cut-off with an adjusted *p*-value of 0.01, while the two dashed lines parallel to the y-axis denote a 2-fold change in relative lipid concentration. Based on these filtering criteria, different PI lipids that significantly accumulate in the adult fly gut (in both female and male) upon CG17192 knockdown are colored and labeled in red.

Expression of CG17192 in S2 cells

Following up on the untargeted lipidomics experiment, next, we wanted to assess the phospholipase activity of CG17192 using biochemical assays. For this, we expressed CG17192 in S2 insect cells, and cloned this putative lipase with a C-terminal FLAG tag. As a negative control for the different biochemical assays, using established site-directed mutagenesis protocols, we also generated an active site S179A mutant in the same plasmid, which based on precedence of other SH enzymes[24, 25], is expected to be catalytically inactive. To account for any “off-target” effects from the plasmid, an empty plasmid (mock) was used as an additional control in all our biochemical experiments. Upon transfecting all the plasmids (i.e. mock, WT

CG17192, and S179A CG17192) in S2 cells, we collected the corresponding transfected cells, and fractionated them into soluble and membrane proteomic fractions using established protocols[34, 40]. Concurrent to harvesting the transfected cells, we also collected the respective secreted media for further biochemical analysis.

First, using reported protocols[11,16], we performed gel-based ABPP assays on the soluble, membrane and secreted media proteomic fractions of the different transfected S2 cells (mock, WT CG17192, and S179A CG17192). Interestingly, we found that WT CG17192 showed maximal activity in the secreted media, to a much less extent in the soluble proteomic fraction, and no activity was observed in the membrane proteomic fraction (**Figure 5.4**). On the other hand, as expected, S2 cells transfected with mock or S179A CG17192 showed no detectable CG17192 activity in any proteomic fraction tested by us (**Figure 5.4**). To assess extent of expression, we performed a Western blot analysis on all proteomic fractions using an anti-FLAG antibody and also did Ponceau S staining for the same samples to ensure equal loading of samples. Based on both these experiments, we found that relative to the mock control, both WT and S179A CG17192 had comparable expression and protein distribution in the soluble and secreted media proteomic fractions, with the protein levels of both WT and S179A CG17192 being highest in the secreted media fractions (**Figure 5.4**). Taken together, these studies collectively show that despite equivalent expression, WT CG17192, but not the S179A mutant, is active and substantially secreted from S2 cells, and that the secreted media from these transfections (i.e. mock, WT C17192, and S179A CG17192) can be used as a proteomic fraction to assay the putative phospholipase activity of CG17192 in subsequent substrate assays.

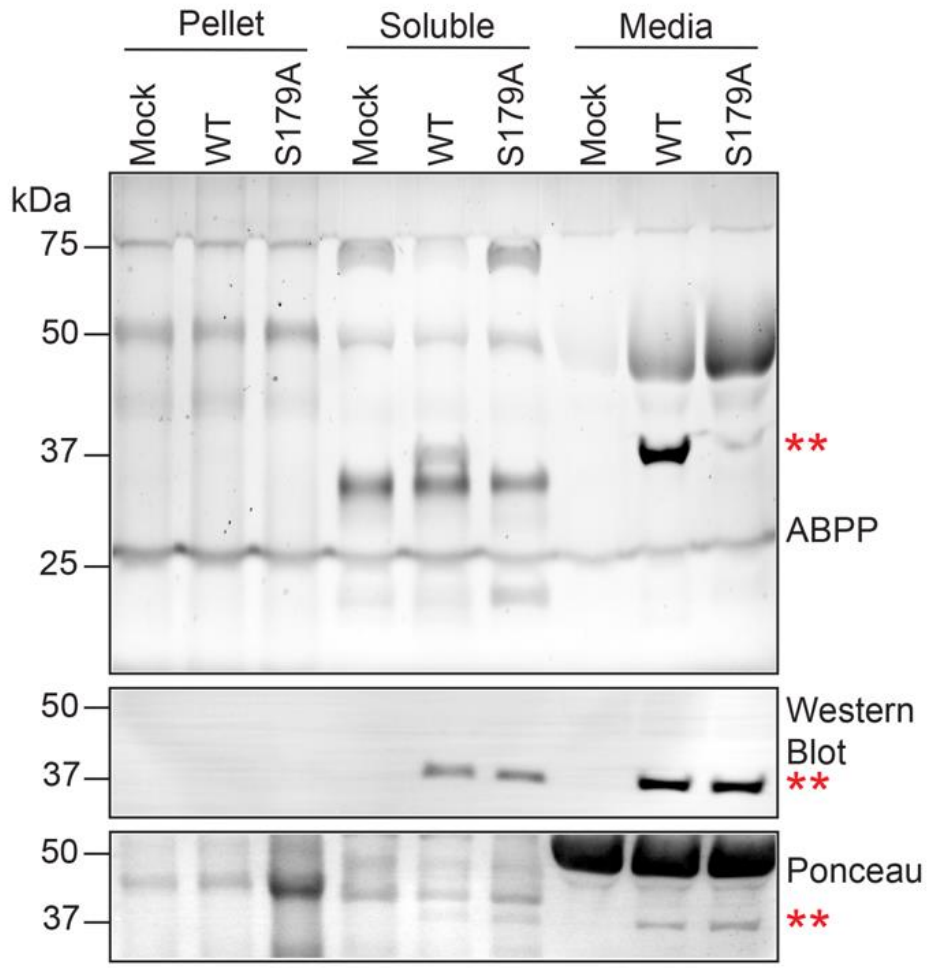

Figure 5.4. Assessing expression and activity of CG17192 in S2 cells.

The various proteomic fractions (membrane, soluble and secreted media) of S2 cells transfected with mock, WT CG17192 or S179A CG17192 were assessed using gel-based ABPP (top panel), Western blot analysis using an anti-FLAG antibody (middle panel), and Ponceau S staining (bottom panel). The double red asterisk corresponds to activity (top panel) or expression (middle and bottom panel) of CG17192. This experiment was done three times with reproducible results each time (Data reproduce from Mrunal MS thesis).

Phospholipase activity of CG17192.

A bioinformatics survey of the polypeptide sequence of CG17192 from UniProt (ID: Q9VB92), showed that besides a canonical lipase domain which contained the invariant catalytic triad (S179, D204 and H269), this putative phospholipase also contained an additional 16-amino acids at N-terminus end of the protein (**Figure 5.5A**).

This 16-amino acid stretch (sequence: MRELFFLAALLVAGNA) corresponds to the sequence of a signaling peptide (as per the Signal algorithm[32] in UniProt) that is predicted to facilitate the secretion of CG17192 from cells (**Figure 5.5A**), and is consistent with our expression studies of CG17192 from S2 cells (**Figure 5.4**). Given this, we hypothesized that perhaps CG17192 is an extracellular (secreted) lipase that acts on membrane phospholipids.

To test, the phospholipase activity of CG17192, we incubated the secreted media from mock, WT CG17192 and S179A C17192 transfected S2 cells with 4 different phospholipids, namely PC, PE, PI and PS. After quenching the reactions, using LC-MS/MS analysis, we looked for all the lipid products arising from the possible PLA1/2-type, PLC-type or PLD-type phospholipase activity of CG17192 (**Figure 5.5B**). From these substrate assays, we found that CG17192 did not possess any PLA1/2-type or PLD-type phospholipase activity. Interestingly, we found that relative to the mock control, WT CG17192, but not the S179A mutant, showed significant PLC-type phospholipase activity against PI (~ 8-fold over mock) and PS (~ 4-fold over mock), with PI being a better substrate for this enzyme (based on the formation of DAG product) (**Figure 5.5C**). Of note, we found that neither PC nor PE were substrates of CG17192 for this PLC-type phospholipase activity (**Figure 5.5C**). Taken together, this PLC-type phospholipase activity of CG17192 fits well with the untargeted lipidomics data (reported earlier in **Figure 5.3B**), in that, the depletion of *CG17192* in the adult fly gut results in a substantial accumulation of PI lipids (substrates for CG17192)

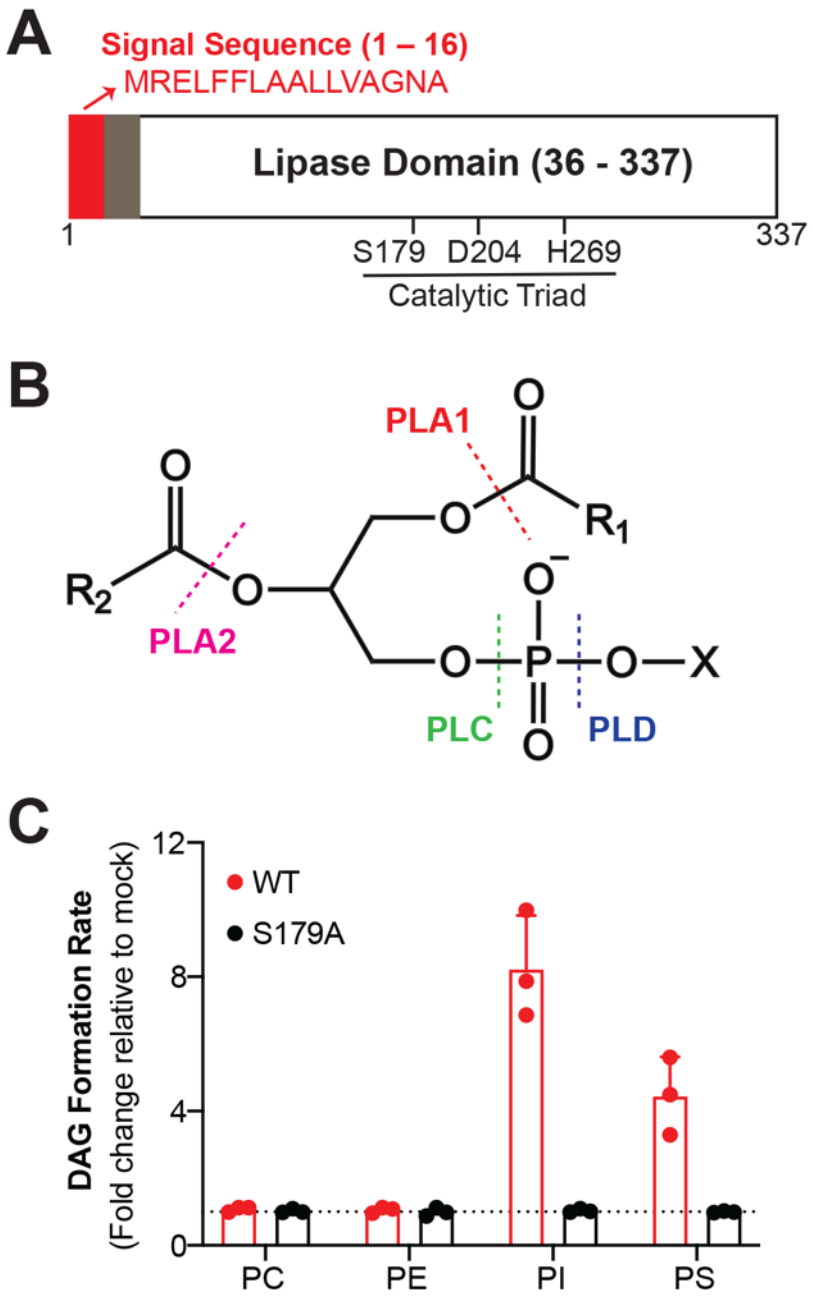

Figure 5.5. Phospholipase activity of CG17192.

(**A**) A bioinformatics analysis shows that full length CG17192 contains a N-terminal signaling peptide and a lipase domain. (**B**) Different types of phospholipase activities. In the phospholipid substrate, X = head group that determines the phospholipid (X = choline for PC, X = ethanolamine for PE, X = inositol for PI, X = serine for PS). (**C**) The PLC-type phospholipase activity shown by WT CG17192, but not the S179A mutant, against various phospholipid substrates tested (PC, PE, PI and PS). The bar data represents mean ± standard deviation from three biological replicates per group. The dashed line parallel to the x-axis denotes a fold change = 1 (i.e. no change in experimental terms relative to the mock control).

Effect of CG17192 activity on PI and DAG levels in the adult gut upon infection

Our untargeted lipidomics analysis on the adult gut upon *CG17192* knockdown, and biochemical assays with recombinant CG17192 taken together showed that PI is the substrate for this PLC-type phospholipase. Therefore, to determine if this was indeed physiologically the case *in vivo* during injury or infection, next, we attempted to quantify the relative levels of both substrate (PI lipids) and product (DAG lipids) of CG17192 in a gut infection paradigm in adult flies. In this experiment, adult WT or *CG17192-KD* flies were subjected to an established gut-specific infection[13,15], and using a previously reported semi-quantitative untargeted lipidomics approach[16,18,34], the relative levels of phospholipids and DAG lipids were quantified across various genotypic groups. We have previously shown that during injury (or infection), CG17192 enzymatic activity increases in adult flies (in the gut) (**Figure 4.5**). From our lipidomics analysis, we find that in WT adult fly guts (female and male), upon infection, the relative levels of PI lipids decrease (substrate of CG17192) (**Figure 5.6A**) with a concomitant increase in the DAG lipids (product of CG17192) (**Figure 5.6B**), consistent with heightened enzymatic activity of CG17192 during a physiological stress.

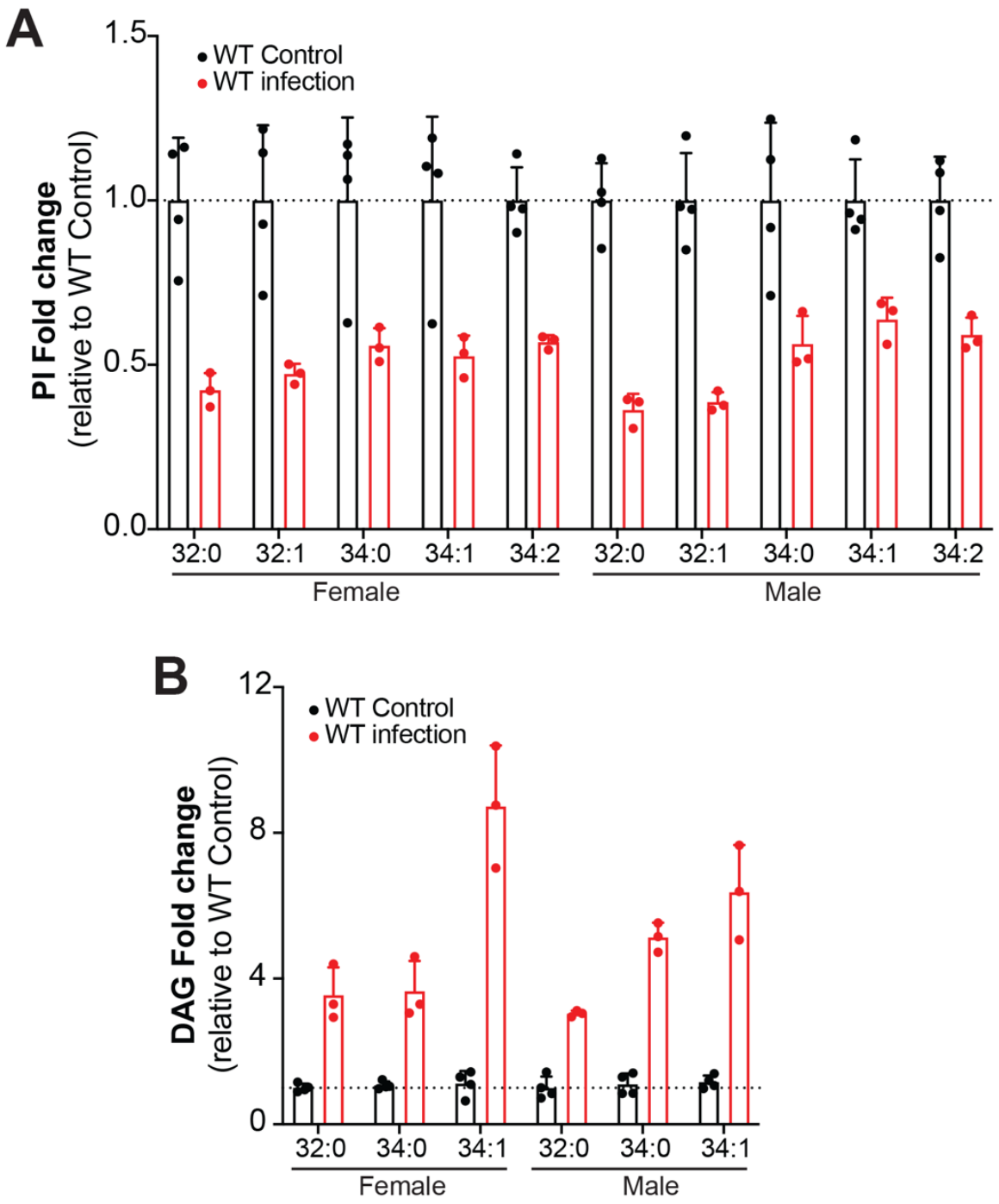

Figure 5.6. Relative PI and DAG levels in the WT adult fly gut upon infection.

Relative levels of (**A**) PI lipid variants and (**B**) DAG lipid variants quantified in the WT adult gut by semi-quantitative untargeted lipidomics measurements as a function of a gut-specific infection paradigm. Bar data represents mean ± standard deviation from three or more biological replicates per genotype. The dashed line parallel to the x-axis denotes a fold change = 1 (i.e. no change in experimental terms relative to the WT uninfected control).

Interestingly, we find that amongst the various phospholipids, this change is unique only to PI lipids, and no other phospholipid class changes consistently in the WT adult gut (female and male) during this infection paradigm (**Figure 5.7**).

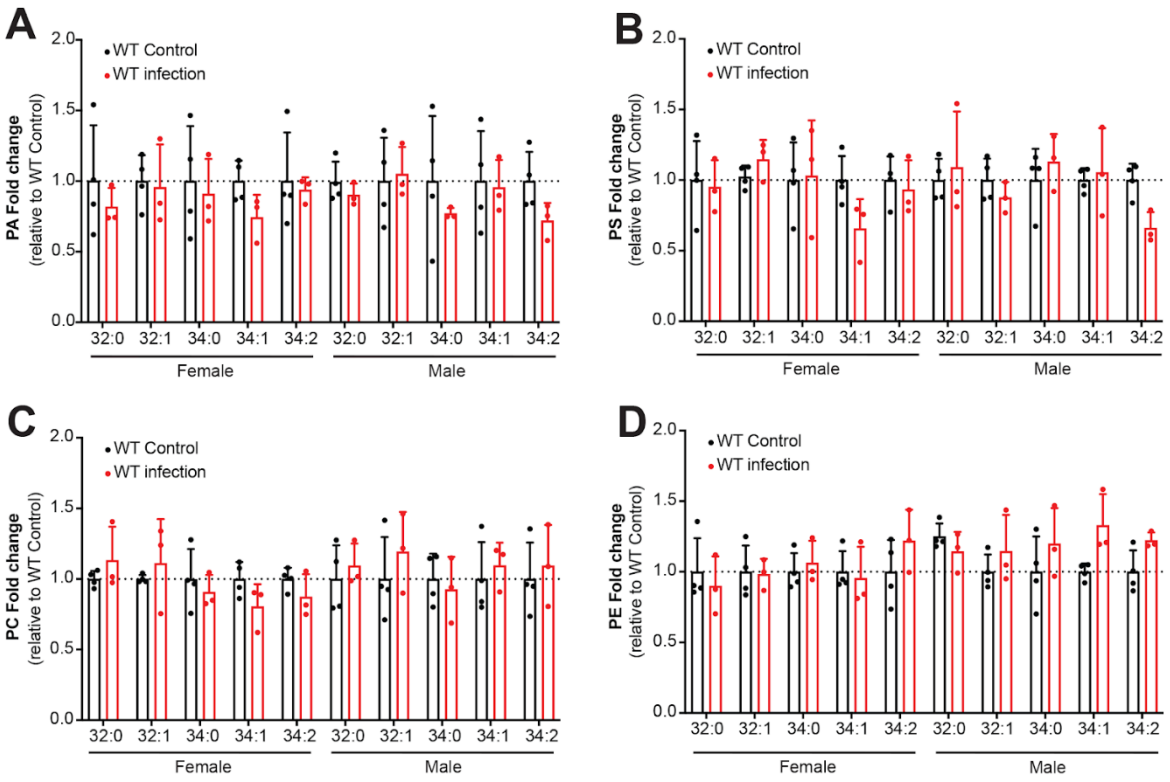

Figure 5.7. Relative phospholipid levels in the WT adult fly gut upon infection. Relative levels of lipid variants of (**A**) Phosphatidic acid (PA), (**B**) Phosphatidylserine (PS), (**C**) Phosphatidylcholine (PC), and (**D**) Phosphatidylethanolamine (PE) quantified in the WT adult gut by semi-quantitative untargeted lipidomics measurements as a function of a gut-specific infection paradigm. Bar data represents mean ± standard deviation from three or more biological replicates per genotype. The dashed line parallel to the x-axis denotes a fold change = 1 (i.e. no change in experimental terms relative to the WT uninfected control).

Finally, relative to adult WT flies, we also quantified the levels of various phospholipids and DAG lipids in the guts of adult *CG17192-KD* flies in the same infection paradigm. Previously, we have seen that under normal physiological conditions, PI metabolism is dysregulated in guts of adult *CG17192-KD* flies (**Figure 5.3B**), and we wanted to see if this metabolic axis is also altered in this genotype during a gut-specific infection. Interestingly, from our semi-quantitative untargeted lipidomics measurements, there was no change in the relative levels of PI lipids in the adult gut (both female and male) upon infection between the WT and *CG17192-KD* flies (**Figure 5.8**). From the same experiment however, we found that corroborating the increased CG17192 activity in adult WT flies and lack thereof in the *CG17192-KD* flies during an infection paradigm, that the relative DAG levels were significantly elevated (~ 3 to 5-fold) in the guts of adult WT flies (but not the *CG17192-KD* flies) (both female and male) upon infection (**Figure 5.8**). In these experiments, we did not observe any change in other phospholipid classes in the adult gut during infection between the WT and *CG17192-KD* genotypes.

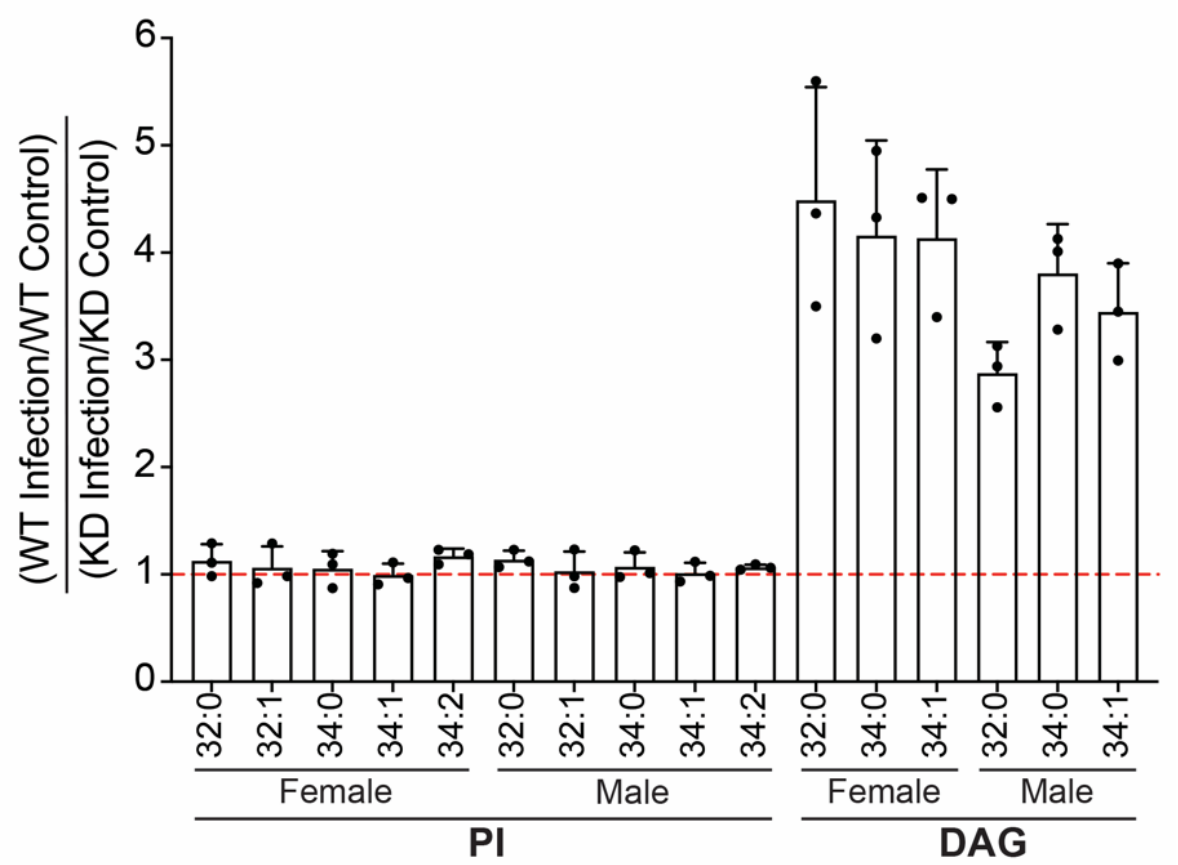

Figure 5.8. PI and DAG levels in the guts of adult WT and *CG17192-KD* flies during an infection.

Relative levels of PI and DAG lipid variants quantified in the guts of adult WT and *CG17192-KD* flies by semi-quantitative untargeted lipidomics measurements during a gut-specific infection. Bar data represents mean ± standard deviation from three independent experiments (three biological replicates per genotype). The dashed line parallel to the x-axis denotes a ratio = 1 (i.e. no change in experimental terms relative to the WT genotype).

CG17192 knockdown favor the host to clear infecting bacteria

We tested the influence of CG7192KD to clear the ingested bacteria. We perform the bacterial clearance test on control and CG7192KD male and female flies. We observe that female CG7192KD flies clear ingested bacteria faster than female control. However, male control and CG7192KD flies clear ingested bacteria simultaneously (**Figure 5.9**).

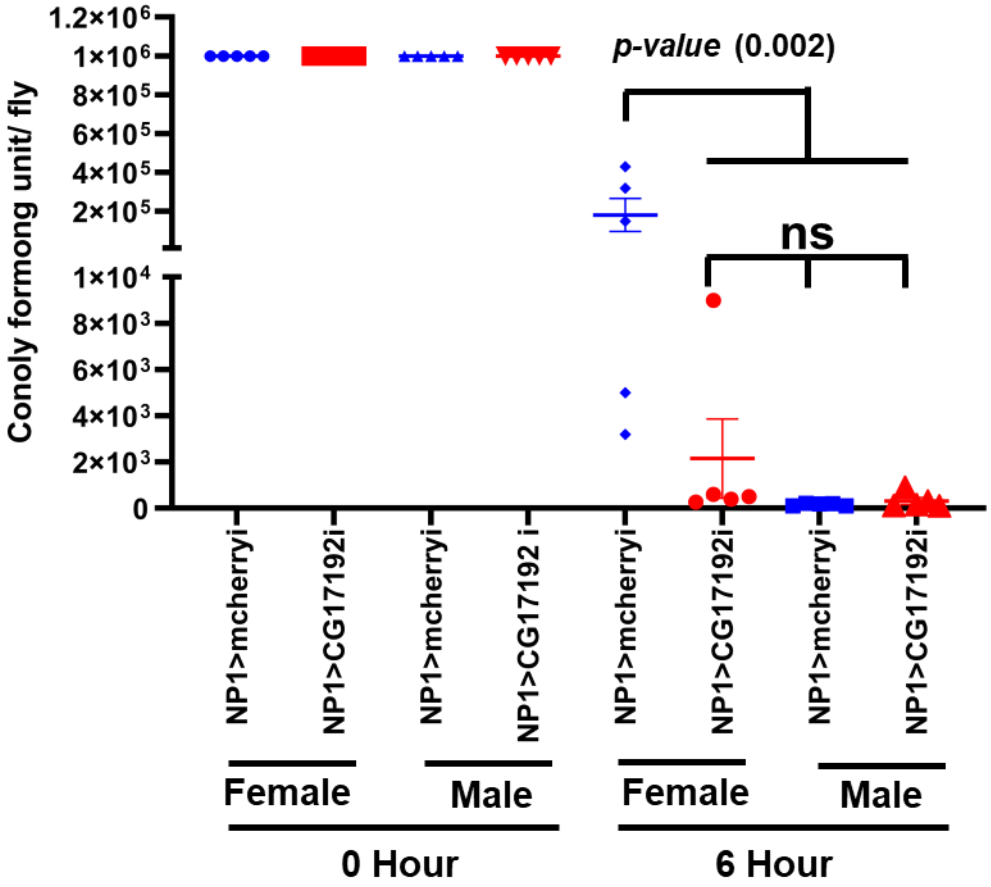

Figure 5.9. CG17192 Show sexually dimorphic host-defence role in the *Drosophila* gut.

Enterocyte-specific *NP1-Gal4^{ts}* was used to knockdown *CG17192 and mcherry RNAi (mcherryi)* act as control. Scatter dot plot represent the Bacterial clearence test as colony-forming units (CFUs) post-gut feeding of *P. entomophilia (O.D.=200).* The student's t-test was performed comparing *NP1>mcherryi* (Blue) and NP1>*CG17192i* (Red) at 0 (ZERO) hour and 6 (SIX) hours. **p = 0.002; *Number of biological replicate (N)=5* ns-*Data not significant.*

Discussion and conclusion

We generated a gut-specific CG17192 knockdown fly line, and using an untargeted lipidomics approach, showed that the guts of adult flies lacking CG17192 have dysregulated PI metabolism during normal physiological conditions (**Figure 5.3B**) and in a gut infection model (**Figure 5.6, 5.8**). Consistent with our lipidomics data, we show

using gel-based ABPP experiments (**Figure 5.4**) and LC-MS/MS substrate assays (**Figure 5.5**) that recombinant WT CG17192 (but not a catalytically dead S179A mutant) is expressed as an active enzyme and has a distinct PLC-type lipase activity with PI being the best substrate for this enzyme (**Figure 5.10**).

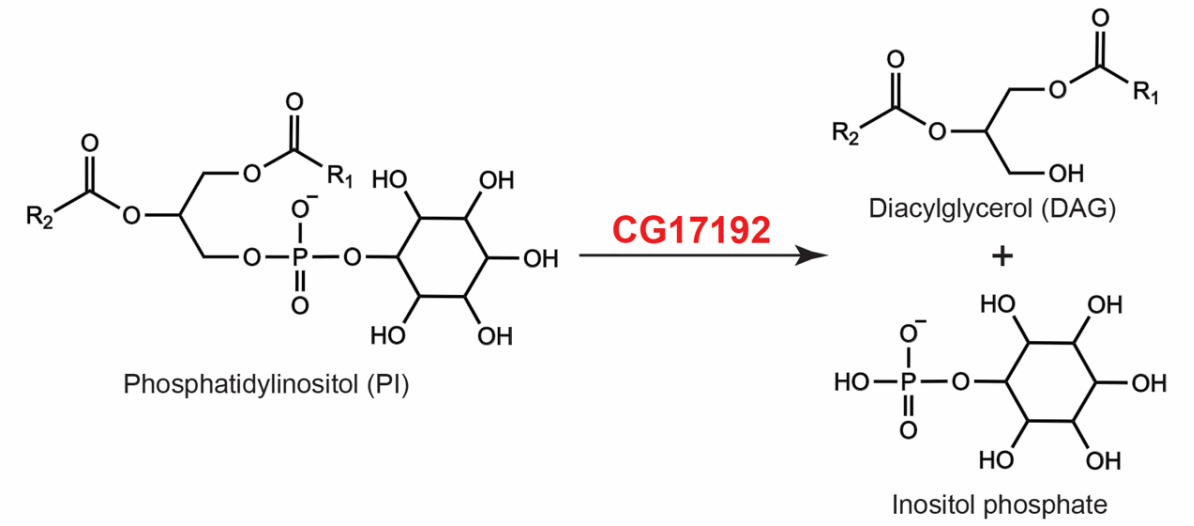

Figure 5.10. Reaction catalyzed by CG17192.
The PLC-type phospholipase activity of CG17192 with PI being the best substrate for this metabolic SH enzyme.

The end products of the PLC-type lipase activity catalyzed by CG17192 from PI substrates are two signaling lipids, namely DAG and inositol phosphate (IP), both of which are known to regulate critical downstream events during receptor mediated activation events[33–40]. That CG17192 activity increases during an injury or infection to elevate cellular levels of DAG and IP strongly suggests an important role for this phospholipase in cellular signaling cascades, and places it at the crossroads of lipid metabolism and an innate immune response in flies. Interestingly, large-scale gene expression studies show that CG17192 has strong, almost exclusive expression in the midgut of an adult fly[11,31,41]. Yet, during an injury (or infection) at a distant site (e.g., thorax), it displays heightened activity, thereby suggesting, that via its PLC-type phospholipase with PI, CG17192 is likely involved in important signaling cascades

during the animal's systemic response. Consistent with this premise, it is now becoming increasingly evident, that the *Drosophila* gut, which contains a rich cocktail of metabolic enzymes, is fast emerging as major nodal organ that regulates the flux of key organismal physiological processes, like the systemic immune response[42–44].

A recent study showed that the *Drosophila* E78 nuclear receptor controls the expression of CG17192, and by doing so, can regulate dietary lipid uptake and systemic lipid levels[70]. Based on a dysregulated lipid phenotype from depleting the E78 nuclear receptor, CG17192 was tentatively annotated as a digestive lipase involved in maintaining adult lipid levels with putative triacylglycerol lipase activity[45]. Further, a bioinformatics survey from FlyBase shows that CG17192 is orthologous to three enzymes from the metabolic SH family, namely LIPC (UniProt ID: P11150), LIPG (UniProt ID: Q9Y5X9) and LIPH (UniProt ID: Q8WWY8), that belong to the mammalian triglyceride lipase family and mutations to these result in dysregulated lipid metabolism in humans. However, despite their tentative annotations as putative triglyceride lipases based largely on the dysregulated lipid phenotypes, exhaustive biochemical studies on these three human lipases, namely LIPC[46–48], LIPG[48–50] and LIPH,[51–53] have now clearly shown that these function as phospholipases. Our studies reported here seem to agree with the dysregulated lipid phenotype observed depletion of *CG17192* (mediated by the E78 nuclear receptor), and from studies done on the three human lipases (LIPC, LIPG, and LIPH), in that, via its phospholipase activity, CG17192 might be responsible for regulating systemic lipid metabolism and dietary lipid uptake. However, more investigations are needed to mechanistically understand this and establish the exact biological role of CG17192 in this process.

Moving forward, our studies open several new questions with regards to the signaling pathways regulated by CG17192 activity. For example, from our recent cataloguing of

SH in adult fly tissues, we find that CG17192 is also active to a lesser extent in the hemolymph[34]. Recently, another extracellular lipase made in the midgut, CG8093, was shown to be secreted in the hemolymph and mediate gut-brain communication and modulate systemic insulin signaling in flies[53]. Along similar lines, CG17192 is also a secreted lipase, and this opens an interesting possibility, on whether the activity of CG17192 in the hemolymph during a systemic immune response plays any role in important organismal signaling pathways. Finally, we would like to add a note of caution that despite having a very high lipid coverage, our LC-MS/MS based lipidomics platforms are not tailored to measure levels of various lesser abundant phosphorylated PI (PIPs), which are known to be potent regulator of several biological processes[54–56]. Therefore, it remains a distinct possibility based on our biochemical studies, that besides PI, CG17192 might also be regulating levels of PIPs in the adult fly gut (and in the hemolymph) and by doing so, may be modulating a far more diverse network of signaling pathways both locally in the gut and systemically. Moving forward, further studies are much needed to tease apart and validate this hypothesis.

Contribution

Mrunal Pazare contributed to the cloning of pRM-CG17192 vectors and assessing expression and activity of CG17192 in S2 cells and also bacterial clearance studies.

Acknowledgments

We thank Arnab Chakravarty, Aakash C. and Saddam Shaikh for technical assistance with mass spectrometry.

References

(1) Gerlt, J. A.; Allen, K. N.; Almo, S. C.; Armstrong, R. N.; Babbitt, P. C.; Cronan, J. E.; Dunaway-Mariano, D.; Imker, H. J.; Jacobson, M. P.; Minor, W.; Poulter, C. D.; Raushel, F. M.; Sali, A.; Shoichet, B. K.; Sweedler, J. V. The Enzyme Function Initiative. *Biochemistry* **2011**, *50* (46), 9950–9962. https://doi.org/10.1021/bi201312u.
(2) Gerlt, J. A.; Babbitt, P. C. Can Sequence Determine Function? *Genome Biol.* **2000**, *1* (5), REVIEWS0005. https://doi.org/10.1186/gb-2000-1-5-reviews0005.

(3) Schnoes, A. M.; Brown, S. D.; Dodevski, I.; Babbitt, P. C. Annotation Error in Public Databases: Misannotation of Molecular Function in Enzyme Superfamilies. *PLOS Comput. Biol.* **2009**, *5* (12), e1000605. https://doi.org/10.1371/journal.pcbi.1000605.
(4) Brown, S. D.; Babbitt, P. C. Inference of Functional Properties from Large-Scale Analysis of Enzyme Superfamilies. *J. Biol. Chem.* **2012**, *287* (1), 35–42. https://doi.org/10.1074/jbc.R111.283408.
(5) Kim, G. B.; Kim, J. Y.; Lee, J. A.; Norsigian, C. J.; Palsson, B. O.; Lee, S. Y. Functional Annotation of Enzyme-Encoding Genes Using Deep Learning with Transformer Layers. *Nat. Commun.* **2023**, *14* (1), 7370. https://doi.org/10.1038/s41467-023-43216-z.
(6) Holliday, G. L.; Davidson, R.; Akiva, E.; Babbitt, P. C. Evaluating Functional Annotations of Enzymes Using the Gene Ontology. *Methods Mol. Biol. Clifton NJ* **2017**, *1446*, 111–132. https://doi.org/10.1007/978-1-4939-3743-1_9.
(7) Morgat, A.; Lombardot, T.; Coudert, E.; Axelsen, K.; Neto, T. B.; Gehant, S.; Bansal, P.; Bolleman, J.; Gasteiger, E.; de Castro, E.; Baratin, D.; Pozzato, M.; Xenarios, I.; Poux, S.; Redaschi, N.; Bridge, A.; UniProt Consortium. Enzyme Annotation in UniProtKB Using Rhea. *Bioinforma. Oxf. Engl.* **2020**, *36* (6), 1896–1901. https://doi.org/10.1093/bioinformatics/btz817.
(8) Yu, T.; Cui, H.; Li, J. C.; Luo, Y.; Jiang, G.; Zhao, H. Enzyme Function Prediction Using Contrastive Learning. *Science* **2023**, *379* (6639), 1358–1363. https://doi.org/10.1126/science.adf2465.
(9) Oberg, N.; Zallot, R.; Gerlt, J. A. EFI-EST, EFI-GNT, and EFI-CGFP: Enzyme Function Initiative (EFI) Web Resource for Genomic Enzymology Tools. *J. Mol. Biol.* **2023**, *435* (14), 168018. https://doi.org/10.1016/j.jmb.2023.168018.
(10) Zallot, R.; Oberg, N.; Gerlt, J. A. The EFI Web Resource for Genomic Enzymology Tools: Leveraging Protein, Genome, and Metagenome Databases to Discover Novel Enzymes and Metabolic Pathways. *Biochemistry* **2019**, *58* (41), 4169–4182. https://doi.org/10.1021/acs.biochem.9b00735.
(11) Kumar, K.; Mhetre, A.; Ratnaparkhi, G. S.; Kamat, S. S. A Superfamily-Wide Activity Atlas of Serine Hydrolases in *Drosophila* Melanogaster. *Biochemistry* **2021**, *60* (16), 1312–1324. https://doi.org/10.1021/acs.biochem.1c00171.
(12) Buchon, N.; Silverman, N.; Cherry, S. Immunity in *Drosophila* Melanogaster--from Microbial Recognition to Whole-Organism Physiology. *Nat. Rev. Immunol.* **2014**, *14* (12), 796–810. https://doi.org/10.1038/nri3763.
(13) Chakrabarti, S.; Liehl, P.; Buchon, N.; Lemaitre, B. Infection-Induced Host Translational Blockage Inhibits Immune Responses and Epithelial Renewal in the *Drosophila* Gut. *Cell Host Microbe* **2012**, *12* (1), 60–70. https://doi.org/10.1016/j.chom.2012.06.001.
(14) Perkins, L. A.; Holderbaum, L.; Tao, R.; Hu, Y.; Sopko, R.; McCall, K.; Yang-Zhou, D.; Flockhart, I.; Binari, R.; Shim, H.-S.; Miller, A.; Housden, A.; Foos, M.; Randkelv, S.; Kelley, C.; Namgyal, P.; Villalta, C.; Liu, L.-P.; Jiang, X.; Huan-Huan, Q.; Wang, X.; Fujiyama, A.; Toyoda, A.; Ayers, K.; Blum, A.; Czech, B.; Neumuller, R.; Yan, D.; Cavallaro, A.; Hibbard, K.; Hall, D.; Cooley, L.; Hannon, G. J.; Lehmann, R.; Parks, A.; Mohr, S. E.; Ueda, R.; Kondo, S.; Ni, J.-Q.; Perrimon, N. The Transgenic RNAi Project at Harvard Medical School: Resources and Validation. *Genetics* **2015**, *201* (3), 843–852. https://doi.org/10.1534/genetics.115.180208.
(15) Soory, A.; Ratnaparkhi, G. S. SUMOylation of Jun Fine-Tunes the *Drosophila* Gut Immune Response. *PLOS Pathog.* **2022**, *18* (3), e1010356. https://doi.org/10.1371/journal.ppat.1010356.

(16) Kelkar, D. S.; Ravikumar, G.; Mehendale, N.; Singh, S.; Joshi, A.; Sharma, A. K.; Mhetre, A.; Rajendran, A.; Chakrapani, H.; Kamat, S. S. A Chemical-Genetic Screen Identifies ABHD12 as an Oxidized-Phosphatidylserine Lipase. *Nat. Chem. Biol.* **2019**, *15* (2), 169–178. https://doi.org/10.1038/s41589-018-0195-0.
(17) Rajendran, A.; Soory, A.; Khandelwal, N.; Ratnaparkhi, G.; Kamat, S. S. A Multi-Omics Analysis Reveals That the Lysine Deacetylase ABHD14B Influences Glucose Metabolism in Mammals. *J. Biol. Chem.* **2022**, *298* (7), 102128. https://doi.org/10.1016/j.jbc.2022.102128.
(18) Abhyankar, V.; Kaduskar, B.; Kamat, S. S.; Deobagkar, D.; Ratnaparkhi, G. S. *Drosophila* DNA/RNA Methyltransferase Contributes to Robust Host Defense in Aging Animals by Regulating Sphingolipid Metabolism. *J. Exp. Biol.* **2018**, *221* (Pt 22), jeb187989. https://doi.org/10.1242/jeb.187989.
(19) Pathak, D.; Mehendale, N.; Singh, S.; Mallik, R.; Kamat, S. S. Lipidomics Suggests a New Role for Ceramide Synthase in Phagocytosis. *ACS Chem. Biol.* **2018**, *13* (8), 2280–2287. https://doi.org/10.1021/acschembio.8b00438.
(20) Hegde, S.; Sreejan, A.; Gadgil, C. J.; Ratnaparkhi, G. S. SUMOylation of Dorsal Attenuates Toll/NF-κB Signaling. *Genetics* **2022**, *221* (3), iyac081. https://doi.org/10.1093/genetics/iyac081.
(21) Chaplot, K.; Pimpale, L.; Ramalingam, B.; Deivasigamani, S.; Kamat, S. S.; Ratnaparkhi, G. S. SOD1 Activity Threshold and TOR Signalling Modulate VAP(P58S) Aggregation via Reactive Oxygen Species-Induced Proteasomal Degradation in a *Drosophila* Model of Amyotrophic Lateral Sclerosis. *Dis. Model. Mech.* **2019**, *12* (2), dmm033803. https://doi.org/10.1242/dmm.033803.
(22) Bhaskar, V.; Valentine, S. A.; Courey, A. J. A Functional Interaction between Dorsal and Components of the Smt3 Conjugation Machinery*. *J. Biol. Chem.* **2000**, *275* (6), 4033–4040. https://doi.org/10.1074/jbc.275.6.4033.
(23) Rajendran, A.; Vaidya, K.; Mendoza, J.; Bridwell-Rabb, J.; Kamat, S. S. Functional Annotation of ABHD14B, an Orphan Serine Hydrolase Enzyme. *Biochemistry* **2019**, *59* (2), 183–196. https://doi.org/10.1021/acs.biochem.9b00703.
(24) Nayak, P.; Kejriwal, A.; Ratnaparkhi, G. S. SUMOylation of Arginyl tRNA Synthetase Modulates the *Drosophila* Innate Immune Response. *Front. Cell Dev. Biol.* **2021**, *9*, 695630. https://doi.org/10.3389/fcell.2021.695630.
(25) Khandelwal, N.; Shaikh, M.; Mhetre, A.; Singh, S.; Sajeevan, T.; Joshi, A.; Balaji, K. N.; Chakrapani, H.; Kamat, S. S. Fatty Acid Chain Length Drives Lysophosphatidylserine-Dependent Immunological Outputs. *Cell Chem. Biol.* **2021**, *28* (8), 1169-1179.e6. https://doi.org/10.1016/j.chembiol.2021.01.008.
(26) Joshi, A.; Shaikh, M.; Singh, S.; Rajendran, A.; Mhetre, A.; Kamat, S. S. Biochemical Characterization of the PHARC-Associated Serine Hydrolase ABHD12 Reveals Its Preference for Very-Long-Chain Lipids. *J. Biol. Chem.* **2018**, *293* (44), 16953–16963. https://doi.org/10.1074/jbc.RA118.005640.
(27) Khandelwal, N.; Shaikh, M.; Mhetre, A.; Singh, S.; Sajeevan, T.; Joshi, A.; Balaji, K. N.; Chakrapani, H.; Kamat, S. S. Fatty Acid Chain Length Drives Lysophosphatidylserine-Dependent Immunological Outputs. *Cell Chem. Biol.* **2021**, *28* (8), 1169-1179.e6. https://doi.org/10.1016/j.chembiol.2021.01.008.
(28) The UniProt Consortium. UniProt: The Universal Protein Knowledgebase in 2023. *Nucleic Acids Res.* **2023**, *51* (D1), D523–D531. https://doi.org/10.1093/nar/gkac1052.
(29) Thurmond, J.; Goodman, J. L.; Strelets, V. B.; Attrill, H.; Gramates, L. S.; Marygold, S. J.; Matthews, B. B.; Millburn, G.; Antonazzo, G.; Trovisco, V.; Kaufman,

T. C.; Calvi, B. R.; the FlyBase Consortium. FlyBase 2.0: The next Generation. *Nucleic Acids Res.* **2019**, *47* (D1), D759–D765. https://doi.org/10.1093/nar/gky1003.
(30) Chintapalli, V. R.; Wang, J.; Dow, J. A. T. Using FlyAtlas to Identify Better *Drosophila* Melanogaster Models of Human Disease. *Nat. Genet.* **2007**, *39* (6), 715–720. https://doi.org/10.1038/ng2049.
(31) Leader, D. P.; Krause, S. A.; Pandit, A.; Davies, S. A.; Dow, J. A. T. FlyAtlas 2: A New Version of the *Drosophila* Melanogaster Expression Atlas with RNA-Seq, miRNA-Seq and Sex-Specific Data. *Nucleic Acids Res.* **2018**, *46* (D1), D809–D815. https://doi.org/10.1093/nar/gkx976.
(32) Nielsen, H.; Tsirigos, K. D.; Brunak, S.; von Heijne, G. A Brief History of Protein Sorting Prediction. *Protein J.* **2019**, *38* (3), 200–216. https://doi.org/10.1007/s10930-019-09838-3.
(33) Shears, S. B. Metabolism of the Inositol Phosphates Produced upon Receptor Activation. *Biochem. J.* **1989**, *260* (2), 313–324.
(34) Posor, Y.; Jang, W.; Haucke, V. Phosphoinositides as Membrane Organizers. *Nat. Rev. Mol. Cell Biol.* **2022**, *23* (12), 797–816. https://doi.org/10.1038/s41580-022-00490-x.
(35) Tu-Sekine, B.; Kim, S. F. The Inositol Phosphate System-A Coordinator of Metabolic Adaptability. *Int. J. Mol. Sci.* **2022**, *23* (12), 6747. https://doi.org/10.3390/ijms23126747.
(36) Chatree, S.; Thongmaen, N.; Tantivejkul, K.; Sitticharoon, C.; Vucenik, I. Role of Inositols and Inositol Phosphates in Energy Metabolism. *Mol. Basel Switz.* **2020**, *25* (21), 5079. https://doi.org/10.3390/molecules25215079.
(37) Hammond, G. R. V.; Burke, J. E. Novel Roles of Phosphoinositides in Signaling, Lipid Transport, and Disease. *Curr. Opin. Cell Biol.* **2020**, *63*, 57–67. https://doi.org/10.1016/j.ceb.2019.12.007.
(38) Balakrishnan, S. S.; Basu, U.; Raghu, P. Phosphoinositide Signalling in *Drosophila*. *Biochim. Biophys. Acta* **2015**, *1851* (6), 770–784. https://doi.org/10.1016/j.bbalip.2014.10.010.
(39) Mérida, I.; Ávila-Flores, A.; Merino, E. Diacylglycerol Kinases: At the Hub of Cell Signalling. *Biochem. J.* **2007**, *409* (1), 1–18. https://doi.org/10.1042/BJ20071040.
(40) Toker, A. The Biology and Biochemistry of Diacylglycerol Signalling. *EMBO Rep.* **2005**, *6* (4), 310–314. https://doi.org/10.1038/sj.embor.7400378.
(41) Cao, X.; Jiang, H. Building a Platform for Predicting Functions of Serine Protease-Related Proteins in *Drosophila* Melanogaster and Other Insects. *Insect Biochem. Mol. Biol.* **2018**, *103*, 53–69. https://doi.org/10.1016/j.ibmb.2018.10.006.
(42) Miguel-Aliaga, I.; Jasper, H.; Lemaitre, B. Anatomy and Physiology of the Digestive Tract of *Drosophila* Melanogaster. *Genetics* **2018**, *210* (2), 357–396. https://doi.org/10.1534/genetics.118.300224.
(43) Lemaitre, B.; Miguel-Aliaga, I. The Digestive Tract of *Drosophila* Melanogaster. *Annu. Rev. Genet.* **2013**, *47*, 377–404. https://doi.org/10.1146/annurev-genet-111212-133343.
(44) Zhao, X.; Karpac, J. The *Drosophila* Midgut and the Systemic Coordination of Lipid-Dependent Energy Homeostasis. *Curr. Opin. Insect Sci.* **2020**, *41*, 100–105. https://doi.org/10.1016/j.cois.2020.07.003.
(45) Praggastis, S. A.; Lam, G.; Horner, M. A.; Nam, H.-J.; Thummel, C. S. The *Drosophila* E78 Nuclear Receptor Regulates Dietary Triglyceride Uptake and Systemic Lipid Levels. *Dev. Dyn. Off. Publ. Am. Assoc. Anat.* **2021**, *250* (5), 640–651. https://doi.org/10.1002/dvdy.287.

(46) Yang, P.; Subbaiah, P. V. Regulation of Hepatic Lipase Activity by Sphingomyelin in Plasma Lipoproteins. *Biochim. Biophys. Acta* **2015**, *1851* (10), 1327–1336. https://doi.org/10.1016/j.bbalip.2015.07.003.
(47) Dugi, K. A.; Dichek, H. L.; Santamarina-Fojo, S. Human Hepatic and Lipoprotein Lipase: The Loop Covering the Catalytic Site Mediates Lipase Substrate Specificity (∗). *J. Biol. Chem.* **1995**, *270* (43), 25396–25401. https://doi.org/10.1074/jbc.270.43.25396.
(48) McCoy, M. G.; Sun, G.-S.; Marchadier, D.; Maugeais, C.; Glick, J. M.; Rader, D. J. Characterization of the Lipolytic Activity of Endothelial Lipase. *J. Lipid Res.* **2002**, *43* (6), 921–929. https://doi.org/10.1016/S0022-2275(20)30466-1.
(49) Jaye, M.; Lynch, K. J.; Krawiec, J.; Marchadier, D.; Maugeais, C.; Doan, K.; South, V.; Amin, D.; Perrone, M.; Rader, D. J. A Novel Endothelial-Derived Lipase That Modulates HDL Metabolism. *Nat. Genet.* **1999**, *21* (4), 424–428. https://doi.org/10.1038/7766.
(50) Hirata, K.; Dichek, H. L.; Cioffi, J. A.; Choi, S. Y.; Leeper, N. J.; Quintana, L.; Kronmal, G. S.; Cooper, A. D.; Quertermous, T. Cloning of a Unique Lipase from Endothelial Cells Extends the Lipase Gene Family. *J. Biol. Chem.* **1999**, *274* (20), 14170–14175. https://doi.org/10.1074/jbc.274.20.14170.
(51) Sonoda, H.; Aoki, J.; Hiramatsu, T.; Ishida, M.; Bandoh, K.; Nagai, Y.; Taguchi, R.; Inoue, K.; Arai, H. A Novel Phosphatidic Acid-Selective Phospholipase A1That Produces Lysophosphatidic Acid*. *J. Biol. Chem.* **2002**, *277* (37), 34254–34263. https://doi.org/10.1074/jbc.M201659200.
(52) Hiramatsu, T.; Sonoda, H.; Takanezawa, Y.; Morikawa, R.; Ishida, M.; Kasahara, K.; Sanai, Y.; Taguchi, R.; Aoki, J.; Arai, H. Biochemical and Molecular Characterization of Two Phosphatidic Acid-Selective Phospholipase A1s, mPA-PLA1α and mPA-PLA1β*. *J. Biol. Chem.* **2003**, *278* (49), 49438–49447. https://doi.org/10.1074/jbc.M213018200.
(53) Singh, A.; Abhilasha, K. V.; Acharya, K. R.; Liu, H.; Nirala, N. K.; Parthibane, V.; Kunduri, G.; Abimannan, T.; Tantalla, J.; Zhu, L. J.; Acharya, J. K.; Acharya, U. R. A Nutrient Responsive Lipase Mediates Gut-Brain Communication to Regulate Insulin Secretion in *Drosophila*. *Nat. Commun.* **2024**, *15*, 4410. https://doi.org/10.1038/s41467-024-48851-8.
(54) Balla, T. Phosphoinositides: Tiny Lipids With Giant Impact on Cell Regulation. *Physiol. Rev.* **2013**, *93* (3), 1019–1137. https://doi.org/10.1152/physrev.00028.2012.
(55) Majerus, P. W.; Ross, T. S.; Cunningham, T. W.; Caldwell, K. K.; Jefferson, A. B.; Bansal, V. S. Recent Insights in Phosphatidylinositol Signaling. *Cell* **1990**, *63* (3), 459–465. https://doi.org/10.1016/0092-8674(90)90442-H.
(56) Fruman, D. A.; Meyers, R. E.; Cantley, L. C. Phosphoinositide Kinases. *Annu. Rev. Biochem.* **1998**, *67*, 481–507. https://doi.org/10.1146/annurev.biochem.67.1.481.

Chapter 6

Uncovering biochemical functions for *Drosophila* CG10038

Chapter 6

Uncovering biochemical functions for *Drosophila* CG10038

Abstract

As we previously discussed in this thesis, only a small fraction of the enzymes has been biochemically characterized and/or have correct biological functions. Many enzymes involved in human diseases and metastasis are awaiting to be characterized for their biochemical functions. Realizing this, we found in Chapter 1 and Chapter 2 that CG10038 is a novel SH enzyme and orthologous to mammalian FAM172A protein, which interacts with NF-κB factor control apoptosis in hepatocellular carcinoma (Shen et. al., *RSC Adv.*, 2017,**7**, 51870-51878). However, FAM172A is also biochemically uncharacterized. Hence. In this Chapter, we chose CG10038 as a potential target to identify its biochemical function in the *Drosophila* model organism. To assign a biological function to this as-of-yet uncharacterized SH, we confirm the CG10038 is cytoplasmic and soluble SH using chemoproteomics and expression in S2 cells. Then, we expressed and purified CG10038 and found that it is a small molecule hydrolase using *p*-Np substrates hydrolysis assays. Following this, we characterize the BL-91433 fly line as a hypomorphic allele using RTqPCR and chemoproteomics. Next, we hypothesized and showed that CG10038 as deacetylase by performing lysine acetated western blotting (adult fly proteome using hypomorphic allele) and immuno-precipitation of CG10038 (S2 cell proteome) followed by in-gel LC-MS/MS. Since CG10038 is a deacetylase, it may regulate the function of its immune-responsive partner proteins by deacetylation. Therefore, we tested and found that the CG10038 hypomorphic allele is susceptible to infection. This Chapter with CG10038 thus demonstrates the complementary use of ABPP platforms, immune-precipitation,

LC-MS/MS and biochemical assays in assigning functions to enzymes in different physiological contexts.

Graphical abstract

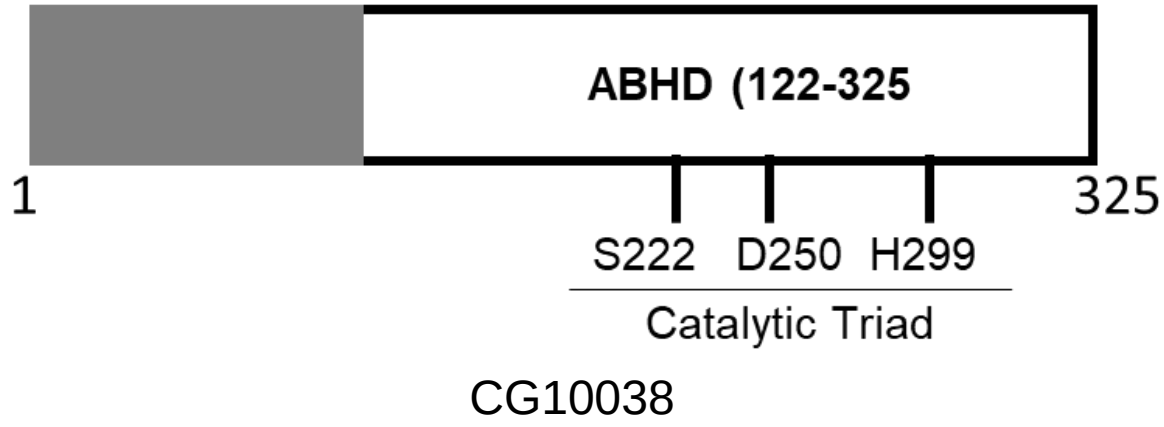

Keywords: CG10038, FAM172A, Serine Hydrolase, , Deacetylase, ABPP, *Drosophila*.

Introduction

A large number of enzymes have identified post-genome sequencing, and determination of their molecular, cellular and pathophysiological functions is the major challenge faced by twenty-first-century scientists[1]. A significant fraction of each organism's proteome consists of uncharacterized enzymes[2]. For example, in Chapter 1, we have built the Serine hydrolase (SH) database (354 SHs, ~2.5 % of total genes) of the *Drosophila melanogaster,* and according to the literature survey, around 84% of them are still uncharacterized[3]. Realizing this gap, in Chapter 2, we generated the activity atlas of SHs during various developmental and adult tissue in the fly using established ABPP platforms[3]. This atlas leads us one step ahead, out of multiple milestones, in characterizing the SH enzymes in pathophysiology. Since Serine hydrolase superfamily members utilize serine as catalytic residue, most have different substrates. Almost all of them have different cellular and molecular functions, with exceptions. So, It becomes massive and less efficient to characterize all enzymes together, taking interest of the present challenge, public interest and human resources as well[1,4]. Henceforth, in Chapter 4, we map the SHs activity in immune response and choose target CG17192, and in Chapter 5, we identify its biochemical functions using biochemical assays and LC-MS/MS platforms.

Similarly, in this Chapter, we identify a novel metabolic SH, CG10038 (uniprot: Q95RN0) from chapter 1 and chapter 2 which is orthologous to human and mouse FAM172A as evident from bioinformatics survey from FlyBase database. The multiple sequence alignment using online clustal omega tool showed that the CG10038 protein sequence is highly conserved and shows 45 and 48% sequence similarity with mouse (uniport: Q3TNH5) and human (uniport:Q8WUF8) FAM172A protein, respectively (**Figure 6.1**). FAM172A is associated with cellular proliferation and apoptosis, which

makes it potentially relevant in cancer biology. FAM172A interact with important signaling players i.e. NF-kB and Notch proteins[5]. Dysregulation of FAM172A is cause CHARGE syndrome (coloboma, heart defects, atresia of choanae, retardation of growth/development, genital abnormalities, and ear anomalies) and co-localized with spliceosome complex[6,7]. Recently, FAM172A has been identified as a serine hydrolase enzyme[6] and has yet to identify its biological substrate to characterize its mechanism in CHARGE syndrome and melanoma pathogenesis.

```
CG10038_Dmel      ------------MWSRLIQIFRPLRS-----------------FRMSHSPPPASNCEEA 30
FAM172A_MOUSE     MSISLSSLIFLPIWINMAQMQQGGSNETEQTAALKDLLSRIDLDELMKKDEPPF----DF 56
FAM172A_Human     MSISLSSLILLPIWINMAQIQQGGPDEKEKTTALKDLLSRIDLDELMKKDEPPL----DF 56
                             :* .: *: :   .                   *.:. **     :

CG10038_Dmel      LIQLKNFGYAFDGEGVLRKVDPATGEPGKELFSYNVSDD-AAENEKHYQKLANQIPEIVY 89
FAM172A_MOUSE     PDTLEGFEYAFNEKGQLRHIKTG------EPFVFNYREDLHRWNQKRYEALGEIITRYVY 110
FAM172A_Human     PDTLEGFEYAFNEKGQLRHIKTG------EPFVFNYREDLHRWNQKRYEALGEIITKYVY 110
                     *:.* ***: :* **::. .      * * :*  :*    *:*:*: *.: * . **

CG10038_Dmel      ALLEKNG-LSRTYIPFDQP-PERSSFVFSQPAKLSQSKKLLVLIHGSGYVKAGQWARSLI 147
FAM172A_MOUSE     ELLESDCNLKKISIPVDATESEPKSFIFMSEDALTNPQKLMVLIHGSGVVRAGQWARRLI 170
FAM172A_Human     ELLEKDCNLKKVSIPVDATESEPKSFIFMSEDALTNPQKLMVLIHGSGVVRAGQWARRLI 170
                   ***.:  *.:  **.*    * .**:* .   *:: :**:******* *:****** **

CG10038_Dmel      INNSLDHGTQLPYVRQAQKLGYDLLITNANDCT-------------------------- 180
FAM172A_MOUSE     INEDLDSGTQIPFIKRAMDEGYGVIVLNPNENYIEVEKQKMHKQSSSSDGTDEPAGKRER 230
FAM172A_Human     INEDLDSGTQIPFIKRAVAEGYGVIVLNPNENYIEVEKPKIHVQS-SSDSSDEPAEKRER 229
                  **:.** ***:*::::*   **.::: * *:

CG10038_Dmel      ------------RFYNGKENP----------IKGVNTSVEHVKYVWKNIVLPAKPESVAI 218
FAM172A_MOUSE     RDKVSKETKKRRDFYEKYRNPQKEKEMMQLFIRENGSPEEHAVYVWDHFIAQAAAENVFF 290
FAM172A_Human     KDKVSKETKKRRDFYEKYRNPQREKEMMQLYIRENGSPEEHAIYVWDHFIAQAAAENVFF 289
                            **:  .**          *:  .:  **. ***.:::  *  *.* :

                     Ser                              Asp
CG10038_Dmel      VAHSYGGSLTLDLVERFPDFFKESVFAIAFTDAAMG----SPQAKNKEYLCDVACDWVAS 274
FAM172A_MOUSE     VAHSYGGLAFVELMIQREADVKSKVTAVALTDSVHNVWHQEAGKTIREWMRENCCNWVSS 350
FAM172A_Human     VAHSYGGLAFVELMIQREADVKNKVTAVALTDSVHNVWHQEAGKTIREWMRENCCNWVSS 349
                  *******   ::*: :    .*..* *:*:**:. .    .   . :*:: : .*:**:*

                                        His
CG10038_Dmel      NTPLDTPVSQSKSSIRRISAGHTKHEWTSYSAIDSVFKFIEEKYEQRANKK--------- 325
FAM172A_MOUSE     SEPLDTSVESMLPDCPRVSAGTDRHELTSWKSFPSIFKFFAEASEAKSSSQKPALTRRSH 410
FAM172A_Human     SEPLDTSVESMLPDCPRVSAGTDRHELTSWKSFPSIFKFFTEASEAKTSSLKPAVTRRSH 409
                  . **** *..   .  *:***  :** **:.:: *:***: *  * ::..

CG10038_Dmel      -------      325
FAM172A_MOUSE     RIKHEEL      417
FAM172A_Human     RIKHEEL      416
```

Figure 6.1. Multiple sequence analysis (MSA) of CG10038.

MSA showing conserved residues between *Drosophila* CG10038 and mouse and Human FAM172 protein. The red box indicates residues of catalytic triad (Ser- Serine, Asp- Aspartate and His- Histidine).

To complement the activity atlas study in Chapter 2, in this Chapter, we chose CG10038 as the target serine hydrolase to characterize biochemically. The human orthologue of *Drosophila* CG10038 is yet to be biochemically unannotated while having the aforementioned important pathophysiological functions. We first validate CG10038 as bona-fide serine hydrolase using ABPP platforms and biochemical assays with purified CG10038 protein. The biochemical assays with various p-Np substrates revealed that CG1008 might be a small molecule hydrolase. Further, using recombinant CG10038 expression in insect cell, we identify that Cg10038 is soluble cytoplasmic protein. To complement the potential small hydrolase function, we validated the BL-91433 fly line as a hypomorphic allele of CG10038 using RTqPCR and ABPP platform. Then, using hypomorphic allele, anti-acetyl lysine western blotting and immunoprecipitation in conjugation with in-gel LC-MS/MS, we showed that the acetylated proteome is dysregulated in adult flies having diminished CG10038 activity. Finally, having a rationale for the immune responsive role of CG10038 partner protein Arc1, we show that CG10038 hypomorph is susceptible to infection.

Material and Methods

Fly Experimentation

The *Drosophila melanogaster* lines, w^{1118}, $CG10038^{CRIMIC}$ (BL-91433) was grown on standard cornmeal agar medium at 25 °C.

Systemic wounding

For Septic wounding five day old male and female flies were pricked separately on thorax with a needle previously dipped into *S. saprophyticus* (O.D.- 0.5) and incubated in medial containing vials as per experiments.

Gel-based and LC-MS/MS ABPP.

The Gel-based and LC-MS/MS based experiments were performed using established procedure (refers to chapter 2 and chapter 4).

Overexpression of CG10038 in Bacteria

The *CG10038* gene and S222A variant of CG10038 cloned using SLiCE technique into the *pet45(b+)* vector with a N-terminal His epitope. The cloned plasmids were sequence verified and transformed into BL21-De3 bacteria for protein expression. Primary culture were grown at 37°C for overnight and secondary cultures were set from the primary culture. The protein expression was induced with IPTG (0.5mM) at 18°C for 14 hours. Cells were pelleted at 6,800g for 15 min at 4 °C. Cell pellet resuspended in lysis buffer (50mM Tris-cl, pH-8.0 with 10nm imidazole, for native purification) and lysed by sonication for 10 min (Pulse: 10 sec ON; 10 sec OFF) at 4°C. Further, lysed cells were centrifuged at 20,000*g for 30 minutes at 4°C to fractioned into supernatant and the pellet. Protein expression were verified using established protocols ABPP and SDS-PAGE & Coomassie staining and western-blotting. The protein were purified using Ni-NTA agarose (Catalogue No:- 30210) as per manufacture protocol. Briefly, 1 litre of secondary culture supernatant incubated with Ni-NTA agarose for 3 hours and followed by 3 washes with 50mM tris-cl containing 10m, 20 and 40 mM imidazole for respective wash. Finally, protein was eluted with 200mM imidazole in 50 mM tris-cl. The purity of purified protein validated using SDS-PAGE followed by Coomassie staining.

pNp hydrolysis: Calorimetric assay

Colorimetric assays were performed using established protocol previously reported by us[8]. Briefly, all pNp substrates hydrolysis were performed in 10 mM Tris buffer or 10 mM Tris buffer with 0.01% triton X100, (pH 8) by observing the release of *p*-nitrophenolate from substrates by at 405 nm in a 96-well plate assay at 37 °C in a Varioskan Flash plate reader (Thermo Fisher Scientific). All assays were performed in biological triplicates to ensure reproducibility. The structure–activity relationship (SAR) assays were performed with 10 µM WT CG10038 and with 500 µM *p*-nitrophenyl (pNp) analogues of varying chain lengths, namely, *p*-Np-acetate, *p*-Np-butyrate, *p*-Np-octanoate, *p*-Np-decanoate, *p*-Np-dodecanoate, and pNp-palmitate as described previously by Rajendra et. al. 2019[8].

Overexpression of CG10038 in Insect Cells

The *CG10038* gene (encoding CG10038) was amplified from a laboratory generated cDNA[9] library of the adult fly, and cloned into the *pRmHa3* vector[10,11] with a C-terminal FLAG epitope. Using site directed mutagenesis techniques, the catalytic serine (S222) was mutated to an alanine, to yield the S222A variant of CG10038 in the same *pRmHa3* vector. All primers used for generating the constructs are listed in **Table 6.1**. To study the biochemical functions of CG10038, we overexpress this protein in Schneider 2 (S2) insect cells using established protocol (See Chapter 5). Expression of CG10038 in the membrane, soluble and secreted media proteomic fractions was confirmed by gel-based ABPP (reported earlier in Chapter 2 and 4) and Western blot analysis using previously reported protocols(Chapter 5)[8,9,12].

Antibody used- Polyclonal anti-His antibody Santa Cruz, Anti-acetyl Lysine antibody, Anti-tubulin antibody.

Real Time qPCR (RT-qPCR)

RNA was extracted from the adult flies using established protocol (refer to chapter 5). The RNA concentration was measured using a nano-drop spectrometer (ThermoFisher Scientific, Catalog No.: ND-2000c), and 1 μg of isolated RNA was used for first-strand cDNA synthesis using the High-Capacity cDNA Reverse Transcription Kit (ThermoFisher Scientific, Catalog No.: 4374966) as per manufacturer's protocols. Next, all real-time quantitative PCR (RT-qPCR) experiments were performed using the iTaq Universal SYBR Green Supermix Kit (Bio-Rad, Catalog No.: 1725124) on a CFX96 Touch Real-Time PCR Detection System (Bio-Rad) using standard RT-qPCR protocols. Fold inductions in transcript levels were determined using the ΔΔCt method and all transcript levels were normalized to *rp49*. The complete list of primers used in this RT-qPCR experiment is listed in **Table 6.1**.

Immunoprecipitation

Mock, C-terminal WT and S222A CG10038 transfected S2 cell proteome were lysed in 1xPBS using established protocol (Chapter 5). The lysate were centrifuge at 21000g to segregate the cell debris. The result supernatant were incubated use for I.P. as per manufacture procedure (Sigma, catalogue No.:- M8823). The CG10038 and its interacting protein complexes eluted by heating at 95°C in 1× Laemmli buffer. Eluted proteins were resolved on a 12% SDS-PAGE which is followed by western blotting (as established protocol) and in-gel trypsin digestion.

In-gel LC-MS/MS

The protein bands (Coomassie stain) on the gel were cut into 1.5 mm cubes and futher distained with in-gelMS-distain buffer (1:1 ratio acetonitrile (ACN) and 50 mM Ammonium bicarbonate). Then, gel pieces were dehydrated in 100% ACN (dehydration step). Dehydrated gels were incubated with 10 mM dithiothreitol, 60°C, for 30 minutes for Reduction followed

by dehydration and alkylation by 20 mM iodoacetamide, 25°C, for 30 minutes. Finally, Gel pieces dehydrated and speed vac for 5 minutes to evaporate remaining CAN. The protein in gels were digested overnight at 37°C with Trypsin at 10 ng/µl concentration in 50mM Ammonium bicarbonate (Promega, sequencing grade trypsin). Digeste peptide were extracted and run for LC-MS/MS analysis using previously reported protocol by us13.

Data Plotting and Analysis

All graphs represented is this study are plotted and analyzed using GraphPad Prism 10 (version 10.3.0) software for macOS.

Table 6.1. Primers used in this study.

S. No.	Primer Sequence (5' to 3')	Primer Description
1	GGAAGTCCCCAAGCGAAGAA	Primer pair for RT-qPCR amplification of CG17192
2	CGATGGCCGAGTAAGAGGTC	
3	GACGCTTCAAGGGACAGTATCTG	Primer pair for RT-qPCR amplification of rp49
4	AAACGCGGTTCTGCATGAG	
5	GAATTCGAGCTCGGTACCATGTGGTCTAGGCTTATTCAAATATTTC	Primers for amplification of CG10038 for cloning into the pRmHa3 vector
6	CTTATCATCATCATCCTTGTAATCTTCAGTTTGCCCGAATG	
7	CAGGTCGACTCTAGAGGATCCCTACTTATCATCATCATCCTTGTAATC	
8	TTGTGGCCCACGCCTATGGTGGCAGTCTTAC	Primer pair for generating the S179A mutant
9	CTGCCACCATAGGCGTGGGCCACAATGGC	
10	TCATTCGAACCGGTACCCACTCACTTCTTATTCGCTCGCTGTTCAT	Primers for amplification of CG10038 for cloning into the pet45(b+) vector
11	CACATCACCACCACCATCACGGTGGTATGTGGTCTAGGCTTATTCAAAT	

Results

Validating CG10038 as active SH using Competitive LC-MS/MS-based ABPP

In Chapter 2, we demonstrated that CG10038 is ubiquitously expressed as active serine hydrolase (chapter 2, Figure 2.3 and Figure 2.4)[3]. For more confidence in the activity of CG10038, by using established LC-MS/MS-based competitive ABPP, we aim to validate that CG10038 is an active serine hydrolase. The adult fly lysate reacted with FP-alkyne (FP-alkyne treated), which quenched the SHs activity. On the other hand, another adult fly lysate reacted with DMSO (DMSO treated), which resulted in SHs activity. Then after, Both the lysates, FP-alkyne and DMSO treated, chased with FP-biotin, which reacts with active SHs, in case of DMSO treated but not in FP-alkyne treated lysate and followed by LC-MS/MS ReDime Procedure (**Figure 4.2.B**). The FP-alkyne DMSO-treated tryptic peptide was labelled with Light and Heavy formaldehyde, respectively. This experiment showed that CG10038 has a Light vs Heavy ratio of around 0.1, which validates CG10038 as an active Serine hydrolase (**Figure 6.2**).

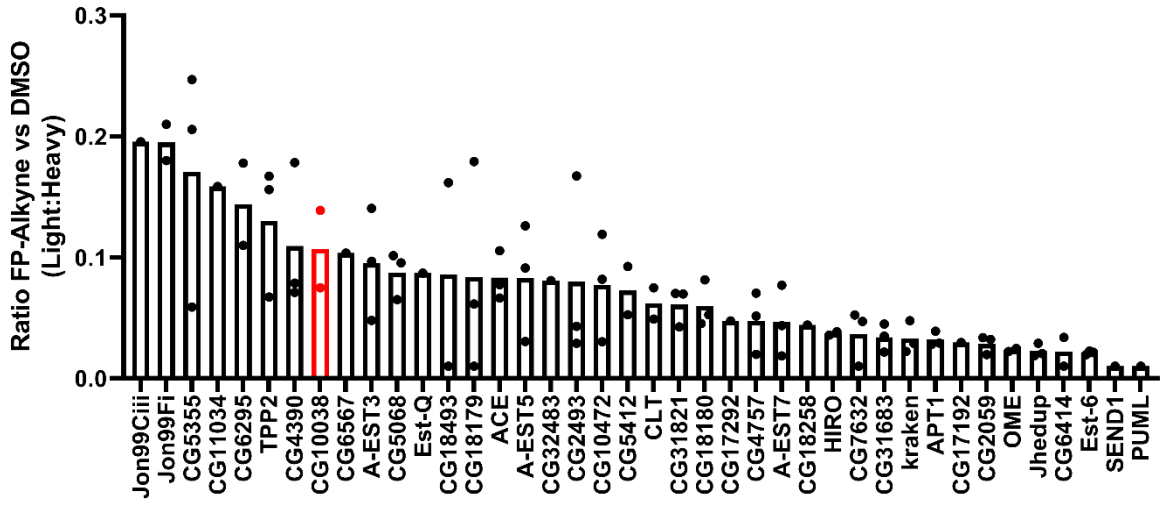

Figure 6.2. Competitive LC-MS/MS-based ABPP

ABPP analysis coupled with post-tryptic ReDiMe labeling strategy to validate CG10038 as active Serine hydrolase in adult fly (light/ heavy; light for inactive SH, FP-Alkyne treated; heavy for native SH, DMSO treated). Bar represents the mean value of L:H ratio from three independent experiments.

Bacterial expression and purification of *Drosophila* CG10038

After validating CG10038 as indeed Serine Hydrolase and previously categorized as metabolic SH, we performed bioinformatic analysis to identify the protein domain and catalytic triad. Our bioinformatics analysis of the protein sequence of CG10038 from UniProt (ID: **Q95RN0**) showed that CG10038 have a canonical ABHD domain, and multiple sequence alignment highlights its catalytic triad (S222, D250 and H299) as discussed in Chapter 1, appendix 1 (**Figure 6.3.A**)[3].

The WT and active site-directed S222A mutant of CG10038 are successfully cloned using SLiCE technique into pet45(b+) vector with N-terminal His tag. Both WT and the S222A mutant of CG10038 were expressed and purified from *E. coli* as described in the protocol earlier in this Chapter. The E3 elution fraction out of E1, E2 and E3 has the highest purity (>90%) for both WT and S222A (**Figure 6.3.B**), which is used for further biochemical assays. The 3-5 mg is the yield of CG10038/L of culture.

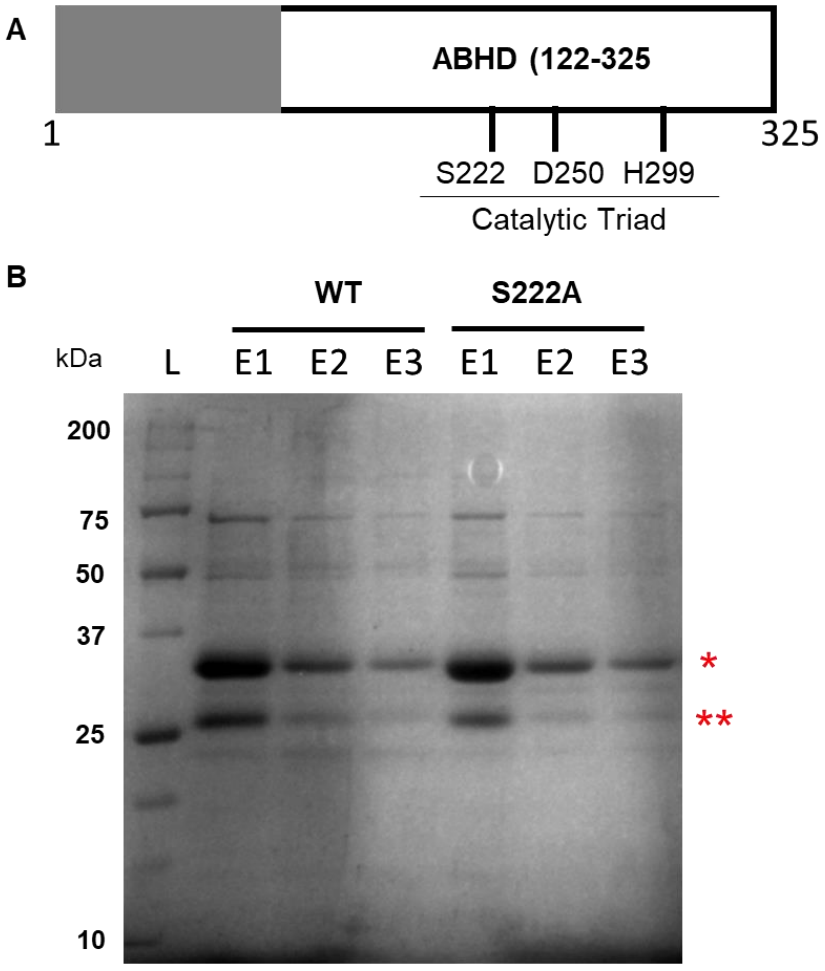

Figure 6.3. Expression and Purification of CG10038 in Bacteria (BL21-DE3).
(A) The bioinformatics analysis showing catalytic triad of full length CG10038 in alpha-beta hydrolase domain (ABHD). (B) WT CG10038 and S222A mutant of CG10038 is expressed and as per protocol described earlier. Representative Coomassie gels for the elution fractions (E1, E2 and E3) scheme towards purifying WT and S222A *Drosophila* CG1008 recombinantly from E. coli.

Biochemical properties of CG10038

To determine whether the S222A mutant was catalytically inactive, we performed the gel-based ABPP assays. We found that WT showed robust activity with the FP-Rh activity probe, whereas unexpectedly, S222A showed partial activity compared to WT protein (**Figure 6.4.A**).

In addition to gel-based ABPP assays, we performed substrate hydrolysis assays against acylated *p*-nitrophenol substrate. In this regard, we incubated WT and S222A CG10038 with *p*-Np-acetate (500 µM) and found that WT produced *p*-nitrophenolate from *p*-Np-acetate approximately 1.5-fold better than S222A CG10038 (**Figure 6.4.B**). The spontaneous hydrolysis of p-Np acetate remains negligible (**Figure 6.4.B**). These experiments suggest that S222A is not catalytically compromised. The diminished activity in S222A suggests the presence of another nearby serine residue in the protein tertiary structure and may be contributing to its activity.

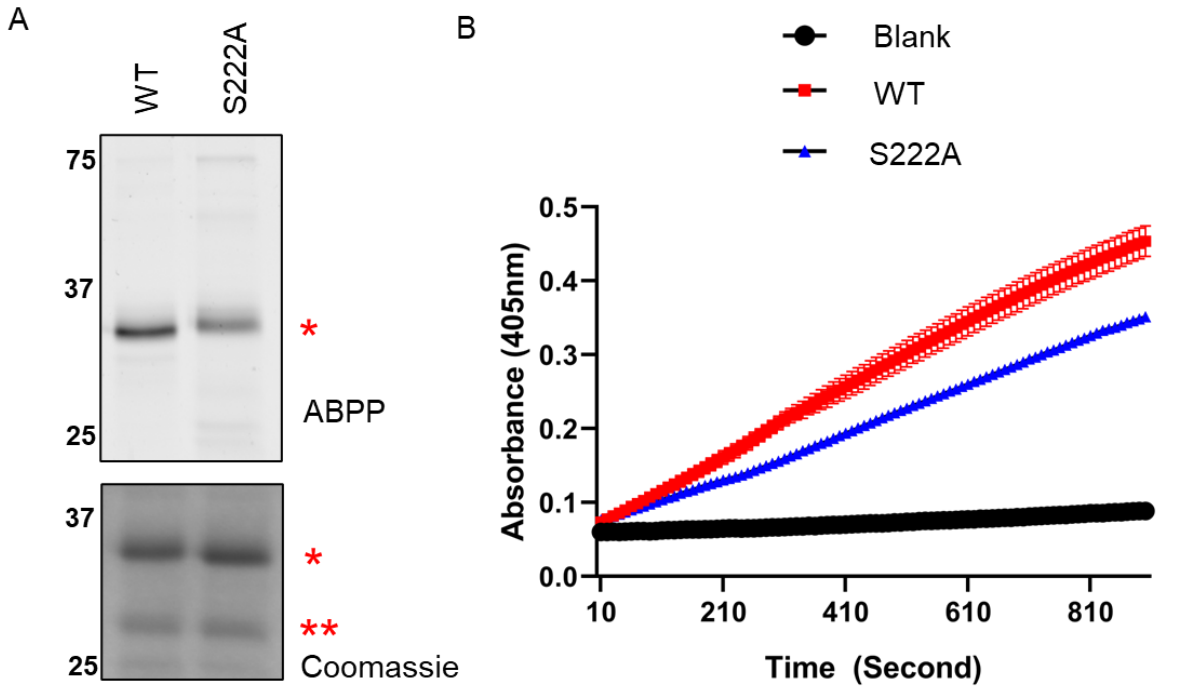

Figure 6.4. S222A mutant of human ABHD14B that is partially catalytically active.

(A) Gel-based ABPP assays with WT and S222A CG10038 showing robust activity of WT and partial activity of S222A. (B) Colorimetric enzymatic assay with *p*-Np-acetate (500 µM) showing ~1.5-fold more activity of WT CG10038, compared to S222A CG10038. These experiments were done three times with reproducible results.

Since WT CG10038 could catalyze acylated p-nitrophenol substrates, we tested with these surrogate substrates to determine if the enzyme preferred the acyl group to *p*-Np. Henceforth, we incubated WT CG10038 (5 µM) with various *p*-Np analogues (500 µM) featuring different chain lengths, ranging from acetate (C2) to palmitate (C16), and observed the release of p-nitrophenolate from these substrates as described earlier in 10 mM Tris-Cl and 10 mM Tris-Cl with 0.01% triton X-100. Our findings revealed a clear trend: WT CG10038 favoured smaller acylated esters of *p*-Np as substrates, with *p*-Np-acetate being the most effective in both buffers (**Figure 6.5.A** and **Figure 6.5.B**). We also observed that the enzyme slowly hydrolyzes pNp-butyrate (C4) but could not hydrolyze acylated esters of *p*-Np with more than 8 carbon atoms (**Figure 6.5**).

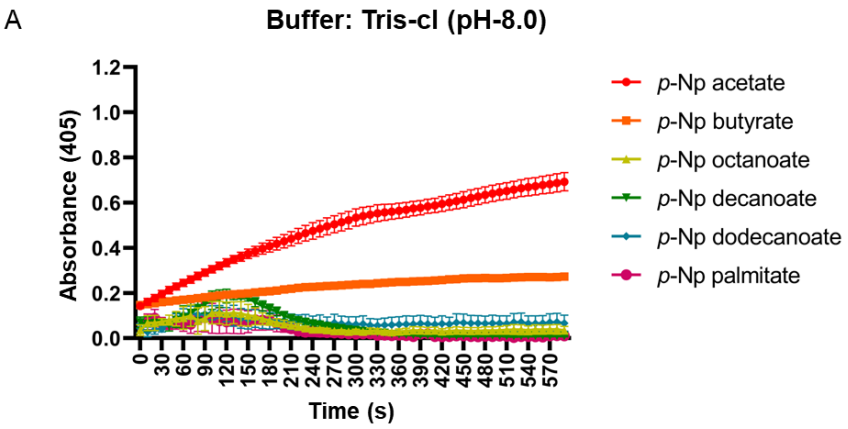

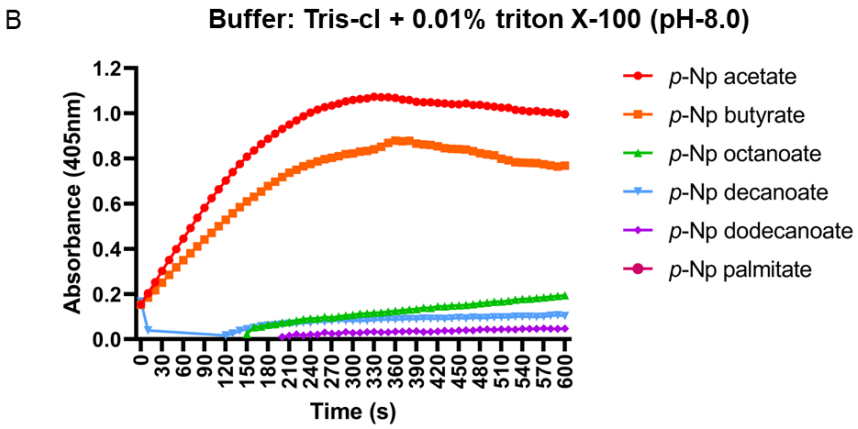

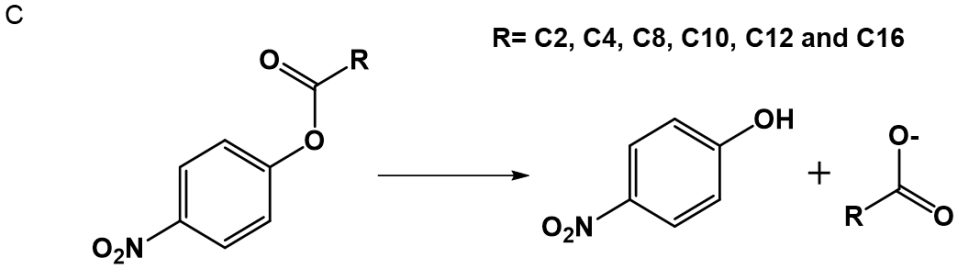

Figure 6.5. CG10038 prefers hydrolysis of the acetyl group from different pNp analogues, that is, substrates having varying acyl chain lengths, (C2, C4, C8, C10, C12 and C16).

(A) The colorimetric assays in Tris-cl buffer pH 8.0. (B) The colorimetric assays in Tris-cl buffer containing 0.01% Triton X-100, pH 8.0. The colorimetric assays were done three independent times with reproducible results. (C) Hydrolysis reaction equation for *p-Np* substrates by WT CG10038.

Cellular localization of CG10038

To date, CG10038 remains an uncharacterized member of the metabolic SH family of enzymes. Next, to determine the cellular localization of CG10038, we cloned N-his and C-flag WT and S222D CG100038 into insect cells expressing vector pRM and transfected and expressed in S2 cell using the established protocol discussed earlier in Chapter 5. After 48 hours of expression, cell and media were harvested. The cells were lysed in 1xPBS and separated into soluble and pellet fractions using benchtop centrifugation. Soluble, pellet and media proteome fraction of mock (empty plasmid control), N-his WT and S222A CG10038 was analyzed for protein expression through gel-based ABPP and western blotting. The ABPP gel shows that WT is active and S222A inactive in the soluble fraction (**Figure 6.6.A**). Western blotting with anti-His antibody shows that both WT and S222A CG100038 expressed at the same level in the soluble fraction (**Figure 6.6.A**), and ponceau staining shows equal loading (**Figure 6.6.A**). CG10038 is neither localized in pellet fraction nor secreted into media (**Figure 6.6.A**). To check the cellular localization of CG10038 in the insect cell, the immunofluorescence using commercially available anti-flag antibody and staining of overexpressed CG10038-C-flag protein shows that CG10038 localized in the cytoplasm, red channel (**Figure 6.6.B**). Green, the Staining of F-actine using Phalloidin, denoting cell boundary and Blue, Staining of DNA using DAPI, denoting nucleus. (**Figure 6.6.B**).

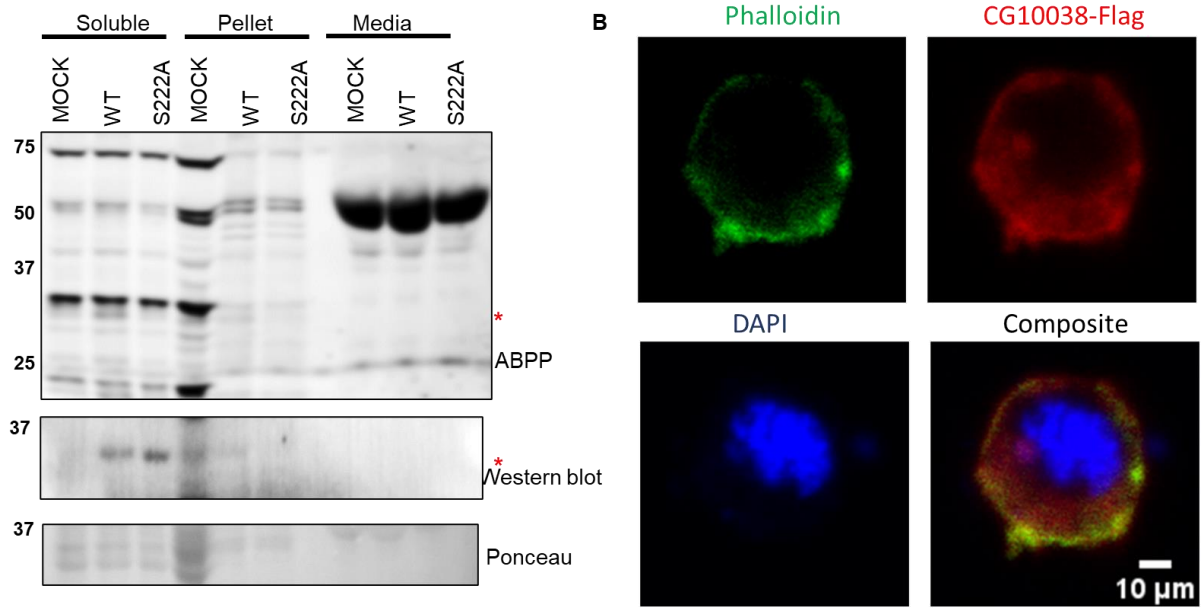

Figure 6.6. CG10038 is a soluble cytoplasmic SH

(A). The various proteomic fractions (membrane, soluble and secreted media) of S2 cells transfected with mock, WT CG10038 or S222A CG10038 were assessed using gel-based ABPP (top panel), Western blot analysis using an anti-His antibody (middle panel), and Ponceau S staining (bottom panel). The red asterisk corresponds to the activity (top panel) or expression (middle panel) of CG10038. (B) Immunostaining showing expression of CG10038 in S2 cell. Green, Staining of F-actin using Phalloidin, denoting cell boundary, Red- immunostaining of CG17192-C-flag and Blue, Staining of DNA using DAPI, denoting nucleus. These experiments were done three times with reproducible results.

Characterization of BL-91433 fly line

To date, CG10038 remains an uncharacterized member of the metabolic SH family of enzymes. Both UniProt[49] (ID: Q95RN0) and FlyBase[50] (DmeI/CG110038) broadly classify CG17192 as co-transcriptional regulator A, based on sequence homology to known FAM172A protein from mammals. To understand biochemical function of CG10038, we decided first to characterize a *CG10038* allele (CG10038-CRIMIC-T2A Gal4) which is generated by a CRIMIC (CRISPR Mediated Integration Cassette) T*2A-GAL4* insertion in the 2nd intron of CG10038/FBgn0038013 gene locus, 3rd

chromosome, right arm (Bloomington stock number:91433) (**Figure 6.7.A**). Insertion of CRIMIC element leads to severe loss-of-function or null alleles by transcription termination and expression of Gal4 under the indigenous promotor of the locus (**Figure 6.7.A**). To check the premature termination transcription of the CG10038 allele, we performed the RTqPCR analysis using the established protocol as discuss earlier in this Chapter. Our RTqPCR analysis suggests that this allele is strong hypomorphic (**Figure 6.7.B**). Further, we assayed the activity of CG10038 in adult flies using LC-MS/MS based ABPP experiment, again which showed that this CRIMIC inserted allele is strong hypomorphic allele (**Figure 6.7.C**). Hence*, CG10038-CRIMIC-T2A Gal4* is now defined as $CG10038^{lof}$. Crossing CG10038lof with UAS-RFP and w1118 generates $CG10038^{lof}$*>UAS-RFP* and $CG10038^{lof}$*> w^{1118}.* To assess the expression of RFP, we observe the fly under the RFP epifluorescence and found that $CG10038^{lof}$*>UAS-RFP express* RFP protein. Whereas $CG10038^{lof}$*> w^{1118}* does not express any RFP protein (**Figure 6.7.D**). Hence, CG10038-CRIMIC-T2A Gal4 is a ubiquitous Gal4.

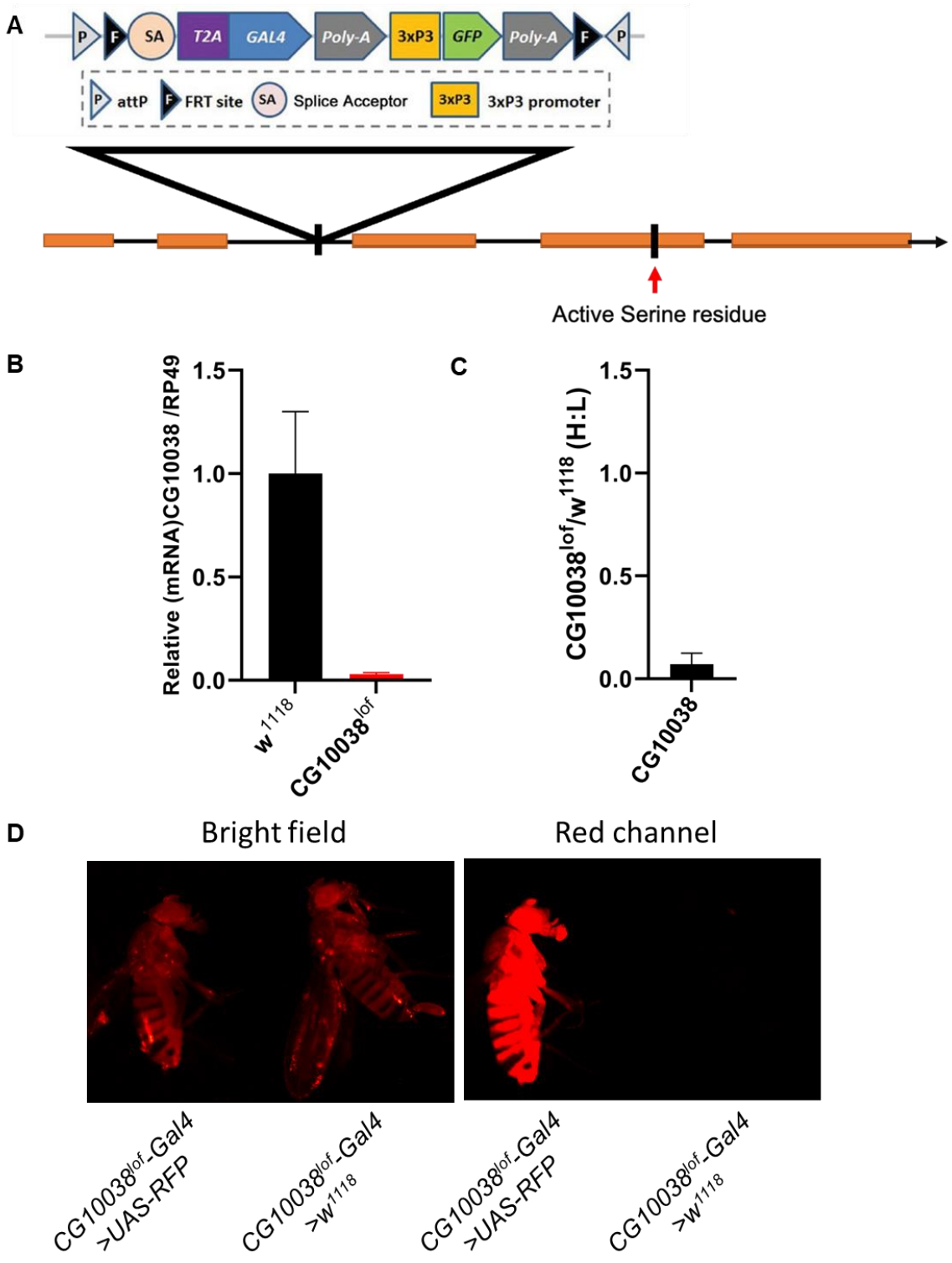

Figure 6.7. Characterization of BL-91433 fly line as CG10038 loss of function. (A) Schematic represents the insertion of CRIMIC element in the second intron (Black dash) of the CG10038 gene region (Image adapted from Lee et. al., 2018)[14]. The red arrow shows catalytic Serine residue in the forth exon (Orange color box) (B) RT-qPCR analysis to check relative CG10038 expression in the adult from *w*^{1118} and the

CG10038^{lof} fly line. (C) Competitive LC-MS/MS-based ABPP assay to check the relative activity of CG10038 in *CG10038^{lof}*. (D) CG10038^{lof} is ubiquitous Gal4 allele. *CG10038^{lof}-Gal4* crossed with UAS-RFP and *w^{1118}. CG10038^{lof}-Gal4>UAS-RFP* shows expression of RFP ubiquitously and *CG10038^{lof}-Gal4>w1118* do not show any expression of RFP.

Since *p*-Np acetate is the most preferred substrate of CG10038 among various *p*-Np analogues (**Figure 6.5**). To understand its biological activity, we hypothesized that CG10038 is a small molecule hydrolase and may hydrolyzed as an acetyl group from acetylated lysine of modified proteins. To test this hypothesis, we performed the western blotting using an anti-acetylated lysine antibody for the lysine acetylation profile of adult fly lysates prepared from *CG10038^{lof}* (test) and *CG10038^{lof}/CG10038^{Df}* (off-target test control). We compared them to lysates prepared from the control *w^{1118}* fly. Consistent with our hypothesis, we found that CG10038lof and CG10038lof/CG10038Df have significantly increased the concentration of acetylated lysine residues compared to *w^{1118}* (**Figure 6.8**). This experiment suggested that CG10038 have protein deacetylase activity. Further, to find the interacting partners of CG10038, we utilize the overexpression system in the S2 cell (**Figure 6.6**) and immuno-precipitate (I.P.) the WT and S222A CG10038 along with its interacting partners in native condition (**Figure 6.8.B**). The I.P. samples were proceeded to perform an in-gel LC-MS/MS analysis to determine the CG10038 interacting partners. We found that 21 proteins were common in WT and S222A with CG10038 and Acr1 with the highest peptide count (**Figure 6.8.C, Table 2**). CG10038 and Arc1 is acetylated in S222A I.P. proteome and not in the WT I.P. proteome (**Figure 6.9**). This experiment provided another lead to annotate CG10038 as protein deacetylase.

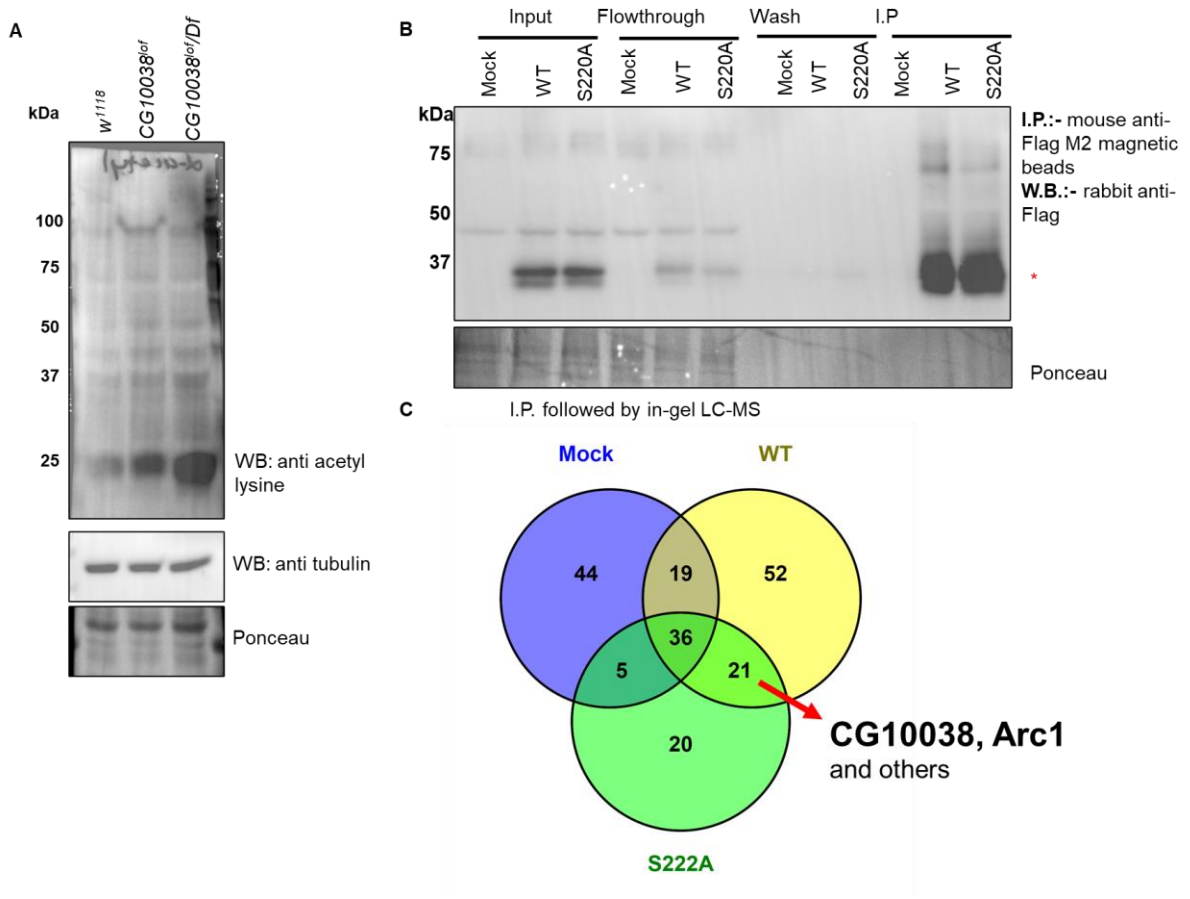

Figure 6.8. CG10038 is possibly a protein deacetylase.

Western blot showing increased levels of protein lysine acetylation CG10038^{lof} and CG10038^{lof}/ (*Df*) [df- Deficiency of CG10038]. Middle (Anti-tubulin western blot) and bottom (ponceau) panel showing equal loading of *proteome* lysate. (B) Using mouse anti-Flag M2 magnetic beads used to immune precipitate (I.P) WT and S222A CG10038 expressed in the S2 cell. Mock (empty plasmid transfected control) used as control. Top panel, Western blot with rabbit anti-flag showing expression and I.P of CG10038, indicated as red asterisk. Bottom panel, ponceau showing loading control. (C) Venn diagram showing proteins identified using in gel LC-MS/MS on I.P proteome of Mock, WT and S222A CG10038. 21 proteins including CG10038 and Arc1 common to WT and S222A (Table 6.3) Proteins unique to WR and S222A also listed in Table 6.4 and 6.5. All experiments were done twice with reproducible results.

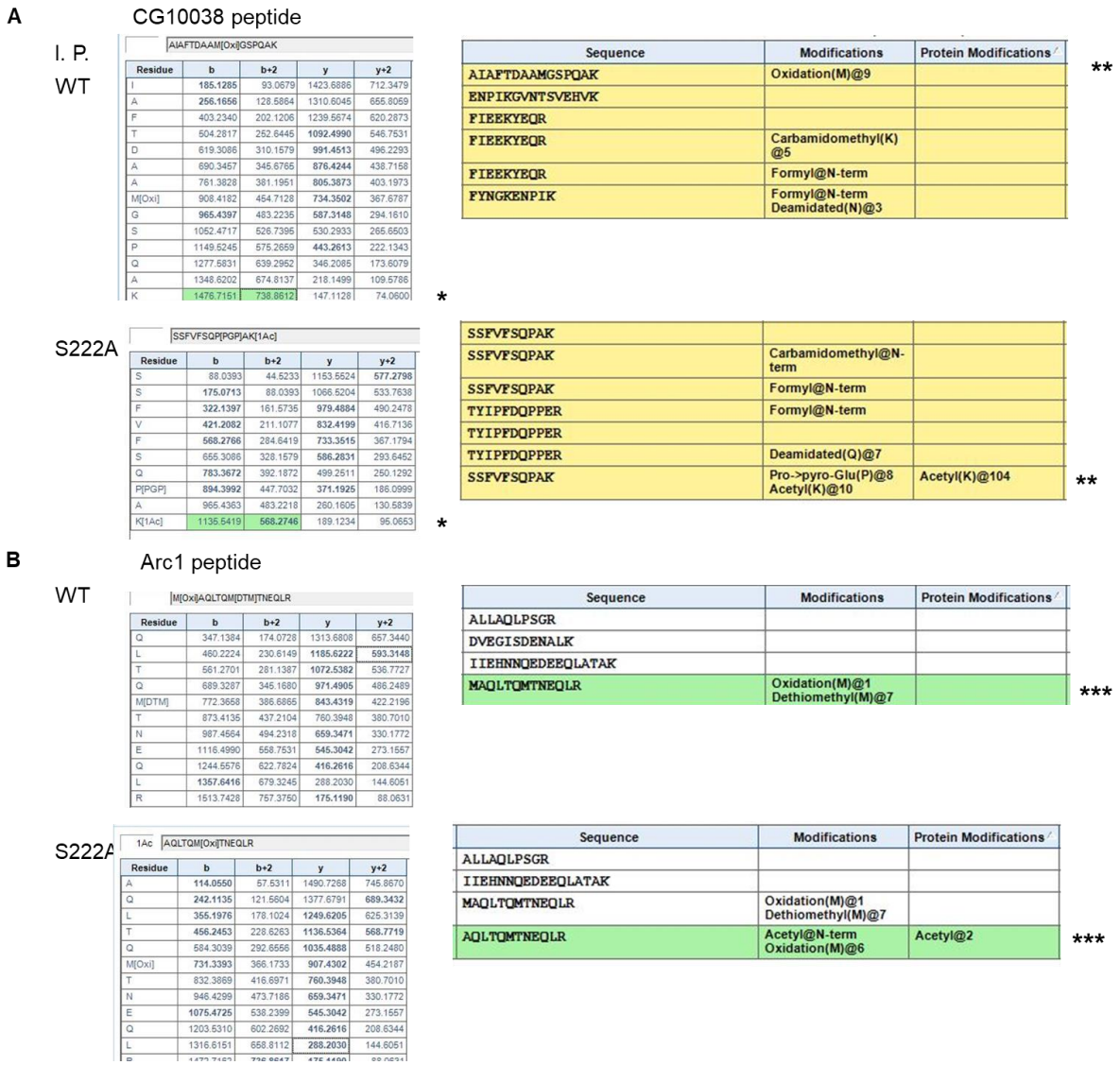

Figure 6.9. Representative snapshot of acetylated peptides of CG10038 and Arc1 proteins from Proteinpilot (Sciex) LC-MS/MS analysis software.

(A)Lysine (K) of the 'SSFVFQPAK' peptide of CG10038 is acetylated in the S222A I.P. Proteome and not in the WT I.P. proteome (single and double asterisk). (B). The N-terminal of the 'AQLTQMTNEQLR' peptide of Arc1 CG10038 is acetylated in the S222A I.P. Proteome and not in the WT I.P. proteome (triple asterisk).

Next, we hypothesized that CG10038, being a potential protein deacetylase enzyme, might be involved in the immune response. Because, acetylation of immune-responsive transcription factor like Jun[15] and NF-κB[16] negatively regulates the immune

response. The CG10038 interacting partner Arc1 (identified earlier in this article) also modulates immune responses to the microbiota[17,18]. Also, The transcript level of CG10038 is increased by 2 fold upon bacterial infection in female mated flies[19]. Having rationale for CG10038 may have the immune role, we performed the immune assays on *CG10038^{lof}*, *Df(3R)Excel7314/*CG10038^{lof} and *Df(3R)Excel6164/*CG10038^{lof} (deficiencies of CG10038; as off-target control (**Figure 6.10.A**)) and found that the CG10038^{lof}, *Df(3R)Excel7314/*CG10038^{lof} and *Df(3R)Excel6164/*CG10038^{lof} are susceptible to infection as compared to wildtype control (**Figure 6.10.B**). Also, CG10038^{lof} does not show spontaneous melanization upon injury (**Figure 6.10.C**) And, representative ABPP gel showed increased in activity of CG10038 in wildtype (red asterisk) and not in CG10038^{lof} upon *S. saprophyticus* infection (**Figure 6.10.D**). Taken together, we propose that *CG10038^{lof}* is unable to deacetylase the acetylated proteins (**Figure 6.8**), and hence acetylated proteins that implicated immune response might lose their function[15,16,18]. Thus, *CG10038^{lof}* flies susceptible to infection (**Figure 6.10**).

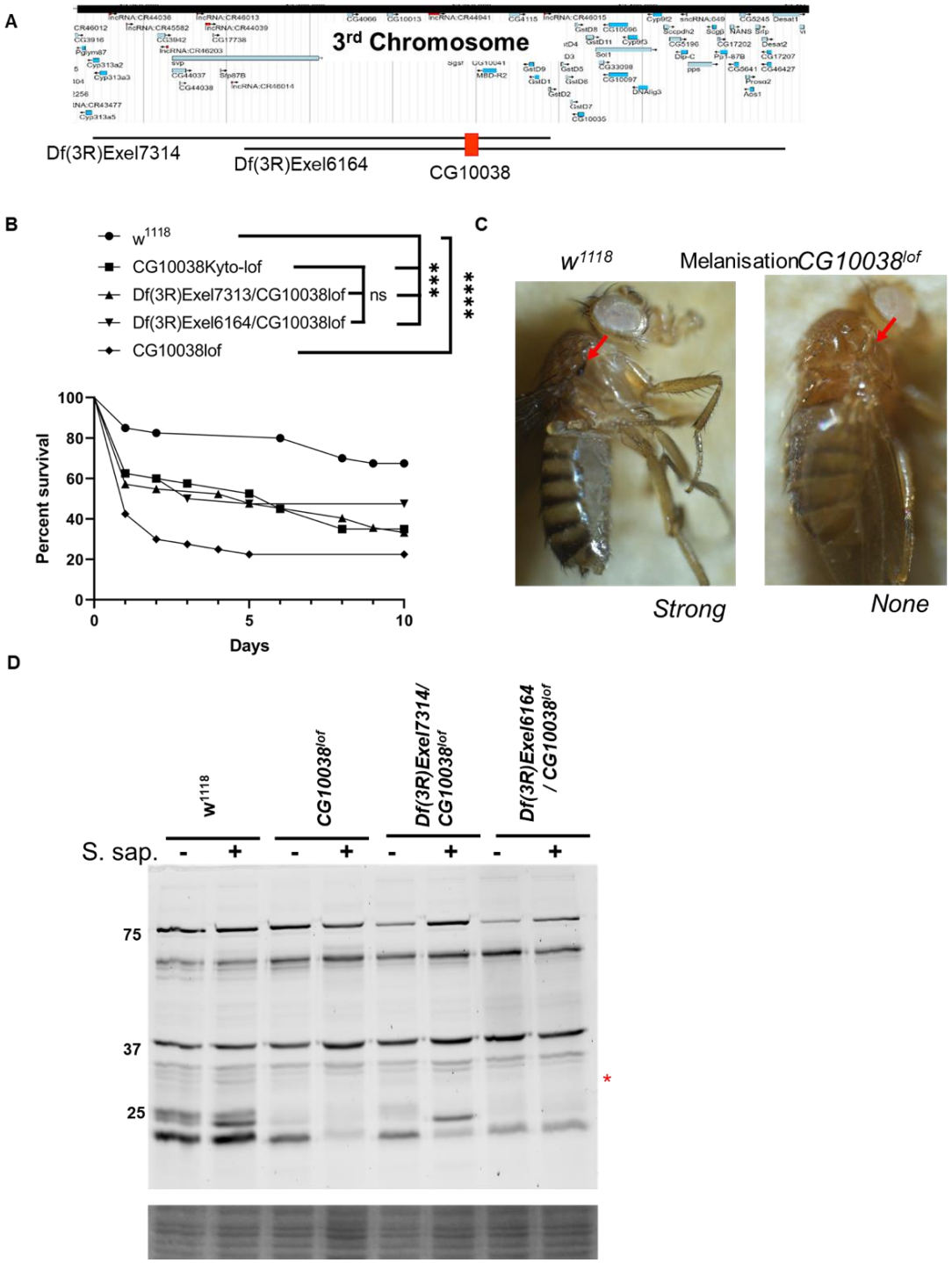

Figure 6.10. CG10038^{lof} is susceptible to infection.

(A) Schematics showing deletion of region of 3rd including *CG10038* gene on *Df(3R)Excel7314* and *Df(3R)Excel6164.* (B) Survival of *w^{1118}, Df(3R)Excel7314* /CG10038^{lof}; *Df(3R)Excel6164*/CG10038^{lof} and CG10038^{lof} flies upon infection (N=75 flies, *** p-value= <0.0001 and **** p-value= <0.00001). (C) *CG10038^{lof}* don't show spontaneous melanization upon infection, whereas *w^{1118}* showed spontaneous melanization. The red arrow indicates the presence of melanization spot in w1118

and not *CG10038^{lof}*. (D) Representative gel-based ABPP experiments showing CG10038 activities in female adult flies at 180 min (indicated as '+') after systemic *S. saprophyticus* infection (red asterisk corresponds to activity of CG10038 in *w^{1118}* and not in *CG10038^{lof}*). The top panel is an ABPP gel while the bottom panel is the loading control (L.C.; Coomassie staining of the ABPP gel). This gel-based ABPP experiment was done twice times, with reproducible results each time.

Discussion and conclusion

Given our interests in assigning functions to hitherto uncharacterized pathophysiologically metabolic SHs in *Drosophila melanogaster* (fruit fly), we chose CG10038 as the target serine hydrolase to characterize biochemically. The rationale behind CG10038 is that it is orthologous to mammalian FAM172A protein. FAM172A is implicated in the CHARGE syndrome (inheritable developmental disorder), cellular proliferation, apoptosis and spliceosome complex[5–7]. FAM172A is physically located in the nucleus and interacts with NF-κB transcription factor[5]. FAM172A protein is essential in cancer cell apoptosis and proliferation, but it is yet to be biochemically annotated. Henceforth, we checked the sequence similarity of CG10038 with mammalian FAM172A and found that the hydrolase domain has high sequence similarity (**Figure 6.1**). Next, we validated CG10038 as bona-fide serine hydrolase and biochemical assays with adult fly proteome (**Figure 6.2**) and purified CG10038 protein (**Figure 6.3 and Figure 6.4.A**) using ABPP platforms, respectively. To understand the enzyme activity of CG10038, we did in-vitro *p*-Np analogues substrate assays. We found that CG10038 preferably hydrolyze the *p*-Np acetate as substrate compared to other *p*-Np analogues (**Figure 6.5**). To understand the cellular function of CG10038, we cloned and expressed it in S2 cells and characterized WT but not S222A CG10038 as active SH (**Figure 6.6.A, top panel**). Both WT and S222A CG10038 of soluble cytoplasmic SH (**Figure 6.6.A middle panel and Figure 6.6.B**). To understand the in-

vivo substrate of CG10038, we first characterized the transgenic BL-91433 fly line as the loss of function allele of CG10038 using RTqPCR and ABPP platform (**Figure 6.7**). Then, we showed that acetylated proteome increased in *CG10038^{lof}* using anti-acetyl lysine western blotting(**Figure 6.8***).* Also, using I.P. and in-gel LC-MS/MS, CG10038 and Arc1 is co-immunoprecipitated and both acetylated in S222A I.P proteome and not acetylated in WT I.P. proteome (**Figure 6.9**). Finally, having a rationale that protein Arc1 has the immune responsive role, we show that CG10038^{lof} is susceptible to infection (Figure 6.10).

To full biochemical characterization of CG10038, we further additional experiments needed to perform. The future experiments will be followings: (1) To test the acetylated protein as substrate for CG10038 and investigate the product formation. (2) Validate the substrate and product in vivo by loss and gain of function studies by other techniques as we primarily shown in this chapter using anti-acetyl lysine western blotting. For pathophysiological role of CG10038, we need to perform rescue experiments to confirm the identified phenotype associated with CG10038^{lof}.

Contribution

Shivani Deshpande (BS-MS IISER Pune) contributed in the parts of cloning of CG10038 vectors and assessing bacterial expression, Purification and activity of CG10038. Dr Kavita Sharma synthesized FP-Biotin Probe which used in this chapter.

Acknowledgments

We thank Saddam Shaikh for technical assistance in MS samples run.

Reference

(1) Saghatelian, A.; Cravatt, B. F. Assignment of Protein Function in the Postgenomic Era. *Nat. Chem. Biol.* **2005**, *1* (3), 130–142. https://doi.org/10.1038/nchembio0805-130.

(2) Walsh, C. *Posttranslational Modification of Proteins: Expanding Nature's Inventory*; Roberts and Co. Publishers: Englewood, Colo, 2006.

(3) Kumar, K.; Mhetre, A.; Ratnaparkhi, G. S.; Kamat, S. S. A Superfamily-Wide Activity Atlas of Serine Hydrolases in *Drosophila* Melanogaster. *Biochemistry* **2021**, *60* (16), 1312–1324. https://doi.org/10.1021/acs.biochem.1c00171.

(4) Gerlt, J. A.; Babbitt, P. C. Divergent Evolution of Enzymatic Function: Mechanistically Diverse Superfamilies and Functionally Distinct Suprafamilies. *Annu. Rev. Biochem.* **2001**, *70* (1), 209–246. https://doi.org/10.1146/annurev.biochem.70.1.209.

(5) Shen, W.; Feng, Z.; Wang, P.; Zhang, J. FAM172A Controls Endoplasmic Reticulum (ER) Stress Related to NF-κB Signaling Pathway in Hepatocellular Carcinoma. *RSC Adv.* **2017**, *7* (82), 51870–51878. https://doi.org/10.1039/C7RA09918E.

(6) Sallis, S.; Bérubé-Simard, F.-A.; Grondin, B.; Leduc, E.; Azouz, F.; Bélanger, C.; Pilon, N. The CHARGE Syndrome-Associated Protein FAM172A Controls AGO2 Nuclear Import. *Life Sci. Alliance* **2023**, *6* (8), e202302133. https://doi.org/10.26508/lsa.202302133.

(7) Bélanger, C.; Bérubé-Simard, F.-A.; Leduc, E.; Bernas, G.; Campeau, P. M.; Lalani, S. R.; Martin, D. M.; Bielas, S.; Moccia, A.; Srivastava, A.; Silversides, D. W.; Pilon, N. Dysregulation of Cotranscriptional Alternative Splicing Underlies CHARGE Syndrome. *Proc. Natl. Acad. Sci.* **2018**, *115* (4), E620–E629. https://doi.org/10.1073/pnas.1715378115.

(8) Rajendran, A.; Vaidya, K.; Mendoza, J.; Bridwell-Rabb, J.; Kamat, S. S. Functional Annotation of ABHD14B, an Orphan Serine Hydrolase Enzyme. *Biochemistry* **2019**, *59* (2), 183–196. https://doi.org/10.1021/acs.biochem.9b00703.

(9) Hegde, S.; Sreejan, A.; Gadgil, C. J.; Ratnaparkhi, G. S. SUMOylation of Dorsal Attenuates Toll/NF-κB Signaling. *Genetics* **2022**, *221* (3), iyac081. https://doi.org/10.1093/genetics/iyac081.

(10) Chaplot, K.; Pimpale, L.; Ramalingam, B.; Deivasigamani, S.; Kamat, S. S.; Ratnaparkhi, G. S. SOD1 Activity Threshold and TOR Signalling Modulate VAP(P58S) Aggregation via Reactive Oxygen Species-Induced Proteasomal Degradation in a *Drosophila* Model of Amyotrophic Lateral Sclerosis. *Dis. Model. Mech.* **2019**, *12* (2), dmm033803. https://doi.org/10.1242/dmm.033803.

(11) Bhaskar, V.; Valentine, S. A.; Courey, A. J. A Functional Interaction between Dorsal and Components of the Smt3 Conjugation Machinery*. *J. Biol. Chem.* **2000**, *275* (6), 4033–4040. https://doi.org/10.1074/jbc.275.6.4033.

(12) Nayak, P.; Kejriwal, A.; Ratnaparkhi, G. S. SUMOylation of Arginyl tRNA Synthetase Modulates the *Drosophila* Innate Immune Response. *Front. Cell Dev. Biol.* **2021**, *9*, 695630. https://doi.org/10.3389/fcell.2021.695630.

(13) Tendulkar, S.; Hegde, S.; Garg, L.; Thulasidharan, A.; Kaduskar, B.; Ratnaparkhi, A.; Ratnaparkhi, G. S. Caspar, an Adapter for VAPB and TER94, Modulates the Progression of ALS8 by Regulating IMD/NFκB-Mediated Glial Inflammation in a *Drosophila* Model of Human Disease. *Hum. Mol. Genet.* **2022**, *31* (17), 2857–2875. https://doi.org/10.1093/hmg/ddac076.

(14) Lee, P.-T.; Zirin, J.; Kanca, O.; Lin, W.-W.; Schulze, K. L.; Li-Kroeger, D.; Tao, R.; Devereaux, C.; Hu, Y.; Chung, V.; Fang, Y.; He, Y.; Pan, H.; Ge, M.; Zuo, Z.; Housden, B. E.; Mohr, S. E.;

Yamamoto, S.; Levis, R. W.; Spradling, A. C.; Perrimon, N.; Bellen, H. J. A Gene-Specific T2A-GAL4 Library for *Drosophila*. *eLife* **2018**, *7*, e35574. https://doi.org/10.7554/eLife.35574.

(15) Zhang, D.; Suganuma, T.; Workman, J. L. Acetylation Regulates Jun Protein Turnover in *Drosophila*. *Biochim. Biophys. Acta BBA - Gene Regul. Mech.* **2013**, *1829* (11), 1218–1224. https://doi.org/10.1016/j.bbagrm.2013.07.007.

(16) Rothgiesser, K. M.; Fey, M.; Hottiger, M. O. Acetylation of P65 at Lysine 314 Is Important for Late NF-κB-Dependent Gene Expression. *BMC Genomics* **2010**, *11* (1), 22. https://doi.org/10.1186/1471-2164-11-22.

(17) Delbare, S. Y. N.; Ahmed-Braimah, Y. H.; Wolfner, M. F.; Clark, A. G. Interactions between the Microbiome and Mating Influence the Female's Transcriptional Profile in *Drosophila* Melanogaster. *Sci. Rep.* **2020**, *10* (1), 18168. https://doi.org/10.1038/s41598-020-75156-9.

(18) Keith, S. A.; Bishop, C.; Fallacaro, S.; McCartney, B. M. Arc1 and the Microbiota Together Modulate Growth and Metabolic Traits in *Drosophila*. *Development* **2021**, *148* (15), dev195222. https://doi.org/10.1242/dev.195222.

(19) Short, S. M.; Lazzaro, B. P. Reproductive Status Alters Transcriptomic Response to Infection in Female *Drosophila Melanogaster*. *G3 GenesGenomesGenetics* **2013**, *3* (5), 827–840. https://doi.org/10.1534/g3.112.005306.

Supplementry Tables

Table 6.2: SH identified from the LC-MS/MS based ABPP experiment shown in Figure 6.2

Flybase ID	Gene Symbol	FP-Alkyne vs DMSO (Heavy:Light Ratio)		
		Replicate 1	**Replicate 2**	**Replicate 3**
FBgn0003357	Jon99Ciii			0.195554
FBgn0039778	Jon99Fi	0.209916		0.179997
FBgn0031741	CG11034			0.158553
FBgn0038013	CG10038	0.074865		0.138746
FBgn0261393	A-EST5	0.091309	0.030551	0.126164
FBgn0039471	CG6295	0.177852		0.109994
FBgn0035951	CG5068	0.095419	0.065127	0.101505
FBgn0015571	A-EST3	0.140462	0.047923	0.096733
FBgn0038806	CG5412	0.052657		0.092527
FBgn0037090	Est-Q			0.086973
FBgn0036024	CG18180	0.052615	0.045455	0.08152
FBgn0052483	CG32483			0.080751
FBgn0000024	ACE	0.105395	0.066444	0.077531
FBgn0015575	A-EST7	0.043598	0.018661	0.077083
FBgn0038771	CG4390	0.078771	0.17827	0.071089
FBgn0027584	CG4757	0.051435	0.019807	0.070416
FBgn0020370	TPP2	0.156037	0.16708	0.067209
FBgn0032242	CG5355	0.246933	0.205709	0.059019
FBgn0000326	CLT	0.074857		0.049033
FBgn0032029	CG17292			0.047425
FBgn0037071	CG7632	0.052344	0.01	0.047076
FBgn0265267	CG18258			0.044077
FBgn0032864	CG2493	0.029052	0.167285	0.043086
FBgn0051821	CG31821	0.069708	0.070307	0.042517
FBgn0042138	APT1	0.029169	0.028068	0.039046
FBgn0035154	HIRO	0.035833		0.038602
FBgn0051683	CG31683	0.04496	0.021691	0.034879
FBgn0029942	CG2059	0.033737	0.019564	0.032105
FBgn0035670	CG10472	0.081865	0.119117	0.030295
FBgn0034076	Jhedup	0.020468	0.018704	0.029093
FBgn0000592	Est-6	0.019544	0.02148	0.02259
FBgn0259175	OME	0.024818		0.022186
FBgn0020545	kraken	0.028968	0.047657	0.022172
FBgn0038701	CG18493		0.161829	0.01
FBgn0036023	CG18179	0.179177	0.06144	0.01
FBgn0031406	SEND1			0.01

FBgn0033226	PUML			0.01
FBgn0029690	CG6414	0.033947	0.01	
FBgn0037842	CG6567	0.103649		
FBgn0039472	CG17192	0.029698		

Table 6.3. CG10038 interacting protein identified common to WT and S222A I.P proteome (Figure 6.8).

Proteins common to WT and S222A			
FBgn I.D.	Gene symbol	Average peptide count	
		WT 90	S222A
FBgn0038013	CG10038	14	10
FBgn0003360	sesB	4	1
FBgn0033926	Arc1	3	3
FBgn0014455	Ahcy	2	1
FBgn0013269	Fkbp39	2	2
FBgn0004587	B52	1	2
FBgn0285937	Rab1	1	1
FBgn0263598	Vha68-2	1	2
FBgn0015756	RpL9	1	1
FBgn0039463	Spag1	1	1
FBgn0037891	CG5214	1	1
FBgn0250814	UQCR-C2	1	1
FBgn0016685	Nlp	1	1
FBgn0015288	RpL22	1	1
FBgn0013325	RpL11	1	1
FBgn0265434	zip	5	1
FBgn0003886	alphaTub85E	2	1
FBgn0053869	His4:CG33869	1	2
FBgn0011230	poe	2	1
FBgn0032455	Pih1D1	1	1
FBgn0002780	mod	1	1

Table 6.4. CG10038 interacting protein identified unique to WT (Figure 6.8).

Proteins unique to WT		
FBgn I.D.	Gene symbol	Average peptide count
FBgn0003279	RpL4	3
FBgn0040232	cmet	3
FBgn0037636	aqz	3
FBgn0086472	RpS25	2
FBgn0011284	RpS4	2
FBgn0040074	retinin	2
FBgn0004867	RpS2	2
FBgn0002622	RpS3	2
FBgn0024957	Irp-1B	2
FBgn0032218	CG5381	2
FBgn0265767	zyd	2
FBgn0015376	cutlet	1
FBgn0037686	RpL34b	1
FBgn0035601	Uev1A	1
FBgn0037090	Est-Q	1
FBgn0000319	Chc	1
FBgn0038535	alt	1
FBgn0053303	CG33303	1
FBgn0003517	sta	1
FBgn0022893	Df31	1
FBgn0039250	Mink	1
FBgn0036824	CG3902	1
FBgn0036544	sff	1
FBgn0035121	Tudor-SN	1
FBgn0034259	P32	1
FBgn0030039	CG12123	1
FBgn0014009	Rab2	1
FBgn0064225	RpL5	1
FBgn0031127	CG1835	1
FBgn0029629	eIF3g1	1
FBgn0001313	kl-2	1
FBgn0039510	CG3339	1
FBgn0085427	CG34398	1
FBgn0011661	Moe	1
FBgn0010173	RpA-70	1

FBgn0038129	TBC1D5	1
FBgn0027567	CG8108	1
FBgn0005593	RpL7	1
FBgn0263220	Hk	1
FBgn0031281	Saf6	1
FBgn0003701	thr	1
FBgn0052017	CG32017	1
FBgn0031980	RpL36A	1
FBgn0261985	Ptpmeg	1
FBgn0036224	Rpt4R	1
FBgn0032298	CG6724	1
FBgn0263968	nonC	1
FBgn0261800	LanB1	1
FBgn0039580	Gfat2	1
FBgn0040377	Vha36-3	1
FBgn0000100	RpLP0	1

Table 6.5. CG10038 interacting protein identified unique to S222A (Figure 6.8).

Proteins unique to S222A		
FBgn I.D.	Gene symbol	Average peptide count
FBgn0020660	eIF4B	1
FBgn0031842		1
FBgn0035422	RpL28	1
FBgn0086710	RpL30	1
FBgn0037328	RpL35A	1
FBgn0033912	RpS23	1
FBgn0032518	RpL24	1
FBgn0028474	CG4119	1
FBgn0285949	RpL31	1
FBgn0033507	CG12909	1
FBgn0083960	CG34124	1
FBgn0039338	XNP	1
FBgn0040294	POSH	1
FBgn0262937	Rabex-5	1
FBgn0000557	eEF1alpha2	3
FBgn0033194	Vps13	2
FBgn0264449	CG43867	1
FBgn0053111	CG33111	1
FBgn0000489	Pka-C3	1
FBgn0004167	kst	1

Annexure 1

A systematic approach for generation of genetic reagents to annotate orphan serine hydrolases

Annexure 1

A systematic approach for generation of genetic and biochemical reagents to annotate orphan serine hydrolases

Aim: To generate the fly and biochemical reagent for study of orphan serine hydrolases in the *Drosophila melanogaster*

Rationale

We have learned in the chapter 1 that *Drosophila* genome encodes 354 non-redundant SH genes and categorized into serine proteases and metabolic SHs, with 210 and 144 members, respectively, of which 84% lacked known physiological function. A systematic approach needs to device for assigning the function of unannotated or orphan SHs in the *Drosophila*'s pathophysiology. If we know the expression and activity of SHs in the different developmental stages, it will be easy and fasten the uncovering of the role SHs. For answering the same, modENCODE and developmental proteome is built to profile the expression of different genes in the fly which include the SHs. In chapter 2, we have also built the activity atlas for SHs using ABPP-mudPIT. However, it is massive and less efficient to assign functions of all SHs together. Therefore, we need to select suitable candidate whose study will benefit to the mankind and associated niche.

The roadmap to identify and annotate candidate SHs, [**1**] Identify of suitable candidate (Methods to identify candidate SHs is discussed in Chapter 3 and 4); [**2**] know the identify family of SH (Chapter 1); [**3**] know the expression profile of SHs (Chapter 2); [**4**] using biochemical (Bacterial and insect cell expression system) and fly reagents, chemo-proteomics and metabolic LC-MS/MS (Lipidomic) technique make easy investigation of candidate SH annotations (Chapter 5 and 6) ().

Henceforth, we needed to **generate of proper reagents** using cloning, protein expression antibody generation, CRISPR/cas9 based knockouts flies for the annotation of each target.

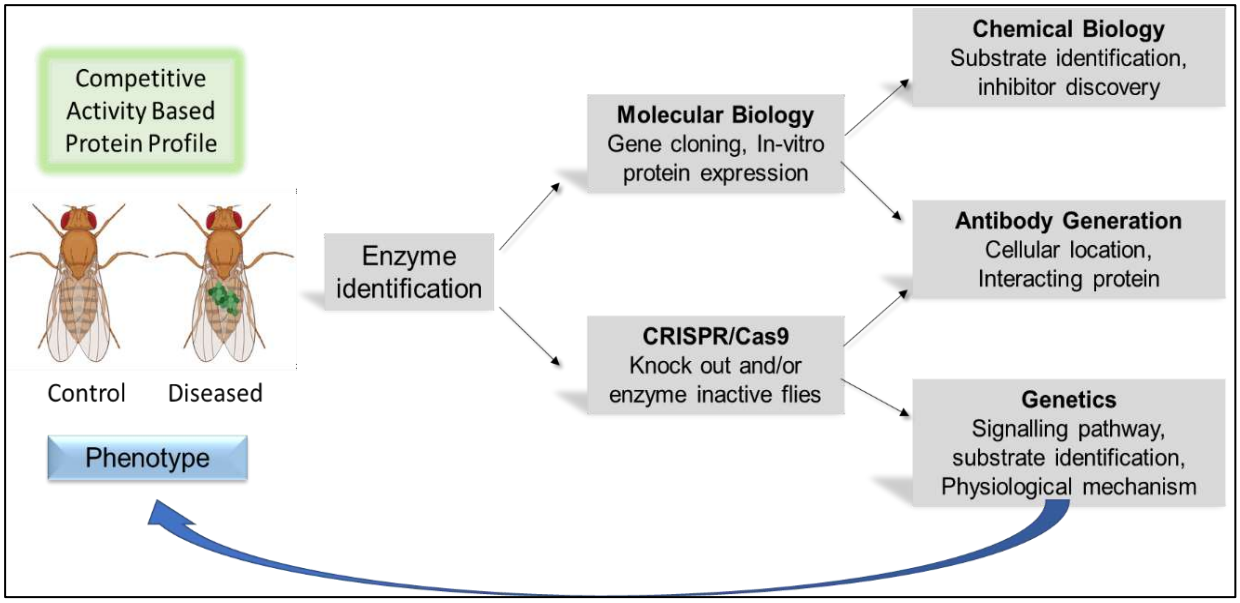

Figure Annexure1.1. Schematic for Genetic and Biochemical approach for the Global Analysis of an enzyme function.

In this annexure, We have following objectives.

Objectives

1). Determine five specific targets (Chapter 2 and 4) to uncover the mechanistic role of novel immune responsive SHs.

2). To clone the target genes into bacterial and insect cell expression vector for annotation of the substrate and enzyme activity.

3). Generation of polyclonal rabbit antibody against target gene.

4). To generate the loss-of-function (*lof*) lines for targeted SHs using CRISPR/Cas9 based genome editing technology.

5). To generate the gain-of-function (*gof*) lines for targeted SHs using UAS system.

Objective 1: Determine Six specific targets to uncover the mechanistic role of novel immune responsive SHs.

CG17192, CG5377, CG6567, CG11309 and CG4757 are selected as candidates target gene annotation of biological and biochemical function from the infection experiment (chapter 4). CG10038 is selected from activity atlas (chapter 2) as its orthologs associated with CHARGE syndrome and tumors in human. All target are metabolic serine hydrolases. The biodata of each candidate gene is listed the Table 5.1.

Table Annexure1.1: Biodata of candidate genes.

Gene		CG17192	CG5377	CG6567	CG11309	CG4757	CG10038
Family		mSH	mSH	mSH	mSH	mSH	mSH
Biological Function		-	-	-	-	-	-
Predicted catalytic activity		Triglyceride lipase	alpha-amino-acid esterase	S-formylglutathione hydrolase	-	carboxylesterase	-
Orthologs		PLA1A, LIPH, LIPC, LIPG	BPHL, PARG	ESD	SERHL2	CES1, CES2, CES3, CES4A, CES5A	FAM172A
Human Orthologs of this gene implicated in several diseases		Cardiovascular system disease, Type 2 diabetes mellitus	-	-	-	Drug metabolism	Charge syndrome, implicated in cancer
Predicted Molecular weight (kDa)		36	32	36	36	62	36
Expression pattern	Expression (mRNA)	Adult gut, Carcass	Ubiquitos	Ubiquitos	Ubiquitos	Prepupa, adult male and female	Ubiquitos
	Activity	Adult gut and Hemolymph	Ubiquitos	Ubiquitos	Embryo, Adult head, carcass, gut, testis	Pupa, Adult head and hemolympd	Ubiquitos
Localization		Extracellular lumen	-	-	-	-	Cytoplasmic

The expression of CG4757 is regulated by the spatzle upon infection (De Gregorio et al. 2001; De Gregorio et al. 2002). There are 36 paralogous genes of CG4757 (FlyBase) and CG3841, Ace, Jhe and CG4382 show the highest sequence similarity. It mostly expresses in the hemolymph, fat body and brain. CG4757 was predicted to be involved in the Glycerophospholipid metabolism (Kegg pathway database). CG4757 expression is upregulated in response to immune challenge (Duneau et al.

2017; De Gregorio et al. 2001; De Gregorio et al. 2002). CG17192 and CG11309 have lipase activity. Predicted to be involved in lipid catabolic process (Flybase database). Predicted to localize to extracellular space. Human ortholog(s) of this gene implicated in hypotrichosis 7, a condition that affects hair growth. Orthologous to human lipase H; lipase I; and phospholipase A1 (Flybase database).

Objective 2: To Clone and express the target gene for annotation of the substrate and enzyme activity.

Material and methods

Cloning and expression: The targets gene CG10038, CG11309. CG17192, CG4757 are cloned in bacterial [pET45(b+), Addgene-] and insect [pRM-HA 3] expressing vector using SLiCE cloning method. For serine to alanine point mutation, site directed mutagenesis technique were used and Primers used for cloning is listed in the Table Annexure 1.1. All cloned were verified using sanger sequencing. The bacterial vector expresses in BL21-DE3 and insect cell vector in the insect cell (S2 cell) using standard protocol. and CG11309 is purified using Ni-NTA based affinity purification in native condition using manufacture procedure (Ni-NTA beads, quiagen).

FPLC Purification of CG11309

Ni-NTA purified CG11309 protein further clean using Sephadex G-75 FPLC system. Column.: - matrix, Sephadex G-75; Eluent.: - Tris-Bbuffer-Saline; flow rate.: - 1 ml/min. Peak in the elution profile represents a protein present in the eluate. CG11309 show elution peak at 8.5ml to 10ml elution volum of superdex-75 analytical column.

Table Annexure1.2: Summary of target SHs gene cloning

Gene	Cloned in bacterial expression vector/ Protein expression	Cloned in insect expression vector
CG17192	Yes/Yes (Mrunal Pazare MS thesis)	Yes/Yes (Mrunal Pazare MS thesis and Chapter 5)
CG10038	Yes/Yes (Chapter 6)	Yes/Yes (Chapter 6)
CG11309	Yes/Yes	No
CG4757	Yes/No	No

Results

Purification of CG11309

The WT CG11309 are successfully cloned using SLiCE technique into pet45(b+) **A** tor with N-terminal His tag. WT CG11309 were expressed and purified from *E. coli* as described in the protocol earlier in this Chapter 5. The E3 elution fraction out of E1, E2 and E3 has the highest purity (>90%) (**Figure Annexure1.2**), which is used for further biochemical assays. The 5-10 mg is the yield of CG11309/L of culture.

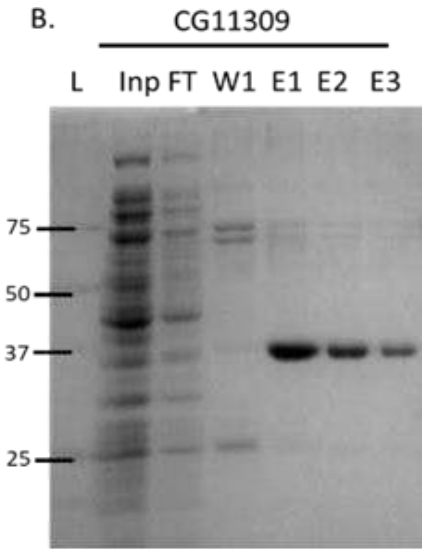

Figure Annexure1. 2. Ni-NTA based affinity purification of the CG11309.
SDS-PAGE based visualization of CG11309. CG11309 run at 37kDA. Acronyms: -inp- input, FT- flowthrough, W1- wash 2, E1- elution 1, E2- elution 2 and E3- elution 3.

FPLC cleanup of CG11309

The Ni-NTA purified CG11309 protein has cleaned through size exclusion chromatography using Fast pressure liquid chromatography (FPLC) and suprdex-75 analytical column (**Figure Annexure1.3**). The chromatogram shows that Ni-NTA purified protein is pure and form dimer in native condition. Since, CG11309 get eluted just after void volume.

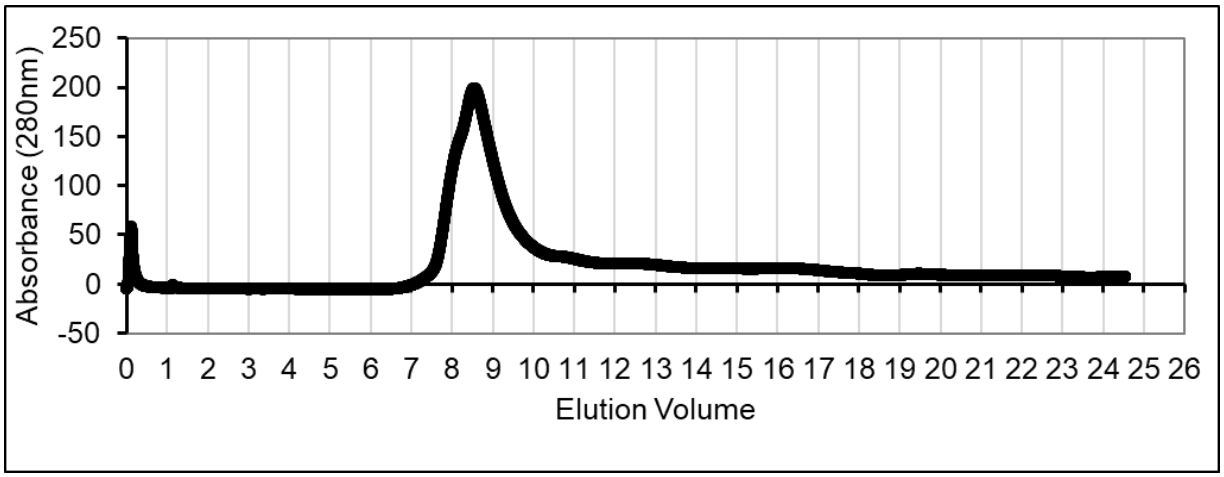

Figure Annexure1.3 Chromatogram of CG11309 protein. The chromatogram shows that CG11309 get eluted just after void volume i.e 7 to 19 minutes on superdex-75 analytical column.

Objective 3: In-house polyclonal rabbit antibody generation against CG10038 and CG11309

Material and methods

The Purified protein of CG10038 and CG11309 elumisfied with complet fruend's adjuvant (CFA) and inject subcutaneously in rabbit (Animal #1 for CG10038 and Animal #2 for CG11309) as plan shown in table 2. The first booster made in incomplete fruend's adjuvant (IFA) and inject subcutaneously. The serum collection and booster immunization perform as per table 2. Pre-immune serum from respective animal was taken as negative control. Western blotting were perform to test the serum for generation of antibody.

Table Annexure1.3: Plan of In-house generation of antibody against CG10038 and CG11309

Procedure	Protocol Day	Date	Description
Control serum collection	Day 0	27/06/2023	Pre-Immune bleed (3ml)
Primary injection	Day 1	27/06/2023	Immunize with 0.25 mg antigen in CFA, SQ 4 sites
1st booster	Day 14	10/07/2023	Boost with 0.10 mg antigen in IFA, 4 SQ sites
Serum collection	Day 28	24/07/2023	Bleed (~2 mL per rabbit)
2nd booster	Day 42	07/08/2023	Boost with 0.10 mg antigen in IFA, 4 SQ sites
Serum collection	Day 56	21/08/2023	Bleed (~2 mL per rabbit)
3rd booster	day 56	21/08/2023	Boost with 0.10 mg antigen in IFA, 4 SQ sites
Serum collection	Day 70, 72	04/09/2023 & 06/09/2023	Two bleeds (~40 mL total per rabbit)

Results

The immune serum for animal #1 shows strong reaction to pure His-CG10038 protein on western blot. There are many unspecific IgG antibody in first bleed for CG10038 anti-serum (**Figure Annexure1.4.A**). Similarly, CG11309 anti-serum was tested and western blotting shows of optimum antibody generation against CG11309 (**Figure Annexure1.4.B and C).**

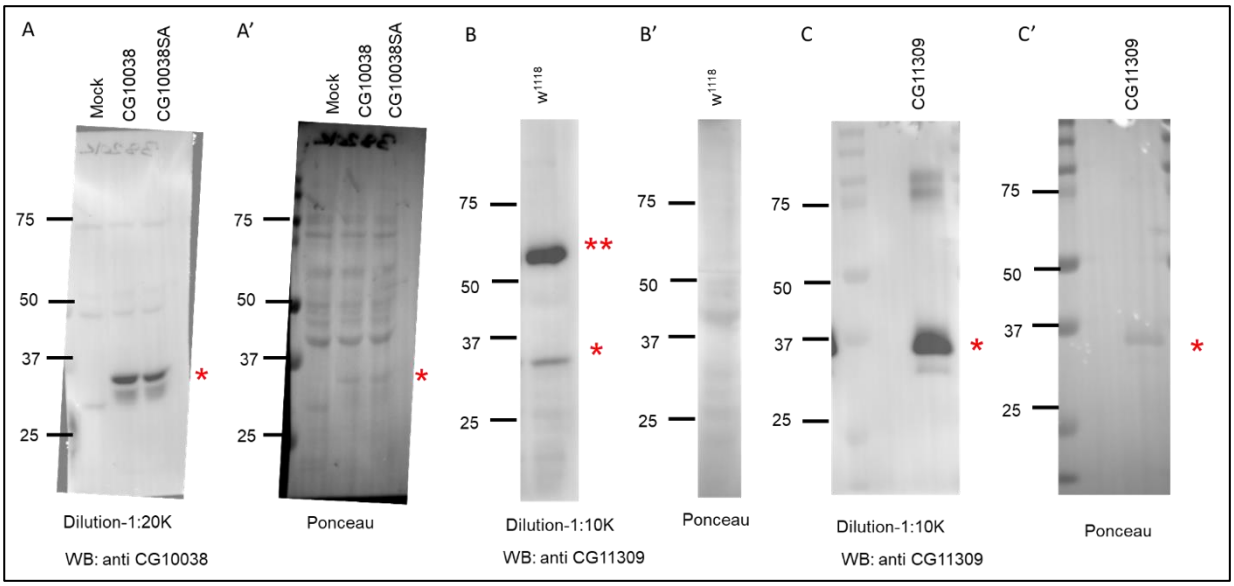

Figure Annexure1.4. Validation of in house generated rabbit polyclonal antibody against (A and A') CG10038 and (B, B', C and C') CG11309 full length protein using western blot technique.

(A) CG10038 anti-serum, dilution 1:20,000 tested on overexpressed wt-CG10038 and S220A-CG10038 protein in S2 cell, mock act as negative control. Band (red asterisk '*') specific to CG10038 observed in wt-CG10038 and S220A-CG10038 transfected lysate but is not present in the mock lysate, confirming specificity of the antibody. (B and C) CG11309 anti-serum, dilution 1:10,000 tested on wildtype adult fly lysate and purified CG11309 protein. Band (red single asterisk '*') specific to CG11309 observed in both wildtype adult fly lysate and purified protein. Double red asterisk shows unspecific band in case of CG11309 anti-serum western blot with adult fly lysate. Ponceau show loading of protein.

Objective 4. To generate the loss-of-function (*lof*) lines for targeted SHs using CRISPR/Cas9 based genome editing technology.

Material and Method

CRISPR Cas9 technology was employed to generate null fly lines for CG17192, CG11309 and CG4757. Dual guide (dg)-RNAs targeting the coding region in the 5'end of Exon 1 and 3' end of last Exon was designed by Deepti Trivedi, fly facility NCBS Bangalore. The dgRNAs were cloned into the *pU6-BbsI-chiRNA* (Addgene # 45946) plasmid, which was then docked into *y1 v1; P{CaryP}attP40 Drosophila* line (BDSC 36304), by transgenic injections, at the NCBS-CCAMP transgenic facility, Bangalore, India. 3 *dual-gRNA* male flies (F0) crossed to *nos-Cas9* (BDSC 54591) animals which produce F1 dual-gRNA/nos-Cas9 progeny. 20 male of dual-gRNA/nos-Cas9 animal (F1, Cas9-gRNA complex form in the germ cell of this animal) cross with balance fly (**Figure Annexure1.5**). Two hundred flies (F2, animal having putative mutation) were balanced over a third chromosome balancer and screened for genomic deletion. The null progeny (F3) self-cross to make independent population.

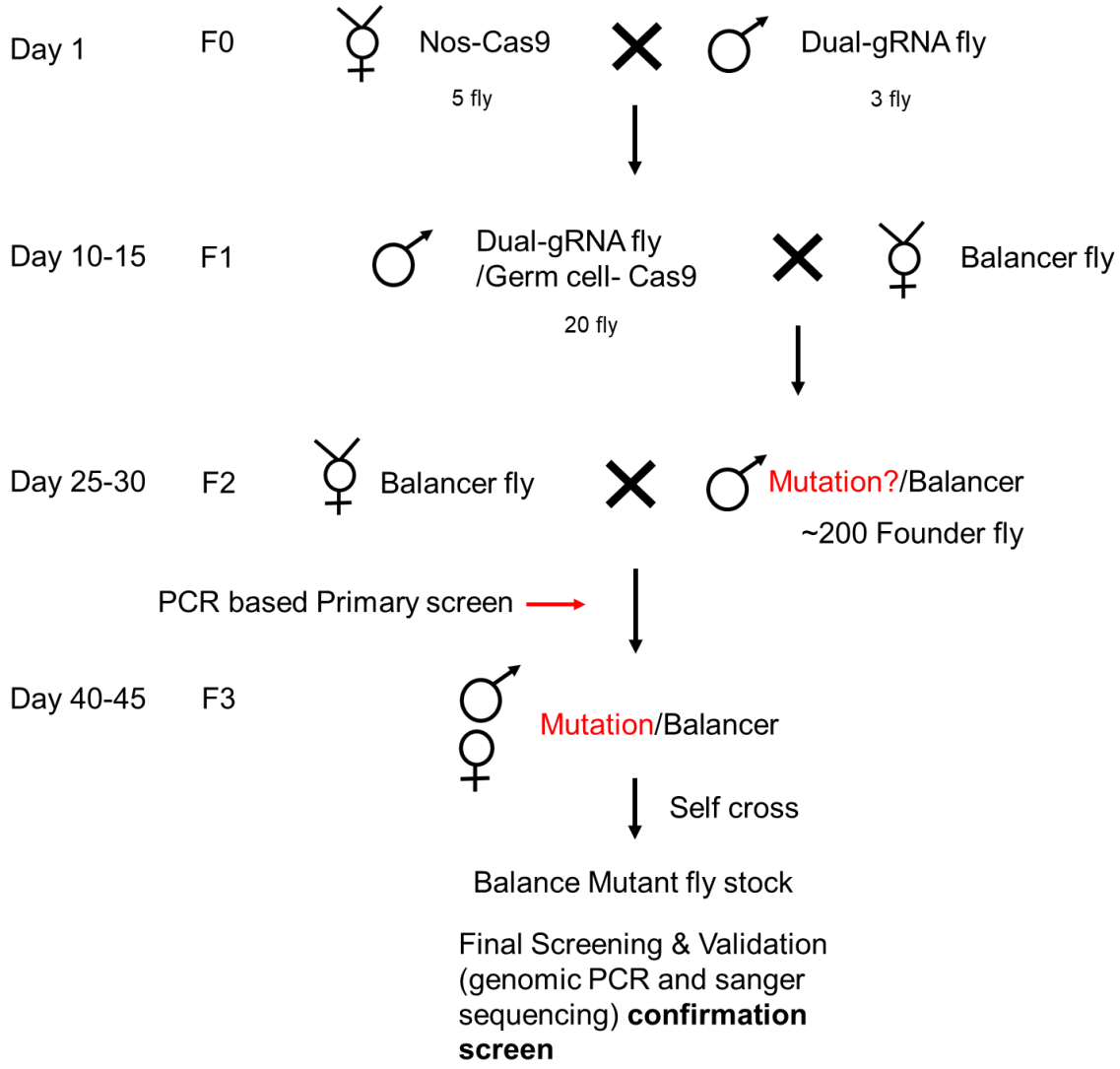

Figure Annexure1.5. *Drosophila* Crosses for excision of the SHs genes locus to generate null fly line of SHs.

Results

The transgenic dgRNA lines were crossed to the nanos-*Cas9* line. The founder male progenies obtained were crossed to *w*⁻*;;Sb/Tb* balancer females wherein the Cas9-dgRNA complex is formed in the germline. In the next generation, three heterozygous female progenies from each cross were maintained as a separate line over a *Sb/Tb* balancer. Since the CG17192 (**Figure Annexure1.6**), CG11309 (**Figure Annexure1.7**) and CG4757 (**Figure Annexure1.8**) gene is located on the III.

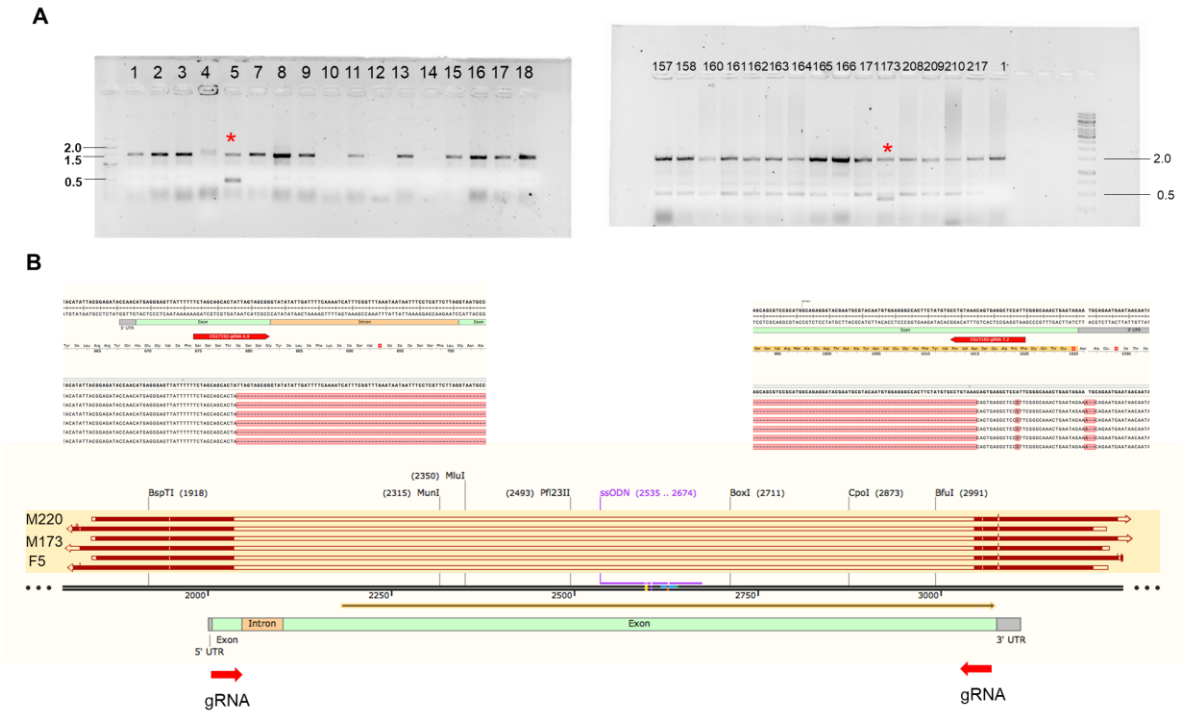

Figure Annexure1.6. PCR based screening of CG17192 knockout using CRISPR/Cas9 genome engineering.

(A) A ~2kb deletion in the CG17192 gene was generated using a dual gRNA strategy, resulting in a loss-of-function (lof) mutant allele. To detect this lof allele in heterozygous flies, PCR primers were designed to flank the expected deletion site. The deletion produces an ~0.5 kb amplicon, while the wildtype chromosome yields a 2 kb PCR product, corresponding to the intact gene. In heterozygous mutants or balancer flies, both PCR products are present. The PCR products were separated on a 1% agarose gel and visualized with Ethidium Bromide staining. **(B)**Schematic showing the deletion of CG17192 gene region in line F5, M173 and M220. A10 and A24, two more deletion were made with Anand Karthik.

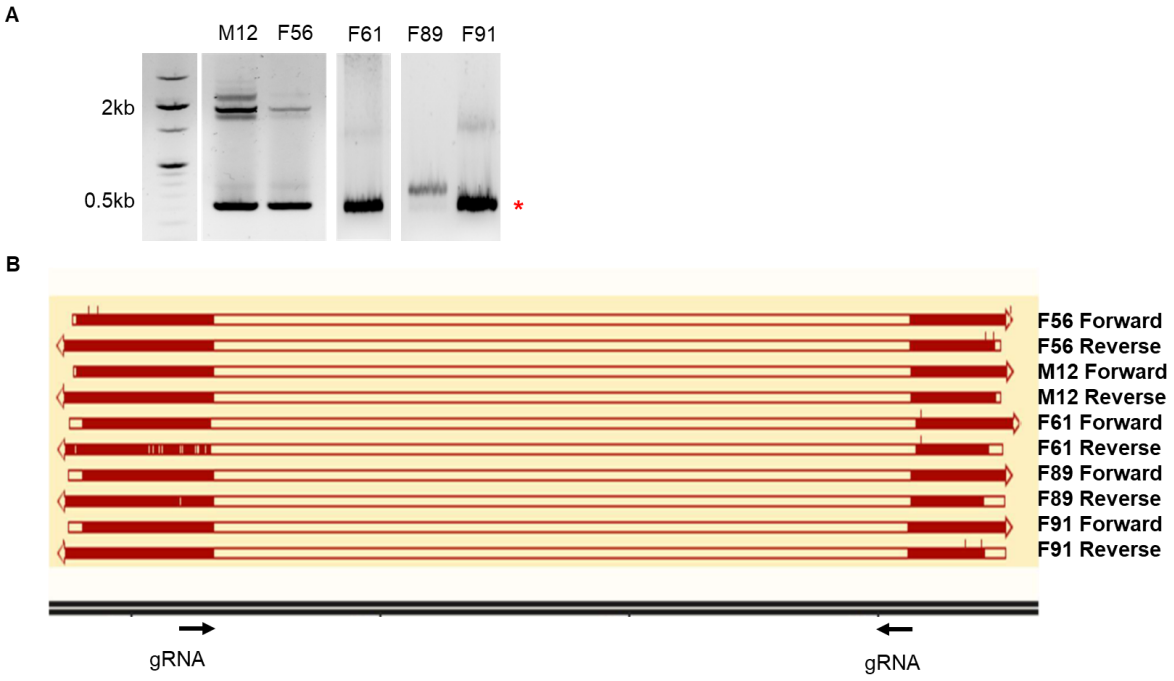

Figure Annexure1.7. PCR based screening of CG11309 knockout using CRISPR/Cas9 genome engineering.

(A) A ~2kb deletion in the CG11309 gene was generated using a dual gRNA strategy, resulting in a loss-of-function (lof) mutant allele. **(B)**Schematic showing the deletion of CG11309 gene region in line F56, M12, F61, F89 and F91. These mutants made with Rishita Ghosh.

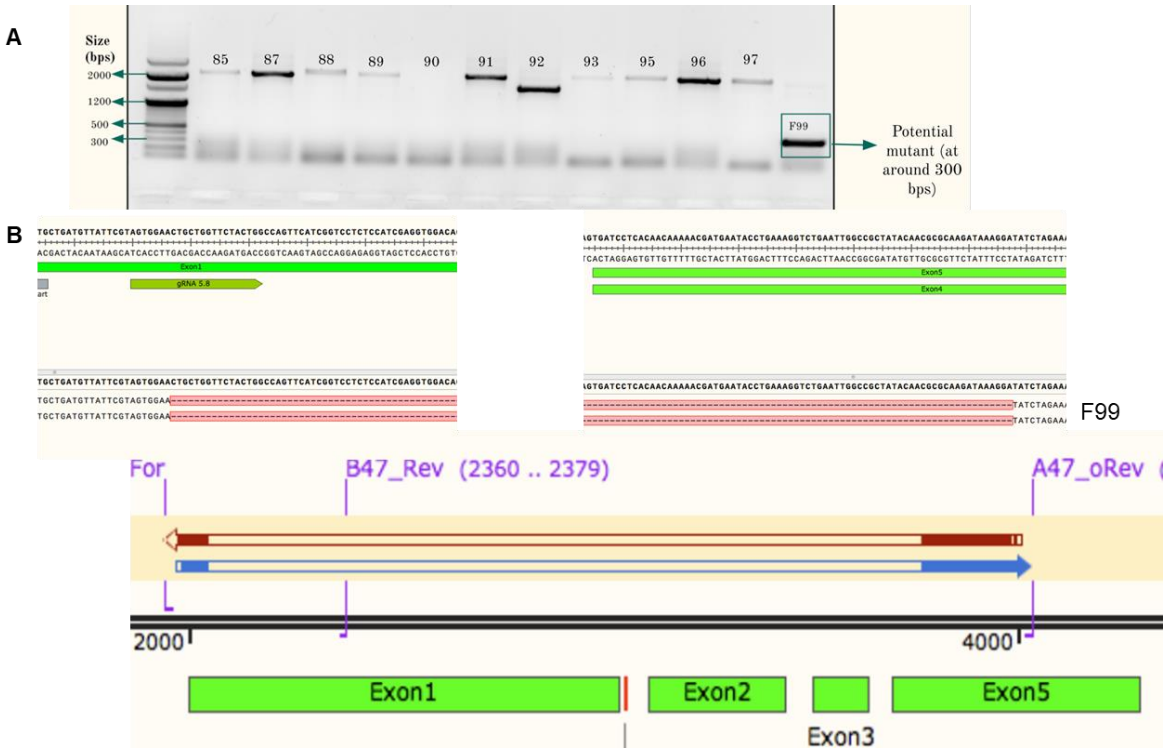

Figure Annexure1.8. PCR based screening of CG4757 knockout using CRISPR/Cas9 genome engineering.

(A) A ~2kb deletion in the CG4757 gene was generated using a dual gRNA strategy, resulting in a loss-of-function (lof) mutant allele. **(B)** Schematic showing the deletion of CG4757 gene region in line F99 and F91. These mutants made with Apoorva Gopal.

Contribution

Fly facility at C_CAMP (NCBS) Bangalore (Dr Deepti Trivedi and her team) has generated the dual gRNA line. Anand Karthik, Apoorva Gopal, Rishita Gosh contributed with generation of CRISPR line as aforementioned.

Objective 5. To generate the gain-of-function (*gof*) lines for targeted SHs using UAS system.

Material and method

pUASp AttB fly lines/strains: UAS-wt-*CG17192* and UAS-*S179A-CG17192* were cloned into *pUASp-attB vector* using a homology-based recombination technique, a

modification of the SLiCE protocol (Zhang et al., 2014). Find PCR primer in the Table Annexure 1.1. Prior to injection, pUASP-wt**-***CG17192* and pUASP-*S179A-CG17192 vector co-transfected with Act-gal4* plasmid in S2 cell for expression using standard protocol (see chapter 5). Then, these cloned vectors were injected into *AttP4O fly* lines for the generation of transgenic fly lines. The injected animal (F0) was self-crossed and the progeny (F1) were screen for the mini-white (**Figure Annexure1.10,** middle fly, red arrow). The founder progeny with mini-white eye were crossed the *w-;Tft/Cyo* balancer fly. Finally, mini-white progeny (F3) was self-cross for make homogenous population transformed pUASP-wt**-***CG17192* and pUASP-*S179A-CG17192* fly line.

[We thank the Fly facility at the National Centre for Biological Science (NCBS), Bangalore, for generating dual gRNA flies and embryonic injections for UAS fly. Dr. Deepti Trivedi for her input on the design of the CRISPR/Cas9 genomic constructs.]

Results

As discussed in Chapter 5 for pRM-CG17192 vectors, ABPP gel for pUASp cloned for WT and S179A CG17192 shows that WT is active and S222A inactive in the soluble fraction. Also, CG17192 get secreted into media as expected from chapter 5 (Figure Annexure1.9).

Acknowledgments

We thanked Dr Swapnil Bangar along with his team at National Facility For Gene Function In Health and Disease for generous effort in generation of antibodies.

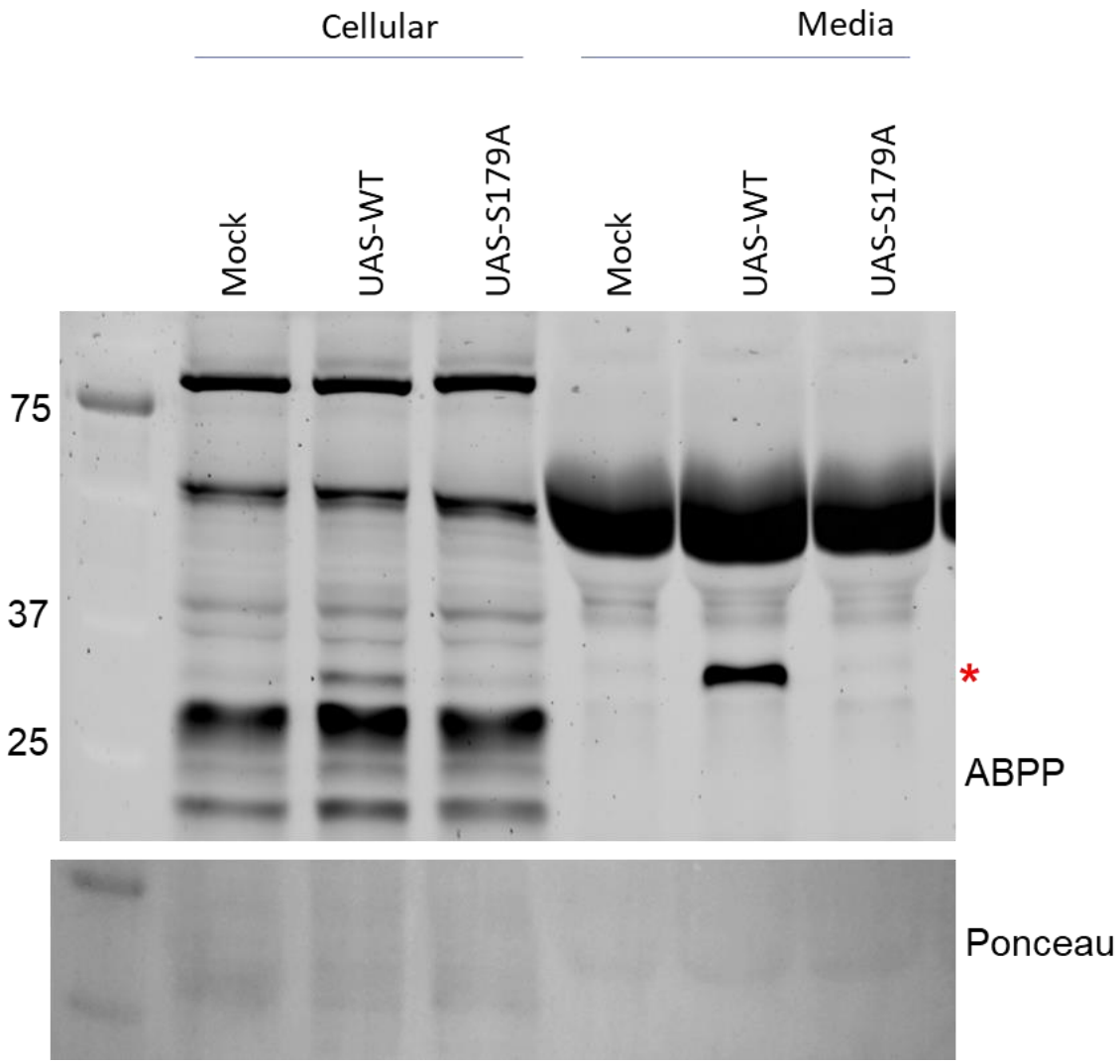

s

Figure Annexure1.9. The various proteomic fractions (membrane, soluble and secreted media) of S2 cells transfected with mock, pUASp WT and S179A CG17192 as described in method, were assessed using gel-based ABPP (top panel) and Ponceau S staining (bottom panel). The red asterisk corresponds to the activity (top panel) or expression (middle panel) of CG10038.

After checking the expression in S2 cells, plasmids were injected into Attb flies as described the method and stable transgenic line generated which have mini-white eye marker (**Figure Annexure1.10,** middle fly, red arrow). For the expression of transgenic fly lines, both UAS-CG17192-WT and UAS-CG17192-S179A were cross with NP1 Gal4 and Tubulin Gal4 and F1 flies were lysed and check foe expression using ABPP assay.

Figure Annexure1.10. Representative image of transgenic flies. Selection of mini-white selection marker based transgenic flies for WT and S222A UAS-CG17192.

Table Annexure 1.4: List of primers

S.No.	Primer name	5' to 3'	Use for
1	Pet45_RP_common	GTGATGGTGGTGGTGATGTG	Clonning of SHs in Pet45(b+)
2	Pet45b_FP_common	GTGGGTACCGGTTCGAATGA	
3	Pet45b CG17192 RP	TCATTCGAACCGGTACCCACCTATTCAGTTTGCCCGAATGGAGC	Clonning of His-CG17192 in Pet45(b+) vector
4	Pet45b CG17192_FP	CACATCACCACCACCATCACGGTGGTATGAGGGAGTTATTTTTTCTAGCAG	
5	Pet45b_CG10038_RP	TCATTCGAACCGGTACCCACTCACTTCTTATTCGCTCGCTGTTCAT	Clonning of His-CG10038 in Pet45(b+) vector
6	Pet45b_CG10038_FP	CACATCACCACCACCATCACGGTGGTATGTGGTCTAGGCTTATTCAAAT	
7	Pet45_CG4757_FP	CACATCACCACCACCATCACGGTGGTATGCTGATGTTATTCGTAGTGG	Clonning of His-CG4757 in Pet45(b+) vector
8	Pet45b_CG4757_RP	TCATTCGAACCGGTACCCACTTAGTGAAAGCTTGAAAGTGGAAATAAATCCTCC	
9	Pet45b_CG11309_FP	CACATCACCACCACCATCACGGTGGTATGGACACGGACGAC	

10	Pet45b_CG11309_RP	TCATTCGAACCGGTACCCACCTAAAGCTTGCTCTCCTTCGCC	Clonning of His-CG11309 in Pet45(b+) vector
11	cPRM_Rev	GTGATGGTGGTGGTGATGCATGGTACCGAGCTCGAATTC	Clonning of SHs in pRMHA-3
12	cPRM_For	GGATCCTCTAGAGTCGACCTGC	
13	pRM CG1309_FP	CATCACCACCACCATCACATGAGTTTCCTAAATTACGTGTTTGGC	Clonning of His-CG11309 in pRMHA-3 vector
14	PRM_CG1309_RP	CAGGTCGACTCTAGAGGATCCTTAGGTGAACACAAATCCCTGCTC	
15	PRMCG17192_FP	CATCACCACCACCATCACATGAGGGAGTTATTTTTTCTAGCAGC	Clonning of His-CG17192 in pRMHA-3 vector
16	PRM17192_RP	CTCTAGAGGATCCCTATTCAGTTTGCCCGAATGGAG	
17	PRMCG4757_FP	CATCACCACCACCATCACATGTTATTCGTAGTGGAACTGCTGG	Clonning of His-CG4757 in pRMHA-3 vector
18	PRMCG4757_RP	CTAGAGGATCCTTAGTGAAAGCTTGAAAGTGGAAATAAATC	
19	PRMCG6567_RP	TCGACTCTAGAGGATCCTCAGAGTTTGTTCTGTACTTGG	Clonning of His-CG6567 in pRMHA-3 vector
20	PRMCG6567_FP	CACCACCACCATCACATGAAGCCAGCCTTGACAAC	
21	PRMCG10038_RP	GTCGACTCTAGAGGATCCTCACTTCTTATTCGCTCGCTG	Clonning of His-CG10038 in pRMHA-3 vector
22	PRMCG10038_For	CATCACCACCACCATCACGGTGGTATGTGGTCTAGGCTTATTC	
23	pUASp_CG17192_FP	GCATAGGCCACTAGTGGATCATGAGGGAGTTATTTTTTCTAGCAGC	Clonning of pUASP-CG17192 in pUASp vector
24	CG17192_flag_RP	CTTATCATCATCATCCTTGTAATCTTCAGTTTGCCCGAATG3	
25	pUASP_cFlag_RP	GGTCGACTCTAGAGGATCCATCACTTATCATCATCATCCTTGTAATC	
26	pUASp_CG10038FP	GCATAGGCCACTAGTGGATCATGTGGTCTAGGCTTATTCAAATATTTC	Clonning of pUASP-CG10038 in pUASp vector
27	CG10038cFlag_RP	TCACTTATCATCATCATCCTTGTAATCCTTCTTATTCGCTCGCTGTTC	
28	pUASP_cFlag_RP	GGTCGACTCTAGAGGATCCATCACTTATCATCATCATCCTTGTAATC	
29	AG_CG11309 For	CGATCACCATGACCTTTGAATC	Screening of CG11309 CRISPR knockout
30	AG_CG11309 iRev	ACAGAATCGGTATGACACCTAC	
31	AG_CG11309 oRev	GCGCAATACAAAAGGGTTAAGC	
32	AG_CG17192 For	AGATAGATGCAACACACGAAAC	Screening of CG17192 CRISPR knockout
33	AG_CG17192 iRev	GAACGGAATTCGAGAGGGGAAA	
34	AG_CG17192 oRev	CGAATTCCAAACAGGATGGGTG	
35	AG_CG4757 For	GCAATCGCATCTGGGTAAAGC	Screening of CG4757 CRISPR knockout
36	AG_CG4757 iRev	CTGGCTGCGGATTCACAAATC	
37	AG_CG4757 oRev	CACCTGACGATAGTTATGCGC	
38	KK10038_CR_For	TATTCCATCCCTAGTTCGGCGTTC	Screening of CG10038 CRISPR knockout
39	KK10038_CR_i_Rev	TCCTACCCACGTGGGCATATG	
40	KK10038_CR_ORev	GTGACAGATTCGGACACTCGC	
41	KK4390_CR_1For	CTGTGCTTTCTGATGCGAGCG	Screening of CG4390 CRISPR knockout
42	KK4390_CR_i1Rev	ATGCACAGCAGTTCATCTGTAAG	
43	KK4390_CR_oRev	TCTTCTGTACATTGGCACCTAGAATG	
44	KK5377_CR_2For	GCCAAATATTCCTCTCTGGACATC	Screening of CG4390 CRISPR knockout
45	KK5377_CR_iRev	CGTTCAAGTAGGCACCTGCTC	
46	KK5377_CR_ORev	ACTTTGAACACCTGCATGCTC	

Annexure 2

Protocol for ‘Active’ Serine Hydrolases staining in *Drosophila*’s embryo using Activity Based Probes (ABPs)

Annexure 2

Protocol for 'Active' Serine Hydrolases staining in *Drosophila*'s embryo using Activity Based Probes (ABPs)

Abstract

Serine hydrolases (SHs) are a superfamily of enzymes. Serine hydrolases superfamily members play essential roles in the various pathophysiological processes and serve as therapeutic targets for many clinical conditions. Activity-based protein profiling (ABPP) is a powerful chemoproteomic approach to study the roles of SHs in complex biological settings through gel-based fluorescence and LC-MS/MS based quantitative identification approach. Both approach cannot reveal the the cell identitiy and its type which is responsible for serine hydrolase activity. *Drosophila*'s embryo harbors around 50 percent serine hydrolases gene at the protein level and 20 percent can be assayed for activity using the current ABPP technique. Here, we develop the protocol to access the in-situ enzyme activity of the *Drosophila* embryo using both broad-spectrum and target-specific activity probes. Our method involves permeabilization of the embryos and in-situ reaction of serine hydrolases with chemical probes. Our protocol advances the ABPP technique to image global and specific SH activity using high-resolution confocal fluorescence imaging in anatomically preserved complex native cellular settings,

Keywords: Activity Based Protein Profiling (ABPP); Activity-based probes (ABPs), Serine Hydrolases, *Drosophila*; Embryo, Microscopy

Introduction

Serine hydrolases (SHs) are an enzyme superfamily characterized by conversed nucleophilic serine at the active site[1]. SHs superfamily is the most significant functional enzyme class across prokaryotes and eukaryotes, constituting 1-3% of the total cellular proteome. SHs superfamily members play important roles in most physiological processes like development, body patterning, digestion, growth, neurotransmission, metabolism, immune response, oxidative stress, inflammation, blood coagulation and signaling cascade[2]. Also, SHs have been reported as therapeutical targets for diseases and disorders such as cancer[3], obesity[4], bacterial infection[5] and neurological disease[4]. Activity-based protein profiling (abbreviated as ABPP) is a technique to profile SHs enzyme activity using activity-based probes (ABPs) in various complex proteome settings such as cells, tissue lysates, or small organism lysate[6]. The SHs activity probes consist of three elements: the reactive warhead, which reacts with enzymes, a tag that allows detection, enrichment and quantitiv identification and a spacer to prevent the steric clash of tag in the enzyme active site and also contributes to selectivity and specificity of the probes[7]. The fluorophosphonate (FP) warhead reacts with most of the members of the SHs superfamily and links to either fluorescent tags (Rhodamine, BODIPYs, Fluorescein) for gel-based-ABPP or Biotin for LC-MS/MS based Multidimensional Protein Identification Technology, often called ABPP-MudPIT. ABPP enables the comparison of SHs amongst various proteomes such as different developmental stages, tissue, cells or wildtype and mutant settings. Gel-based ABPP allows qualitative or semi-quantitative readout of SHs activity, and ABPP-MudPIT uses biotin-avidin-based enrichment and subsequent LC/MS-MS-based quantitively target identification[8]. The identification of SHs in tissues is a trivial task as compared to the lysates and hence the procedure for the same remains unexplored.[9]. Aaltonen et al. Biological Procedures Online, 2020, was the first to develop a procedure for labeling and high-resolution microscopy imaging of the ‘active’ SHs in the mice brain section[9]. Using inhibitor sensitivity of ABPs or competitive ABPP assay, authors rule out the unspecific reactivity of the FP-probes in-vivo. Like, FP-probes, β lactone-based ABPs (MB064, MB108) also react with a broad range of the SHs[10]. The imaging of active SHs with broad-spectrum probes define the cellular localization of all SHs but not

specific SHs. However, Specific or tailored ABPs like HT01, and WHP01 determine the cellular localization of an active SH[11].

Drosophila melanogaster is a popular model organism used to study many biological processes and disease mechanisms using its short life cycle and powerful genetic tool kit[12]. *Drosophila melanogaster is* used to study organism development and patterning process. A Cascade of serine proteases mediate the activation of toll signaling and, thus, dorsal-ventral patterning[13]. The serine proteases cascade and localization have been discovered using biochemical and genetics respectively[14]. Around 80 serine hydrolase enzyme are deposited maternally in the embryo, and 80% of the them are orphans (Chapter 1 and 2). The localization of 'active' SHs in developing embryos is the major factor to contribute the annotation of the orphan SHs.

Here, we advance the ABPP methodology enabling high-resolution confocal fluorescence imaging of superfamily-wide and specific SHs activity in *Drosophila* embryos using Broad Spectrum (FP-Rh) and tailored (WHP01) ABPs. We chemically permeabilized the embryo[15] and incubated the embryo with FP-Rh or WHP01 for labeling of active SHs. The rhodamine azide taken as a control for SH activity. The ABPs labels the active SHs and rhodamine-azide fail to do so. The WHO01 show the localization of specific SHs in the embryo.

Materials

1. *Drosophila* Embryo
2. 100% Bleach
3. Embryo basket
4. Paintbrush (size 10)
5. Isopropanol
6. D-limonene
7. Heptane
8. Paper towel
9. Flat bottom glass dish 1.5cmX1cm
10. Flurophosphoonate-rhodamine
11. WHP01

12. 4% Paraformaldehyde
13. Methanol, Glass vials
14. 1x Phosphate buffer saline (1xPBS)
15. Triton-X 100
16. Hoechst
17. Glass slides
18. Coverslip

Mounting media (90% glycerol, 0.01% n-propyl gallate),

Equipment

- Thermoxiture (Eppendorf, city, state if applicable, country; Cat. no.: XXX)
- Rotator (Manufacturer's name, city, state if applicable, country; Cat. no.: XXX)
- Light stereo microscope
- Confocal microscope

Procedure

1. **Collection of *Drosophila* embryo**: Collect and age the Drosophila embryo as per experimental design [16]. Transfer the embryos to a embryo basket and wash the embryos using running tap water. The wash basket help transfer embryo from one solution to another.

2. ***Drosophila* Embryo Dichlorination:** Dechlorinate the embryo in 50% bleach for 90 seconds and rinse with running tap water for 1-2 minutes to remove the excess bleach[17]. After dichlorination, Blot the embryo basket on a paper towel to remove excess water as much as possible. Over-incubation may damage the embryo**. (See** *Drosophila* Embryo Dichlorination (ref doi:10.1101/pdb. prot4826).

⚠ CRITICAL STEPs Permeabilization [Steps 3 to 5]

3. The embryo basket dips into 100% isopropanol for 5 to 10 seconds. All embryos sank to the bottom. Again, blot the embryo basket on the paper tawel to remove excess isopropanol. Dry the embryo basket with blowing humid air until the basket mesh becomes see-through. NOTE- Isopropanol uses to remove water. It is critical to remove the isopropanol. The combination of isopropanol and hexane is toxic to embryos.

4. The embryo basket dips into D-limonene and heptane mixture (1:4) for 10 seconds. This step permeabilizes the embryo. Again, blot the embryo basket of a paper towel.
5. Embryo basket dip into heptane for 5 seconds. This step removes the D-limonene from the embryo. Finally, air-dry the heptane from the embryo[15].

⚠ CRITICAL STEPs SHs reaction with activity probes

6. **In-vivo labelling of 'active' Serine Hydrolases:** transfer the permeabilized embryo into 1.5 ml microcentrifuge tubes with the help of a wet brush which contains required reaction mixture. Incubate embryo with reaction mixture at 37°C, 750rpm for 15 minutes on thermos-mixture.
7. Aspirate the reaction mixture after the reaction. Then, wash the embryo with 1XPBS thrice.

Embryo Fixation [Step 8 to 10] (see

8. Transfer the embryo in a glass vial and fix the embryo with 1:1 mixture of the 4% paraformaldehyde (in 1X PBS, called fix) and n-heptane for 25 minutes on a mutator.
9. **Embryo floats at interface of n-heptane and fix.** Remove the lower phase (fix), add equal volume of chilled methanol, and shake for 15-20 seconds to remove the vitelline membrane. At this strep, Devitellinized embryo sink to the bottom.
10. **PAUSE STEP:** Remove the upper liquid and rinse the embryo with methanol twice. The embryo can store at -20°C for a week at this step.
11. Rehydrate the embryo thrice with 0.1% 1X PBST for 15 minutes.
12. **OPTIONAL STEP**: Embryo can be used for immune staining using standard protocols.
13. Add 1X DAPI in 0.1% PBST and incubate for 15 minutes on the mutator. And wash the embryo with 0.1% PBST for 10 minutes.
14. Transfer the embryo to a glass slide the soaked the PBST, and add mounting medium. Cover the embryo with a cover slip and seal the sides with colourless nail paint.
15. Image the embryo under a confocal microscope.
16. Analyse images using ImageJ Software (Figure Annexure2.1).

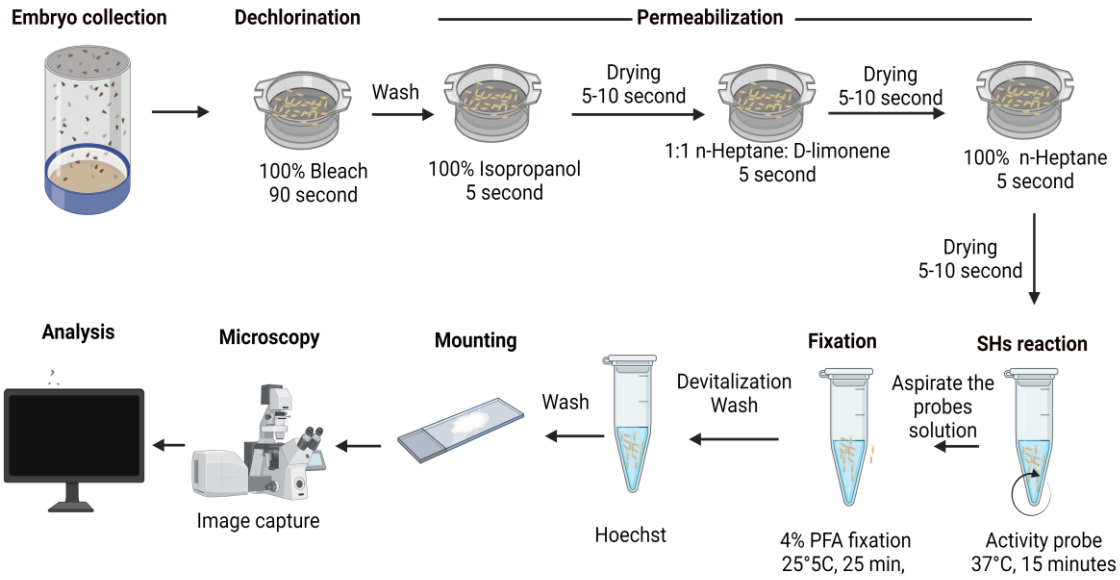

Figure Annexure2.1. Work scheme for high-resolution imaging of the active Serine hydrolases.

Expected Results

Titration of FP-Rh with in-vivo activity of SHs of *Drosophila* embryo

The titration of the four different concentrations (0.025, 0.1. 0.25 and 0.5µM) of the FP-Rh with Serine hydrolase activity of chemical permeabilized *Drosophila*'s embryo shows that Active SHs reaction get saturated at 0.5µM. FP-Rh concentration. As the concentration of FP-Rh increases, the fluorescence intensity of FP-reacted SHs increases and saturates at 0.5 µM concentration. The FP-Rh fluorescence shows that SHs are distributed in the embryo's central, yolk and peripheral cellular regions. Nuclear Hoechst staining shows that the embryo is at the cellularization stage. The warhead deficient control Rhodamine-azide reaction at the maximum concentration (0.5 µM) shows that absence of fluorescence in the embryo (**Figure Annexure2.2**). Henceforth, FP-Rh reacts with active SHs in the embryo and the reaction get saturated at 0.5µM

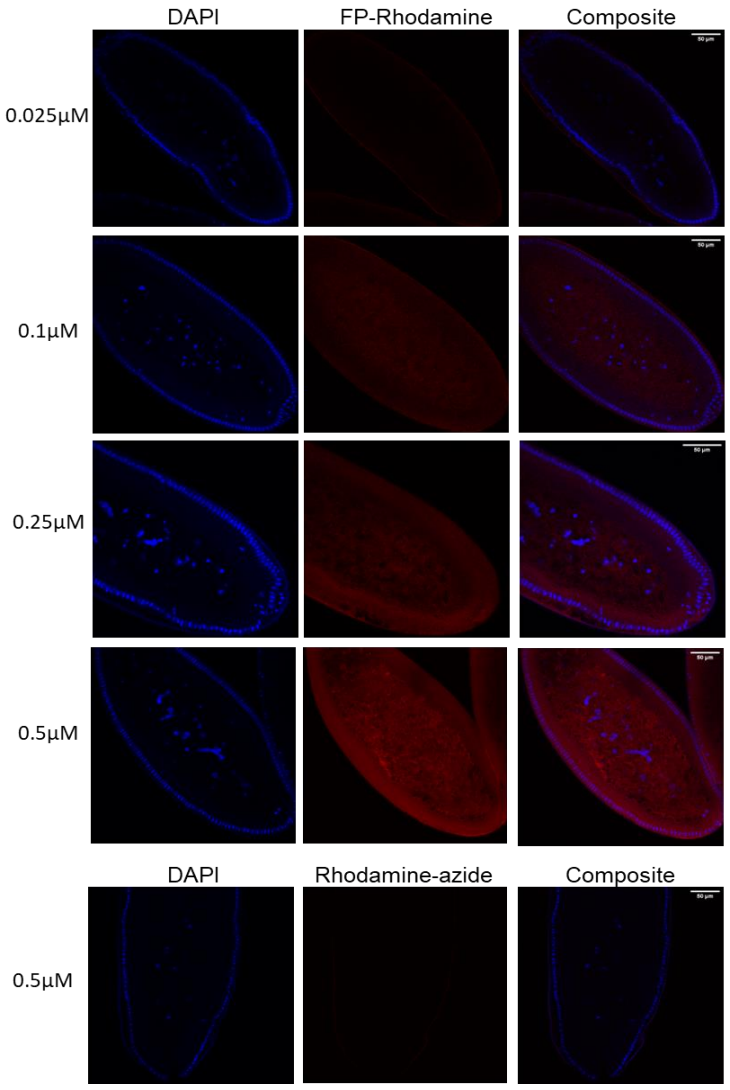

Figure Annexure2.2. Titration of FP-Rh with active of SHs in *Drosophila* embryo in-vivo.

Reaction of tailored ABPs (WHP01) with active SHs in the *Drosophila* embryo

The tailored ABPs WHP01 reacts with specific SHs in the *Drosophila* embryo and the location of the reacted SHs in the basal and apical region of the developing embryo. The Rhodamine-azide is act as negative reaction control. (**Figure Annexure2.3**). Henceforth, in-vivo imaging of active SHs with WHP01 shows that protocol applies for tailored ABPs.

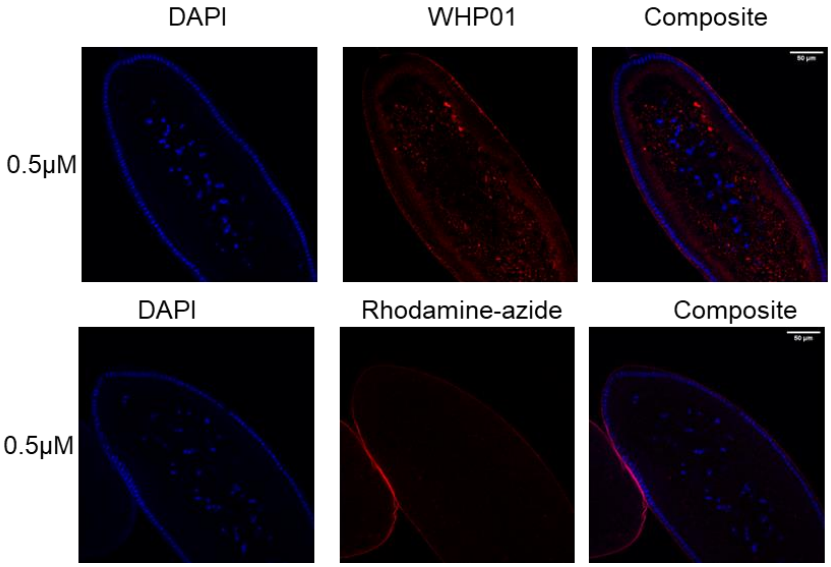

Figure Annexure2.3. Image of tailored ABPs (WHP01) Reaction with active SHs in the *Drosophila* embryo.

Summary

This protocol will enable study of Serine hydrolase enzyme activity in-vivo and may followed by biochemical analysis. For example, role of SHs can be screen by inhibiting SHs using FP probes in the *Drosophila* embryo.

References

[1] G. Dodson and A. Wlodawer, “Catalytic triads and their relatives,” *Trends Biochem. Sci.*, vol. 23, no. 9, pp. 347–352, Sep. 1998, doi: 10.1016/s0968-0004(98)01254-7.

[2] J. Z. Long and B. F. Cravatt, “The Metabolic Serine Hydrolases and Their Functions in Mammalian Physiology and Disease,” *Chem. Rev.*, vol. 111, no. 10, pp. 6022–6063, Oct. 2011, doi: 10.1021/cr200075y.

[3] J. A. Menendez and R. Lupu, “Fatty acid synthase and the lipogenic phenotype in cancer pathogenesis,” *Nat. Rev. Cancer*, vol. 7, no. 10, pp. 763–777, Oct. 2007, doi: 10.1038/nrc2222.

[4] D. A. Bachovchin and B. F. Cravatt, “The Pharmacological Landscape and Therapeutic Potential of Serine Hydrolases,” *Nat. Rev. Drug Discov.*, vol. 11, no. 1, pp. 52–68, Jan. 2012, doi: 10.1038/nrd3620.

[5] B. Zou *et al.*, “Acyloxyacyl hydrolase promotes the resolution of lipopolysaccharide-induced acute lung injury,” *PLOS Pathog.*, vol. 13, no. 6, p. e1006436, Jun. 2017, doi: 10.1371/journal.ppat.1006436.

[6] G. M. Simon and B. F. Cravatt, “Activity-based Proteomics of Enzyme Superfamilies: Serine Hydrolases as a Case Study*,” *J. Biol. Chem.*, vol. 285, no. 15, pp. 11051–11055, Apr. 2010, doi: 10.1074/jbc.R109.097600.
[7] “Strategies for Tuning the Selectivity of Chemical Probes that Target Serine Hydrolases,” *Cell Chem. Biol.*, vol. 27, no. 8, pp. 937–952, Aug. 2020, doi: 10.1016/j.chembiol.2020.07.008.
[8] K. Kumar, A. Mhetre, G. S. Ratnaparkhi, and S. S. Kamat, “A Superfamily-wide Activity Atlas of Serine Hydrolases in *Drosophila melanogaster*,” *Biochemistry*, vol. 60, no. 16, pp. 1312–1324, Apr. 2021, doi: 10.1021/acs.biochem.1c00171.
[9] N. Aaltonen *et al.*, “High-Resolution Confocal Fluorescence Imaging of Serine Hydrolase Activity in Cryosections – Application to Glioma Brain Unveils Activity Hotspots Originating from Tumor-Associated Neutrophils,” *Biol. Proced. Online*, vol. 22, no. 1, p. 6, Mar. 2020, doi: 10.1186/s12575-020-00118-4.
[10] M. P. Baggelaar *et al.*, “ABHD2 Inhibitor Identified by Activity-Based Protein Profiling Reduces Acrosome Reaction,” *ACS Chem. Biol.*, vol. 14, no. 10, pp. 2295–2304, Oct. 2019, doi: 10.1021/acschembio.9b00640.
[11] J. M. G. Nagano *et al.*, “Selective inhibitors and tailored activity probes for lipoprotein-associated phospholipase A2,” *Bioorg. Med. Chem. Lett.*, vol. 23, no. 3, pp. 839–843, Feb. 2013, doi: 10.1016/j.bmcl.2012.11.061.
[12] K. G. Hales, C. A. Korey, A. M. Larracuente, and D. M. Roberts, “Genetics on the Fly: A Primer on the *Drosophila* Model System,” *Genetics*, vol. 201, no. 3, pp. 815–842, Nov. 2015, doi: 10.1534/genetics.115.183392.
[13] C. Nüsslein-Volhard, “The Toll gene in *Drosophila* pattern formation,” *Trends Genet.*, vol. 38, no. 3, pp. 231–245, Mar. 2022, doi: 10.1016/j.tig.2021.09.006.
[14] E. K. LeMosy, Y.-Q. Tan, and C. Hashimoto, “Activation of a protease cascade involved in patterning the *Drosophila* embryo,” *Proc. Natl. Acad. Sci. U. S. A.*, vol. 98, no. 9, pp. 5055–5060, Apr. 2001, doi: 10.1073/pnas.081026598.
[15] M. D. Rand, A. L. Kearney, J. Dao, and T. Clason, “Permeabilization of *Drosophila* embryos for introduction of small molecules,” *Insect Biochem. Mol. Biol.*, vol. 40, no. 11, pp. 792–804, Nov. 2010, doi: 10.1016/j.ibmb.2010.07.007.
[16] W. F. Rothwell and W. Sullivan, “*Drosophila* Embryo Collection,” *Cold Spring Harb. Protoc.*, vol. 2007, no. 9, p. pdb.prot4825, Sep. 2007, doi: 10.1101/pdb.prot4825.
[17] W. F. Rothwell and W. Sullivan, “*Drosophila* Embryo Dechorionation,” *Cold Spring Harb. Protoc.*, vol. 2007, no. 9, p. pdb.prot4826, Sep. 2007, doi: 10.1101/pdb.prot4826.

Annexure 3

Modulation of Phosphatidylinositol upon *Wunen* and *Sac1* knockdown

Annexure 3
Modulation of Phosphatidylinositol upon *Wunen* and *Sac1* knockdown in *Drosophila* embryo

Project leader: Dr. Girish Deshpande, Princeton University

Aim

To investigate the modulation in the phospholipids upon Wunen (Wun) and Sac1 knockdown and Wunen overexpression

Rationale

Wun is required for proper germ cell migration and tentatively annotated as *Drosophila* transmembrane Type 2 phosphatidic acid phosphatase[1]. Loss of *wun in germ cell leads to germ cell death, whereas loss of wun in somatic cell leads to mis-migration of germ cell*[2]*.* Wun hydrolyses the glycerophosphate bond of phospholipid and releases phosphate[3]*.* While having the prominent function in germ cell migration*,* the in-vivo biochemical characterization of wun is still remaining. We test the phospholipid's dysregulation upon Wun knockdown in the embryo. Similar to Wunen activity, Sac1 is lipid phosphatase and dephosphorylates phosphatidylinositol 4-phosphate to generate phosphatidylinositol[4]. Hence, we use Sac1 knockdown as control for Wun.

Material and methods

To knockdown the Wun and Sac1 in 6 to 9 hours aged *Drosophila* embryo, the 13.4 double maternal gal4 were crossed with the UAS-Wun RNAi (BDSC-32430) fly and Sac1 (VDRC-37216), respectively and collected embryo for 3 hours and aged for 6 hours. For control experiment, 13.4 double maternal gal4 were crossed with the UAS-mcherry RNAi (BDSC-35785) fly. For LC-MS for lipid profiling, the embryos

were lysed and lipid species were analyzed using the same procedure described in Chapter 5.

Results

Wun is characterized as lipid phosphate phosphatase and hydrolyzes the glycerophosphate bond of lysophosphatidic acid in vitro. However, Wun has yet to be biochemically characterized in vivo. Wun has the highest and specific expression in the developing gut of the embryo. Given this specific anatomical localization and enzymatic activity, we decided to knockdown *Wun* in the embryo by crossing male UAS-*Wun*^{RNAi} with female *13.4 MAT-Gal4* to generate the *Wun*^{RNAi} embryo (referred to as *Wun-KD* embryo from here on). For the control experiments, the embryo generated by crossing male *UAS-mCherry*^{RNAi} with female *13.4 MAT-Gal4* (referred to as WT from here on) and the embryo generated by crossing male *UAS-mCherry*^{RNAi} with female *13.4 MAT-Gal4*.

The depletion of Wunen expression was established before, and we assessed the influenced lipid classes. For this, we collected *WT* and *Wun-KD* embryos, 6 to 9 hours old and extracted lipids using established protocols (Chapter 5). We used these embryonic lipidomic extracts to perform an untargeted LC-MS/MS based lipidomics experiment. For any lipid species to be considered significantly changing (or altered) following Wun-KD in this LC-MS/MS based lipidomics analysis relative to the WT, it must have > 1.5-fold change (increased or decreased) with a stringent *p*-value cut-off < 0.05. Our untargeted lipidomics experiments led to the identification and quantification of lipid species spanning almost all lipid classes (e.g. neutral lipids, phospholipids, sterols, sphingolipids) (**Figure Annexure 3.1**). The lipid class that showed consistent increase upon Wunen-KD was phosphatidylinositol (PI), Lysophosphatidylinositol (LysoPI) and lysophosphatidic Acid (LysoPA 18:0) (**Figure**

Annexure 3.1). This untargeted lipidomics experiment thus strongly suggested that Wunen might function as a phospholipase with PI and LysoPI as the best possible substrate in the embryos.

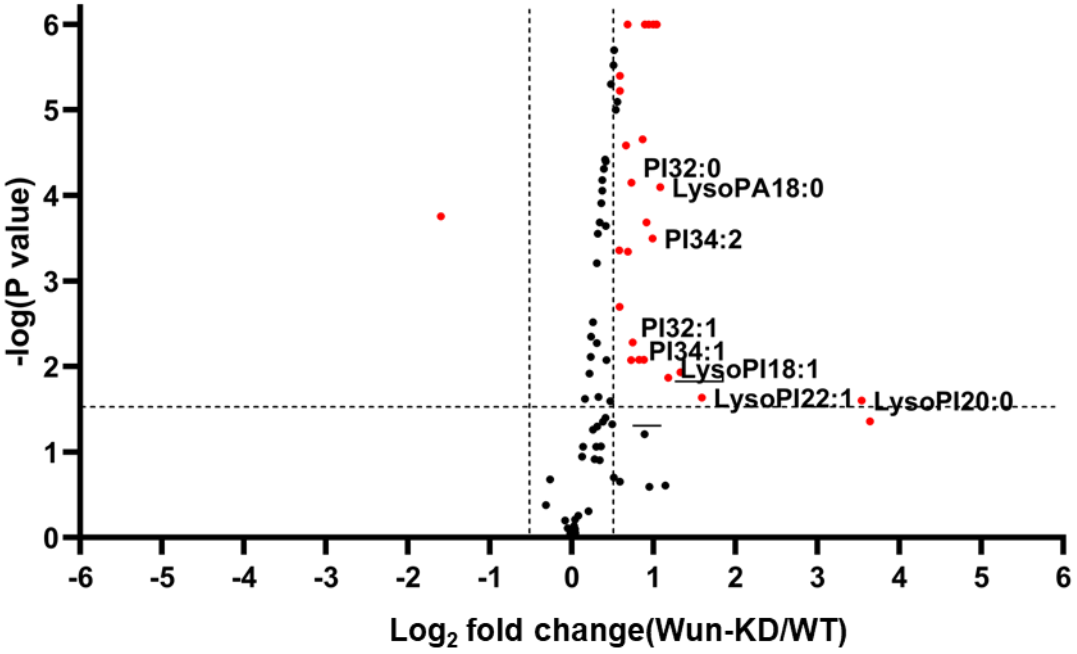

Figure Annexure 3.1. Untargeted lipidomics experiment on the Wun-KD embryo. Volcano plots show differentially changing lipids in the embryo from the Wun-KD relative to the WT embryo, as determined by LC-MS/MS analysis. Each data point represents the mean value from three independent biological replicates. The dashed line parallel to the x-axis denotes a cut-off with an adjusted *p*-value of 0.05, while the two dashed lines parallel to the y-axis denote a 1.5-fold change in relative lipid concentration. PI and LysoPI species showed accumulation upon Wun-KD compared to WT.

Next, the knockdown of Sac1 (Sac1-KD) leads to the accumulation of phosphatidylinositol triphosphate lipids. Here, we aim to study the influence of Sac1-KD on phospholipid metabolism as a control experiment for Wun-KD. We performed the lipidomic experiment and found that PI species accumulate in Sac1-KD by more than 10-fold compared to WT (**Figure Annexure 3.2**). We observed from our

experiment that the Wun-KD leads to increase in PI lipid by 1.5-fold, whereas Sac1-KD leads to increase in PI lipid by more the 10-fold. This difference in activity of Wun and Sac1 because of difference in level and distribution of Wun and Sac1 protein (**Figure Annexure 4.3**). Henceforth, we concluded that PI is the substrate for both Wun and Sac1.

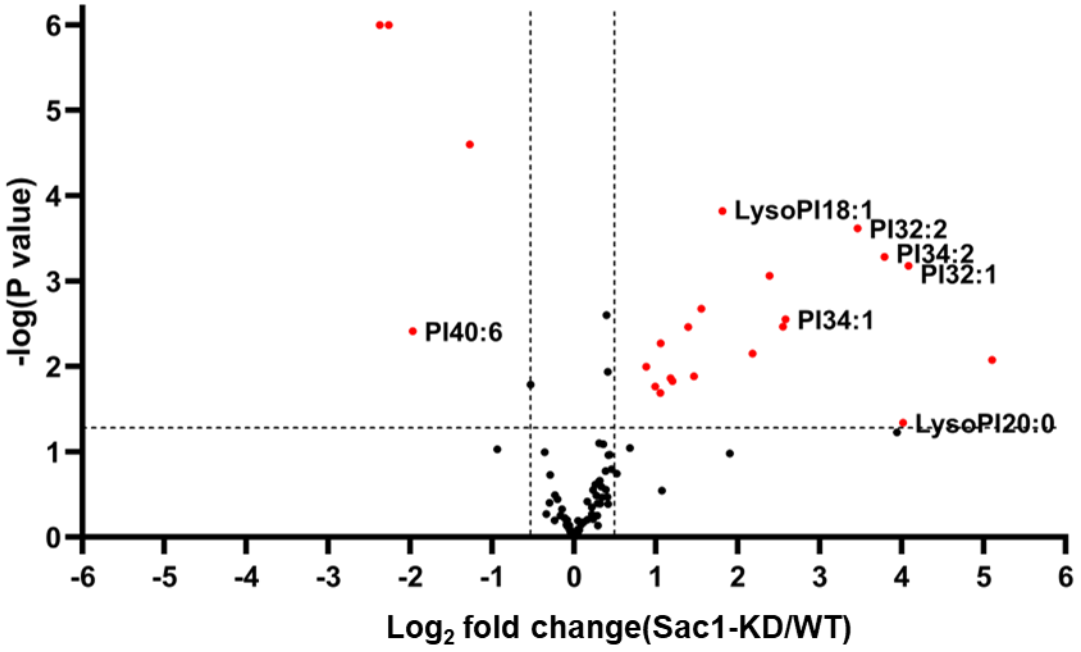

Figure Annexure 3.2. Untargeted lipidomics experiment on the Sac1-KD embryo. Volcano plots show differentially changing lipids in the embryo from the Sac1-KD relative to the WT embryo, as determined by LC-MS/MS analysis. Each data point represents the mean value from three independent biological replicates. The dashed line parallel to the x-axis denotes a cut-off with an adjusted *p*-value of 0.05, while the two dashed lines parallel to the y-axis denote a 1.5-fold change in relative lipid concentration. PI and LysoPI species showed accumulation upon Sac1-KD compared to WT.

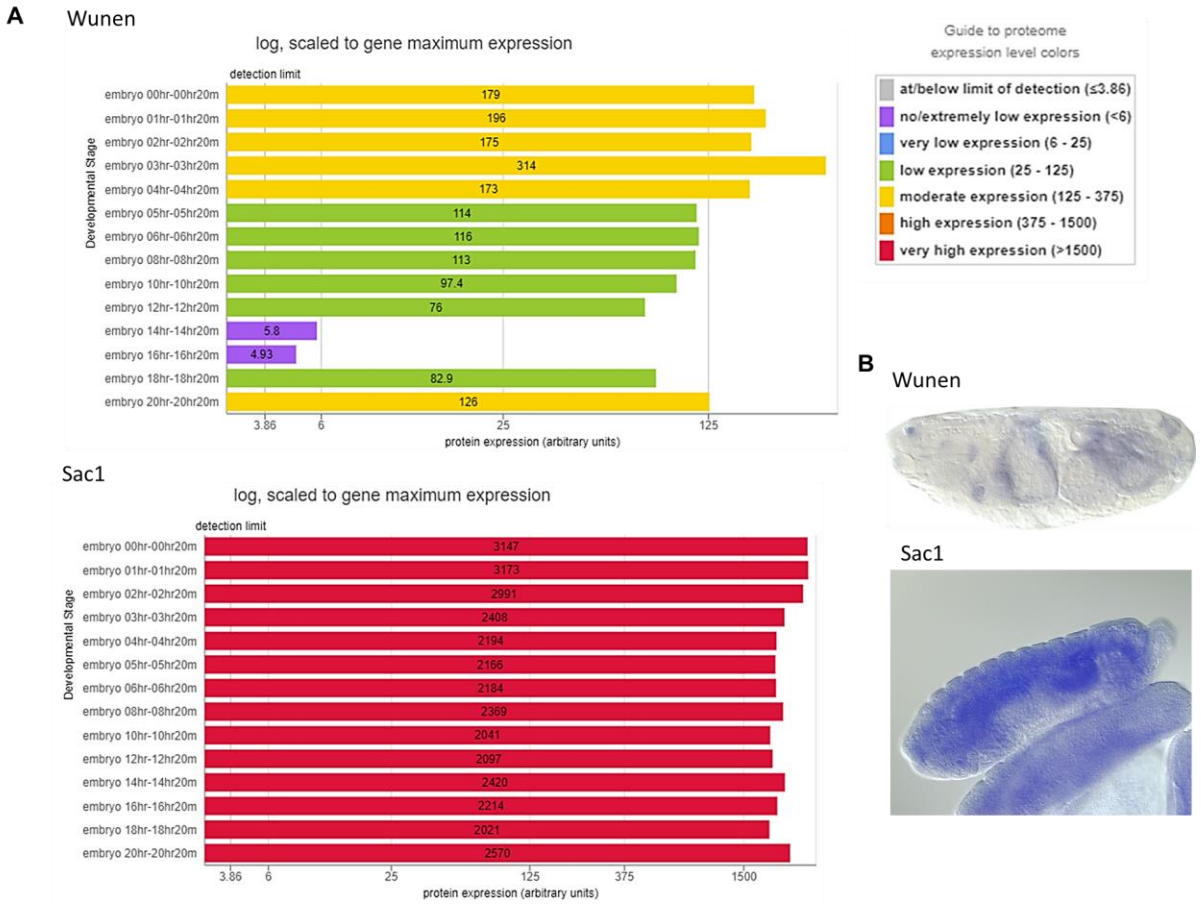

Figure Annexure 3.3. Expression of Wun and Sac1 protein in *Drosophila* embryo.

(A) Snapshot represents protein expression level of Wun (Top panel) and Sac1 (bottom panel). The Wun protein express moderately, whereas Sac1 expressed at very high level. Adapted from Casas-Vila et al. 2017[5] and Flybase database[6]. (B) Image showing RNA-situ hybridization of Wun (Top panel) and Sac1 (bottom panel) embryo (Stage 13-16). Sac1 mRNA is distributed widely compared to Wun mRNA. Adapted from Weiszman et al. 2009[7], Kumar et al. 2011[8] and BDPG database[9–11].

Acknowledgments

We thank Arnab Chakravarty, Aakash C. and Saddam Shaikh for technical assistance in MS samples run.

Reference

(1) Deshpande, G.; Ng, C.; Jourjine, N.; Chiew, J. W.; Dasilva, J.; Schedl, P. Hedgehog Signaling Guides Migration of Primordial Germ Cells to the *Drosophila*

Somatic Gonad. *Genetics* **2023**, *225* (3), iyad165. https://doi.org/10.1093/genetics/iyad165.
(2) Renault, A. D.; Kunwar, P. S.; Lehmann, R. Lipid Phosphate Phosphatase Activity Regulates Dispersal and Bilateral Sorting of Embryonic Germ Cells in *Drosophila*. *Development* **2010**, *137* (11), 1815–1823. https://doi.org/10.1242/dev.046110.
(3) Burnett, C.; Howard, K. Fly and Mammalian Lipid Phosphate Phosphatase Isoforms Differ in Activity Both in Vitro and in Vivo. *EMBO Rep.* **2003**, *4* (8), 793–799. https://doi.org/10.1038/sj.embor.embor900.
(4) Yavari, A.; Nagaraj, R.; Owusu-Ansah, E.; Folick, A.; Ngo, K.; Hillman, T.; Call, G.; Rohatgi, R.; Scott, M. P.; Banerjee, U. Role of Lipid Metabolism in Smoothened Derepression in Hedgehog Signaling. *Dev. Cell* **2010**, *19* (1), 54–65. https://doi.org/10.1016/j.devcel.2010.06.007.
(5) Casas-Vila, N.; Bluhm, A.; Sayols, S.; Dinges, N.; Dejung, M.; Altenhein, T.; Kappei, D.; Altenhein, B.; Roignant, J.-Y.; Butter, F. The Developmental Proteome of *Drosophila* Melanogaster. *Genome Res.* **2017**, *27* (7), 1273–1285. https://doi.org/10.1101/gr.213694.116.
(6) Leader, D. P.; Krause, S. A.; Pandit, A.; Davies, S. A.; Dow, J. A. T. FlyAtlas 2: A New Version of the *Drosophila* Melanogaster Expression Atlas with RNA-Seq, miRNA-Seq and Sex-Specific Data. *Nucleic Acids Res.* **2018**, *46* (D1), D809–D815. https://doi.org/10.1093/nar/gkx976.
(7) Weiszmann, R.; Hammonds, A. S.; Celniker, S. E. Determination of Gene Expression Patterns Using High-Throughput RNA in Situ Hybridization to Whole-Mount *Drosophila* Embryos. *Nat. Protoc.* **2009**, *4* (5), 605–618. https://doi.org/10.1038/nprot.2009.55.
(8) Kumar, S.; Konikoff, C.; Van Emden, B.; Busick, C.; Davis, K. T.; Ji, S.; Wu, L.-W.; Ramos, H.; Brody, T.; Panchanathan, S.; Ye, J.; Karr, T. L.; Gerold, K.; McCutchan, M.; Newfeld, S. J. FlyExpress: Visual Mining of Spatiotemporal Patterns for Genes and Publications in *Drosophila* Embryogenesis. *Bioinforma. Oxf. Engl.* **2011**, *27* (23), 3319–3320. https://doi.org/10.1093/bioinformatics/btr567.
(9) Hammonds, A. S.; Bristow, C. A.; Fisher, W. W.; Weiszmann, R.; Wu, S.; Hartenstein, V.; Kellis, M.; Yu, B.; Frise, E.; Celniker, S. E. Spatial Expression of Transcription Factors in *Drosophila* embryonic Organ Development. *Genome Biol.* **2013**, *14* (12), R140. https://doi.org/10.1186/gb-2013-14-12-r140.
(10) Tomancak, P.; Beaton, A.; Weiszmann, R.; Kwan, E.; Shu, S.; Lewis, S. E.; Richards, S.; Ashburner, M.; Hartenstein, V.; Celniker, S. E.; Rubin, G. M. Systematic Determination of Patterns of Gene Expression during *Drosophila* Embryogenesis. *Genome Biol.* **2002**, *3* (12), research0088.1. https://doi.org/10.1186/gb-2002-3-12-research0088.
(11) Tomancak, P.; Berman, B. P.; Beaton, A.; Weiszmann, R.; Kwan, E.; Hartenstein, V.; Celniker, S. E.; Rubin, G. M. Global Analysis of Patterns of Gene Expression during *Drosophila*embryogenesis. *Genome Biol.* **2007**, *8* (7), R145. https://doi.org/10.1186/gb-2007-8-7-r145.

Annexure 4

Database of Serine Hydrolases

S.No		Refseq I.D.	Annotation symbol	Gene Symbol	Predicted Molecular Funtion	Catalytic Serine Residue or Catalytic Triad	Category	Clan	Family	HMMER	Domain	M.W.
1	FBgn0039494	NP_733197.1	CG5896	grass	serine-type endopeptidase activity	H121; D181; S276	Serine protease/peptidase	PA	S1	CL0124	clip_Trypsin	335
2	FBgn0039759	NP_651784.2	CG9733	CG9733	serine-type endopeptidase activity	H208; D272; S369	Serine protease/peptidase	PA	S1	CL0124	clip_Trypsin	417
3	FBgn0039798	NP_651821.3	CG11313	CG11313	serine-type endopeptidase activity	H62; D225;S321	Serine protease/peptidase	PA	S1	CL0124	clip_Trypsin	367
4	FBgn0038113	NP_650254.1	CG11668	CG11668	serine-type endopeptidase activity	H204; D250; S344	Serine protease/peptidase	PA	S1	CL0124	clip_Trypsin	398
5	FBgn0085438	NP_001097728.2	CG34409	CG34409	serine-type endopeptidase activity	H296; D34; S450	Serine protease/peptidase	PA	S1	CL0124	clip_Trypsin	511
6	FBgn0039108	NP_651175.4	CG10232	CG10232	serine-type endopeptidase activity	H303; D366; S456	Serine protease/peptidase	PA	S1	CL0124	clip_Trypsin	509
7	FBgn0039101	NP_651167.3	CG16710	CG16710	serine-type endopeptidase activity	H156;D219; S316	Serine protease/peptidase	PA	S1	CL0124	clip_Trypsin	372
8	FBgn0035501	NP_647862.1	CG1299	CG1299	serine-type endopeptidase activity	H305;D351; S456	Serine protease/peptidase	PA	S1	CL0124	clip_Trypsin	442
9	FBgn0038727	NP_650825.2	CG7432	CG7432	serine-type endopeptidase activity	H519; D574; S672	Serine protease/peptidase	PA	S1	CL0124	clip_Trypsin	721
10	FBgn0051220	NP_732440.2	CG31220	CG31220	serine-type endopeptidase activity	H154; D216; S310	Serine protease/peptidase	PA	S1	CL0124	clip_Trypsin	363
11	FBgn0052260	NP_728942.1	CG32260	CG32260	serine-type endopeptidase activity	H375; D421; S521	Serine protease/peptidase	PA	S1	CL0124	clip_Trypsin	395
12	FBgn0000533	NP_524362.2	CG4920	ea	serine-type endopeptidase activity	H173; D240; S338	Serine protease/peptidase	PA	S1	CL0124	clip_Trypsin	261

13	FBgn0027930	NP_649450.3	CG1102	MP1	serine-type endopeptidase activity	H173; D238; S336	Serine protease/peptidase	PA	S1	CL0124	clip_Trypsin	390
14	FBgn0003450	NP_524338.2	CG7996	snk	serine-type endopeptidase activity	H235; D283; S381	Serine protease/peptidase	PA	S1	CL0124	clip_Trypsin	252
15	FBgn0030926	NP_573297.1	CG6367	psh	serine-type endopeptidase activity	H187; D234; S339	Serine protease/peptidase	PA	S1	CL0124	clip_Trypsin	394
16	FBgn0019929	NP_572582.1	CG2045	Ser7	serine-type endopeptidase activity	H177; D238; S339	Serine protease/peptidase	PA	S1	CL0124	clip_Trypsin	397
17	FBgn0030925	NP_573296.2	CG6361	Hayan	serine-type endopeptidase activity	H170; D218; S323	Serine protease/peptidase	PA	S1	CL0124	clip_Trypsin	378
18	FBgn0033362	NP_610438.2	CG8172	CG8172	serine-type endopeptidase activity	H344; D394; S493	Serine protease/peptidase	PA	S1	CL0124	clip_Trypsin	192
19	FBgn0030051	NP_727276.1	CG2056	spirit	serine-type endopeptidase activity	H178; D224; S319	Serine protease/peptidase	PA	S1	CL0124	clip_Trypsin	393
20	FBgn0036891	NP_649132.1	CG9372	CG9372	serine-type endopeptidase activity	H216; D265; S358	Serine protease/peptidase	PA	S1	CL0124	clip_Trypsin	408
21	FBgn0284244	NP_723797.3	CG31728	l(2)k05911	serine-type endopeptidase activity	H440; D492; S591	Serine protease/peptidase	PA	S1	CL0124	clip_Trypsin	639
22	FBgn0038144	NP_731802.1	CG8870	CG8870	serine-type endopeptidase activity	H132; D197; S288	Serine protease/peptidase	PA	S1	CL0124	clip_Trypsin	356
23	FBgn0039102	NP_651168.1	CG16705	SPE	serine-type endopeptidase activity	H181; D249; S346	Serine protease/peptidase	PA	S1	CL0124	clip_Trypsin	400
24	FBgn0034139	NP_001033953.1	CG4927	CG4927	serine-type endopeptidase activity	H151; D216; S309	Serine protease/peptidase	PA	S1	CL0124	clip_Trypsin	362
25	FBgn0034796	NP_611736.1	CG3700	CG3700	serine-type endopeptidase activity	H150; D215; S307	Serine protease/peptidase	PA	S1	CL0124	clip_Trypsin	360

26	FBgn0039758	NP_651783.1	CG9737	CG9737	serine-type endopeptidase activity	H191; D257; S360	Serine protease/peptidase	PA	S1	CL0124	clip_Trypsin	424
27	FBgn0033365	NP_610441.2	CG8170	CG8170	serine-type endopeptidase activity	H651; D703; S802	Serine protease/peptidase	PA	S1	CL0124	clip_Trypsin	778
28	FBgn0003319	NP_476709.1	CG4316	Sb	serine-type endopeptidase activity	H590; D640; S738	Serine protease/peptidase	PA	S1	CL0124	clip_Trypsin	787
29	FBgn0265011	NP_610437.2	CG34350	Np	serine-type endopeptidase activity	H872; D892; S990	Serine protease/peptidase	PA	S1	CL0124	clip_Trypsin	1041
30	FBgn0042106	NP_652652.3	CG18754	CG18754	serine-type endopeptidase activity	H140; D199; S287	Serine protease/peptidase	PA	S1	CL0124	clip_Trypsin	296
31	FBgn0033363	NP_610439.1	CG13744	CG13744	serine-type endopeptidase activity	H181; D237; S337	Serine protease/peptidase	PA	S1	CL0124	clip_Trypsin	389
32	FBgn0037515	NP_731175.2	CG3066	Sp7	serine-type endopeptidase activity	H182; D244; S341	Serine protease/peptidase	PA	S1	CL0124	clip_Trypsin	391
33	FBgn0039495	NP_651544.1	CG5909	CG5909	serine-type endopeptidase activity	H174; D234; S239	Serine protease/peptidase	PA	S1	CL0124	clip_Trypsin	381
34	FBgn0001285	NP_724699.1	CG8579	Jon44E	serine-type endopeptidase activity	H82; D216; S221	Serine protease/peptidase	PA	S1	CL0124	Trypsin	271
35	FBgn0003863	NP_476771.1	CG18444	alphaTry	serine-type endopeptidase activity	H71;D116; S210	Serine protease/peptidase	PA	S1	CL0124	Trypsin	256
36	FBgn0031249	NP_608518.1	CG11911	CG11911	serine-type endopeptidase activity	H80; D126; S221	Serine protease/peptidase	PA	S1	CL0124	Trypsin	277
37	FBgn0035795	NP_648134.1	CG16998	CG16998	serine-type endopeptidase activity	H65; D108; S203	Serine protease/peptidase	PA	S1	CL0124	Trypsin	258
38	FBgn0035669	NP_648016.1	CG6592	CG6592	serine-type endopeptidase activity	H166; D215; S311	Serine protease/peptidase	PA	S1	CL0124	Trypsin	438

39	FBgn0015316	NP_523518.2	CG9564	Try29F	serine-type endopeptidase activity	H167; D215; S309	Serine protease/peptidase	PA	S1	CL0124	Trypsin	267
40	FBgn0051954	NP_722915.1	CG31954	CG31954	serine-type endopeptidase activity	H90; D135; S231	Serine protease/peptidase	PA	S1	CL0124	Trypsin	277
41	FBgn0029827	NP_572282.1	CG6048	CG6048	serine-type endopeptidase activity	H177; D224; S320	Serine protease/peptidase	PA	S1	CL0124	Trypsin	362
42	FBgn0011556	NP_523691.1	CG12387	zetaTry	serine-type endopeptidase activity	H87; D134; S234	Serine protease/peptidase	PA	S1	CL0124	Trypsin	280
43	FBgn0031654	NP_608882.1	CG8869	Jon25Bii	serine-type endopeptidase activity	H86; D131; S226	Serine protease/peptidase	PA	S1	CL0124	Trypsin	276
44	FBgn0042187	NP_722785.1	CG17234	CG17234	serine-type endopeptidase activity	H67; D117; S206	Serine protease/peptidase	PA	S1	CL0124	Trypsin	251
45	FBgn0040060	NP_523944.1	CG6457	yip7	serine-type endopeptidase activity	H83; D128; S224	Serine protease/peptidase	PA	S1	CL0124	Trypsin	270
46	FBgn0250815	NP_648012.1	CG6467	Jon65Aiv	serine-type endopeptidase activity	H82; D127; S223	Serine protease/peptidase	PA	S1	CL0124	Trypsin	271
47	FBgn0085487	NP_001097340.1	CG34458	CG34458	serine-type endopeptidase activity	H72; D118; S212	Serine protease/peptidase	PA	S1	CL0124	Trypsin	257
48	FBgn0010357	NP_524904.1	CG18211	betaTry	serine-type endopeptidase activity	H71; D116; S210	Serine protease/peptidase	PA	S1	CL0124	Trypsin	253
49	FBgn0033277	NP_610366.1	CG14760	CG14760	serine-type endopeptidase activity	H319; D374; S421; D473	Serine protease/peptidase	PA	S1	CL0124	Trypsin	529
50	FBgn0003356	NP_524554.1	CG31034	Jon99Cii	serine-type endopeptidase activity	H78; D123; S215	Serine protease/peptidase	PA	S1	CL0124	Trypsin	265
51	FBgn0035678	NP_648025.1	CG10469	CG10469	serine-type endopeptidase activity	H70; D118; S216	Serine protease/peptidase	PA	S1	CL0124	Trypsin	267

52	FBgn0052269	NP_647788.1	CG32269	CG32269	serine-type endopeptidase activity	H148; D194; S286	Serine protease/peptidase	PA	S1	CL0124	Trypsin	332
53	FBgn0052270	NP_728837.1	CG32270	CG32270	serine-type endopeptidase activity	H71; D116; S209	Serine protease/peptidase	PA	S1	CL0124	Trypsin	259
54	FBgn0051265	NP_650599.1	CG31265	CG31265	serine-type endopeptidase activity	H78; D213; S216	Serine protease/peptidase	PA	S1	CL0124	Trypsin	266
55	FBgn0051269	NP_001097818.1	CG31269	CG31269	serine-type endopeptidase activity	H79; D124; S217	Serine protease/peptidase	PA	S1	CL0124	Trypsin	273
56	FBgn0035663	NP_648011.1	CG6462	CG6462	serine-type endopeptidase activity	H121; D169; S267	Serine protease/peptidase	PA	S1	CL0124	Trypsin	319
57	FBgn0015001	NP_523695.1	CG7754	iotaTry	serine-type endopeptidase activity	H68; D113; S206	Serine protease/peptidase	PA	S1	CL0124	Trypsin	252
58	FBgn0032551	NP_995714.2	CG18636	CG18636	serine-type endopeptidase activity	H86; D139; S233	Serine protease/peptidase	PA	S1	CL0124	Trypsin	349
59	FBgn0038481	NP_650600.2	CG17475	CG17475	serine-type endopeptidase activity	H91; D136; S229	Serine protease/peptidase	PA	S1	CL0124	Trypsin	288
60	FBgn0038595	NP_650703.1	CG7142	CG7142	serine-type endopeptidase activity	H125; D177; S274	Serine protease/peptidase	PA	S1	CL0124	Trypsin	334
61	FBgn0038002	NP_650166.2	CG12256	CG12256	serine-type endopeptidase activity	H93;D138; D159; S235	Serine protease/peptidase	PA	S1	CL0124	Trypsin	283
62	FBgn0263234	NP_609550.1	CG16996	Phae1	serine-type endopeptidase activity	H76; D125; S223	Serine protease/peptidase	PA	S1	CL0124	Trypsin	270
63	FBgn0039777	NP_651799.1	CG2229	Jon99Fii	serine-type endopeptidase activity	H80; D215; S217	Serine protease/peptidase	PA	S1	CL0124	Trypsin	267
64	FBgn0039703	NP_651732.1	CG7829	CG7829	serine-type endopeptidase activity	H68; D114; S206	Serine protease/peptidase	PA	S1	CL0124	Trypsin	253

65	FBgn0020906	NP_001033873.1	CG8867	Jon25Bi	serine-type endopeptidase activity	H79; D123; S215	Serine protease/peptidase	PA	S1	CL0124	Trypsin	266
66	FBgn0042186	NP_722784.1	CG17239	CG17239	serine-type endopeptidase activity	H64; D108; S198	Serine protease/peptidase	PA	S1	CL0124	Trypsin	248
67	FBgn0011555	NP_523693.1	CG12385	thetaTry	serine-type endopeptidase activity	H76; D121; S216	Serine protease/peptidase	PA	S1	CL0124	Trypsin	262
68	FBgn0031248	NP_608517.1	CG11912	CG11912	serine-type endopeptidase activity	H71; D117; S219	Serine protease/peptidase	PA	S1	CL0124	Trypsin	271
69	FBgn0038485	NP_650604.1	CG5255	CG5255	serine-type endopeptidase activity	H72; D118; S211	Serine protease/peptidase	PA	S1	CL0124	Trypsin	273
70	FBgn0003357	NP_733330.1	CG31362	Jon99Ciii	serine-type endopeptidase activity	H78; D123; S215	Serine protease/peptidase	PA	S1	CL0124	Trypsin	265
71	FBgn0035667	NP_648015.1	CG10475	Jon65Ai	serine-type endopeptidase activity	H81; D119; S212	Serine protease/peptidase	PA	S1	CL0124	cTrypsin	262
72	FBgn0263235	NP_609551.2	CG16997	Phae2	serine-type endopeptidase activity	H72; D121; S219	Serine protease/peptidase	PA	S1	CL0124	Trypsin	265
73	FBgn0052374	NP_729270.1	CG32374	CG32374	serine-type endopeptidase activity	H114; D158; S253	Serine protease/peptidase	PA	S1	CL0124	Trypsin	299
74	FBgn0052376	NP_729271.1	CG32376	CG32376	serine-type endopeptidase activity	H106; D150; S245	Serine protease/peptidase	PA	S1	CL0124	Trypsin	291
75	FBgn0038001	NP_650165.2	CG17404	CG17404	serine-type endopeptidase activity	H80; D124; S225	Serine protease/peptidase	PA	S1	CL0124	Trypsin	275
76	FBgn0033469	NP_610540.2	CG12133	CG12133	serine-type endopeptidase activity	H109; D172; S269	Serine protease/peptidase	PA	S1	CL0124	Trypsin	340
77	FBgn0003358	NP_524555.1	CG31039	Jon99Ci	serine-type endopeptidase activity	H84; D124; S222	Serine protease/peptidase	PA	S1	CL0124	Trypsin	272

78	FBgn0036024	NP_648341.1	CG18180	CG18180	serine-type endopeptidase activity	H81; D124; S216	Serine protease/peptidase	PA	S1	CL0124	Trypsin	264
79	FBgn0036023	NP_648340.1	CG18179	CG18179	serine-type endopeptidase activity	H85; D128; S220	Serine protease/peptidase	PA	S1	CL0124	Trypsin	268
80	FBgn0035666	NP_648014.1	CG6580	Jon65Aii	serine-type endopeptidase activity	H81; D114; S209	Serine protease/peptidase	PA	S1	CL0124	Trypsin	259
81	FBgn0038003	NP_650167.1	CG3916	CG3916	serine-type endopeptidase activity	H74; D120; S215	Serine protease/peptidase	PA	S1	CL0124	Trypsin	267
82	FBgn0038431	NP_001036717.1	CG10405	CG10405	serine-type endopeptidase activity	H77; D124; S221	Serine protease/peptidase	PA	S1	CL0124	Trypsin	268
83	FBgn0031058	NP_608345.2	CG14227	CG14227	serine-type endopeptidase activity	H85; D140; S232	Serine protease/peptidase	PA	S1	CL0124	Trypsin	286
84	FBgn0035070	NP_611971.1	CG3650	CG3650	serine-type endopeptidase activity	H67; D112; S204	Serine protease/peptidase	PA	S1	CL0124	Trypsin	249
85	FBgn0025378	NP_569939.2	CG3795	CG3795	serine-type endopeptidase activity	H94; D147; S239	Serine protease/peptidase	PA	S1	CL0124	Trypsin	305
86	FBgn0031406	NP_608662.1	CG17012	Send1	serine-type endopeptidase activity	H70; D112; S201	Serine protease/peptidase	PA	S1	CL0124	Trypsin	255
87	FBgn0035887	NP_648217.1	CG7170	Jon66Cii	serine-type endopeptidase activity	H80; D118; S211	Serine protease/peptidase	PA	S1	CL0124	Trypsin	262
88	FBgn0037039	NP_649273.1	CG10587	CG10587	serine-type endopeptidase activity	H87; D133; S226	Serine protease/peptidase	PA	S1	CL0124	Trypsin	225
89	FBgn0037036	NP_649270.1	CG10586	Sems	serine-type endopeptidase activity	H85; D131; S224	Serine protease/peptidase	PA	S1	CL0124	Trypsin	275
90	FBgn0034661	NP_611611.1	CG4386	tpr	serine-type endopeptidase activity	H167; D215; S309	Serine protease/peptidase	PA	S1	CL0124	Trypsin	372

91	FBgn0036022	NP_648339.1	CG8329	CG8329	serine-type endopeptidase activity	H75; D118; S210	Serine protease/peptidase	PA	S1	CL0124	Trypsin	259
92	FBgn0035886	NP_729372.1	CG7118	Jon66Ci	serine-type endopeptidase activity	H77; D114; S209	Serine protease/peptidase	PA	S1	CL0124	Trypsin	260
93	FBgn0038479	NP_650598.1	CG17477	CG17477	serine-type endopeptidase activity	H68; D113; S209	Serine protease/peptidase	PA	S1	CL0124	Trypsin	267
94	FBgn0038447	NP_650562.1	CG14892	CG14892	serine-type endopeptidase activity	H127; D178; S389	Serine protease/peptidase	PA	S1	CL0124	Trypsin	442
95	FBgn0052271	NP_728833.1	CG32271	CG32271	serine-type endopeptidase activity	H65; D110; S203	Serine protease/peptidase	PA	S1	CL0124	Trypsin	248
96	FBgn0053159	NP_788455.1	CG33159	CG33159	serine-type endopeptidase activity	H66; D112; S207	Serine protease/peptidase	PA	S1	CL0124	Trypsin	257
97	FBgn0031653	NP_608881.1	CG8871	Jon25Biii	serine-type endopeptidase activity	H77; D115; S208	Serine protease/peptidase	PA	S1	CL0124	Trypsin	258
98	FBgn0038014	NP_650177.2	CG10041	CG10041	serine-type endopeptidase activity	H83; D128; S221	Serine protease/peptidase	PA	S1	CL0124	Trypsin	287
99	FBgn0010359	NP_725034.1	CG30028	gammaTry	serine-type endopeptidase activity	H71; D116; S210	Serine protease/peptidase	PA	S1	CL0124	Trypsin	253
100	FBgn0039778	NP_651800.2	CG18030	Jon99Fi	serine-type endopeptidase activity	H80; D125; S217	Serine protease/peptidase	PA	S1	CL0124	Trypsin	267
101	FBgn0052277	NP_728835.1	CG32277	CG32277	serine-type endopeptidase activity	H67; D118; S213	Serine protease/peptidase	PA	S1	CL0124	Trypsin	261
102	FBgn0053160	NP_788456.1	CG33160	CG33160	serine-type endopeptidase activity	H73; D119; S212	Serine protease/peptidase	PA	S1	CL0124	Trypsin	258
103	FBgn0038482	NP_650601.2	CG4053	CG4053	serine-type endopeptidase activity	H76; D122; S215	Serine protease/peptidase	PA	S1	CL0124	Trypsin	265

104	FBgn0000808	NP_001303552.1	CG1505	gd	serine-type endopeptidase activity	H292; D347; D468, S368	Serine protease/peptidase	PA	S1	CL0124	Trypsin	179
105	FBgn0039568	NP_651607.1	CG4815	CG4815	serine-type endopeptidase activity	H76; D125; S217	Serine protease/peptidase	PA	S1	CL0124	Trypsin	265
106	FBgn0264253	NP_609708.2	CG18125	Send2	serine-type endopeptidase activity	H67; D104; S188	Serine protease/peptidase	PA	S1	CL0124	Trypsin	239
107	FBgn0037038	NP_649272.1	CG11037	CG11037	serine-type endopeptidase activity	H103; D149; S242	Serine protease/peptidase	PA	S1	CL0124	Trypsin	292
108	FBgn0040341	NP_569865.1	CG11664	CG11664	serine-type endopeptidase activity	H62; D108; S198	Serine protease/peptidase	PA	S1	CL0124	Trypsin	254
109	FBgn0034666	NP_995920.1	CG9294	CG9294	serine-type endopeptidase activity	H141; D190; S288	Serine protease/peptidase	PA	S1	CL0124	cTrypsin	352
110	FBgn0031619	NP_723001.1	CG3355	CG3355	serine-type endopeptidase activity	H119; D165; S259	Serine protease/peptidase	PA	S1	CL0124	Trypsin	216
111	FBgn0053329	NP_996209.2	CG33329	Sp212	serine-type endopeptidase activity	H321; D371; S464	Serine protease/peptidase	PA	S1	CL0124	Trypsin	516
112	FBgn0010358	NP_523694.2	CG12351	deltaTry	serine-type endopeptidase activity	H71; D116; S210	Serine protease/peptidase	PA	S1	CL0124	Trypsin	253
113	FBgn0050025	NP_725036.1	CG30025	CG30025	serine-type endopeptidase activity	H71; D116; S210	Serine protease/peptidase	PA	S1	CL0124	Trypsin	253
114	FBgn0050082	NP_001188942.1	CG30082	CG30082	serine-type endopeptidase activity	H80; D135; S226	Serine protease/peptidase	PA	S1	CL0124	Trypsin	280
115	FBgn0050083	NP_725492.3	CG30083	CG30083	serine-type endopeptidase activity	H79; D119; S210	Serine protease/peptidase	PA	S1	CL0124	Trypsin	279
116	FBgn0050087	NP_725489.2	CG30087	CG30087	serine-type endopeptidase activity	H82; D134; S225	Serine protease/peptidase	PA	S1	CL0124	Trypsin	277

117	FBgn0050088	NP_725488.3	CG30088	CG30088	serine-type endopeptidase activity	H85; D136; S227	Serine protease/peptidase	PA	S1	CL0124	Trypsin	281
118	FBgn0042098	NP_652645.1	CG18735	CG18735	serine-type endopeptidase activity	H123; D171; S267	Serine protease/peptidase	PA	S1	CL0124	Trypsin	364
119	FBgn0050090	NP_725487.1	CG30090	CG30090	serine-type endopeptidase activity	H80; D134; S228	Serine protease/peptidase	PA	S1	CL0124	Trypsin	291
120	FBgn0050098	NP_725573.2	CG30098	CG30098	serine-type endopeptidase activity	H75; D121; S210	Serine protease/peptidase	PA	S1	CL0124	Trypsin	264
121	FBgn0050187	NP_726265.4	CG30187	CG30187	serine-type endopeptidase activity	H76; D120; S214	Serine protease/peptidase	PA	S1	CL0124	Trypsin	489
122	FBgn0050286	NP_726082.3	CG30286	CG30286	serine-type endopeptidase activity	H75; D219; S223	Serine protease/peptidase	PA	S1	CL0124	Trypsin	152
123	FBgn0050287	NP_726083.1	CG30287	CG30287	serine-type endopeptidase activity	H82; D136; S232	Serine protease/peptidase	PA	S1	CL0124	Trypsin	284
124	FBgn0050288	NP_001097398.1	CG30288	CG30288	serine-type endopeptidase activity	H83; D132; S225	Serine protease/peptidase	PA	S1	CL0124	Trypsin	282
125	FBgn0050289	NP_726081.1	CG30289	CG30289	serine-type endopeptidase activity	H80; D134; S224	Serine protease/peptidase	PA	S1	CL0124	Trypsin	316
126	FBgn0051219	NP_001097837.1	CG31219	CG31219	serine-type endopeptidase activity	H135; D202; S294	Serine protease/peptidase	PA	S1	CL0124	Trypsin	345
127	FBgn0039272	NP_733078.1	CG11836	CG11836	serine-type endopeptidase activity	H27; D76; S169	Serine protease/peptidase	PA	S1	CL0124	Trypsin	223
128	FBgn0051681	NP_722789.1	CG31681	CG31681	serine-type endopeptidase activity	H69; D115; S207	Serine protease/peptidase	PA	S1	CL0124	Trypsin	264
129	FBgn0052755	NP_727055.1	CG32755	CG32755	serine-type endopeptidase activity	H86; D142; S232	Serine protease/peptidase	PA	S1	CL0124	Trypsin	315

130	FBgn0052808	NP_726740.1	CG32808	CG32808	serine-type endopeptidase activity	H72; D119; S213	Serine protease/peptidase	PA	S1	CL0124	Trypsin	284
131	FBgn0053458	NP_995854.2	CG33458	CG33458	serine-type endopeptidase activity	H78; D132; S226	Serine protease/peptidase	PA	S1	CL0124	Trypsin	281
132	FBgn0053459	NP_995855.2	CG33459	CG33459	serine-type endopeptidase activity	H78; D130; S227	Serine protease/peptidase	PA	S1	CL0124	Trypsin	284
133	FBgn0053461	NP_995843.3	CG33461	CG33461	serine-type endopeptidase activity	H82; D136; S233	Serine protease/peptidase	PA	S1	CL0124	Trypsin	287
134	FBgn0053462	NP_995844.2	CG33462	CG33462	serine-type endopeptidase activity	H76; D130; S224	Serine protease/peptidase	PA	S1	CL0124	Trypsin	300
135	FBgn0069056	NP_995917.3	CG33226	CG33226	serine-type endopeptidase activity	H187; D140; S237	Serine protease/peptidase	PA	S1	CL0124	Trypsin	292
136	FBgn0085319	NP_001097899.2	CG34290	CG34290	serine-type endopeptidase activity	H89; D135; S233	Serine protease/peptidase	PA	S1	CL0124	Trypsin	282
137	FBgn0260474	NP_001163100.1	CG30002	CG30002	serine-type endopeptidase activity	H105; D166; S254	Serine protease/peptidase	PA	S1	CL0124	Trypsin	311
138	FBgn0262570	NP_001286532.1	CG43110	CG43110	serine-type endopeptidase activity	H76; D118; S209	Serine protease/peptidase	PA	S1	CL0124	Trypsin	483
139	FBgn0263999	NP_001261130.1	CG43742	CG43742	serine-type endopeptidase activity	H73; D121; S207	Serine protease/peptidase	PA	S1	CL0124	Trypsin	474
140	FBgn0038114	NP_001368950.1	CG11670	CG11670	serine-type endopeptidase activity	H215; D265; S363	Serine protease/peptidase	PA	S1	CL0124	Trypsin	404
141	FBgn0037222	NP_730791.1	CG14642	CG14642	serine-type endopeptidase activity	H189; D239; S337	Serine protease/peptidase	PA	S1	CL0124	Trypsin	200
142	FBgn0036287	NP_001097593.2	CG10663	CG10663	serine-type endopeptidase activity	H548; D952; S688	Serine protease/peptidase	PA	S1	CL0124	Trypsin	748

143	FBgn0036436	NP_648711.1	CG4914	CG4914	serine-type endopeptidase activity	H168; D215; S315	Serine protease/peptidase	PA	S1	CL0124	Trypsin	374
144	FBgn0036427	NP_648707.2	CG4613	CG4613	serine-type endopeptidase activity	H177; D224; S320	Serine protease/peptidase	PA	S1	CL0124	Trypsin	374
145	FBgn0039630	NP_651663.1	CG11843	CG11843	serine-type endopeptidase activity	H114; D164; S263	Serine protease/peptidase	PA	S1	CL0124	Trypsin	316
146	FBgn0039628	NP_651661.1	CG11841	CG11841	serine-type endopeptidase activity	H117; D167; S264	Serine protease/peptidase	PA	S1	CL0124	Trypsin	319
147	FBgn0031141	NP_608418.1	CG1304	CG1304	serine-type endopeptidase activity	H72; D124; D144; S214	Serine protease/peptidase	PA	S1	CL0124	Trypsin	260
148	FBgn0011834	NP_523426.1	CG2071	Ser6	serine-type endopeptidase activity	H72; D124; D144; S214	Serine protease/peptidase	PA	S1	CL0124	Trypsin	259
149	FBgn0050091	NP_725484.1	CG30091	CG30091	serine-type endopeptidase activity	H77; D133; S228	Serine protease/peptidase	PA	S1	CL0124	Trypsin	526
150	FBgn0052523	NP_728401.1	CG32523	CG32523	serine-type endopeptidase activity	H77; D125; S216	Serine protease/peptidase	PA	S1	CL0124	Trypsin	262
151	FBgn0035661	NP_648010.1	CG10477	CG10477	serine-type endopeptidase activity	H83; D128; S224	Serine protease/peptidase	PA	S1	CL0124	Trypsin	272
152	FBgn0030688	NP_573072.1	CG8952	CG8952	serine-type endopeptidase activity	H80; D123; S222	Serine protease/peptidase	PA	S1	CL0124	Trypsin	276
153	FBgn0051217	NP_536776.2	CG31217	modSP	serine-type endopeptidase activity	H414; D472; S563	Serine protease/peptidase	PA	S1	CL0124	Trypsin	628
154	FBgn0038211	NP_650343.1	CG9649	CG9649	serine-type endopeptidase activity	H301; D353; S451	Serine protease/peptidase	PA	S1	CL0124	Trypsin	504
155	FBgn0011554	NP_523692.1	CG12386	etaTry	serine-type endopeptidase activity	H74; D120; S215	Serine protease/peptidase	PA	S1	CL0124	Trypsin	262

156	FBgn0050031	NP_725035.1	CG30031	CG30031	serine-type endopeptidase activity	H71; D116; S210	Serine protease/peptidase	PA	S1	CL0124	Trypsin	253
157	FBgn0027563	NP_650345.1	CG9631	CG9631	serine-type endopeptidase activity	H240; D290; S387	Serine protease/peptidase	PA	S1	CL0124	Trypsin	439
158	FBgn0050414	NP_611789.2	CG30414	CG30414	serine-type endopeptidase activity	H79; D155; S245	Serine protease/peptidase	PA	S1	CL0124	Trypsin	305
159	FBgn0036817	NP_001246825.1	CG6865	CG6865	serine-type endopeptidase activity	H75; D134; S237	Serine protease/peptidase	PA	S1	CL0124	Trypsin	285
160	FBgn0034052	NP_611066.1	CG8299	CG8299	serine-type endopeptidase activity	H71; D117; S213	Serine protease/peptidase	PA	S1	CL0124	Trypsin	260
161	FBgn0039629	NP_651662.1	CG11842	CG11842	serine-type endopeptidase activity	H118; D168; S266	Serine protease/peptidase	PA	S1	CL0124	Trypsin	319
162	FBgn0034518	NP_001027442.1	CG13430	CG13430	serine-type endopeptidase activity	H72; D119; S216	Serine protease/peptidase	PA	S1	CL0124	Trypsin	267
163	FBgn0036738	NP_648995.3	CG7542	CG7542	serine-type endopeptidase activity	H70; D119; S216	Serine protease/peptidase	PA	S1	CL0124	Trypsin	270
164	FBgn0263040	NP_001247121.1	CG43335	CG43335	serine-type endopeptidase activity	H82; D133; S227	Serine protease/peptidase	PA	S1	CL0124	Trypsin	281
165	FBgn0263041	NP_001247122.1	CG43336	CG43336	serine-type endopeptidase activity	H79; D132; S226	Serine protease/peptidase	PA	S1	CL0124	Trypsin	279
166	FBgn0033439	NP_610512.1	CG1773	CG1773	serine-type endopeptidase activity	H105;D166; S254	Serine protease/peptidase	PA	S1	CL0124	Trypsin	317
167	FBgn0033192	NP_995773.1	CG2105	Corin	serine-type endopeptidase activity	H1114; D1198; S1297	Serine protease/peptidase	PA	S1	CL0124	Trypsin	1397
168	FBgn0043470	NP_610673.1	CG12350	lambdaTry	serine-type endopeptidase activity	H76; D125; S217	Serine protease/peptidase	PA	S1	CL0124	Trypsin	272

169	FBgn0034221	NP_611213.2	CG10764	CG10764	serine-type endopeptidase activity	H76; D121; S214;D385; S471	Serine protease/peptidase	PA	S1	CL0124	Trypsin	523
170	FBgn0035670	NP_648017.1	CG10472	CG10472	serine-type endopeptidase activity	H90; D140; S236	Serine protease/peptidase	PA	S1	CL0124	Trypsin	290
171	FBgn0050371	NP_610370.1	CG30371	CG30371	serine-type endopeptidase activity	H193; D245; S343	Serine protease/peptidase	PA	S1	CL0124	Trypsin	399
172	FBgn0050375	NP_724665.1	CG30375	CG30375	serine-type endopeptidase activity	H195; D248; S344	Serine protease/peptidase	PA	S1	CL0124	Trypsin	398
173	FBgn0034507	NP_611479.2	CG11192	CG11192	serine-type endopeptidase activity	H68; D114; S214	Serine protease/peptidase	PA	S1	CL0124	Trypsin	279
174	FBgn0259998	NP_610109.1	CG17571	CG17571	serine-type endopeptidase activity	H72; D117; S212	Serine protease/peptidase	PA	S1	CL0124	Trypsin	258
175	FBgn0036264	NP_648558.1	CG11529	CG11529	serine-type endopeptidase activity	H74; D121; S213	Serine protease/peptidase	PA	S1	CL0124	Trypsin	287
176	FBgn0023197	NP_001189126.2	CG6298	Jon74E	serine-type endopeptidase activity	H76; D121; S216	Serine protease/peptidase	PA	S1	CL0124	Trypsin	271
177	FBgn0029826	NP_572281.1	CG6041	CG6041	serine-type endopeptidase activity	H83; D137; S230	Serine protease/peptidase	PA	S1	CL0124	Trypsin	308
178	FBgn0037677	NP_649880.1	CG12951	CG12951	serine-type endopeptidase activity	H71;D118; S217	Serine protease/peptidase	PA	S1	CL0124	Trypsin	265
179	FBgn0010425	NP_525112.1	CG18681	epsilonTry	serine-type endopeptidase activity	H71; D116; S210	Serine protease/peptidase	PA	S1	CL0124	Trypsin	256
180	FBgn0002926	NP_523947.2	CG10129	ndl	serine-type endopeptidase activity	H1185; D1233; S1332	Serine protease/peptidase	PA	S1	CL0124	DUF1986	2616
181	FBgn0019928	NP_610874.1	CG4812	Ser8	serine-type endopeptidase activity	H75; D121; S214	Serine protease/peptidase	PA	S1	CL0124	Trypsin	260

182	FBgn0037678	NP_649881.1	CG16749	CG16749	serine-type endopeptidase activity	H71; D118; S217	Serine protease/peptidase	PA	S1	CL0124	Trypsin	265
183	FBgn0011832	NP_523456.1	CG17240	Ser12	serine-type endopeptidase activity	H64; D110; S199	Serine protease/peptidase	PA	S1	CL0124	Trypsin	245
184	FBgn0025383	NP_569920.2	CG14780	CG14780	serine-type endopeptidase activity	H80; D134; S321	Serine protease/peptidase	PA	S1	CL0124	Trypsin	302
185	FBgn0038484	NP_650603.1	CG5246	CG5246	serine-type endopeptidase activity	H83; D127; S222	Serine protease/peptidase	PA	S1	CL0124	Trypsin	272
186	FBgn0035665	NP_648013.1	CG6483	Jon65Aiii	serine-type endopeptidase activity	H83; D128; S224	Serine protease/peptidase	PA	S1	CL0124	Trypsin	274
187	FBgn0030773	NP_728008.1	CG9676	CG9676	serine-type endopeptidase activity	H68; D115; S206	Serine protease/peptidase	PA	S1	CL0124	Trypsin	251
188	FBgn0038233	NP_650366.1	CG8464	HtrA2	serine-type endopeptidase activity	H157; D189; S266	Serine protease/peptidase	PA	S1	CL0124	Trypsin_2	422
189	FBgn0286782	NP_610435.4	CG8213	flz	serine-type endopeptidase activity	H1476; D1525; S1623	Serine protease/peptidase	PA	S1	CL0124	Trypsin	1430
190	FBgn0035065	NP_611968.1	CG3589	CG3589	serine-type endopeptidase activity	H323; 357; S431	Serine protease/peptidase	PA	S1	CL0124	Trypsin_2	509
191	FBgn0051973	NP_722590.2	CG31973	Cda5	hydrolase activity, acting on carbon-nitrogen	H1311; D1672; S1975	Serine protease/peptidase			CL0155	CBM_14	1890
192	FBgn0023479	NP_648288.2	CG4821	teq	serine-type endopeptidase activity	H2592; D2641; S2438	Serine protease/peptidase	PA	S1	CL0155	CBM_14	2379
193	FBgn0033672	NP_523704.1	CG8972	rho-7	endopeptidase activity	S174; H235	Serine protease/peptidase	ST	S54	CL0207	Rhomboid	351
194	FBgn0020248	NP_788451.1	CG33166	stet	calcium ion binding	S180; H257	Serine protease/peptidase	ST	S54	CL0207	Rhomboid	330

195	FBgn0003295	NP_524790.1	CG1214	ru	serine-type endopeptidase activity	S202; H266	Serine protease/peptidase	ST	S54	CL0207	Rhomboid	341
196	FBgn0004635	NP_523883.2	CG1004	rho	serine-type endopeptidase activity	S217; H281	Serine protease/peptidase	ST	S54	CL0207	Rhomboid	355
197	FBgn0032415	NP_788038.1	CG17212	rho-6	serine-type endopeptidase activity	S174; H235	Serine protease/peptidase	ST	S54	CL0207	Rhomboid	166
198	FBgn0030318	NP_727538.1	CG1697	rho-4	serine-type endopeptidase activity	S299; H358	Serine protease/peptidase	ST	S54	CL0207	Rhomboid	417
199	FBgn0036892	NP_730435.2	CG8798	Lon	ATP binding	S898; K941	Serine protease/peptidase	SJ	S16	CL0329	Lon_C	1006
200	FBgn0034535	NP_611501.1	CG11110	CG11110	serine-type peptidase activity	S34; K81	Serine protease/peptidase	SF	S26	CL0299	Peptidase_S24	171
201	FBgn0030669	NP_573054.2	CG9240	CG9240	serine-type peptidase activity	S38; K81	Serine protease/peptidase	SF	S26	CL0299	Peptidase_S24	128
202	FBgn0262801	NP_649676.1	CG2358	twr	serine-type peptidase activity	S62; K110	Serine protease/peptidase	SF	S26	CL0299	Peptidase_S24	185
203	FBgn0260779	NP_650775.2	CG6007	GatA	amidase activity	K79; S160; S184	Serine protease/peptidase				Amidase	508
204	FBgn0037105	NP_649337.2	CG7169	S1P	serine-type endopeptidase activity	D129; H200; D220; S365	Serine protease/peptidase	SB	S8		Peptidase_S8	1012
205	FBgn0023179	NP_477318.1	CG6438	amon	serine-type endopeptidase activity	D196; D217; H237; D261; S412	Serine protease/peptidase	SB	S8		Peptidase_S8	654
206	FBgn0004509	NP_996294.2	CG10772	Fur1	serine-type endopeptidase activity	D372; D393; H413; S587	Serine protease/peptidase	SB	S8		Peptidase_S8	285
207	FBgn0004598	NP_996486.1	CG18734	Fur2	serine-type endopeptidase activity	D417; D438; H456; S637	Serine protease/peptidase	SB	S8		Peptidase_S8	586

208	FBgn0020370	NP_725252.1	CG3991	TppII	serine-type endopeptidase activity	H359; S549	Serine protease/peptidase	SB	S8		TPPII_N	1354
209	FBgn0039120	NP_651187.2	CG10198	CG10198	chromatin DNA binding	S1029	Serine protease/peptidase	SP	S59	CL0661	Nucleoporin autopeptidase	
210	FBgn0032229	NP_609388.1	CG5045	ClpP	ATPase binding	S124; H149; D198	Serine protease/peptidase	SK	S14	CL0127	CLP_protease	253
211	FBgn0038974	NP_651052.1	CG5377	CG5377	-	S213; D191; H218	Metabolic serine hydrolase	SC	S33	CL0028	Abhydrolase_1	278
212	FBgn0265264	NP_609429.1	CG17097	CG17097	sterol esterase activity	S855; D1029; H1060	Metabolic serine hydrolase	SC	S33	CL0028	Abhydrolase_1	1087
213	FBgn0014906	NP_608751.2	CG3488	Hydr2	acetylesterase activity	S192; D328; H359	Metabolic serine hydrolase			CL0028	Abhydrolase_1	311
214	FBgn0033382	NP_724757.2	CG8058	Hydr1	lipase activity	S198; D331; H36O	Metabolic serine hydrolase			CL0028	Abhydrolase_1	438
215	FBgn0032271	NP_609425.1	CG7329	CG7329	-	S172; D336; H365	Metabolic serine hydrolase			CL0028	Abhydrolase_1	457
216	FBgn0051871	NP_723607.1	CG31871	CG31871	sterol esterase activity	S208; D382; H413	Metabolic serine hydrolase			CL0028	Abhydrolase_1	531
217	FBgn0034990	NP_611897.2	CG11406	CG11406	sterol esterase activity	S90; D265; H295	Metabolic serine hydrolase			CL0028	Abhydrolase_1	266
218	FBgn0037842	NP_001097742.1	CG6567	CG6567	carboxylic ester hydrolase activity	S118; D174; H206	Metabolic serine hydrolase			CL0028	Abhydrolase_2	235
219	FBgn0042138	NP_996056.1	CG18815	Apt1	palmitoyl-(protein) hydrolase activity	S112; D165;H197	Metabolic serine hydrolase			CL0028	Abhydrolase_2	216
220	FBgn0287695	AAF52391.1	CG9542	KFase	arylformamidase activity	S157; D244; H276	Metabolic serine hydrolase	SC	S9	CL0028	Abhydrolase_3	

221	FBgn0035951	NP_648277.3	CG5068	CG5068	protein methylesterase activity	S151; D350; H372	Metabolic serine hydrolase	SC	S33	CL0028	Abhydrolase_6	409
222	FBgn0037090	NP_649321.1	CG7529	Est-Q	-	S226; D345; H473	Metabolic serine hydrolase	SC	S9	CL0028	COesterase	559
223	FBgn0000592	NP_788500.1	CG6917	Est-6	short-chain carboxylesterase activity	S209; D340; H466	Metabolic serine hydrolase	SC	S9	CL0028	COesterase	544
224	FBgn0000594	NP_788501.1	CG17148	Est-P	carboxylic ester hydrolase activity	S206; D337; H466	Metabolic serine hydrolase			CL0028	COesterase	544
225	FBgn0038771	NP_732486.2	CG4390	CG4390	S-formylglutathione hydrolase activity	S150, D227, H262	Metabolic serine hydrolase			CL0028	esterase	
226	FBgn0030057	NP_727284.1	CG12108	Ppt1	palmitoyl-(protein) hydrolase activity	S123; D241; H295	Metabolic serine hydrolase			CL0028	Palm_thioest	314
227	FBgn0261244	NP_788901.1	CG33174	inaE	lipoprotein lipase activity	S478; D530;	Metabolic serine hydrolase			CL0028	Lipase_3	644
228	FBgn0035453	NP_647821.2	CG10357	CG10357	carboxylic ester hydrolase activity	S137; D161; H236	Metabolic serine hydrolase			CL0028	Lipase	321
229	FBgn0032029	NP_723380.1	CG17292	CG17292	carboxylic ester hydrolase activity	S143; D173; H242	Metabolic serine hydrolase			CL0028	Lipase	340
230	FBgn0085476	NP_001259940.1	CG34447	CG34447	carboxylic ester hydrolase activity	S157; D181; H249	Metabolic serine hydrolase			CL0028	Lipase	389
231	FBgn0085477	NP_001097059.1	CG34448	CG34448	triglyceride lipase activity	S160; D184; H254	Metabolic serine hydrolase			CL0028	Lipase	344
232	FBgn0034166	NP_611166.2	CG6472	CG6472	carboxylic ester hydrolase activity	S163; D190; H264	Metabolic serine hydrolase			CL0028	Lipase	389
233	FBgn0032289	NP_609442.2	CG6431	CG6431	carboxylic ester hydrolase activity	S172; D196; H264	Metabolic serine hydrolase			CL0028	Lipase	346

234	FBgn0039473	NP_651523.1	CG17191	CG17191	phospholipase A1 activity	S179; D204; H269	Metabolic serine hydrolase			CL0028	Lipase	337
235	FBgn0039472	NP_651522.1	CG17192	CG17192	phospholipase A1 activity	S179; D204; H269	Metabolic serine hydrolase			CL0028	Lipase	337
236	FBgn0030162	NP_572590.1	CG1986	CG1986	carboxylic ester hydrolase activity	S180; D204; H282	Metabolic serine hydrolase			CL0028	Lipase	404
237	FBgn0039471	NP_651521.1	CG6295	CG6295	phospholipase A1 activity	S180; D205; H270	Metabolic serine hydrolase			CL0028	Lipase	338
238	FBgn0039474	NP_651524.1	CG6283	CG6283	phospholipase A1 activity	S181;D206; H271	Metabolic serine hydrolase			CL0028	Lipase	339
239	FBgn0039476	NP_651526.1	CG6271	CG6271	phospholipase A1 activity	S184; D208; H273	Metabolic serine hydrolase			CL0028	Lipase	341
240	FBgn0039475	NP_651525.1	CG6277	CG6277	phospholipase A1 activity	S184; D208; H273	Metabolic serine hydrolase			CL0028	Lipase	341
241	FBgn0039470	NP_651520.1	CG6296	CG6296	phospholipase A1 activity	S187; D212; H277	Metabolic serine hydrolase			CL0028	Lipase	676
242	FBgn0038398	NP_650522.1	CG4979	sxe2	carboxylic ester hydrolase activity	S189; D214; H284	Metabolic serine hydrolase			CL0028	Lipase	387
243	FBgn0031426	NP_608682.3	CG18641	CG18641	carboxylic ester hydrolase activity	S189; D216; H285	Metabolic serine hydrolase			CL0028	Lipase	369
244	FBgn0032612	NP_609814.1	CG13282	CG13282	carboxylic ester hydrolase activity	S195; D220; H287	Metabolic serine hydrolase			CL0028	Lipase	484
245	FBgn0035697	NP_648042.1	CG10163	CG10163	carboxylic ester hydrolase activity	S197; D225; H290	Metabolic serine hydrolase			CL0028	Lipase	378
246	FBgn0029831	NP_572286.1	CG5966	CG5966	carboxylic ester hydrolase activity	S199; D227; H312	Metabolic serine hydrolase			CL0028	Lipase	436

247	FBgn0036977	NP_649213.2	CG5665	CG5665	carboxylic ester hydrolase activity	S200; D228; H291	Metabolic serine hydrolase			CL0028	Lipase	376
248	FBgn0264979	NP_608661.1	CG4267	CG4267	carboxylic ester hydrolase activity	S202; D227; H288	Metabolic serine hydrolase			CL0028	Lipase	374
249	FBgn0030828	NP_573202.1	CG5162	CG5162	carboxylic ester hydrolase activity	S214; D242; H305	Metabolic serine hydrolase			CL0028	Lipase	411
250	FBgn0031976	NP_609175.2	CG7367	CG7367	carboxylic ester hydrolase activity	S224; D248; H317	Metabolic serine hydrolase			CL0028	Lipase	358
251	FBgn0032973	NP_610132.3	CG6675	CG6675	carboxylic ester hydrolase activity	S236; D261; H322	Metabolic serine hydrolase			CL0028	Lipase	386
252	FBgn0039344	NP_651403.1	CG4582	CG4582	carboxylic ester hydrolase activity	S249; D274; H336	Metabolic serine hydrolase			CL0028	Lipase	432
253	FBgn0030884	NP_573259.2	CG6847	CG6847	carboxylic ester hydrolase activity	S275; D298; H387	Metabolic serine hydrolase			CL0028	Lipase	1000
254	FBgn0265267	NP_573201.1	CG18258	CG18258	carboxylic ester hydrolase activity	S287; D316; H382	Metabolic serine hydrolase			CL0028	Lipase	468
255	FBgn0005391	NP_511102.3	CG2979	Yp2	carboxylic ester hydrolase activity	D284; H311; S334	Metabolic serine hydrolase			CL0028	Lipase	442
256	FBgn0004047	NP_511148.2	CG11129	Yp3	carboxylic ester hydrolase activity	D273; H300; S323	Metabolic serine hydrolase			CL0028	Lipase	420
257	FBgn0004045	NP_511103.1	CG2985	Yp1	carboxylic ester hydrolase activity	D283; H310; S340	Metabolic serine hydrolase			CL0028	Lipase	439
258	FBgn0051872	NP_723603.1	CG31872	CG31872	sterol esterase activity	S845	Metabolic serine hydrolase		-	CL0028	Partial Abhydrolase	1073
259	FBgn0038069	NP_650218.3	CG11608	CG11608	triglyceride lipase activity	S185	Metabolic serine hydrolase		-	CL0028	Partial Abhydrolase	430

260	FBgn0043825	NP_609428.1	CG18284	CG18284	triglyceride lipase activity	S228	Metabolic serine hydrolase		-	CL0028	Partial Abhydrolase	457
261	FBgn0034928	NP_611849.1	CG13562	CG13562	carboxylic ester hydrolase activity	S148; D175; S198	Metabolic serine hydrolase		-	CL0028	Lipase	342
262	FBgn0035206	NP_728590.1	CG9186	sturkopf	-	S119; D254; H283	Metabolic serine hydrolase			CL0028	LIDHydrolase	307
263	FBgn0051683	NP_724265.2	CG31683	CG31683	O-acyltransferase activity	S205; D369; H401	Metabolic serine hydrolase			CL0028	LCAT	421
264	FBgn0042175	NP_652700.1	CG18858	CG18858	O-acyltransferase activity	S205; D369; H401	Metabolic serine hydrolase			CL0028	LCAT	421
265	FBgn0034491	NP_725942.1	CG11055	Hsl	sterol esterase activity	S473; D794; H824	Metabolic serine hydrolase	SC	S9		HSL_N	881
266	FBgn0038806	NP_650895.1	CG5412	CG5412	-	S133; D191; H218	Metabolic serine hydrolase			CL0028	FSH1	279
267	FBgn0259175	NP_524739.1	CG42280	ome	serine-type peptidase activity	S662; D739; H771	Metabolic serine hydrolase	SC	S9	CL0186	DPPIV_N	784
268	FBgn0039240	NP_996292.2	CG3744	CG3744	serine-type peptidase activity	S910; D988; H1020	Metabolic serine hydrolase	SC	S15	CL0186	DPPIV_N	1042
269	FBgn0031835	NP_609051.1	CG11319	CG11319	serine-type peptidase activity	S783;D861;H893	Metabolic serine hydrolase	SC	S9	CL0186	DPPIV_N	935
270	FBgn0031741	NP_608961.2	CG11034	CG11034	serine-type peptidase activity	S610; D689; H721	Metabolic serine hydrolase	SC	S9	CL0186	DPPIV_N	
271	FBgn0035154	NP_612051.1	CG3344	hiro	serine-type carboxypeptidase activity	S161; D368; H425	Metabolic serine hydrolase	SC	S10	CL0028	Peptidase_S10	446

272	FBgn0038738	NP_732457.1	CG4572	CG4572	serine-type carboxypeptidase activity	S217; D403; H460	Metabolic serine hydrolase	SC	S10	CL0028	Peptidase_S10	482
273	FBgn0052483	NP_728540.1	CG32483	CG32483	serine-type carboxypeptidase activity	S156; D361; H418	Metabolic serine hydrolase	SC	S10	CL0028	Peptidase_S10	439
274	FBgn0051823	NP_723939.1	CG31823	CG31823	serine-type carboxypeptidase activity	S164; D349; H406	Metabolic serine hydrolase	SC	S10	CL0028	Peptidase_S10	427
275	FBgn0051821	NP_609771.2	CG31821	CG31821	serine-type carboxypeptidase activity	S158; D344; H401	Metabolic serine hydrolase	SC	S10	CL0028	Peptidase_S10	427
276	FBgn0035726	NP_648067.2	CG9953	CG9953	serine-type peptidase activity	S183; D445; H470	Metabolic serine hydrolase	SC	S28	CL0028	Peptidase_S28	508
277	FBgn0038702	NP_650804.2	CG3739	CG3739	serine-type peptidase activity	S179; D432; H453	Metabolic serine hydrolase	SC	S28	CL0028	Peptidase_S28	485
278	FBgn0038700	NP_650802.1	CG3734	CG3734	serine-type peptidase activity	S172; D421; H442	Metabolic serine hydrolase	SC	S28	CL0028	Peptidase_S28	473
279	FBgn0032864	NP_610037.1	CG2493	CG2493	serine-type peptidase activity	S166; D417; H442	Metabolic serine hydrolase	SC	S28	CL0028	Peptidase_S28	475
280	FBgn0038701	NP_650803.1	CG18493	CG18493	serine-type peptidase activity	S181; D428; H449	Metabolic serine hydrolase	SC	S28	CL0028	Peptidase_S28	480
281	FBgn0038705	NP_001369023.1	CG11626	CG11626	serine-type peptidase activity	S177; D435; H456	Metabolic serine hydrolase	SC	S28	CL0028	Peptidase_S28	379
282	FBgn0030447	NP_572852.1	CG2200	CG2200	serine-type peptidase activity	S125; D140; H162	Metabolic serine hydrolase	PC	S51	CL0014	Peptidase_S51	240
283	FBgn0032242	NP_609397.2	CG5355	CG5355	serine-type endopeptidase activity	S599; D686; H725	Metabolic serine hydrolase	SC	S9	CL0186	Peptidase_S9_N	756

284	FBgn0032969	NP_610129.3	CG2528	CG2528	serine-type endopeptidase activity	S574; D661; H700	Metabolic serine hydrolase	SC	S9	CL0186	Peptidase_S9_N	727
285	FBgn0030362	NP_572775.1	regucalcin	regucalcin	calcium ion binding	S159	Metabolic serine hydrolase			CL0186	SGL	
286	FBgn0038257	NP_524353.2	smp-30	smp-30	calcium ion binding	S159	Metabolic serine hydrolase			CL0186	SGL	
287	FBgn0000024	NP_476953.1	CG17907	Ace	acetylcholinesterase activity	S276; E405; H518	Metabolic serine hydrolase	SC	S9	CL0028	COesterase	636
288	FBgn0015568	NP_524269.3	CG1031	alpha-Est1	carboxylic ester hydrolase activity	S219; E352; H471	Metabolic serine hydrolase	SC	S9	CL0028	COesterase	565
289	FBgn0015569	NP_524257.3	CG1131	alpha-Est10	carboxylic ester hydrolase activity	S220; E353; H473	Metabolic serine hydrolase	SC	S9	CL0028	COesterase	550
290	FBgn0015570	NP_524268.3	CG2505	alpha-Est2	carboxylic ester hydrolase activity	S219; E352; H470	Metabolic serine hydrolase	SC	S9	CL0028	COesterase	566
291	FBgn0015571	NP_524267.2	CG1257	alpha-Est3	carboxylic ester hydrolase activity	S189; E322; H446	Metabolic serine hydrolase	SC	S9	CL0028	COesterase	99
292	FBgn0015572	NP_524266.1	CG1082	alpha-Est4	carboxylic ester hydrolase activity	S194; E322;H444	Metabolic serine hydrolase	SC	S9	CL0028	COesterase	541
293	FBgn0261393	NP_524265.3	CG1089	alpha-Est5	carboxylic ester hydrolase activity	S195; E326; H448	Metabolic serine hydrolase	SC	S9	CL0028	COesterase	542
294	FBgn0015574	NP_524262.1	CG1108	alpha-Est6	carboxylic ester hydrolase activity	S227; E353; H476	Metabolic serine hydrolase	SC	S9	CL0028	COesterase	568
295	FBgn0015575	NP_524261.1	CG1112	alpha-Est7	carboxylic ester hydrolase activity	S218; E352; H472	Metabolic serine hydrolase	SC	S9	CL0028	COesterase	572
296	FBgn0015576	NP_524259.2	CG1121	alpha-Est8	carboxylic ester hydrolase activity	S218; E353; H472	Metabolic serine hydrolase	SC	S9	CL0028	COesterase	574

297	FBgn0015577	NP_731165.2	CG1128	alpha-Est9	cholinesterase activity	S235; E368; H489	Metabolic serine hydrolase	SC	S9	CL0028	COesterase	569
298	FBgn0039084	NP_732875.1	CG10175	CG10175	carboxylic ester hydrolase activity	S161; E305; H421	Metabolic serine hydrolase	SC	S9	CL0028	COesterase	524
299	FBgn0032131	NP_609300.1	CG3841	CG3841	carboxylic ester hydrolase activity	S209; E331; H447	Metabolic serine hydrolase	SC	S9	CL0028	COesterase	564
300	FBgn0027584	NP_650043.1	CG4757	CG4757	carboxylic ester hydrolase activity	S202; E332; H452	Metabolic serine hydrolase	SC	S9	CL0028	COesterase	550
301	FBgn0029690	NP_570089.1	CG6414	CG6414	carboxylic ester hydrolase activity	S217; E349; H473	Metabolic serine hydrolase	SC	S9	CL0028	COesterase	583
302	FBgn0000326	NP_536784.1	CG9858	clt	carboxylic ester hydrolase activity	S205; E343; H461	Metabolic serine hydrolase	SC	S9	CL0028	COesterase	562
303	FBgn0034736	NP_611678.1	CG6018	gas	-	S219; E353; H472	Metabolic serine hydrolase	SC	S9	CL0028	COesterase	566
304	FBgn0010052	NP_523758.3	CG8425	Jhe	protein binding	S218; E351; H476	Metabolic serine hydrolase	SC	S9	CL0028	COesterase	579
305	FBgn0034076	NP_611085.2	CG8424	Jhedup	carboxylic ester hydrolase activity	S207; E342; H466	Metabolic serine hydrolase	SC	S9	CL0028	COesterase	559
306	FBgn0037070	NP_730617.1	CG11309	CG11309	hydrolase activity	S133; E280; D286; H307; H310	Metabolic serine hydrolase	SC	S33	CL0028	Abhydrolase_1	348
307	FBgn0025109	NP_477372.1	CG18642	Bem46	palmitoyl-(protein) hydrolase activity	S187	Metabolic serine hydrolase	SC	S9	CL0028	Hydrolase_4	338
308	FBgn0035519	NP_647880.1	CG1309	CG1309	phospholipase activity	S319	Metabolic serine hydrolase	SC	S9	CL0028	Abhydrolase_1	524
309	FBgn0034419	NP_725856.1	CG15111	CG15111	lysophospholipase activity	S259	Metabolic serine hydrolase	SC	S9	CL0028	Hydrolase_4	393

310	FBgn0035312	NP_647696.1	CG15820	CG15820	hydrolase activity	S105	Metabolic serine hydrolase	SC	S33	CL0028	Abhydrolase_1	308
311	FBgn0035309	NP_647694.1	CG15879	CG15879	hydrolase activity	S104;	Metabolic serine hydrolase	SC	S33	CL0028	Abhydrolase_6	342
312	FBgn0032265	NP_609419.1	CG18301	CG18301	triglyceride lipase activity	S175	Metabolic serine hydrolase			CL0028	Abhydrolase_1	422
313	FBgn0029942	NP_572388.1	CG2059	CG2059	carboxylic ester hydrolase activity	S127	Metabolic serine hydrolase	SC	S33	CL0028	Abhydrolase_1	308
314	FBgn0052333	NP_728588.1	CG32333	CG32333	-	S1300	Metabolic serine hydrolase			CL0028	DUF676	236
315	FBgn0053096	NP_788737.1	CG33096	CG33096	palmitoyl-(protein) hydrolase activity	S169	Metabolic serine hydrolase	SC	S9	CL0028	Hydrolase_4	286
316	FBgn0026570	NP_652068.1	CG5704	CG5704	hydrolase activity	S107	Metabolic serine hydrolase	SC	S33	CL0028	Abhydrolase_1	335
317	FBgn0026593	NP_652065.1	CG5707	CG5707	hydrolase activity	S117	Metabolic serine hydrolase	SC	S33	CL0028	Abhydrolase_1	357
318	FBgn0037071	NP_649302.1	CG7632	CG7632	hydrolase activity	S132	Metabolic serine hydrolase	SC	S33	CL0028	Abhydrolase_6	312
319	FBgn0020545	NP_477265.1	CG3943	kraken	hydrolase activity	S138	Metabolic serine hydrolase	SC	S33	CL0028	Abhydrolase_1	331
320	FBgn0032264	NP_609418.1	CG6113	Lip4	sterol esterase activity	S200	Metabolic serine hydrolase	SC	S33	CL0028	Abhydrolase_1	432
321	FBgn0029789	NP_572245.1	CG3160	PGAP1	phosphatidylinositol deacylase activity	S170	Metabolic serine hydrolase			CL0028	PGAP1	980
322	FBgn0033226	NP_724611.1	CG1882	puml	lysophosphatidic acid acyltransferase activity	S123	Metabolic serine hydrolase	SC	S33	CL0028	Abhydrolase_1	387

323	FBgn0051146	NP_731172.2	CG31146	Nlg1	neuroligin family protein binding	C221; S366	Metabolic serine hydrolase			CL0028	COesterase	1354
324	FBgn0034405	NP_788413.4	CG15102	Jheh2	cis-stilbene-oxide hydrolase activity	S201	Metabolic serine hydrolase	SC	S33	CL0028	EHN	463
325	FBgn0010053	NP_611385.1	CG15101	Jheh1	cis-stilbene-oxide hydrolase activity	S206	Metabolic serine hydrolase	SC	S33	CL0028	EHN	474
326	FBgn0034406	NP_611387.1	CG15106	Jheh3	cis-stilbene-oxide hydrolase activity	S201	Metabolic serine hydrolase	SC	S33	CL0028	EHN	468
327	FBgn0265271	NP_650106.1	CG14717	CG14717	lysophosphatidic acid acyltransferase activity	S87	Metabolic serine hydrolase	SC	S33	CL0028	Abhydrolase_6	306
328	FBgn0039430	NP_733152.1	CG5455	CG5455	molecular_function	S538	Metabolic serine hydrolase		-			688
329	FBgn0038013	NP_731685.1	CG10038	CG10038	siRNA binding	S206	Metabolic serine hydrolase	SC	S9			325
330	FBgn0032699	NP_609896.1	CG10383	CG10383	hydrolase activity, acting on ester bonds	S579	Metabolic serine hydrolase		-			784
331	FBgn0033897	NP_725358.1	CG8233	Rcd1	hydrolase activity	S650	Metabolic serine hydrolase		-	CL0028	DLH	1066
332	FBgn0037964	NP_650130.1	CG14731	CG14731	catalytic activity	S270	Metabolic serine hydrolase		-	CL0088	DUF229	641
333	FBgn0021979	NP_726286.1	CG3082	l(2)k09913	molecular_function	S145	Metabolic serine hydrolase		-	CL0028	DUF829	389
334	FBgn0037958	NP_650124.1	CG6962	CG6962	sphingomyelin phosphodiesterase D activity	S462	Metabolic serine hydrolase		-		mit_SMPDase	767
335	FBgn0043070	NP_995916.1	CG15669	MESK2	-	S4	Metabolic serine hydrolase		-	CL0028	Ndr	365

336	FBgn0032358	NP_609500.1	CG4851	Ppt2	palmitoyl-(protein) hydrolase activity	S98	Metabolic serine hydrolase		-	CL0028	Palm_thioest	288
337	FBgn0036939	NP_649178.1	CG7365	CG7365	lysophospholipase activity	S113	Metabolic serine hydrolase			CL0264	Lipase_GDSL	424
338	FBgn0031735	NP_608955.1	CG11029	CG11029	lysophospholipase activity	S141	Metabolic serine hydrolase			CL0264	Lipase_GDSL	
339	FBgn0287184	NP_001015405.3	CG17374	FASN3	hydrolase activity, acting on ester bonds	C178;; S605; H707; D1048;; S2188; H2355	Metabolic serine hydrolase			CL0046	ketoacyl-synt	2394
340	FBgn0042627	NP_647613.1	CG3524	FASN2	hydrolase activity, acting on ester bonds	C179;; S606; H709; D1049;;S2225; H2388	Metabolic serine hydrolase			CL0046	ketoacyl-synt	2410
341	FBgn0283427	NP_608748.1	CG3523	FASN1	hydrolase activity, acting on ester bonds	C199;; S619; H721; D1062;; S2249; H24216	Metabolic serine hydrolase			CL0046	Acyl_transf_1	2540
342	FBgn0029720	NP_572180.1	CG3009	CG3009	calcium-dependent phospholipase A2 activity	H135; D165, S226	Metabolic serine hydrolase			CL0629	Phospholip_A2_2	342
343	FBgn0250862	NP_572855.1	CG42237	CG42237	calcium-dependent phospholipase A2 activity	S217; H286; D316	Metabolic serine hydrolase			CL0629	Phospholip_A2_2	309
344	FBgn0039655	NP_001097964.1	CG14507	CG14507	phospholipase A2 activity	S253; H288; D339	Metabolic serine hydrolase			CL0629	Phospholip_A2_1	373
345	FBgn0004611	NP_995606.1	CG4574	Plc21C	calcium ion binding	H326; H333; H378; S555	Metabolic serine hydrolase			CL0384	PI-PLC-X	1250
346	FBgn0003416	NP_476726.2	CG4200	sl	phosphatidylinositol phospholipase C activity	H339; H384; S806	Metabolic serine hydrolase			CL0384	PI-PLC-X	1236

347	FBgn0082831	NP_650193.1	CG6525	pps	hydrolase activity, acting on acid anhydrides	S1856	Metabolic serine hydrolase		-		TFIIS_M	2018
348	FBgn0037623	NP_996184.1	CG9801	CG9801	catalytic activity	S388	Metabolic serine hydrolase		-	CL0238	PP2C_2	709
349	FBgn0030607	NP_572995.1	CG5560	dob	triglyceride lipase activity	S44	Metabolic serine hydrolase		-	CL0323	Patatin	480
350	FBgn0036449	NP_648723.1	CG5295	bmm	triglyceride lipase activity	S38	Metabolic serine hydrolase		-	CL0323	Patatin	553
351	FBgn0036053	NP_648366.2	iPLA2-VIA	iPLA2-VIA	calcium-independent phospholipase A2 activity	S592	Metabolic serine hydrolase			CL0323	Patatin	
352	FBgn0035734	NP_729206.1	CG14823	CG14823	lysozyme activity	S43	Metabolic serine hydrolase	S-	S81	CL0037	Destabilase	
353	FBgn0034165	NP_611165.2	CG6435	CG6435	lysozyme activity	S17	Metabolic serine hydrolase	S-	S81	CL0037	Destabilase	
354	FBgn0031990	NP_609185.1	PAPLA1	PAPLA1	metal ion binding	S1517	Metabolic serine hydrolase				DDHD	

Annexure 5

Activity atlas of Serine Hydrolases in *Drosophila melanogaster*

Table Annexure 5.1:Serine proteases in development

GENE SYMBOL	AVERAGE PEPTIDE COUNTS FROM 3 BIOLOGICAL REPLICATES									
	SOLUBLE					MEMBRANE				
	EMBRYO	LARVA	PUPA	ADULT (FEMALE)	ADULT (MALE)	EMBRYO	LARVA	PUPA	ADULT (FEMALE)	ADULT (MALE)
alphaTry	0	0	0	4	0	0	0	0	0	0
betaTry	0	0	0	3	0	0	1	0	0	0
CG10198	5	0	0	0	0	2	0	0	0	0
CG10469	2	0	0	0	0	0	0	0	0	0
CG10472	0	7	0	2	0	1	5	0	1	1
CG11313	0	1	0	0	0	0	0	0	0	0
CG11911	0	2	0	0	0	0	2	0	0	0
CG11912	0	2	0	0	0	0	0	0	0	0
CG17475	0	0	0	0	0	0	0	1	0	0
CG17571	0	2	0	0	0	0	0	0	0	0
CG18179	0	0	5	0	0	0	0	5	0	0
CG18180	0	5	0	0	5	0	2	0	0	0
CG18735	0	0	4	0	0	0	0	0	0	0
CG30025	0	4	0	0	0	0	0	0	0	0
CG31681	2	0	0	0	0	1	0	0	0	0
CG3355	0	0	6	0	0	0	0	8	0	0
CG4914	0	0	0	0	0	0	0	2	0	0
ClpP	4	0	0	3	4	1	0	0	0	0

epsilonTry	0	2	0	0	0	0	0	0	0	0
etaTry	0	0	0	0	0	0	2	0	0	0
GatA	2	0	0	0	0	0	0	0	0	0
iotaTry	0	3	0	0	0	0	3	0	0	0
Jon65Ai	0	4	0	0	0	0	0	0	0	0
Jon65Aiv	2	10	0	6	0	0	5	0	0	0
Jon66Cii	0	4	0	0	0	0	0	0	0	0
Jon99Cii	0	0	0	3	0	0	0	0	0	0
Jon99Ciii	5	11	0	4	3	3	3	0	0	0
Jon99Fi	5	9	0	2	0	2	1	0	0	0
Jon99Fii	0	0	0	0	0	4	0	0	0	0
Lon	1	0	0	0	0	4	0	0	0	0
MP1	0	0	2	0	0	0	0	0	0	0
Np	0	0	3	0	0	0	0	4	0	0
TppII	44	15	0	4	5	22	8	14	0	0
yip7	0	3	0	0	0	0	0	0	0	0
zetaTry	0	2	0	0	0	0	3	2	2	2

Table Annexure 5.2:Metabolic serine hydrolases in development

GENE SYMBOL	AVERAGE PEPTIDE COUNTS FROM 3 BIOLOGICAL REPLICATES									
	SOLUBLE					MEMBRANE				
	EMBRYO	LARVA	PUPA	ADULT (FEMALE)	ADULT (MALE)	EMBRYO	LARVA	PUPA	ADULT (FEMALE)	ADULT (MALE)
Ace	0	0	0	0	0	0	0	11	1	2
alpha-Est3	2	2	0	0	1	0	0	0	0	0
alpha-Est5	9	9	3	4	3	4	0	0	0	0
alpha-Est7	0	7	0	0	0	0	7	22	4	6
Apt1	9	7	7	7	7	6	3	6	2	2
CG10038	16	3	2	4	3	5	0	0	0	0
CG11309	3	0	0	0	0	0	0	0	0	0
CG1309	0	0	0	0	0	4	0	4	1	2
CG17097	0	0	0	0	0	0	0	0	0	15
CG18493	0	3	0	0	0	0	3	0	2	0
CG18858	8	0	0	0	0	7	0	10	0	0
CG2059	3	0	0	2	2	0	0	0	0	0
CG2493	5	4	4	0	0	4	2	6	0	0
CG31683	0	5	4	0	0	5	0	0	0	0
CG31821	0	14	0	0	0	0	0	0	0	0
CG31872	0	0	0	0	0	0	0	0	0	15
CG32483	0	4	0	0	0	0	0	0	0	0
CG33096	0	0	0	0	0	3	0	0	0	0
CG3739	4	0	0	0	0	0	0	0	0	0
CG4390	10	3	6	3	2	0	0	4	0	0

CG4572	10	7	16	5	8	4	0	10	0	0
CG4757	0	0	7	0	0	0	0	0	0	0
CG5068	3	0	0	3	3	0	0	0	0	0
CG5162	0	0	0	0	0	0	0	0	0	3
CG5355	47	17	12	18	25	25	0	9	0	0
CG5377	5	2	0	5	6	2	0	4	0	0
CG5412	5	2	2	2	0	0	0	2	0	0
CG6567	5	8	3	3	0	0	0	5	0	0
CG7632	3	0	0	3	4	0	0	3	0	0
CG9953	6	2	0	3	2	7	0	5	0	0
clt	2	0	0	0	0	0	0	0	0	0
Est-6	3	6	3	7	28	0	0	0	0	5
Est-P	0	4	0	0	0	0	0	0	0	0
FASN1	4	126	7	8	24	18	16	62	25	30
FASN2	0	0	0	0	0	0	0	0	7	7
hiro	0	4	0	0	0	0	0	0	0	0
iPLA2-VIA	3	0	0	0	0	0	0	0	0	0
Jheh1	0	0	0	0	0	0	2	5	2	2
Jheh2	0	0	0	0	0	3	0	4	0	0
Jheh3	0	0	0	0	0	0	0	5	0	0
kraken	0	0	0	2	2	0	0	0	0	0
l(2)k09913	0	0	0	0	0	0	3	6	2	2
Lip4	0	0	0	0	0	0	0	2	0	0
MESK2	0	0	0	0	0	0	0	2	0	2
ome	0	3	0	0	0	0	3	6	2	2

PAPLA1	0	6	0	0	0	0	0	0	0	0
PPT1	0	0	0	0	0	0	0	4	0	0
puml	0	0	0	0	0	4	0	3	2	3
regucalcin	0	46	43	12	17	0	3	43	4	10
smp-30	0	10	6	0	0	0	0	0	0	0
sturkopf	0	2	0	0	0	4	2	9	2	3
Yp1	128	0	0	30	4	104	0	0	9	0
Yp2	86	0	0	26	5	75	0	0	11	0
Yp3	106	0	0	23	4	102	0	0	7	0

Table Annexure 5.3:Serine Proteases in adult organs

Gene Symbol	Average peptide counts from 3 biological replicates													
	Head				Carcass		Hemolymph		Gut				Reproductive Organs	
	Soluble		Membrane		Whole		Whole		Soluble		Membrane		Whole	
	Female	Male	Female	Male	Female	Male	Female	Male	Female	Male	Female	Male	Ovary	Testis
alphaTry	0	0	0	0	0	0	2	0	18	10	32	11	0	0
amon	3	3	0	0	0	0	0	0	0	0	0	0	0	0
betaTry	0	0	0	0	3	0	3	2	19	21	24	14	0	0
CG10041	0	0	0	0	0	0	0	0	0	0	0	0	0	2
CG10198	2	2	0	0	0	0	0	0	0	2	0	0	2	0
CG10469	0	0	0	0	0	0	0	0	0	0	5	0	0	0

CG10472	0	0	0	0	0	2	5	0	7	10	33	11	0	0
CG10477	0	0	0	0	0	0	0	0	0	6	0	4	0	0
CG10587	0	0	0	0	0	0	0	0	0	0	0	0	0	3
CG11037	0	0	0	0	0	0	0	2	0	0	0	2	0	5
CG11911	0	0	0	0	0	0	2	0	0	3	5	2	0	0
CG16749	0	0	0	0	0	0	0	0	0	7	20	9	0	0
CG17475	0	0	0	0	0	0	0	0	0	0	9	4	0	0
CG17477	0	0	0	0	0	0	0	0	0	0	4	2	0	0
CG17571	0	0	0	0	0	0	0	0	0	5	4	2	0	0
CG18179	0	0	0	0	0	0	0	0	0	5	0	0	0	0
CG18180	0	0	0	0	0	2	5	2	4	12	4	7	0	0
CG31265	0	0	0	0	0	0	0	0	0	0	5	4	0	0
CG4053	0	0	0	0	0	0	0	0	0	0	2	0	0	0
CG8329	6	5	3	2	0	0	2	0	0	0	0	4	0	0
CG8952	0	0	0	0	0	0	0	0	0	2	0	0	0	0
CG9372	0	2	0	0	0	2	3	3	0	0	0	0	0	0

CG9676	5	3	0	0	0	0	0	0	0	0	0	0	0
ClpP	3	5	0	0	0	3	0	0	0	4	0	0	3	5
etaTry	0	0	0	0	0	0	0	0	0	0	0	3	0	0
grass	2	1	0	0	0	0	0	0	0	0	0	0	0	0
HtrA2	0	0	2	0	0	0	0	0	0	0	0	0	0	2
iotaTry	0	0	0	0	0	0	2	0	0	7	16	9	0	0
Jon25Bi	0	0	0	0	0	0	0	0	0	6	0	5	0	0
Jon25Bii	0	0	0	0	0	0	0	0	0	5	0	5	0	0
Jon25Biii	0	0	0	0	0	0	0	0	0	6	0	0	0	0
Jon65Ai	0	0	0	0	0	0	0	0	5	7	0	5	0	0
Jon65Aiii	0	0	0	0	0	0	0	0	0	16	0	10	0	0
Jon65Aiv	0	0	0	0	4	4	6	0	10	22	6	10	0	0
Jon74E	0	0	0	0	0	0	0	0	4	9	4	5	0	0
Jon99Ci	0	0	0	0	0	0	0	0	0	2	0	0	0	0
Jon99Cii	0	0	0	0	0	0	4	3	10	21	16	13	0	0
Jon99Ciii	0	0	0	0	2	2	4	3	10	21	16	13	0	0

Jon99Fi	0	0	0	0	0	2	4	0	10	14	0	9	0	0
Jon99Fii	0	0	0	0	0	0	4	0	9	15	0	9	0	0
MP1	0	0	0	0	0	0	0	0	0	0	0	0	0	0
Sems	0	0	0	0	0	0	0	0	0	0	0	0	0	2
Send1	0	0	0	0	0	0	0	0	4	0	10	0	0	
Ser7	0	2	0	0	0	0	0	0	0	0	0	0	0	0
SPE	5	4	0	0	3	2	5	5	0	0	0	0	0	0
thetaTry	0	0	0	0	0	0	0	0	3	4	6	3	0	
TppII	18	19	11	7	11	9	9	3	3	21	8	4	6	11
twr	0	0	3	2	0	0	0	0	0	0	0	3	0	3
yip7	0	0	0	0	0	0	0	0	8	15	10	5	0	0
zetaTry	0	0	0	0	0	0	0	0	4	3	21	7	0	0

Table Annexure 5.4:Metabolic serine hydrolase in adult organs

Gene Symbol	**Average peptide counts from 3 biological replicates**

	Head				Carcass		Hemolymph		Gut				Reproductive Organs	
	Soluble		Membrane		Whole		Whole		Soluble		Membrane		Whole	
	Female	Male	Female	Male	Female	Male	Female	Male	Female	Male	Female	Male	Ovary	Testis
Ace	16	15	14	15	4	4	0	0	0	0	0	0	0	0
alpha-Est1	0	0	0	0	0	0	0	0	0	0	2	2	0	0
alpha-Est10	0	0	0	0	0	0	0	0	0	0	0	4	0	0
alpha-Est5	0	0	0	0	0	0	3	2	4	2	2	2	0	0
alpha-Est7	6	5	11	11	3	3	2	0	6	11	26	21	0	0
Apt1	8	11	5	5	6	5	6	3	6	0	3	5	7	4
CG10038	5	3	0	0	0	0	1	0	0	0	0	0	3	3
CG10175	0	0	0	0	0	0	0	0	0	0	0	0	0	2
CG11034	0	0	0	0	0	0	0	0	0	0	19	10	0	5
CG11309	2	3	0	0	5	5	0	0	0	8	0	2	0	4
CG11319	0	0	4	3	0	0	0	0	0	0	0	0	0	0
CG11608	0	0	0	0	0	0	0	0	0	0	0	5	0	7
CG1309	0	0	0	2	0	0	0	0	0	0	0	4	0	3

CG13282	0	0	0	0	0	0	0	0	0	0	0	0	0	2
CG17097	0	0	0	0	0	0	0	15	0	0	0	23	0	41
CG17192	0	0	0	0	0	0	2	0	0	3	0	0	0	0
CG18258	0	0	0	0	0	0	0	11	0	3	0	2	0	14
CG18301	0	0	0	0	0	0	0	0	0	0	0	3	0	0
CG18493	0	0	0	0	0	0	2	0	0	9	44	16	0	0
CG18858	0	0	0	0	0	4	0	0	0	6	0	2	0	6
CG2059	2	2	0	0	5	5	0	0	0	2	0	0	0	0
CG2200	2	0	0	0	0	0	0	0	0	3	0	0	0	0
CG2493	4	4	3	2	2	2	0	0	0	4	5	3	0	3
CG2528	0	0	0	0	0	0	0	0	0	0	0	0	0	4
CG31683	4	7	3	2	6	0	0	0	0	6	0	3	0	6
CG31821	3	3	0	0	0	0	19	14	0	0	0	0	0	0
CG31872	0	0	0	0	0	0	0	15	0	0	0	10	0	37
CG32483	0	0	0	0	0	0	0	0	6	5	5	4	0	0
CG34447	0	0	0	0	0	0	0	0	0	0	0	0	0	3
CG3734	0	0	0	0	0	0	0	0	0	2	15	11	0	0

CG3739	0	0	0	0	0	0	0	0	0	7	0	0	0	0
CG3841	0	0	0	0	0	0	0	0	0	0	23	8	0	0
CG4390	2	5	0	0	5	6	4	0	12	5	0	0	4	5
CG4572	10	10	5	3	8	12	2	0	9	10	5	4	3	9
CG4757	3	5	0	0	0	2	7	5	0	0	0	0	0	0
CG5068	4	4	0	0	0	0	0	0	0	0	0	0	0	0
CG5162	0	0	2	2	0	3	4	13	0	6	0	4	0	18
CG5355	26	29	2	0	28	19	15	8	4	38	2	2	13	32
CG5377	8	9	0	0	12	12	0	0	0	7	0	0	0	5
CG5412	2	2	0	0	0	0	0	0	0	0	0	0	2	0
CG5707	0	0	0	0	0	1	0	0	0	5	0	0	0	0
CG6295	0	0	0	0	0	0	0	0	0	4	0	0	0	0
CG6567	3	4	0	0	0	0	0	0	0	0	0	0	2	0
CG7632	6	7	0	0	10	7	0	0	0	2	0	0	0	0
CG9953	2	0	0	0	0	0	0	0	0	0	0	4	2	2
Est-6	17	18	7	3	10	19	29	63	0	27	0	4	0	58
Est-Q	0	0	0	0	0	0	4	4	0	0	0	0	0	0

FASN1	3	5	12	10	9	4	58	44	6	48	0	14	4	5
FASN2	0	0	0	0	0	0	0	0	0	13	0	7	0	0
gas	0	0	0	0	0	0	0	0	0	2	0	2	0	0
hiro	0	0	0	0	0	0	3	0	4	6	5	0	0	0
Jhedup	6	6	0	0	0	0	0	0	0	0	0	0	0	0
Jheh1	0	0	2	4	0	0	0	0	0	2	6	8	0	2
Jheh2	0	0	3	3	0	0	0	0	0	0	0	7	0	3
Jheh3	0	0	0	0	0	0	0	0	0	0	7	8	0	0
kraken	2	2	0	0	3	3	0	0	0	5	0	0	0	0
l(2)k09913	0	0	6	4	2	3	0	0	0	0	0	4	0	0
MESK2	0	0	0	2	0	0	0	0	0	0	0	0	0	0
ome	0	0	3	3	0	0	1	0	2	4	30	24	0	3
Ppt1	0	0	0	0	0	0	0	0	0	0	0	2	0	3
puml	0	0	3	3	0	0	0	0	3	3	8	9	0	0
regucalcin	23	22	9	7	11	20	14	15	3	13	0	3	2	26
smp-30	4	5	0	0	3	4	0	0	0	9	0	0	0	0
sturkopf	0	0	3	5	0	0	3	0	0	0	6	3	0	3

sxe2	0	0	1	0	0	0	0	0	0	0	0	0	0	0
Yp1	28	24	8	8	22	0	132	5	5	0	0	0	96	0
Yp2	29	18	9	12	20	0	86	3	12	0	0	0	63	0
Yp3	26	15	5	5	14	0	96	5	7	0	0	0	74	0

Table Annexure 5.5:SHs identified

Serine Proteases Identified			
Embryo	**Larva**	**Pupa**	**Adult**
CG10198	etaTry	Np	CG16749
Jon99Fi	iotaTry	CG18735	CG10472
Jon99Fii	CG18180	MP1	Jon99Ciii
Lon	Jon99Fi	CG18179	TppII
TppII	Jon99Ciii	CG3355	CG18180
Jon99Ciii	zetaTry	zetaTry	betaTry
CG31681	Jon65Aiv	CG4914	alphaTry
GatA	CG10472	twr	ClpP
Jon65Aiv	TppII	TppII	Jon65Aiv
ClpP	CG11911		Jon99Cii
CG10469	yip7		Jon99Fi
	CG11912		amon

	CG30025		CG10041
	CG17571		CG10198
	epsilonTry		CG10477
	Jon66Cii		CG10587
	Jon65Ai		CG11037
			CG11911
			CG17475
			CG17477
			CG17571
			CG18179
			CG31265
			CG8329
			CG8952
			CG9372
			CG9676
			etaTry

			grass
			HtrA2
			iotaTry
			Jon25Bi
			Jon25Bii
			Jon25Biii
			Jon65Ai
			Jon65Aiii
			Jon74E
			Jon99Ci
			Jon99Fii
			MP1
			Sems
			Ser7
			SPE
			thetaTry

			twr
			yip7
			zetaTry
			CG10469
			Send1
			CG4053

Serine Proteases Unique to 1 Stage of life Cycle			
Embryo	**Larva**	**Pupa**	**Adult**
Lon	CG11912	Np	CG16749
CG31681	CG30025	CG18735	betaTry
GatA	epsilonTry	CG3355	alphaTry
	Jon66Cii	CG4914	Jon99Cii
			amon

			CG10041
			CG10477
			CG10587
			CG11037
			CG17475
			CG17477
			CG31265
			CG8329
			CG8952
			CG9372
			CG9676
			grass
			HtrA2
			Jon25Bi
			Jon25Bii
			Jon25Biii
			Jon65Aiii

			Jon74E
			Jon99Ci
			Sems
			Ser7
			SPE
			thetaTry
			Send1
			CG4053

Serine Proteases Present in more than 1 Stage of life Cycle					
Embryo & Adult	**Embryo, Larva & Adult**	**All life forms**	**Larva & Adult**	**Larva, Pupa & Adult**	**Pupa & Adult**
CG10198	Jon99Fi	TppII	etaTry	zetaTry	MP1
Jon99Fii	Jon99Ciii		iotaTry		CG18179
ClpP	Jon65Aiv		CG18180		twr

CG10469			CG10472		
			CG11911		
			yip7		
			CG17571		
			Jon65Ai		

Metabolic SHs Identified			
Embryo	**Larva**	**Pupa**	**Adult**
Jheh2	ome	MESK2	Jheh1
CG5377	CG18493	CG7632	MESK2
CG4572	CG9953	CG4390	Apt1
CG33096	CG5412	CG6567	ome
alpha-Est5	CG5377	Lip4	l(2)k09913
CG1309	alpha-Est3	CG5377	CG5162

CG2493	CG4390	puml	Est-6
puml	CG2493	Jheh2	Ace
sturkopf	CG10038	Ppt1	regucalcin
Apt1	hiro	Jheh1	alpha-Est7
FASN1	Est-6	CG1309	FASN2
CG9953	Est-P	l(2)k09913	CG17097
CG10038	CG31683	ome	CG31872
CG18858	alpha-Est7	CG9953	FASN1
CG31683	CG6567	Jheh3	Yp1
CG5355	Apt1	Apt1	alpha-Est3
Yp2	PAPLA1	CG2493	kraken
Yp1	alpha-Est5	CG5355	CG10038
Yp3	CG4572	CG4572	CG2059
alpha-Est3	smp-30	Ace	CG5068
CG2059	CG31821	sturkopf	Yp3
CG5068	CG5355	CG18858	Yp2
CG7632	regucalcin	alpha-Est7	CG7632

iPLA2-VIA	FASN1	regucalcin	CG5377
CG11309	Jheh1	FASN1	CG4572
Est-6	sturkopf	CG5412	CG5355
CG3739	l(2)k09913	CG10038	CG1309
CG5412	CG32483	Est-6	sturkopf
CG6567		CG31821	CG18493
CG4390		alpha-Est5	puml
clt		CG4757	CG4390
		smp-30	CG5412
		CG31683	alpha-Est5
			CG9953
			CG6567
			alpha-Est1
			alpha-Est10
			CG10175
			CG11034
			CG11309

			CG11319
			CG11608
			CG13282
			CG17192
			CG18258
			CG18301
			CG18858
			CG2200
			CG2493
			CG2528
			CG31683
			CG31821
			CG32483
			CG34447
			CG3734
			CG3739
			CG3841

			CG4757
			CG5707
			CG6295
			Est-Q
			gas
			hiro
			Jhedup
			Jheh2
			Jheh3
			Ppt1
			smp-30
			sxe2

Metabolic SHs Unique to 1 Stage of life Cycle			
Embryo:	**Larva:**	**Pupa:**	**Adult:**
CG33096	Est-P	Lip4	CG5162
iPLA2-VIA	PAPLA1		FASN2
clt			CG17097
			CG31872
			kraken
			alpha-Est1
			alpha-Est10
			CG10175
			CG11034
			CG11319
			CG11608

			CG13282
			CG17192
			CG18258
			CG18301
			CG2200
			CG2528
			CG34447
			CG3734
			CG3841
			CG5707
			CG6295
			Est-Q
			gas
			Jhedup
			sxe2

Metabolic SHs Present in more than 1 Stage of life Cycle						
Embryo & Adult	**Larva & Adult**	**Pupa & Adult**	**Embryo, Larva & Adult**	**Embryo, Pupa & Adult**	**Larva, Pupa & Adult**	**All life forms**
Yp2	CG18493	MESK2	alpha-Est3	Jheh2	ome	CG5377
Yp1	hiro	Ppt1		CG1309	alpha-Est7	CG4572
Yp3	CG32483	Jheh3		puml	smp-30	alpha-Est5
CG2059		Ace		CG18858	CG31821	CG2493
CG5068		CG4757		CG7632	regucalcin	sturkopf
CG11309					Jheh1	Apt1
CG3739					l(2)k09913	FASN1

						CG9953
						CG10038
						CG31683
						CG5355
						Est-6
						CG5412
						CG6567
						CG4390

Annexure 6

Literature survey of Serine Hydrolases in *Drosophila's* immune response

S.No.	*FlyBase ID*	*Gene symbol*	*Up / Down Regulated*	*Treatment*	*Time Point*	*Value of Expression Parameter*	*Developmental stage/Tissue*	*Reference*
1	*FBgn0000024*	Ace	Down-Regulation	ECC15	4 Hours	-2	Gut	Buchon et al. 2009
								Chakrabarti et al. 2012
				Pseudomonas entomophila	4 Hours	-2.1	Gut	Chakrabarti et al. 2012
						-0.9628	Gut	Soory and Ratnaparkhi 2022
			Up-Regulation	*Gamasodes queenslandicus*	-	-	Adult male	Benoit et al. 2020
				Providencia rettgeri,	-	1.37	Adult	Short and Lazzaro 2013
				Pseudomonas entomophila	-	0.6036995414	Adult	Ragheb et al. 2017
						1.046566702	Adult	Ragheb et al. 2017
2	*FBgn0000533*	ea	Up-Regulation	S–W– vs S+W–	24 Hours	1.026600405	Adult	Higareda Alvear et al. 2021
3	*FBgn0000592*	Est-6	Down-Regulation	*Pseudomonas entomophila*	-	-0.7925487997	Adult	Ragheb et al. 2017
						-0.4100738623	Adult	Ragheb et al. 2017
			Up-Regulation	*DCV, Serratia, Beauveria, Octosporea*	-	-	Adult	Roxstrom-Lindquist et al. 2004
4	*FBgn0001285*	Jon44E	-	ECC15	8 Hours	-	Adult	Erkosar et al. 2014
			Down-Regulation	A.fumigatus	24 Hours	-0.302	Adult	De Gregorio et al. 2002
				E. coli and Micrococcus luteus	3 Hours	0.4	Adult	Brun et al. 2006
				Pseudomonas entomophila	-	-1.71424465	Adult	Ragheb et al. 2017

						-0.5568803518	Adult	Ragheb et al. 2017
					16 Hours	-44.9	Gut	Chakrabarti et al. 2012
					4 Hours	-0.6521	Gut	Soory and Ratnaparkhi 2022
5	*FBgn0002926*	ndl	-	*Wolbachia pipientis*		-	Ovary	Christensen et al. 2016
			Down-Regulation	*Pseudomonas entomophila*	-	-1.739481711	Adult	Ragheb et al. 2017
						-1.363503285	Adult	Ragheb et al. 2017
			Up-Regulation	*Aspergillus flavus*	-	-	Adult	Ramirez-Camejo and Bayman 2020
				DCV	-	-	Adult	Merkling et al. 2015a; Merkling et al. 2015b
6	*FBgn0003319*	Sb	Down-Regulation	S–W– vs S+W–	24 Hours	-1.998065632	Adult	Higareda Alvear et al. 2021
				S–W– vs. S–Lh	24 Hours	-1.497406388	Adult	Higareda Alvear et al. 2021
7	*FBgn0003356*	Jon99Cii	Down-Regulation	*Pseudomonas entomophila*	4 Hours	-0.7995	Gut	Soory and Ratnaparkhi 2022
				S. aureus	45 min	-4.95	Plasmatocyte	Ramond et al. 2020
8	*FBgn0003357*	Jon99Ciii		*Photor/nematode*	-	-	Adult	Castillo et al. 2015
			Down-Regulation	*Pseudomonas entomophila*	4 Hours	-0.7379	Gut	Soory and Ratnaparkhi 2022
				S. aureus	45 min	-8.32	Plasmatocyte	Ramond et al. 2020
9	*FBgn0003358*	Jon99Ci	-	Lipopolysaccharide	-	-	Adult	Schlamp et al. 2021

				ECC15	8 Hours	-	Adult	Erkosar et al. 2014
			Down-Regulation	10 different bacteria	-	-1.846145778	Adult	Troha et al. 2018
				Photor/nematode	-	-	Adult	Castillo et al. 2015
				Pseudomonas entomophila	-	-0.8620418734	Adult	Ragheb et al. 2017
					16 Hours	-30.4	Gut	Chakrabarti et al. 2012
					4 Hours	-0.8652	Gut	Soory and Ratnaparkhi 2022
10	*FBgn0003450*	snk	Down-Regulation	*C virus*		-	S2 cell	Zhu et al. 2013
11	*FBgn0003863*	alphaTry	-	*Lipopolysaccharide*	-	-	Adult	Schlamp et al. 2021
				ECC15	8 Hours	-	Adult	Erkosar et al. 2014
			Down-Regulation	*Pseudomonas entomophila*	4 Hours	-0.6349	Gut	Soory and Ratnaparkhi 2022
12	*FBgn0004045*	Yp1	-	*Wolbachia pipientis*		-	Ovary	Christensen et al. 2016
			Down-Regulation	*Pseudomonas entomophila*	-	-0.6610666535	Adult	Ragheb et al. 2017
						-0.3340136772	Adult	Ragheb et al. 2017
			Up-Regulation	*Serratia marcescens and Enterococcos faecalis*	12 Hours	4.251126184	Adult	Sackton et al. 2010
13	*FBgn0004047*	Yp3	-	*Wolbachia pipientis*		-	Ovary	Christensen et al. 2016
			Down-Regulation	*Micrococcus luteus*	-	-7.46985	Adult male	Wei et al. 2018
				Pseudomonas entomophila	-	-0.8028673313	Adult	Ragheb et al. 2017
						-0.3679845502	Adult	Ragheb et al. 2017

			Up-Regulation	*Aspergillus flavus*	-	-	Adult	Ramirez-Camejo and Bayman 2020
				E. coli and Micrococcus luteus	3 Hours	2.2	Adult	Brun et al. 2006
				S–W– vs S+W–	24 Hours	1.098344595	Adult	Higareda Alvear et al. 2021
14	*FBgn0004509*	Fur1	Up-Regulation	*Gamasodes queenslandicus*	-	-	Adult male	Benoit et al. 2020
				Heterorhabditis bacteriophora	-	-	Larva	Arefin et al. 2014
				Pseudomonas entomophila	16 Hours	2.9	Gut	Chakrabarti et al. 2012
						4	Gut	Chakrabarti et al. 2012
				Serratia marcescens and Enterococcos faecalis	12 Hours	1.67768696	Adult	Sackton et al. 2010
15	*FBgn0004598*	Fur2	Up-Regulation	*Gamasodes queenslandicus*	-	-	Adult male	Benoit et al. 2020
16	*FBgn0004611*	Plc21C	Up-Regulation	clean injury	45 min	2.67	Plasmatocyte	Ramond et al. 2020
				Gamasodes queenslandicus	-	-	Adult male	Benoit et al. 2020
17	*FBgn0004635*	rho	Up-Regulation	*ECC15*	4 Hours	4.2	Gut	Buchon et al. 2009
								Chakrabarti et al. 2012
				Pseudomonas entomophila	-	0.7170176055	Adult	Ragheb et al. 2017
					16 Hours	3	Gut	Chakrabarti et al. 2012
					4 Hours	2.7	Gut	Chakrabarti et al. 2012
18	*FBgn0005391*	Yp2	-	*Wolbachia pipientis*		-	Ovary	Christensen et al. 2016
			Down-Regulation	*Micrococcus luteus*	-	-9.98421	Adult male	Wei et al. 2018
				Pseudomonas entomophila	-	-0.7669171883	Adult	Ragheb et al. 2017
						-0.3215202179	Adult	Ragheb et al. 2017

						-0.2691988079	Adult	Ragheb et al. 2017
			Up-Regulation	*E. coli and Micrococcus luteus*	3 Hours	2	Adult	Brun et al. 2006
19	*FBgn0010052*	Jhe	-	Lipopolysaccharide	-	-	Adult	Schlamp et al. 2021
			Down-Regulation	*Heterorhabditis bacteriophora*	-	-	Larva	Arefin et al. 2014
20	*FBgn0010053*	Jheh1	-	*Wolbachia pipientis*		-	Ovary	Christensen et al. 2016
			Down-Regulation	10 different bacteria	-	-0.8538539234	Adult	Troha et al. 2018
				A.fumigatus	24 Hours	-0.526	Adult	De Gregorio et al. 2002
				clean injury	45 min	-2.79	Plasmatocyte	Ramond et al. 2020
				E.coli, M.luteus	3 Hours	-1.175	Adult male	De Gregorio et al. 2001
				Providencia rettgeri,	-	-0.81	Adult	Short and Lazzaro 2013
				Pseudomonas entomophila	16 Hours	-2.6	Gut	Chakrabarti et al. 2012
21	*FBgn0010357*	betaTry	-	Lipopolysaccharide	-	-	Adult	Schlamp et al. 2021
			Down-Regulation	*E. coli and Micrococcus luteus*	3 Hours	0.4	Adult	Brun et al. 2006
				Pseudomonas entomophila	16 Hours	-11	Gut	Chakrabarti et al. 2012
					4 Hours	-1.032	Gut	Soory and Ratnaparkhi 2022
22	*FBgn0010358*	deltaTry	-	Lipopolysaccharide	-	-	Adult	Schlamp et al. 2021
			Down-Regulation	*A.fumigatus*	24 Hours	-0.471	Adult	De Gregorio et al. 2002
				E.coli, M.luteus	3 Hours	-1.219	Adult male	De Gregorio et al. 2001

				Pseudomonas entomophila	-	-0.2564361546	Adult	Ragheb et al. 2017
23	*FBgn0010359*	gammaTry	-	Lipopolysaccharide	-	-	Adult	Schlamp et al. 2021
			Down-Regulation	*Pseudomonas entomophila*	-	-0.2423209659	Adult	Ragheb et al. 2017
				S–Gh vs. S+Gh	24 Hours	-2.05253997	Adult	Higareda Alvear et al. 2021
24	*FBgn0010425*	epsilonTry	-	Lipopolysaccharide	-	-	Adult	Schlamp et al. 2021
			Down-Regulation	*Pseudomonas entomophila*	-	-0.5609685655	Adult	Ragheb et al. 2017
					16 Hours	-5.4	Gut	Chakrabarti et al. 2012
					4 Hours	-0.6139	Gut	Soory and Ratnaparkhi 2022
25	*FBgn0011554*	etaTry	Down-Regulation	*Pseudomonas entomophila*	16 Hours	-2.3	Gut	Chakrabarti et al. 2012
26	*FBgn0011555*	thetaTry	-	ECC15	8 Hours	-	Adult	Erkosar et al. 2014
			Down-Regulation	*A.fumigatus*	24 Hours	-0.146	Adult	De Gregorio et al. 2002
				E. coli and Micrococcus luteus	3 Hours	0.3	Adult	Brun et al. 2006
				E.coli, M.luteus	3 Hours	-1.721	Adult male	De Gregorio et al. 2001
				ECC15	4 Hours	-2.1	Gut	Buchon et al. 2009
								Chakrabarti et al. 2012
				Pseudomonas entomophila	-	-0.5102853378	Adult	Ragheb et al. 2017
					16 Hours	-3.8	Gut	Chakrabarti et al. 2012
					4 Hours	-0.9405	Gut	Soory and Ratnaparkhi 2022

27	*FBgn0011556*	zetaTry	-	ECC15	8 Hours	-	Adult	Erkosar et al. 2014
			Down-Regulation	*Pseudomonas entomophila*	16 Hours	-13.2	Gut	Chakrabarti et al. 2012
28	*FBgn0011834*	Ser6	Up-Regulation	*Pseudomonas entomophila*	4 Hours	0.6103	Gut	Soory and Ratnaparkhi 2022
29	*FBgn0014906*	Hydr2	Up-Regulation	clean injury	45 min	2.96	Plasmatocyte	Ramond et al. 2020
30	*FBgn0015001*	iotaTry	-	Lipopolysaccharide	-	-	Adult	Schlamp et al. 2021
			Down-Regulation	ECC15	4 Hours	-4.6	Gut	Buchon et al. 2009
								Chakrabarti et al. 2012
				Pseudomonas entomophila	16 Hours	-25.7	Gut	Chakrabarti et al. 2012
					4 Hours	-3.3	Gut	Chakrabarti et al. 2012
						-0.8588	Gut	Soory and Ratnaparkhi 2022
31	*FBgn0015316*	CG17192	Up-Regulation	*Providencia rettgeri,*	-	0.95	Adult	Short and Lazzaro 2013
		Try29F	-	Lipopolysaccharide	-	-	Adult	Schlamp et al. 2021
			Down-Regulation	10 different bacteria	-	-1.513733982	Adult	Troha et al. 2018
				DCV, Serratia, Beauveria, Octosporea	-	-	Adult	Roxstrom-Lindquist et al. 2004
				Pseudomonas entomophila	16 Hours	-4.8	Gut	Chakrabarti et al. 2012
					4 Hours	-0.932	Gut	Soory and Ratnaparkhi 2022
			Up-Regulation	*Providencia rettgeri,*	-	1.41	Adult	Short and Lazzaro 2013

32	*FBgn0015568*	alpha-Est1	Down-Regulation	clean injury	45 min	-3.87	Plasmatocyte	Ramond et al. 2020
				ECC15	4 Hours	-3.2	Gut	Buchon et al. 2009
								Chakrabarti et al. 2012
			Up-Regulation	C virus		-	S2 cell	Zhu et al. 2013
33	*FBgn0015569*	alpha-Est10	Up-Regulation	*Pseudomonas entomophila*	4 Hours	3.6	Gut	Chakrabarti et al. 2012
34	*FBgn0015570*	alpha-Est2	-	Lipopolysaccharide	-	-	Adult	Schlamp et al. 2021
			Down-Regulation	10 different bacteria	-	-1.084555357	Adult	Troha et al. 2018
				Pseudomonas entomophila	-	-0.8541567951	Adult	Ragheb et al. 2017
			Up-Regulation	*Pseudomonas entomophila*	16 Hours	3.8	Gut	Chakrabarti et al. 2012
35	*FBgn0015571*	alpha-Est3	Down-Regulation	*Pseudomonas entomophila*	4 Hours	-0.6994	Gut	Soory and Ratnaparkhi 2022
36	*FBgn0015572*	alpha-Est4	Down-Regulation	ECC15	4 Hours	-3.2	Gut	Buchon et al. 2009
								Chakrabarti et al. 2012
				Pseudomonas entomophila	16 Hours	-2.1	Gut	Chakrabarti et al. 2012
			Up-Regulation	*Pseudomonas entomophila*	-	0.6908253458	Adult	Ragheb et al. 2017
37	*FBgn0015575*	alpha-Est7	Down-Regulation	10 different bacteria	-	-0.7575296355	Adult	Troha et al. 2018
				ECC15	4 Hours	-3.7	Gut	Buchon et al. 2009
								Chakrabarti et al. 2012
				Pseudomonas entomophila	-	-0.7372168784	Adult	Ragheb et al. 2017

						-0.2896502427	Adult	Ragheb et al. 2017
						-0.2417493217	Adult	Ragheb et al. 2017
					4 Hours	-0.9017	Gut	Soory and Ratnaparkhi 2022
				S. aureus	45 min	-2.75	Plasmatocyte	Ramond et al. 2020
38	*FBgn0015576*	alpha-Est8	Down-Regulation	clean injury	45 min	-3.94	Plasmatocyte	Ramond et al. 2020
39	*FBgn0015577*	alpha-Est9	Down-Regulation	ecdysone	-	-8.915845808	Larval Hemocyte	Regan et al. 2013
			Up-Regulation	LPS and E. coli		3.52	mbn cell	Johansson et al. 2005
				Pseudomonas entomophila	4 Hours	0.6209	Gut	Soory and Ratnaparkhi 2022
						3	Gut	Chakrabarti et al. 2012
40	*FBgn0019928*	Ser8	-	Lipopolysaccharide	-	-	Adult	Schlamp et al. 2021
			Down-Regulation	*A.fumigatus*	24 Hours	-0.328	Adult	De Gregorio et al. 2002
				E. coli and Micrococcus luteus	3 Hours	0.3	Adult	Brun et al. 2006
				E.coli, M.luteus	3 Hours	-2.043	Adult male	De Gregorio et al. 2001
				ECC15	4 Hours	-19.2	Gut	Buchon et al. 2009
								Chakrabarti et al. 2012
				Pseudomonas entomophila	16 Hours	-51.5	Gut	Chakrabarti et al. 2012
					4 Hours	-18.7	Gut	Chakrabarti et al. 2012

41	*FBgn0019929*	Ser7	Down-Regulation	*DCV, Serratia, Beauveria, Octosporea*	-	-	Adult	Roxstrom-Lindquist et al. 2004
				Pseudomonas entomophila	-	-0.3804038373	Adult	Ragheb et al. 2017
			Up-Regulation	*A.fumigatus*	24 Hours	1.206	Adult	De Gregorio et al. 2002
				ECC15	-	6	larval Trachea	Gendrin et al. 2013
				Pseudomonas entomophila	-	0.1695348717	Adult	Ragheb et al. 2017
				Spiroplasma	Endosymbiont	4.544853994	hemolymph proteome	Masson et al. 2021
42	*FBgn0020248*	stet	Up-Regulation	*ecdysone*	-	1.97859591	Larval Hemocyte	Regan et al. 2013
43	*FBgn0020370*	TppII	-	*Wolbachia pipientis*		-	Ovary	Christensen et al. 2016
44	*FBgn0020545*	kraken	Up-Regulation	*LPS and E. coli*		2.33	mbn cell	Johansson et al. 2005
				Pseudomonas entomophila	4 Hours	2.1	Gut	Chakrabarti et al. 2012
45	*FBgn0020906*	Jon25Bi	-	*Lipopolysaccharide*	-	-	Adult	Schlamp et al. 2021
			Down-Regulation	*E.coli, M.luteus*	3 Hours	-0.792	Adult male	De Gregorio et al. 2001
				Pseudomonas entomophila	-	-0.6969293021	Adult	Ragheb et al. 2017
					16 Hours	-31.4	Gut	Chakrabarti et al. 2012
					4 Hours	-0.9785	Gut	Soory and Ratnaparkhi 2022
			Up-Regulation	*A.fumigatus*	24 Hours	0.04	Adult	De Gregorio et al. 2002
46	*FBgn0021979*	l(2)k09913	Up-Regulation	*ecdysone*	-	1.495181199	Larval Hemocyte	Regan et al. 2013
47	*FBgn0023179*	amon	Up-Regulation	*Gamasodes queenslandicus*	-	-	Adult male	Benoit et al. 2020

48	*FBgn0023197*	Jon74E	-	*Lipopolysaccharide*	-	-	Adult	Schlamp et al. 2021
				ECC15	8 Hours	-	Adult	Erkosar et al. 2014
			Down-Regulation	*DCV, Serratia, Beauveria, Octosporea*	-	-	Adult	Roxstrom-Lindquist et al. 2004
				E. coli and Micrococcus luteus	3 Hours	0.4	Adult	Brun et al. 2006
				Pseudomonas entomophila	-	-0.8134007522	Adult	Ragheb et al. 2017
					16 Hours	-18.6	Gut	Chakrabarti et al. 2012
					4 Hours	-1.0524	Gut	Soory and Ratnaparkhi 2022
49	*FBgn0023479*	teq	Down-Regulation	*Pseudomonas entomophila*	-	-0.403793091	Adult	Ragheb et al. 2017
			Up-Regulation	*CrPV*	-	-	Adult	Merkling et al. 2015a; Merkling et al. 2015b
				ECC15	6 Hours	2.02	Larval	Vodovar et al. 2005
				ecdysone	-	6.120103283	Larval Hemocyte	Regan et al. 2013
				Gamasodes queenslandicus	-	-	Adult male	Benoit et al. 2020
				LPS and E. coli		1.59	mbn cell	Johansson et al. 2005
50	*FBgn0026570*	CG5704	Up-Regulation	*Pseudomonas entomophila*	4 Hours	1.2735	Gut	Soory and Ratnaparkhi 2022
51	*FBgn0026593*	CG5707	Down-Regulation	*C virus*		-	S2 cell	Zhu et al. 2013
			Up-Regulation	*ECC15*	4 Hours	2	Gut	Buchon et al. 2009
								Chakrabarti et al. 2012

				ecdysone	-	1.536716463	Larval Hemocyte	Regan et al. 2013
				Pseudomonas entomophila	16 Hours	3.7	Gut	Chakrabarti et al. 2012
					4 Hours	1.3196	Gut	Soory and Ratnaparkhi 2022
						4.8	Gut	Chakrabarti et al. 2012
52	*FBgn0027563*	CG9631	Down-Regulation	*Pseudomonas entomophila*	-	-0.4400828801	Adult	Ragheb et al. 2017
			Up-Regulation	*A.fumigatus*	24 Hours	0.274	Adult	De Gregorio et al. 2002
				E. coli and Micrococcus luteus	3 Hours	2.4	Adult	Brun et al. 2006
				E.coli, M.luteus	3 Hours	1.716	Adult male	De Gregorio et al. 2001
				LPS and E. coli		1.3	mbn cell	Johansson et al. 2005
53	*FBgn0027584*	CG4757	-	*Lipopolysaccharide*	-	-	Adult	Schlamp et al. 2021
			Down-Regulation	*CrPV*	-	-	Adult	Merkling et al. 2015a; Merkling et al. 2015b
				Pseudomonas entomophila	-	-3.183616099	Adult	Ragheb et al. 2017
			Up-Regulation	*10 different bacteria*	-	4.498161491	Adult	Troha et al. 2018
				A.fumigatus	24 Hours	2.448	Adult	De Gregorio et al. 2002
				E.coli, M.luteus	3 Hours	0.267	Adult male	De Gregorio et al. 2001
				ECC15	-	7.9	larval Trachea	Gendrin et al. 2013
				Gamasodes queenslandicus	-	-	Adult male	Benoit et al. 2020
				Heterorhabditis bacteriophora	-	-	Larva	Arefin et al. 2014
				Pseudomonas entomophila	-	1.13769197	Adult	Ragheb et al. 2017

				Serratia marcescens and Enterococcos faecalis	12 Hours	21.68867194	Adult	Sackton et al. 2010
				Spiroplasma	Endosymbiont	5.043868753	hemolymph proteome	Masson et al. 2021
54	*FBgn0027930*	MP1	Down-Regulation	*Pseudomonas entomophila*	4 Hours	-1.4835	Gut	Soory and Ratnaparkhi 2022
			Up-Regulation	*A.fumigatus*	24 Hours	0.638	Adult	De Gregorio et al. 2002
				B. bassiana	-	-	Hemolymph	Levy et al. 2004b
				E. coli and Micrococcus luteus	3 Hours	2.7	Adult	Brun et al. 2006
				ecdysone	-	1.78643778	Larval Hemocyte	Regan et al. 2013
				fungus	-	14	Larval fat body	Seto and Tamura 2013
				Micrococcus luteus	-	1.55077	Adult male	Wei et al. 2018
				Pseudomonas entomophila	16 Hours	2.2	Gut	Chakrabarti et al. 2012
				Spiroplasma	Endosymbiont	2.816824473	hemolymph proteome	Masson et al. 2021
55	*FBgn0029690*	CG6414	Down-Regulation	*S–W– vs S+W–*	24 Hours	-1.316422774	Adult	Higareda Alvear et al. 2021
				S–W– vs. S–Lh	24 Hours	-1.115443433	Adult	Higareda Alvear et al. 2021
			Up-Regulation	*ecdysone*	-	4.77522485	Larval Hemocyte	Regan et al. 2013
56	*FBgn0029789*	PGAP1	Up-Regulation	*ecdysone*	-	1.605636146	Larval Hemocyte	Regan et al. 2013
57	*FBgn0029826*	CG6041	Down-Regulation	*Heterorhabditis bacteriophora*	-	-	Larva	Arefin et al. 2014
			Up-Regulation	*Pseudomonas entomophila*	4 Hours	2	Gut	Chakrabarti et al. 2012
58	*FBgn0029827*	CG6048	-	*Lipopolysaccharide*	-	-	Adult	Schlamp et al. 2021
			Down-Regulation	*Pseudomonas entomophila*	-	-0.5964769895	Adult	Ragheb et al. 2017

					16 Hours	-2.4	Gut	Chakrabarti et al. 2012
			Up-Regulation	*ECC15*	4 Hours	2.7	Gut	Buchon et al. 2009
								Chakrabarti et al. 2012
				Pseudomonas entomophila	4 Hours	0.506	Gut	Soory and Ratnaparkhi 2022
59	*FBgn0029831*	CG5966	Down-Regulation	*ECC15*	4 Hours	-2.1	Gut	Buchon et al. 2009
								Chakrabarti et al. 2012
				Pseudomonas entomophila	16 Hours	-3	Gut	Chakrabarti et al. 2012
					4 Hours	-2.6	Gut	Chakrabarti et al. 2012
			Up-Regulation	*ecdysone*	-	2.736339049	Larval Hemocyte	Regan et al. 2013
				Pseudomonas entomophila	-	0.4550841345	Adult	Ragheb et al. 2017
				S–Lh vs. S+Lh	24 Hours	1.639537094	Adult	Higareda Alvear et al. 2021
60	*FBgn0030051*	spirit	-	*Lipopolysaccharide*	-	-	Adult	Schlamp et al. 2021
			Down-Regulation	*A.fumigatus*	24 Hours	-0.313	Adult	De Gregorio et al. 2002
				Pseudomonas entomophila	-	-1.087843255	Adult	Ragheb et al. 2017
			Up-Regulation	*fungus*	-	22	Larval fat body	Seto and Tamura 2013
				Micrococcus luteus	-	2.20244	Adult male	Wei et al. 2018
				Photor/nematode	-	-	Adult	Castillo et al. 2015
				S–Lh vs. S+Lh	24 Hours	1.342811163	Adult	Higareda Alvear et al. 2021

61	*FBgn0030057*	Ppt1	Down-Regulation	*Pseudomonas entomophila*	16 Hours	-2.1	Gut	Chakrabarti et al. 2012
			Up-Regulation	*ecdysone*	-	1.645798067	Larval Hemocyte	Regan et al. 2013
62	*FBgn0030162*	CG1986	Down-Regulation	*S–W– vs S+W–*	24 Hours	-2.495843607	Adult	Higareda Alvear et al. 2021
63	*FBgn0030318*	rho-4	Up-Regulation	*A.fumigatus*	24 Hours	0.761	Adult	De Gregorio et al. 2002
				ECC15	4 Hours	2.2	Gut	Buchon et al. 2009
								Chakrabarti et al. 2012
						2.4	Gut	Buchon et al. 2009
				ecdysone	-	2.523480025	Larval Hemocyte	Regan et al. 2013
				Pseudomonas entomophila	16 Hours	2.4	Gut	Chakrabarti et al. 2012
						2.7	Gut	Chakrabarti et al. 2012
					4 Hours	2.3	Gut	Chakrabarti et al. 2012
						2.6	Gut	Chakrabarti et al. 2012
64	*FBgn0030362*	regucalcin	Down-Regulation	*10 different bacteria*	-	-0.8230218543	Adult	Troha et al. 2018
				clean injury	45 min	-2.43	Plasmatocyte	Ramond et al. 2020
				Pseudomonas entomophila	16 Hours	-3.5	Gut	Chakrabarti et al. 2012
						-2.7	Gut	Chakrabarti et al. 2012
			Up-Regulation	*LPS and E. coli*		1.82	mbn cell	Johansson et al. 2005
				protein expression upon LPS infection	-	3.38 ± 0.57	larval hemolymph	Vierstraete et al. 2004

				protein expression upon M. luteus infection	-	7.11 ± 1.33	larval hemolymph	Vierstraete et al. 2004
				protein expression upon S. cereviseae infection	-	3.60 ± 0.95	larval hemolymph	Vierstraete et al. 2004
65	*FBgn0030607*	dob	-	*Lipopolysaccharide*	-	-	Adult	Schlamp et al. 2021
			Down-Regulation	*10 different bacteria*	-	-0.8465818296	Adult	Troha et al. 2018
			Up-Regulation	*S–Lh vs. S+Lh*	24 Hours	1.158902413	Adult	Higareda Alvear et al. 2021
66	*FBgn0030688*	CG8952	-	*Lipopolysaccharide*	-	-	Adult	Schlamp et al. 2021
			Down-Regulation	*DCV, Serratia, Beauveria, Octosporea*	-	-	Adult	Roxstrom-Lindquist et al. 2004
				Pseudomonas entomophila	-	-0.3944095665	Adult	Ragheb et al. 2017
						-0.3155161702	Adult	Ragheb et al. 2017
67	*FBgn0030773*	CG9676	Up-Regulation	*CrPV*	-	-	Adult	Merkling et al. 2015a; Merkling et al. 2015b
				Pseudomonas entomophila	-	0.1642385832	Adult	Ragheb et al. 2017
					16 Hours	2.3	Gut	Chakrabarti et al. 2012
68	*FBgn0030828*	CG5162	-	*Wolbachia pipientis*		-	Ovary	Christensen et al. 2016
			Down-Regulation	*Pseudomonas entomophila*	-	-0.2817502522	Adult	Ragheb et al. 2017
			Up-Regulation	*10 different bacteria*	-	0.719113427	Adult	Troha et al. 2018
				Aspergillus flavus	-	-	Adult	Ramirez-Camejo and Bayman 2020
				S–W– vs S+W–	24 Hours	1.267598075	Adult	Higareda Alvear et al. 2021

				Spiroplasma	Endosymbiont	2.034302863	hemolymph proteome	Masson et al. 2021
69	*FBgn0030925*	Hayan	-	*Lipopolysaccharide*	-	-	Adult	Schlamp et al. 2021
			Down-Regulation	*Pseudomonas entomophila*	-	-0.5860550136	Adult	Ragheb et al. 2017
			Up-Regulation	*A.fumigatus*	24 Hours	0.245	Adult	De Gregorio et al. 2002
				CrPV	-	-	Adult	Merkling et al. 2015a; Merkling et al. 2015b
				E. coli and Micrococcus luteus	3 Hours	2.2	Adult	Brun et al. 2006
				E.coli, M.luteus	3 Hours	1.289	Adult male	De Gregorio et al. 2001
				fungus	-	15	Larval fat body	Seto and Tamura 2013
				Gamasodes queenslandicus	-	-	Adult male	Benoit et al. 2020
				Micrococcus luteus	-	1.90455	Adult male	Wei et al. 2018
				Photor/nematode	-	-	Adult	Castillo et al. 2015
70	*FBgn0030926*	psh	Down-Regulation	*Pseudomonas entomophila*	-	-0.6068502573	Adult	Ragheb et al. 2017
			Up-Regulation	*fungus*	-	3	Larval fat body	Seto and Tamura 2013
71	*FBgn0031141*	CG1304	Down-Regulation	*Pseudomonas entomophila*	16 Hours	-4.5	Gut	Chakrabarti et al. 2012
72	*FBgn0031248*	CG11912	-	*Lipopolysaccharide*	-	-	Adult	Schlamp et al. 2021
			Down-Regulation	*ECC15*	4 Hours	-2.1	Gut	Buchon et al. 2009
								Chakrabarti et al. 2012
				Pe 6 12 Hours	12 Hours	0.18	Larval	Vodovar et al. 2005
				Pseudomonas entomophila	-	-0.7892434336	Adult	Ragheb et al. 2017

						-0.3757850377	Adult	Ragheb et al. 2017
					16 Hours	-94.3	Gut	Chakrabarti et al. 2012
					4 Hours	-2	Gut	Chakrabarti et al. 2012
						-0.8612	Gut	Soory and Ratnaparkhi 2022
			Up-Regulation	*CrPV*	-	-	Adult	Merkling et al. 2015a; Merkling et al. 2015b
				E. coli	45 min	7.31	Plasmatocyte	Ramond et al. 2020
				Photor/nematode	-	-	Adult	Castillo et al. 2015
				S–Lh vs. S+Lh	24 Hours	1.860368299	Adult	Higareda Alvear et al. 2021
				Serratia marcescens and Enterococcos faecalis	12 Hours	1.746700253	Adult	Sackton et al. 2010
73	*FBgn0031249*	CG11911	-	*ECC15*	8 Hours	-	Adult	Erkosar et al. 2014
			Down-Regulation	*E. coli and Micrococcus luteus*	3 Hours	0.4	Adult	Brun et al. 2006
				ECC15	6 Hours	0.62	Larval	Vodovar et al. 2005
				Pseudomonas entomophila	-	-0.8424668455	Adult	Ragheb et al. 2017
					16 Hours	-4.1	Gut	Chakrabarti et al. 2012
			Up-Regulation	*CrPV*	-	-	Adult	Merkling et al. 2015a; Merkling et al. 2015b
				D. pneumoniae, N. catarrhalis, S. aureus, K. pneumoniae, H. influenza, S. pyogenes	6 Hours	45 ± 3.2%m	Adult	de Morais Guedes et al. 2005
				Serratia marcescens and Enterococcos faecalis	12 Hours	1.867971183	Adult	Sackton et al. 2010

74	*FBgn0031426*	CG18641	Down-Regulation	*S–W– vs S+W–*	24 Hours	-1.454522147	Adult	Higareda Alvear et al. 2021
75	*FBgn0031619*	CG3355	Down-Regulation	*S–W– vs S+W–*	24 Hours	-1.963707598	Adult	Higareda Alvear et al. 2021
			Up-Regulation	*Providencia rettgeri,*	-	1.11	Adult	Short and Lazzaro 2013
76	*FBgn0031653*	Jon25Biii	-	*Lipopolysaccharide*	-	-	Adult	Schlamp et al. 2021
				ECC15	8 Hours	-	Adult	Erkosar et al. 2014
			Down-Regulation	*A.fumigatus*	24 Hours	-0.192	Adult	De Gregorio et al. 2002
				E. coli and Micrococcus luteus	3 Hours	0.3	Adult	Brun et al. 2006
				E.coli, M.luteus	3 Hours	-0.845	Adult male	De Gregorio et al. 2001
				ECC15	6 Hours	0.71	Larval	Vodovar et al. 2005
				Gamasodes queenslandicus	-	-	Adult male	Benoit et al. 2020
				Pseudomonas entomophila	-	-0.5386275615	Adult	Ragheb et al. 2017
					16 Hours	-47.1	Gut	Chakrabarti et al. 2012
				S. aureus	45 min	-4.55	Plasmatocyte	Ramond et al. 2020
			Up-Regulation	*DCV, Serratia, Beauveria, Octosporea*	-	-	Adult	Roxstrom-Lindquist et al. 2004
77	*FBgn0031654*	Jon25Bii	-	*Lipopolysaccharide*	-	-	Adult	Schlamp et al. 2021
				ECC15	8 Hours	-	Adult	Erkosar et al. 2014
			Down-Regulation	*A.fumigatus*	24 Hours	-0.402	Adult	De Gregorio et al. 2002
				DCV, Serratia, Beauveria, Octosporea	-	-	Adult	Roxstrom-Lindquist et al. 2004
				E. coli and Micrococcus luteus	3 Hours	0.2	Adult	Brun et al. 2006

				E.coli, M.luteus	3 Hours	-1.635	Adult male	De Gregorio et al. 2001
				Heterorhabditis bacteriophora	-	-	Larva	Arefin et al. 2014
				Pseudomonas entomophila	-	-1.158110108	Adult	Ragheb et al. 2017
					16 Hours	-47.7	Gut	Chakrabarti et al. 2012
					4 Hours	-3.3	Gut	Chakrabarti et al. 2012
						-1.7387	Gut	Soory and Ratnaparkhi 2022
78	*FBgn0031735*	CG11029	Up-Regulation	*S–W– vs S+W–*	24 Hours	1.095925984	Adult	Higareda Alvear et al. 2021
				S–W– vs. S–Gh	24 Hours	1.003463118	Adult	Higareda Alvear et al. 2021
				S–W– vs. S–Lh	24 Hours	1.452544866	Adult	Higareda Alvear et al. 2021
79	*FBgn0031741*	CG11034	Down-Regulation	*Pseudomonas entomophila*	16 Hours	-2.5	Gut	Chakrabarti et al. 2012
80	*FBgn0031835*	CG11319	Down-Regulation	*C virus*		-	S2 cell	Zhu et al. 2013
			Up-Regulation	*Gamasodes queenslandicus*	-	-	Adult male	Benoit et al. 2020
81	*FBgn0031990*	PAPLA1	Down-Regulation	*Pseudomonas entomophila*	4 Hours	-0.7581	Gut	Soory and Ratnaparkhi 2022
			Up-Regulation	*clean injury*	45 min	2.89	Plasmatocyte	Ramond et al. 2020
				Gamasodes queenslandicus	-	-	Adult male	Benoit et al. 2020
82	*FBgn0032029*	CG17292	Down-Regulation	*A.fumigatus*	24 Hours	-0.489	Adult	De Gregorio et al. 2002
				E.coli, M.luteus	3 Hours	-1.272	Adult male	De Gregorio et al. 2001
				ECC15	4 Hours	-3.1	Gut	Buchon et al. 2009
								Chakrabarti et al. 2012

				ecdysone	-	-2.32819409	Larval Hemocyte	Regan et al. 2013
83	*FBgn0032131*	CG3841	-	*ECC15*	8 Hours	-	Adult	Erkosar et al. 2014
84	*FBgn0032242*	CG5355	-	*Wolbachia pipientis*		-	Ovary	Christensen et al. 2016
85	*FBgn0032264*	Lip4	-	*Lipopolysaccharide*	-	-	Adult	Schlamp et al. 2021
				Micrococcus luteus	-	0	Adult male	Wei et al. 2018
			Down-Regulation	*C virus*		-	S2 cell	Zhu et al. 2013
				E. coli and Micrococcus luteus	3 Hours	0.4	Adult	Brun et al. 2006
				Pseudomonas entomophila	-	-0.3794982679	Adult	Ragheb et al. 2017
			Up-Regulation	*LPS and E. coli*		1.43	mbn cell	Johansson et al. 2005
				Pseudomonas entomophila	-	0.8009195858	Adult	Ragheb et al. 2017
86	*FBgn0032265*	CG18301	-	*Micrococcus luteus*	-	0	Adult male	Wei et al. 2018
			Down-Regulation	*A.fumigatus*	24 Hours	-0.193	Adult	De Gregorio et al. 2002
				DCV, Serratia, Beauveria, Octosporea	-	-	Adult	Roxstrom-Lindquist et al. 2004
				E.coli, M.luteus	3 Hours	-0.414	Adult male	De Gregorio et al. 2001
87	*FBgn0032358*	Ppt2	-	*Lipopolysaccharide*	-	-	Adult	Schlamp et al. 2021
			Down-Regulation	*Pseudomonas entomophila*	4 Hours	-1.3101	Gut	Soory and Ratnaparkhi 2022
88	*FBgn0032612*	CG13282	Down-Regulation	*S–W– vs S+W–*	24 Hours	-1.356550985	Adult	Higareda Alvear et al. 2021
89	*FBgn0032699*	CG10383	Down-Regulation	*A.fumigatus*	24 Hours	-0.059	Adult	De Gregorio et al. 2002
			Up-Regulation	*E.coli, M.luteus*	3 Hours	1.177	Adult male	De Gregorio et al. 2001

				ECC15	-	2	larval Trachea	Gendrin et al. 2013
				ecdysone	-	3.223198412	Larval Hemocyte	Regan et al. 2013
				Gamasodes queenslandicus	-	-	Adult male	Benoit et al. 2020
				Heterorhabditis bacteriophora	-	-	Larva	Arefin et al. 2014
				Pseudomonas entomophila	-	0.6843151237	Adult	Ragheb et al. 2017
					16 Hours	2.5	Gut	Chakrabarti et al. 2012
					4 Hours	3.3	Gut	Chakrabarti et al. 2012
90	*FBgn0032864*	CG2493	-	*Lipopolysaccharide*	-	-	Adult	Schlamp et al. 2021
91	*FBgn0032973*	CG6675	Up-Regulation	*A.fumigatus*	24 Hours	1.478	Adult	De Gregorio et al. 2002
				DCV, Serratia, Beauveria, Octosporea	-	-	Adult	Roxstrom-Lindquist et al. 2004
				E.coli, M.luteus	3 Hours	2.512	Adult male	De Gregorio et al. 2001
				Micrococcus luteus	-	3.73777	Adult male	Wei et al. 2018
				Pseudomonas entomophila	-	2.032858175	Adult	Ragheb et al. 2017
92	*FBgn0033192*	Corin	Down-Regulation	*ecdysone*	-	-4.175910138	Larval Hemocyte	Regan et al. 2013
93	*FBgn0033226*	puml	Up-Regulation	*clean injury*	45 min	2.05	Plasmatocyte	Ramond et al. 2020
				Pseudomonas entomophila	4 Hours	0.4713	Gut	Soory and Ratnaparkhi 2022
94	*FBgn0033362*	CG8172	Down-Regulation	*S–W– vs S+W–*	24 Hours	-1.416970928	Adult	Higareda Alvear et al. 2021
				S–W– vs. S–Lh	24 Hours	-1.160917263	Adult	Higareda Alvear et al. 2021
95	*FBgn0033363*	CG13744	Up-Regulation	*S–W– vs. S–Gh*	24 Hours	1.340385115	Adult	Higareda Alvear et al. 2021

96	*FBgn0033365*	CG8170	-	*Lipopolysaccharide*	-	-	Adult	Schlamp et al. 2021
			Down-Regulation	*S–W– vs S+W–*	24 Hours	-1.86847904	Adult	Higareda Alvear et al. 2021
				S–W– vs. S–Lh	24 Hours	-1.359189057	Adult	Higareda Alvear et al. 2021
97	*FBgn0033382*	Hydr1	Down-Regulation	*ecdysone*	-	-4.746775	Larval Hemocyte	Regan et al. 2013
				Pseudomonas entomophila	4 Hours	-0.626	Gut	Soory and Ratnaparkhi 2022
98	*FBgn0033439*	CG1773	-	*Lipopolysaccharide*	-	-	Adult	Schlamp et al. 2021
			Up-Regulation	*CrPV*	-	-	Adult	Merkling et al. 2015a; Merkling et al. 2015b
				DCV	-	-	Adult	Merkling et al. 2015a; Merkling et al. 2015b
99	*FBgn0033897*	Rcd1	Up-Regulation	*Pseudomonas entomophila*	4 Hours	0.8494	Gut	Soory and Ratnaparkhi 2022
100	*FBgn0034052*	CG8299	Down-Regulation	*Heterorhabditis bacteriophora*	-	-	Larva	Arefin et al. 2014
				Pseudomonas entomophila	16 Hours	-3	Gut	Chakrabarti et al. 2012
101	*FBgn0034139*	CG4927	-	*Lipopolysaccharide*	-	-	Adult	Schlamp et al. 2021
			Down-Regulation	*ecdysone*	-	-4.066395859	Larval Hemocyte	Regan et al. 2013
102	*FBgn0034166*	CG6472	-	*Lipopolysaccharide*	-	-	Adult	Schlamp et al. 2021
103	*FBgn0034221*	CG10764	Down-Regulation	*C virus*		-	S2 cell	Zhu et al. 2013
				ecdysone	-	-2.787327777	Larval Hemocyte	Regan et al. 2013
				S–W– vs. S–Lh	24 Hours	-1.212977304	Adult	Higareda Alvear et al. 2021

			Up-Regulation	*S–Lh vs. S+Lh*	24 Hours	2.223816706	Adult	Higareda Alvear et al. 2021
				S–W– vs. S–Gh	24 Hours	2.736408075	Adult	Higareda Alvear et al. 2021
104	*FBgn0034405*	Jheh2	-	*Wolbachia pipientis*		-	Ovary	Christensen et al. 2016
			Down-Regulation	*ECC15*	4 Hours	-2.4	Gut	Buchon et al. 2009
								Chakrabarti et al. 2012
				ecdysone	-	-2.327331414	Larval Hemocyte	Regan et al. 2013
				Pseudomonas entomophila	16 Hours	-2.1	Gut	Chakrabarti et al. 2012
					4 Hours	-2.8	Gut	Chakrabarti et al. 2012
105	*FBgn0034406*	Jheh3	Down-Regulation	*C virus*		-	S2 cell	Zhu et al. 2013
				Pseudomonas entomophila	-	-0.4208671479	Adult	Ragheb et al. 2017
					16 Hours	-3.2	Gut	Chakrabarti et al. 2012
					4 Hours	-2.4	Gut	Chakrabarti et al. 2012
106	*FBgn0034419*	CG15111	Up-Regulation	*Pseudomonas entomophila*	4 Hours	2.2	Gut	Chakrabarti et al. 2012
107	*FBgn0034491*	Hsl	Up-Regulation	*clean injury*	45 min	2.22	Plasmatocyte	Ramond et al. 2020
108	*FBgn0034507*	CG11192	Up-Regulation	*S–W– vs. S–Lh*	24 Hours	1.569820206	Adult	Higareda Alvear et al. 2021
109	*FBgn0034535*	CG11110	Down-Regulation	*clean injury*	45 min	-2.08	Plasmatocyte	Ramond et al. 2020
110	*FBgn0034661*	tpr	Down-Regulation	*S–W– vs S+W–*	24 Hours	-2.253710634	Adult	Higareda Alvear et al. 2021
			Up-Regulation	*E. coli and Micrococcus luteus*	3 Hours	2.7	Adult	Brun et al. 2006
111	*FBgn0034666*	CG9294	Down-Regulation	*E. coli and Micrococcus luteus*	3 Hours	0.4	Adult	Brun et al. 2006

112	*FBgn0034736*	gas	-	*Lipopolysaccharide*	-	-	Adult	Schlamp et al. 2021
			Down-Regulation	*clean injury*	45 min	-2.25	Plasmatocyte	Ramond et al. 2020
				ecdysone	-	-3.059252811	Larval Hemocyte	Regan et al. 2013
			Up-Regulation	*Pseudomonas entomophila*	4 Hours	1.0578	Gut	Soory and Ratnaparkhi 2022
113	*FBgn0034796*	CG3700	Up-Regulation	*10 different bacteria*	-	0.643025177	Adult	Troha et al. 2018
				LPS and E. coli		1.44	mbn cell	Johansson et al. 2005
				Spiroplasma	Endosymbiont	3.445258204	hemolymph proteome	Masson et al. 2021
114	*FBgn0034928*	CG13562	Down-Regulation	*S–W– vs S+W–*	24 Hours	-1.335205081	Adult	Higareda Alvear et al. 2021
115	*FBgn0035065*	CG3589	-	*Lipopolysaccharide*	-	-	Adult	Schlamp et al. 2021
116	*FBgn0035070*	CG3650	Up-Regulation	*S–Gh vs. S+Gh*	24 Hours	1.096211089	Adult	Higareda Alvear et al. 2021
				S–W– vs. S–Lh	24 Hours	1.860123845	Adult	Higareda Alvear et al. 2021
117	*FBgn0035154*	hiro	Down-Regulation	*Heterorhabditis bacteriophora*	-	-	Larva	Arefin et al. 2014
				Pe 6 12 Hours	12 Hours	0.39	Larval	Vodovar et al. 2005
				Pseudomonas entomophila	-	-0.5195321359	Adult	Ragheb et al. 2017
				S. aureus	45 min	-6.60	Plasmatocyte	Ramond et al. 2020
118	*FBgn0035206*	sturkopf	-	*Wolbachia pipientis*		-	Ovary	Christensen et al. 2016
			Down-Regulation	*Pseudomonas entomophila*	-	-0.8993835796	Adult	Ragheb et al. 2017
			Up-Regulation	*A.fumigatus*	24 Hours	0.223	Adult	De Gregorio et al. 2002
				E. coli and Micrococcus luteus	3 Hours	2	Adult	Brun et al. 2006

				LPS and E. coli		1.33	mbn cell	Johansson et al. 2005
119	*FBgn0035309*	CG15879	Down-Regulation	*S. aureus*	45 min	-2.12	Plasmatocyte	Ramond et al. 2020
120	*FBgn0035312*	CG15820	Down-Regulation	*C virus*		-	S2 cell	Zhu et al. 2013
121	*FBgn0035501*	CG1299	Up-Regulation	*E. coli and Micrococcus luteus*	3 Hours	2.1	Adult	Brun et al. 2006
122	*FBgn0035519*	CG1309	Up-Regulation	*LPS and E. coli*		1.47	mbn cell	Johansson et al. 2005
123	*FBgn0035661*	CG10477	-	*ECC15*	8 Hours	-	Adult	Erkosar et al. 2014
			Down-Regulation	*Aspergillus flavus*	-	-	Adult	Ramirez-Camejo and Bayman 2020
				Pseudomonas entomophila	-	-0.1412526608	Adult	Ragheb et al. 2017
					16 Hours	-15.9	Gut	Chakrabarti et al. 2012
					4 Hours	-0.962	Gut	Soory and Ratnaparkhi 2022
			Up-Regulation	*DCV, Serratia, Beauveria, Octosporea*	-	-	Adult	Roxstrom-Lindquist et al. 2004
				Pseudomonas entomophila	-	0.4198934873	Adult	Ragheb et al. 2017
124	*FBgn0035665*	Jon65Aiii	Down-Regulation	*DCV, Serratia, Beauveria, Octosporea*	-	-	Adult	Roxstrom-Lindquist et al. 2004
				Pseudomonas entomophila	-	-0.7052375012	Adult	Ragheb et al. 2017
						-0.3686632576	Adult	Ragheb et al. 2017
					16 Hours	-2.7	Gut	Chakrabarti et al. 2012

					4 Hours	-0.8708	Gut	Soory and Ratnaparkhi 2022
			Up-Regulation	*10 different bacteria*	-	0.8242677313	Adult	Troha et al. 2018
				ecdysone	-	3.400947338	Larval Hemocyte	Regan et al. 2013
125	*FBgn0035666*	Jon65Aii	-	*Lipopolysaccharide*	-	-	Adult	Schlamp et al. 2021
				ECC15	8 Hours	-	Adult	Erkosar et al. 2014
				Photor/nematode	-	-	Adult	Castillo et al. 2015
			Down-Regulation	*ECC15*	6 Hours	0.37	Larval	Vodovar et al. 2005
				Gamasodes queenslandicus	-	-	Adult male	Benoit et al. 2020
				Pseudomonas entomophila	-	-1.559910233	Adult	Ragheb et al. 2017
						-0.03516068846	Adult	Ragheb et al. 2017
					16 Hours	-5.5	Gut	Chakrabarti et al. 2012
					4 Hours	-0.4836	Gut	Soory and Ratnaparkhi 2022
126	*FBgn0035667*	Jon65Ai	-	*ECC15*	8 Hours	-	Adult	Erkosar et al. 2014
			Down-Regulation	*A.fumigatus*	24 Hours	-1.135	Adult	De Gregorio et al. 2002
				E. coli and Micrococcus luteus	3 Hours	0.3	Adult	Brun et al. 2006
				E.coli, M.luteus	3 Hours	-1.752	Adult male	De Gregorio et al. 2001
				ECC15	6 Hours	0.48	Larval	Vodovar et al. 2005
				Heterorhabditis bacteriophora	-	-	Larva	Arefin et al. 2014
				Pseudomonas entomophila	-	-1.139583386	Adult	Ragheb et al. 2017

					16 Hours	-4.1	Gut	Chakrabarti et al. 2012
				S. aureus	45 min	-4.44	Plasmatocyte	Ramond et al. 2020
127	*FBgn0035670*	CG10472	Down-Regulation	*E. coli and Micrococcus luteus*	3 Hours	0.4	Adult	Brun et al. 2006
				Pseudomonas entomophila	-	-0.6451717755	Adult	Ragheb et al. 2017
						-0.2492223836	Adult	Ragheb et al. 2017
					4 Hours	-0.4124	Gut	Soory and Ratnaparkhi 2022
				S. aureus	45 min	-4.94	Plasmatocyte	Ramond et al. 2020
			Up-Regulation	*10 different bacteria*	-	1.993020018	Adult	Troha et al. 2018
128	*FBgn0035678*	CG10469	-	*Lipopolysaccharide*	-	-	Adult	Schlamp et al. 2021
			Down-Regulation	*C virus*		-	S2 cell	Zhu et al. 2013
129	*FBgn0035697*	CG10163	Down-Regulation	*Pseudomonas entomophila*	-	-0.05597883305	Adult	Ragheb et al. 2017
			Up-Regulation	*Pseudomonas entomophila*	4 Hours	3.4	Gut	Chakrabarti et al. 2012
130	*FBgn0035726*	CG9953	-	*Lipopolysaccharide*	-	-	Adult	Schlamp et al. 2021
				Wolbachia pipientis		-	Ovary	Christensen et al. 2016
			Down-Regulation	*ECC15*	4 Hours	-2	Gut	Buchon et al. 2009
								Chakrabarti et al. 2012
				Pseudomonas entomophila	16 Hours	-2.5	Gut	Chakrabarti et al. 2012
131	*FBgn0035734*	CG14823	-	*Lipopolysaccharide*	-	-	Adult	Schlamp et al. 2021

			Down-Regulation	*E.coli, M.luteus*	3 Hours	-1.462	Adult male	De Gregorio et al. 2001
				Pseudomonas entomophila	-	-0.2115800333	Adult	Ragheb et al. 2017
			Up-Regulation	*A.fumigatus*	24 Hours	0.085	Adult	De Gregorio et al. 2002
132	*FBgn0035886*	Jon66Ci	-	*Lipopolysaccharide*	-	-	Adult	Schlamp et al. 2021
				ECC15	8 Hours	-	Adult	Erkosar et al. 2014
			Down-Regulation	*ECC15*	6 Hours	0.49	Larval	Vodovar et al. 2005
				Pseudomonas entomophila	-	-1.775723585	Adult	Ragheb et al. 2017
						-0.8735445509	Adult	Ragheb et al. 2017
					16 Hours	-3.6	Gut	Chakrabarti et al. 2012
					4 Hours	-0.6546	Gut	Soory and Ratnaparkhi 2022
				S. aureus	45 min	-9.84	Plasmatocyte	Ramond et al. 2020
			Up-Regulation	*clean injury*	45 min	8.20	Plasmatocyte	Ramond et al. 2020
				CrPV	-	-	Adult	Merkling et al. 2015a; Merkling et al. 2015b
				ECC15	4 Hours	2.4	Gut	Buchon et al. 2009
								Chakrabarti et al. 2012
133	*FBgn0035887*	Jon66Cii	-	*ECC15*	8 Hours	-	Adult	Erkosar et al. 2014
			Down-Regulation	*Pe 6 12 Hours*	12 Hours	0.45	Larval	Vodovar et al. 2005
				Pseudomonas entomophila	-	-1.492620595	Adult	Ragheb et al. 2017

					16 Hours	-3.2	Gut	Chakrabarti et al. 2012
			Up-Regulation	*CrPV*	-	-	Adult	Merkling et al. 2015a; Merkling et al. 2015b
				ECC15	4 Hours	3.9	Gut	Buchon et al. 2009
								Chakrabarti et al. 2012
134	*FBgn0036022*	CG8329	Up-Regulation	*CrPV*	-	-	Adult	Merkling et al. 2015a; Merkling et al. 2015b
				Serratia marcescens and Enterococcos faecalis	12 Hours	1.807938524	Adult	Sackton et al. 2010
135	*FBgn0036023*	CG18179	-	*ECC15*	8 Hours	-	Adult	Erkosar et al. 2014
			Down-Regulation	*A.fumigatus*	24 Hours	-0.964	Adult	De Gregorio et al. 2002
				E.coli, M.luteus	3 Hours	-1.442	Adult male	De Gregorio et al. 2001
				Pseudomonas entomophila	-	-1.031162999	Adult	Ragheb et al. 2017
					16 Hours	-16.1	Gut	Chakrabarti et al. 2012
			Up-Regulation	*ECC15*	4 Hours	4.7	Gut	Buchon et al. 2009
								Chakrabarti et al. 2012
136	*FBgn0036024*	CG18180	-	*ECC15*	8 Hours	-	Adult	Erkosar et al. 2014
			Down-Regulation	*E.coli, M.luteus*	3 Hours	-0.97	Adult male	De Gregorio et al. 2001
				Pseudomonas entomophila	-	-0.6402974551	Adult	Ragheb et al. 2017
				S. aureus	45 min	-5.46	Plasmatocyte	Ramond et al. 2020
			Up-Regulation	*A.fumigatus*	24 Hours	-0.13	Adult	De Gregorio et al. 2002

137	*FBgn0036053*	iPLA2-VIA	Up-Regulation	*clean injury*	45 min	2.47	Plasmatocyte	Ramond et al. 2020
				Gamasodes queenslandicus	-	-	Adult male	Benoit et al. 2020
138	*FBgn0036264*	CG11529	Down-Regulation	*S–Gh vs. S+Gh*	24 Hours	-1.00900985	Adult	Higareda Alvear et al. 2021
			Up-Regulation	*S–W– vs S+W–*	24 Hours	1.14250247	Adult	Higareda Alvear et al. 2021
				S–W– vs. S–Gh	24 Hours	1.070474469	Adult	Higareda Alvear et al. 2021
				S–W– vs. S–Lh	24 Hours	1.753696875	Adult	Higareda Alvear et al. 2021
139	*FBgn0036427*	CG4613	Down-Regulation	*S–W– vs S+W–*	24 Hours	-2.595722764	Adult	Higareda Alvear et al. 2021
140	*FBgn0036436*	CG4914	Down-Regulation	*S–W– vs S+W–*	24 Hours	-1.258640513	Adult	Higareda Alvear et al. 2021
141	*FBgn0036449*	bmm	-	*Lipopolysaccharide*	-	-	Adult	Schlamp et al. 2021
			Down-Regulation	*C virus*		-	S2 cell	Zhu et al. 2013
			Up-Regulation	*LPS and E. coli*		1.45	mbn cell	Johansson et al. 2005
				Pseudomonas entomophila	-	0.3634419216	Adult	Ragheb et al. 2017
142	*FBgn0036738*	CG7542	-	*Lipopolysaccharide*	-	-	Adult	Schlamp et al. 2021
				ECC15	8 Hours	-	Adult	Erkosar et al. 2014
			Down-Regulation	*DCV, Serratia, Beauveria, Octosporea*	-	-	Adult	Roxstrom-Lindquist et al. 2004
				E. coli and Micrococcus luteus	3 Hours	0.4	Adult	Brun et al. 2006
				Pseudomonas entomophila	-	-0.556427844	Adult	Ragheb et al. 2017
					4 Hours	-1.2591	Gut	Soory and Ratnaparkhi 2022

143	*FBgn0036817*	CG6865	Up-Regulation	*S–W– vs. S–Lh*	24 Hours	2.901505753	Adult	Higareda Alvear et al. 2021
144	*FBgn0036891*	CG9372	Down-Regulation	*Pseudomonas entomophila*	-	-0.03260037777	Adult	Ragheb et al. 2017
			Up-Regulation	*B. bassiana*	-	6	Hemolymph	Levy et al. 2004b
				Spiroplasma	Endosymbiont	2.744687003	hemolymph proteome	Masson et al. 2021
145	*FBgn0036939*	CG7365	Up-Regulation	*ECC15*	4 Hours	2.7	Gut	Buchon et al. 2009
								Chakrabarti et al. 2012
				Pseudomonas entomophila	16 Hours	2.1	Gut	Chakrabarti et al. 2012
				S–W– vs. S–Lh	24 Hours	1.312189765	Adult	Higareda Alvear et al. 2021
146	*FBgn0036977*	CG5665	-	*Wolbachia pipientis*		-	Ovary	Christensen et al. 2016
			Down-Regulation	*S–W– vs S+W–*	24 Hours	-1.043851976	Adult	Higareda Alvear et al. 2021
147	*FBgn0037038*	CG11037	-	*Wolbachia*	-	1.314	spermathecae and seminal receptacles	Yuan et al. 2015
			Up-Regulation	*Wolbachia*	-	2.407	spermathecae and seminal receptacles	Yuan et al. 2015
						3.093	spermathecae and seminal receptacles	Yuan et al. 2015
148	*FBgn0037070*	CG11309	Down-Regulation	*E. coli and Micrococcus luteus*	3 Hours	0.4	Adult	Brun et al. 2006
				Pseudomonas entomophila	16 Hours	-2.1	Gut	Chakrabarti et al. 2012
					4 Hours	-2	Gut	Chakrabarti et al. 2012
149	*FBgn0037090*	Est-Q	-	*Lipopolysaccharide*	-	-	Adult	Schlamp et al. 2021

				ECC15	8 Hours	-	Adult	Erkosar et al. 2014
			Down-Regulation	*10 different bacteria*	-	-0.7127294218	Adult	Troha et al. 2018
				E. coli and Micrococcus luteus	3 Hours	0.4	Adult	Brun et al. 2006
				ECC15	-	-2.7	larval Trachea	Gendrin et al. 2013
			Up-Regulation	*10 different bacteria*	-	0.940836072	Adult	Troha et al. 2018
				Spiroplasma	Endosymbiont	2.92757781	hemolymph proteome	Masson et al. 2021
150	*FBgn0037222*	CG14642	Up-Regulation	*ecdysone*	-	3.374513831	Larval Hemocyte	Regan et al. 2013
151	*FBgn0037515*	Sp7	Up-Regulation	*A.fumigatus*	24 Hours	0.341	Adult	De Gregorio et al. 2002
				E.coli, M.luteus	3 Hours	2.398	Adult male	De Gregorio et al. 2001
				fungus	-	35	Larval fat body	Seto and Tamura 2013
				Micrococcus luteus	-	1.34369	Adult male	Wei et al. 2018
				Pseudomonas entomophila	16 Hours	3.1	Gut	Chakrabarti et al. 2012
					4 Hours	2.1	Gut	Chakrabarti et al. 2012
152	*FBgn0037623*	CG9801	Up-Regulation	*ecdysone*	-	14.64019637	Larval Hemocyte	Regan et al. 2013
				S–Lh vs. S+Lh	24 Hours	1.077912937	Adult	Higareda Alvear et al. 2021
153	*FBgn0037678*	CG16749	-	*Lipopolysaccharide*	-	-	Adult	Schlamp et al. 2021
				ECC15	8 Hours	-	Adult	Erkosar et al. 2014
			Down-Regulation	*10 different bacteria*	-	-0.7001410977	Adult	Troha et al. 2018
				A.fumigatus	24 Hours	-0.254	Adult	De Gregorio et al. 2002
				E. coli and Micrococcus luteus	3 Hours	0.4	Adult	Brun et al. 2006

				E.coli, M.luteus	3 Hours	-1.149	Adult male	De Gregorio et al. 2001
				ECC15	4 Hours	-2.1	Gut	Buchon et al. 2009
								Chakrabarti et al. 2012
				Pseudomonas entomophila	-	-0.2656684492	Adult	Ragheb et al. 2017
					16 Hours	-12	Gut	Chakrabarti et al. 2012
					4 Hours	-0.6854	Gut	Soory and Ratnaparkhi 2022
				Spiroplasma	Endosymbiont	0.022239121	hemolymph proteome	Masson et al. 2021
154	*FBgn0037958*	CG6962	Down-Regulation	*ecdysone*	-	-1.919246034	Larval Hemocyte	Regan et al. 2013
155	*FBgn0038013*	CG10038	Up-Regulation	*Providencia rettgeri,*	-	0.56	Adult	Short and Lazzaro 2013
156	*FBgn0038014*	CG10041	Down-Regulation	*Gamasodes queenslandicus*	-	-	Adult male	Benoit et al. 2020
			Up-Regulation	*Providencia rettgeri,*	-	1.73	Adult	Short and Lazzaro 2013
157	*FBgn0038113*	CG11668	Down-Regulation	*C virus*		-	S2 cell	Zhu et al. 2013
158	*FBgn0038211*	CG9649	Down-Regulation	*E.coli, M.luteus*	3 Hours	-0.079	Adult male	De Gregorio et al. 2001
				Pseudomonas entomophila	-	-0.4637067479	Adult	Ragheb et al. 2017
			Up-Regulation	*A.fumigatus*	24 Hours	0.826	Adult	De Gregorio et al. 2002
				S–W– vs. S–Gh	24 Hours	1.032855251	Adult	Higareda Alvear et al. 2021
				S–W– vs. S–Lh	24 Hours	1.258673014	Adult	Higareda Alvear et al. 2021
159	*FBgn0038233*	HtrA2	Up-Regulation	*Prion-exposed PrP transgenic Drosophila*	-	-		Thackray et al. 2020

160	*FBgn0038257*	smp-30	-	*Lipopolysaccharide*	-	-	Adult	Schlamp et al. 2021
				Photor/nematode	-	-	Adult	Castillo et al. 2015
				Wolbachia	-	0.74	spermathecae and seminal receptacles	Yuan et al. 2015
			Down-Regulation	*ECC15*	4 Hours	-6.8	Gut	Buchon et al. 2009
								Chakrabarti et al. 2012
				Pseudomonas entomophila	16 Hours	-12.1	Gut	Chakrabarti et al. 2012
					4 Hours	-3.2	Gut	Chakrabarti et al. 2012
				Wolbachia	-	0.526	spermathecae and seminal receptacles	Yuan et al. 2015
			Up-Regulation	*Wolbachia*	-	1.535	spermathecae and seminal receptacles	Yuan et al. 2015
161	*FBgn0038398*	sxe2	-	*Micrococcus luteus*	-	0	Adult male	Wei et al. 2018
			Down-Regulation	*E. coli and Micrococcus luteus*	3 Hours	0.3	Adult	Brun et al. 2006
				FHV	-	0.2	Adult	Go et al. 2006
162	*FBgn0038447*	CG14892	Up-Regulation	*E. coli and Micrococcus luteus*	3 Hours	2.1	Adult	Brun et al. 2006
163	*FBgn0038479*	CG17477	-	*ECC15*	8 Hours	-	Adult	Erkosar et al. 2014
			Down-Regulation	*Pseudomonas entomophila*	16 Hours	-12.4	Gut	Chakrabarti et al. 2012
					4 Hours	-8.2	Gut	Chakrabarti et al. 2012
164	*FBgn0038481*	CG17475	Down-Regulation	*Pseudomonas entomophila*	16 Hours	-11.7	Gut	Chakrabarti et al. 2012
					4 Hours	-4	Gut	Chakrabarti et al. 2012

165	*FBgn0038482*	CG4053	Down-Regulation	*Pseudomonas entomophila*	16 Hours	-28.1	Gut	Chakrabarti et al. 2012
					4 Hours	-4	Gut	Chakrabarti et al. 2012
						-0.6807	Gut	Soory and Ratnaparkhi 2022
166	*FBgn0038484*	CG5246	-	*Lipopolysaccharide*	-	-	Adult	Schlamp et al. 2021
				ECC15	8 Hours	-	Adult	Erkosar et al. 2014
			Up-Regulation	*C virus*		-	S2 cell	Zhu et al. 2013
				CrPV	-	-	Adult	Merkling et al. 2015a; Merkling et al. 2015b
				Pseudomonas entomophila	-	0.3049213192	Adult	Ragheb et al. 2017
					4 Hours	5.9	Gut	Chakrabarti et al. 2012
				Spiroplasma	Endosymbiont	4.652746847	hemolymph proteome	Masson et al. 2021
167	*FBgn0038485*	CG5255	Down-Regulation	*ECC15*	-	-3.4	larval Trachea	Gendrin et al. 2013
168	*FBgn0038595*	CG7142	-	*Lipopolysaccharide*	-	-	Adult	Schlamp et al. 2021
				Photor/nematode	-	-	Adult	Castillo et al. 2015
			Down-Regulation	*Pseudomonas entomophila*	-	-0.1477913581	Adult	Ragheb et al. 2017
			Up-Regulation	*ECC15*	4 Hours	4.6	Gut	Buchon et al. 2009
								Chakrabarti et al. 2012
				Heterorhabditis bacteriophora	-	-	Larva	Arefin et al. 2014
				Pseudomonas entomophila	16 Hours	12.9	Gut	Chakrabarti et al. 2012

					4 Hours	1.966	Gut	Soory and Ratnaparkhi 2022
						12.9	Gut	Chakrabarti et al. 2012
169	*FBgn0038700*	CG3734	-	*Lipopolysaccharide*	-	-	Adult	Schlamp et al. 2021
				ECC15	8 Hours	-	Adult	Erkosar et al. 2014
			Down-Regulation	*E. coli and Micrococcus luteus*	3 Hours	0.4	Adult	Brun et al. 2006
				ECC15	4 Hours	-2.5	Gut	Buchon et al. 2009
								Chakrabarti et al. 2012
				Pseudomonas entomophila	16 Hours	-3.2	Gut	Chakrabarti et al. 2012
					4 Hours	-2.1	Gut	Chakrabarti et al. 2012
170	*FBgn0038701*	CG18493	-	*Lipopolysaccharide*	-	-	Adult	Schlamp et al. 2021
			Down-Regulation	*E. coli and Micrococcus luteus*	3 Hours	0.4	Adult	Brun et al. 2006
				Gamasodes queenslandicus	-	-	Adult male	Benoit et al. 2020
				Pseudomonas entomophila	-	-0.7313025359	Adult	Ragheb et al. 2017
					16 Hours	-3.7	Gut	Chakrabarti et al. 2012
					4 Hours	-0.4784	Gut	Soory and Ratnaparkhi 2022
			Up-Regulation	*10 different bacteria*	-	1.936213438	Adult	Troha et al. 2018
171	*FBgn0038702*	CG3739	-	*Lipopolysaccharide*	-	-	Adult	Schlamp et al. 2021
				ECC15	8 Hours	-	Adult	Erkosar et al. 2014

			Down-Regulation	*10 different bacteria*	-	-1.332102716	Adult	Troha et al. 2018
				ECC15	4 Hours	-3.3	Gut	Buchon et al. 2009
								Chakrabarti et al. 2012
				Photor/nematode	-	-	Adult	Castillo et al. 2015
				Pseudomonas entomophila	-	-0.2880588835	Adult	Ragheb et al. 2017
					16 Hours	-4.9	Gut	Chakrabarti et al. 2012
					4 Hours	-2.7	Gut	Chakrabarti et al. 2012
						-1.0337	Gut	Soory and Ratnaparkhi 2022
172	*FBgn0038727*	CG7432	Down-Regulation	*E. coli and Micrococcus luteus*	3 Hours	0.4	Adult	Brun et al. 2006
				S–W– vs S+W–	24 Hours	-1.566316513	Adult	Higareda Alvear et al. 2021
173	*FBgn0038738*	CG4572	-	*Wolbachia pipientis*		-	Ovary	Christensen et al. 2016
			Down-Regulation	*Pseudomonas entomophila*	4 Hours	-0.9704	Gut	Soory and Ratnaparkhi 2022
174	*FBgn0038771*	CG4390	-	*Wolbachia pipientis*		-	Ovary	Christensen et al. 2016
175	*FBgn0038974*	CG5377	Up-Regulation	*Pseudomonas entomophila*	4 Hours	2.5	Gut	Chakrabarti et al. 2012
176	*FBgn0039084*	CG10175	Down-Regulation	*Pseudomonas entomophila*	4 Hours	-1.5191	Gut	Soory and Ratnaparkhi 2022
			Up-Regulation	*Gamasodes queenslandicus*	-	-	Adult male	Benoit et al. 2020
177	*FBgn0039101*	CG16710	Up-Regulation	*Pseudomonas entomophila*	16 Hours	2.5	Gut	Chakrabarti et al. 2012

178	*FBgn0039102*	SPE	-	*Lipopolysaccharide*	-	-	Adult	Schlamp et al. 2021
			Down-Regulation	*Pseudomonas entomophila*	-	-0.4742215693	Adult	Ragheb et al. 2017
			Up-Regulation	*A.fumigatus*	24 Hours	1.496	Adult	De Gregorio et al. 2002
				B. bassiana	-	6	Hemolymph	Levy et al. 2004b
				DCV, Serratia, Beauveria, Octosporea	-	-	Adult	Roxstrom-Lindquist et al. 2004
				E.coli, M.luteus	3 Hours	1.289	Adult male	De Gregorio et al. 2001
				fungus	-	3	Larval fat body	Seto and Tamura 2013
				Micrococcus luteus	-	1.27854	Adult male	Wei et al. 2018
				Serratia marcescens and Enterococcos faecalis	12 Hours	2.913219855	Adult	Sackton et al. 2010
				Spiroplasma	Endosymbiont	5.436986468	hemolymph proteome	Masson et al. 2021
179	*FBgn0039108*	CG10232	Up-Regulation	*E. coli*	45 min	2.98	Plasmatocyte	Ramond et al. 2020
				S–W– vs. S–Gh	24 Hours	1.148198474	Adult	Higareda Alvear et al. 2021
180	*FBgn0039120*	CG10198	Down-Regulation	*ecdysone*	-	-1.865277571	Larval Hemocyte	Regan et al. 2013
			Up-Regulation	*Gamasodes queenslandicus*	-	-	Adult male	Benoit et al. 2020
				Pseudomonas entomophila	4 Hours	0.7866	Gut	Soory and Ratnaparkhi 2022
181	*FBgn0039272*	CG11836	Down-Regulation	*Pseudomonas entomophila*	16 Hours	-3.3	Gut	Chakrabarti et al. 2012
				S–W– vs S+W–	24 Hours	-1.320262939	Adult	Higareda Alvear et al. 2021
182	*FBgn0039430*	CG5455	Down-Regulation	*C virus*		-	S2 cell	Zhu et al. 2013
			Up-Regulation	*clean injury*	45 min	2.36	Plasmatocyte	Ramond et al. 2020

				ecdysone	-	2.366173724	Larval Hemocyte	Regan et al. 2013
183	*FBgn0039470*	CG6296	-	*Lipopolysaccharide*	-	-	Adult	Schlamp et al. 2021
				ECC15	8 Hours	-	Adult	Erkosar et al. 2014
			Down-Regulation	*Pseudomonas entomophila*	-	-0.1289212909	Adult	Ragheb et al. 2017
			Up-Regulation	*Photor/nematode*	-	-	Adult	Castillo et al. 2015
184	*FBgn0039471*	CG6295	-	*Lipopolysaccharide*	-	-	Adult	Schlamp et al. 2021
			Down-Regulation	*E. coli and Micrococcus luteus*	3 Hours	0.3	Adult	Brun et al. 2006
				Micrococcus luteus	-	-1.40523	Adult male	Wei et al. 2018
				Pseudomonas entomophila	-	-0.723876243	Adult	Ragheb et al. 2017
					16 Hours	-35.1	Gut	Chakrabarti et al. 2012
					4 Hours	-0.7264	Gut	Soory and Ratnaparkhi 2022
			Up-Regulation	*CrPV*	-	-	Adult	Merkling et al. 2015a; Merkling et al. 2015b
				DCV, Serratia, Beauveria, Octosporea	-	-	Adult	Roxstrom-Lindquist et al. 2004
185	*FBgn0039472*	CG17192	-	*Micrococcus luteus*	-	0	Adult male	Wei et al. 2018
			Down-Regulation	*A.fumigatus*	24 Hours	-0.27	Adult	De Gregorio et al. 2002
				E. coli and Micrococcus luteus	3 Hours	0.4	Adult	Brun et al. 2006
				E.coli, M.luteus	3 Hours	-1.13	Adult male	De Gregorio et al. 2001
				Pseudomonas entomophila	-	-1.149329102	Adult	Ragheb et al. 2017

					16 Hours	-31.8	Gut	Chakrabarti et al. 2012
					4 Hours	-0.7935	Gut	Soory and Ratnaparkhi 2022
186	*FBgn0039473*	CG17191	Down-Regulation	*Pseudomonas entomophila*	16 Hours	-2.1	Gut	Chakrabarti et al. 2012
187	*FBgn0039474*	CG6283	-	*Photor/nematode*	-	-	Adult	Castillo et al. 2015
			Down-Regulation	*DCV, Serratia, Beauveria, Octosporea*	-	-	Adult	Roxstrom-Lindquist et al. 2004
				Pseudomonas entomophila	16 Hours	-12	Gut	Chakrabarti et al. 2012
					4 Hours	-3.2	Gut	Chakrabarti et al. 2012
						-0.8713	Gut	Soory and Ratnaparkhi 2022
				S. aureus	45 min	-6.31	Plasmatocyte	Ramond et al. 2020
			Up-Regulation	*clean injury*	-	7.60	Plasmatocyte	Ramond et al. 2020
				S–Lh vs. S+Lh	24 Hours	1.019428436	Adult	Higareda Alvear et al. 2021
				S–W– vs S+W–	24 Hours	1.225128911	Adult	Higareda Alvear et al. 2021
188	*FBgn0039475*	CG6277	-	*Micrococcus luteus*	-	0	Adult male	Wei et al. 2018
				Photor/nematode	-	-	Adult	Castillo et al. 2015
			Down-Regulation	*ECC15*	4 Hours	-2	Gut	Buchon et al. 2009
				S. aureus	45 min	-22.98	Plasmatocyte	Ramond et al. 2020
			Up-Regulation	*clean injury*	45 min	12.58	Plasmatocyte	Ramond et al. 2020

				S–Gh vs. S+Gh	24 Hours	1.400375713	Adult	Higareda Alvear et al. 2021
				S–Lh vs. S+Lh	24 Hours	3.819853218	Adult	Higareda Alvear et al. 2021
				S–W– vs S+W–	24 Hours	1.928386951	Adult	Higareda Alvear et al. 2021
				Serratia marcescens and Enterococcos faecalis	12 Hours	2.572867067	Adult	Sackton et al. 2010
189	*FBgn0039476*	CG6271	Down-Regulation	*Pseudomonas entomophila*	16 Hours	-5.1	Gut	Chakrabarti et al. 2012
					4 Hours	-2.1	Gut	Chakrabarti et al. 2012
			Up-Regulation	*S–Lh vs. S+Lh*	24 Hours	1.772720598	Adult	Higareda Alvear et al. 2021
190	*FBgn0039494*	grass	-	*Micrococcus luteus*	-	0	Adult male	Wei et al. 2018
			Up-Regulation	*E. coli and Micrococcus luteus*	3 Hours	2	Adult	Brun et al. 2006
				ecdysone	-	2.66024478	Larval Hemocyte	Regan et al. 2013
				fungus	-	3	Larval fat body	Seto and Tamura 2013
				Spiroplasma	Endosymbiont	2.346143456	hemolymph proteome	Masson et al. 2021
191	*FBgn0039495*	CG5909	-	*Lipopolysaccharide*	-	-	Adult	Schlamp et al. 2021
			Up-Regulation	*A.fumigatus*	24 Hours	0.619	Adult	De Gregorio et al. 2002
				DCV, Serratia, Beauveria, Octosporea	-	-	Adult	Roxstrom-Lindquist et al. 2004
				E.coli, M.luteus	3 Hours	2.217	Adult male	De Gregorio et al. 2001
				Pseudomonas entomophila	-	1.096238633	Adult	Ragheb et al. 2017
					4 Hours	2.4	Gut	Chakrabarti et al. 2012
192	*FBgn0039628*	CG11841	Down-Regulation	*E.coli, M.luteus*	3 Hours	-0.342	Adult male	De Gregorio et al. 2001

				Pseudomonas entomophila	-	-0.5593281218	Adult	Ragheb et al. 2017
			Up-Regulation	*A.fumigatus*	24 Hours	1.344	Adult	De Gregorio et al. 2002
				DCV, Serratia, Beauveria, Octosporea	-	-	Adult	Roxstrom-Lindquist et al. 2004
				Spiroplasma	Endosymbiont	3.468796124	hemolymph proteome	Masson et al. 2021
193	*FBgn0039629*	CG11842	-	*Lipopolysaccharide*	-	-	Adult	Schlamp et al. 2021
			Up-Regulation	*10 different bacteria*	-	2.370238462	Adult	Troha et al. 2018
				A.fumigatus	24 Hours	0.824	Adult	De Gregorio et al. 2002
				DCV, Serratia, Beauveria, Octosporea	-	-	Adult	Roxstrom-Lindquist et al. 2004
				E.coli, M.luteus	3 Hours	0.232	Adult male	De Gregorio et al. 2001
				Spiroplasma	Endosymbiont	2.598617513	hemolymph proteome	Masson et al. 2021
194	*FBgn0039655*	CG14507	Up-Regulation	*Pseudomonas entomophila*	4 Hours	1.6377	Gut	Soory and Ratnaparkhi 2022
195	*FBgn0039703*	CG7829	Up-Regulation	*CrPV*	-	-	Adult	Merkling et al. 2015a; Merkling et al. 2015b
196	*FBgn0039758*	CG9737	Down-Regulation	*S–W– vs S+W–*	24 Hours	-2.044172898	Adult	Higareda Alvear et al. 2021
				S–W– vs. S–Gh	24 Hours	-1.621115119	Adult	Higareda Alvear et al. 2021
				S–W– vs. S–Lh	24 Hours	-1.61253121	Adult	Higareda Alvear et al. 2021
197	*FBgn0039759*	CG9733	-	*Lipopolysaccharide*	-	-	Adult	Schlamp et al. 2021
			Down-Regulation	*Pseudomonas entomophila*	-	-0.2915727182	Adult	Ragheb et al. 2017

			Up-Regulation	*A.fumigatus*	24 Hours	0.259	Adult	De Gregorio et al. 2002
				E. coli and Micrococcus luteus	3 Hours	2.1	Adult	Brun et al. 2006
				E.coli, M.luteus	3 Hours	2.37	Adult male	De Gregorio et al. 2001
				Pseudomonas entomophila	-	2.107127208	Adult	Ragheb et al. 2017
						2.301000092	Adult	Ragheb et al. 2017
				S–W– vs. S–Gh	24 Hours	2.37829	Adult	Higareda Alvear et al. 2021
198	*FBgn0039777*	Jon99Fii	-	*Lipopolysaccharide*	-	-	Adult	Schlamp et al. 2021
				Photor/nematode	-	-	Adult	Castillo et al. 2015
			Down-Regulation	*10 different bacteria*	-	-1.003747104	Adult	Troha et al. 2018
				Pseudomonas entomophila	-	-0.04126229399	Adult	Ragheb et al. 2017
					4 Hours	-1.2153	Gut	Soory and Ratnaparkhi 2022
199	*FBgn0039778*	Jon99Fi	-	*ECC15*	8 Hours	-	Adult	Erkosar et al. 2014
			Down-Regulation	*A.fumigatus*	24 Hours	-0.238	Adult	De Gregorio et al. 2002
				D. pneumoniae, N. catarrhalis, S. aureus, K. pneumoniae, H. influenza, S. pyogenes	6 Hours	28 ± 2.1%m 44 ± 0.9%. 28 ± 1.3%.	Adult	de Morais Guedes et al. 2005
				ECC15	6 Hours	0.49	Larval	Vodovar et al. 2005
				Pseudomonas entomophila	16 Hours	-8.1	Gut	Chakrabarti et al. 2012
					4 Hours	-0.8086	Gut	Soory and Ratnaparkhi 2022

			Up-Regulation	*DCV, Serratia, Beauveria, Octosporea*	-	-	Adult	Roxstrom-Lindquist et al. 2004
200	*FBgn0039798*	CG11313	Up-Regulation	*10 different bacteria*	-	1.385752706	Adult	Troha et al. 2018
				S–W– vs. S–Gh	24 Hours	2.464553421	Adult	Higareda Alvear et al. 2021
201	*FBgn0040060*	yip7	Down-Regulation	*Pseudomonas entomophila*	-	-0.1151919373	Adult	Ragheb et al. 2017
					16 Hours	-2.8	Gut	Chakrabarti et al. 2012
					4 Hours	-1.0977	Gut	Soory and Ratnaparkhi 2022
				S. aureus	45 min	-8.57	Plasmatocyte	Ramond et al. 2020
			Up-Regulation	*DCV, Serratia, Beauveria, Octosporea*	-	-	Adult	Roxstrom-Lindquist et al. 2004
202	*FBgn0042106*	CG18754	-	*Lipopolysaccharide*	-	-	Adult	Schlamp et al. 2021
			Up-Regulation	*clean injury*	45 min	3.10	Plasmatocyte	Ramond et al. 2020
				Pseudomonas entomophila	-	0.7260631772	Adult	Ragheb et al. 2017
				S–W– vs. S–Gh	24 Hours	3.174545128	Adult	Higareda Alvear et al. 2021
203	*FBgn0042138*	Apt1	-	*Wolbachia pipientis*		-	Ovary	Christensen et al. 2016
			Up-Regulation	*Serratia marcescens and Enterococcos faecalis*	12 Hours	1.559211381	Adult	Sackton et al. 2010
204	*FBgn0042175*	CG18858	Up-Regulation	*Pseudomonas entomophila*	-	0.5027440544	Adult	Ragheb et al. 2017
						0.56219672	Adult	Ragheb et al. 2017
205	*FBgn0042186*	CG17239	Up-Regulation	*Providencia rettgeri,*	-	1.05	Adult	Short and Lazzaro 2013

						1.38	Adult	Short and Lazzaro 2013
206	*FBgn0042187*	CG17234	Up-Regulation	*Photor/nematode*	-	-	Adult	Castillo et al. 2015
207	*FBgn0042627*	FASN2	-	*Wolbachia pipientis*		-	Ovary	Christensen et al. 2016
			Up-Regulation	*Gamasodes queenslandicus*	-	-	Adult male	Benoit et al. 2020
208	*FBgn0043070*	MESK2	Down-Regulation	*Pseudomonas entomophila*	4 Hours	-2	Gut	Chakrabarti et al. 2012
209	*FBgn0043470*	lambdaTry	-	*Lipopolysaccharide*	-	-	Adult	Schlamp et al. 2021
			Down-Regulation	*ECC15*	4 Hours	-2	Gut	Buchon et al. 2009
								Chakrabarti et al. 2012
				Pseudomonas entomophila	-	-0.260390973	Adult	Ragheb et al. 2017
					16 Hours	-4.5	Gut	Chakrabarti et al. 2012
			Up-Regulation	*DCV, Serratia, Beauveria, Octosporea*	-	-	Adult	Roxstrom-Lindquist et al. 2004
				Pseudomonas entomophila	-	0.0622400009	Adult	Ragheb et al. 2017
210	*FBgn0043825*	CG18284	Up-Regulation	*10 different bacteria*	-	1.525075538	Adult	Troha et al. 2018
211	*FBgn0050025*	CG30025	-	*Lipopolysaccharide*	-	-	Adult	Schlamp et al. 2021
212	*FBgn0050031*	CG30031	-	*Lipopolysaccharide*	-	-	Adult	Schlamp et al. 2021
			Down-Regulation	*Pseudomonas entomophila*	-	-0.3553654172	Adult	Ragheb et al. 2017
213	*FBgn0050083*	CG30083	Up-Regulation	*10 different bacteria*	-	1.205461799	Adult	Troha et al. 2018
214	*FBgn0050087*	CG30087	Up-Regulation	*DCV, Serratia, Beauveria, Octosporea*	-	-	Adult	Roxstrom-Lindquist et al. 2004
				LPS and E. coli		4.27	mbn cell	Johansson et al. 2005

				Pseudomonas entomophila	-	4.841324288	Adult	Ragheb et al. 2017
215	*FBgn0050088*	CG30088	Up-Regulation	*ecdysone*	-	24.0655307	Larval Hemocyte	Regan et al. 2013
				Pseudomonas entomophila	-	2.603603683	Adult	Ragheb et al. 2017
216	*FBgn0050090*	CG30090	Down-Regulation	*C virus*		-	S2 cell	Zhu et al. 2013
			Up-Regulation	*ECC15*	4 Hours	3.1	Gut	Buchon et al. 2009
								Chakrabarti et al. 2012
				S–W– vs. S–Gh	24 Hours	1.867704939	Adult	Higareda Alvear et al. 2021
217	*FBgn0050091*	CG30091	-	*Lipopolysaccharide*	-	-	Adult	Schlamp et al. 2021
			UP all except_S.mar	*10 different bacteria*	-	2.868283177	Adult	Troha et al. 2018
			Up-Regulation	*Gamasodes queenslandicus*	-	-	Adult male	Benoit et al. 2020
				Heterorhabditis bacteriophora	-	-	Larva	Arefin et al. 2014
				S–Lh vs. S+Lh	24 Hours	2.106653584	Adult	Higareda Alvear et al. 2021
				S–W– vs. S–Gh	24 Hours	3.087748677	Adult	Higareda Alvear et al. 2021
218	*FBgn0050098*	CG30098	-	*Lipopolysaccharide*	-	-	Adult	Schlamp et al. 2021
			Down-Regulation	*Providencia rettgeri,*	-	-1.26	Adult	Short and Lazzaro 2013
						-1.19	Adult	Short and Lazzaro 2013
			Up-Regulation	*ecdysone*	-	6.366603859	Larval Hemocyte	Regan et al. 2013
				Gamasodes queenslandicus	-	-	Adult male	Benoit et al. 2020
				Photor/nematode	-	-	Adult	Castillo et al. 2015
				Pseudomonas entomophila	-	1.475500206	Adult	Ragheb et al. 2017

219	*FBgn0050187*	CG30187	Down-Regulation	*ecdysone*	-	-3.560522575	Larval Hemocyte	Regan et al. 2013
220	*FBgn0050287*	CG30287	-	*Lipopolysaccharide*	-	-	Adult	Schlamp et al. 2021
			Up-Regulation	*Gamasodes queenslandicus*	-	-	Adult male	Benoit et al. 2020
221	*FBgn0050288*	CG30288	Up-Regulation	*S–W– vs. S–Gh*	24 Hours	3.089152547	Adult	Higareda Alvear et al. 2021
222	*FBgn0050289*	CG30289	Up-Regulation	*10 different bacteria*	-	2.85217816	Adult	Troha et al. 2018
223	*FBgn0050371*	CG30371	Up-Regulation	*Aspergillus flavus*	-	-	Adult	Ramirez-Camejo and Bayman 2020
224	*FBgn0050414*	CG30414	Down-Regulation	*ecdysone*	-	-8.789087156	Larval Hemocyte	Regan et al. 2013
			Up-Regulation	*S–W– vs. S–Gh*	24 Hours	1.366656929	Adult	Higareda Alvear et al. 2021
225	*FBgn0051146*	Nlg1	Up-Regulation	*Gamasodes queenslandicus*	-	-	Adult male	Benoit et al. 2020
226	*FBgn0051217*	modSP	Up-Regulation	*ecdysone*	-	2.462171634	Larval Hemocyte	Regan et al. 2013
				fungus	-	10	Larval fat body	Seto and Tamura 2013
227	*FBgn0051219*	CG31219	Up-Regulation	*clean injury*	45 min	2.10	Plasmatocyte	Ramond et al. 2020
				S–W– vs. S–Gh	24 Hours	8.777144804	Adult	Higareda Alvear et al. 2021
228	*FBgn0051265*	CG31265	-	*ECC15*	8 Hours	-	Adult	Erkosar et al. 2014
			Down-Regulation	*Pseudomonas entomophila*	16 Hours	-13	Gut	Chakrabarti et al. 2012
					4 Hours	-3.5	Gut	Chakrabarti et al. 2012
229	*FBgn0051269*	CG31269	-	*ECC15*	8 Hours	-	Adult	Erkosar et al. 2014
			Down-Regulation	*Pseudomonas entomophila*	16 Hours	-13.1	Gut	Chakrabarti et al. 2012
					4 Hours	-2.5	Gut	Chakrabarti et al. 2012

230	*FBgn0051683*	CG31683	Up-Regulation	*Pseudomonas entomophila*	-	0.5628939556	Adult	Ragheb et al. 2017
						0.5978185773	Adult	Ragheb et al. 2017
231	*FBgn0051821*	CG31821	Down-Regulation	*Pseudomonas entomophila*	16 Hours	-4.6	Gut	Chakrabarti et al. 2012
					4 Hours	-2.3	Gut	Chakrabarti et al. 2012
232	*FBgn0051823*	CG31823	Down-Regulation	*Pseudomonas entomophila*	16 Hours	-4	Gut	Chakrabarti et al. 2012
					4 Hours	-2.4	Gut	Chakrabarti et al. 2012
233	*FBgn0051871*	CG31871	Down-Regulation	*S–W– vs S+W–*	24 Hours	-1.771068254	Adult	Higareda Alvear et al. 2021
				S–W– vs. S–Gh	24 Hours	-1.192079072	Adult	Higareda Alvear et al. 2021
				S–W– vs. S–Lh	24 Hours	-1.288520381	Adult	Higareda Alvear et al. 2021
234	*FBgn0051872*	CG31872	-	*Wolbachia*	-	1.411	spermathecae and seminal receptacles	Yuan et al. 2015
			Down-Regulation	*DCV, Serratia, Beauveria, Octosporea*	-	-	Adult	Roxstrom-Lindquist et al. 2004
			Up-Regulation	*10 different bacteria*	-	1.859453391	Adult	Troha et al. 2018
				Wolbachia	-	2.267	spermathecae and seminal receptacles	Yuan et al. 2015
						3.212	spermathecae and seminal receptacles	Yuan et al. 2015
235	*FBgn0051954*	CG31954	Down-Regulation	*ECC15*	-	-2	larval Trachea	Gendrin et al. 2013
236	*FBgn0052260*	CG32260	Up-Regulation	*Pseudomonas entomophila*	-	0.3144840714	Adult	Ragheb et al. 2017
237	*FBgn0052374*	CG32374	Up-Regulation	*S–W– vs. S–Gh*	24 Hours	1.963292857	Adult	Higareda Alvear et al. 2021

				S–W– vs. S–Lh	24 Hours	1.225564843	Adult	Higareda Alvear et al. 2021
238	*FBgn0052376*	CG32376	Up-Regulation	*S–W– vs. S–Gh*	24 Hours	1.077424226	Adult	Higareda Alvear et al. 2021
239	*FBgn0052483*	CG32483	Down-Regulation	*Heterorhabditis bacteriophora*	-	-	Larva	Arefin et al. 2014
				Pseudomonas entomophila	16 Hours	-2.5	Gut	Chakrabarti et al. 2012
240	*FBgn0052523*	CG32523	Up-Regulation	*CrPV*	-	-	Adult	Merkling et al. 2015a; Merkling et al. 2015b
241	*FBgn0052808*	CG32808	Down-Regulation	*ECC15*	-	-2.1	larval Trachea	Gendrin et al. 2013
			Up-Regulation	*S. aureus*	45 min	2.03	Plasmatocyte	Ramond et al. 2020
242	*FBgn0053096*	CG33096	Down-Regulation	*Gamasodes queenslandicus*	-	-	Adult male	Benoit et al. 2020
243	*FBgn0053329*	Sp212	-	*Lipopolysaccharide*	-	-	Adult	Schlamp et al. 2021
			Down-Regulation	*C virus*		-	S2 cell	Zhu et al. 2013
			Up-Regulation	*clean injury*	45 min	2.96	Plasmatocyte	Ramond et al. 2020
				Pseudomonas entomophila	-	0.9010521737	Adult	Ragheb et al. 2017
244	*FBgn0053458*	CG33458	Up-Regulation	*E. coli*	45 min	2.40	Plasmatocyte	Ramond et al. 2020
				ecdysone	-	8.958486404	Larval Hemocyte	Regan et al. 2013
				S. aureus	45 min	2.10	Plasmatocyte	Ramond et al. 2020
245	*FBgn0053459*	CG33459	Down-Regulation	*ecdysone*	-	-3.726264283	Larval Hemocyte	Regan et al. 2013
			Up-Regulation	*E. coli*	45 min	2.08	Plasmatocyte	Ramond et al. 2020
				S–W– vs. S–Gh	24 Hours	1.289019826	Adult	Higareda Alvear et al. 2021

246	*FBgn0053461*	CG33461	Up-Regulation	*S–W– vs. S–Gh*	24 Hours	5.431068635	Adult	Higareda Alvear et al. 2021
247	*FBgn0053462*	CG33462	Up-Regulation	*E. coli*	45 min	2.07	Plasmatocyte	Ramond et al. 2020
				Heterorhabditis bacteriophora	-	-	Larva	Arefin et al. 2014
				S–W– vs. S–Gh	24 Hours	9.439864908	Adult	Higareda Alvear et al. 2021
248	*FBgn0069056*	CG33226	Up-Regulation	*S–W– vs. S–Gh*	24 Hours	3.359906038	Adult	Higareda Alvear et al. 2021
249	*FBgn0082831*	pps	Up-Regulation	*10 different bacteria*	-	0.5173048884	Adult	Troha et al. 2018
				Gamasodes queenslandicus	-	-	Adult male	Benoit et al. 2020
250	*FBgn0085476*	CG34447	-	*Wolbachia pipientis*		-	Ovary	Christensen et al. 2016
			Down-Regulation	*Gamasodes queenslandicus*	-	-	Adult male	Benoit et al. 2020
				S–W– vs S+W–	24 Hours	-1.053972671	Adult	Higareda Alvear et al. 2021
251	*FBgn0250815*	Jon65Aiv	Down-Regulation	*Pseudomonas entomophila*	-	-0.6309752656	Adult	Ragheb et al. 2017
					16 Hours	-6.4	Gut	Chakrabarti et al. 2012
				S. aureus	45 min	-3.06	Plasmatocyte	Ramond et al. 2020
			Up-Regulation	*A.fumigatus*	24 Hours	0.229	Adult	De Gregorio et al. 2002
				E.coli, M.luteus	3 Hours	1.189	Adult male	De Gregorio et al. 2001
252	*FBgn0250862*	CG42237	Down-Regulation	*S–W– vs S+W–*	24 Hours	-1.326341777	Adult	Higareda Alvear et al. 2021
253	*FBgn0259175*	ome	Down-Regulation	*Pseudomonas entomophila*	4 Hours	-0.6513	Gut	Soory and Ratnaparkhi 2022
			Up-Regulation	*10 different bacteria*	-	0.4485676156	Adult	Troha et al. 2018
				clean injury	45 min	3.34	Plasmatocyte	Ramond et al. 2020
				Gamasodes queenslandicus	-	-	Adult male	Benoit et al. 2020

254	*FBgn0259998*	CG17571	-	*Photor/nematode*	-	-	Adult	Castillo et al. 2015
			Down-Regulation	*DCV, Serratia, Beauveria, Octosporea*	-	-	Adult	Roxstrom-Lindquist et al. 2004
				E. coli and Micrococcus luteus	3 Hours	0.4	Adult	Brun et al. 2006
				ECC15	6 Hours	0.58	Larval	Vodovar et al. 2005
				Heterorhabditis bacteriophora	-	-	Larva	Arefin et al. 2014
				Pseudomonas entomophila	-	-0.8636776347	Adult	Ragheb et al. 2017
						-0.2066421286	Adult	Ragheb et al. 2017
			Up-Regulation	*10 different bacteria*	-	2.237867582	Adult	Troha et al. 2018
255	*FBgn0260474*	CG30002	-	*Lipopolysaccharide*	-	-	Adult	Schlamp et al. 2021
			Up-Regulation	*10 different bacteria*	-	1.81972956	Adult	Troha et al. 2018
				Gamasodes queenslandicus	-	-	Adult male	Benoit et al. 2020
				Spiroplasma	Endosymbiont	5.119840791	hemolymph proteome	Masson et al. 2021
256	*FBgn0261244*	inaE	Down-Regulation	*ecdysone*	-	-2.67485249	Larval Hemocyte	Regan et al. 2013
			Up-Regulation	*Gamasodes queenslandicus*	-	-	Adult male	Benoit et al. 2020
				Pseudomonas entomophila	4 Hours	0.8536	Gut	Soory and Ratnaparkhi 2022
257	*FBgn0261393*	alpha-Est5	-	*Lipopolysaccharide*	-	-	Adult	Schlamp et al. 2021
			Up-Regulation	*Pseudomonas entomophila*	16 Hours	5.3	Gut	Chakrabarti et al. 2012
					4 Hours	4.4	Gut	Chakrabarti et al. 2012
258	*FBgn0262570*	CG43110	-	*Photor/nematode*		-	Adult	Castillo et al. 2015
			Up-Regulation	*ecdysone*	-	2.467818569	Larval Hemocyte	Regan et al. 2013

259	*FBgn0262801*	twr	-	*Wolbachia pipientis*		-	Ovary	Christensen et al. 2016
			Down-Regulation	*clean injury*	45 min	-2.23	Plasmatocyte	Ramond et al. 2020
260	*FBgn0263234*	Phae1	-	*Lipopolysaccharide*	-	-	Adult	Schlamp et al. 2021
				ECC15	8 Hours	-	Adult	Erkosar et al. 2014
261	*FBgn0263235*	Phae2	-	*Lipopolysaccharide*	-	-	Adult	Schlamp et al. 2021
				ECC15	8 Hours	-	Adult	Erkosar et al. 2014
			Down-Regulation	*Pseudomonas entomophila*	4 Hours	-0.5779	Gut	Soory and Ratnaparkhi 2022
			Up-Regulation	*DCV, Serratia, Beauveria, Octosporea*	-	-	Adult	Roxstrom-Lindquist et al. 2004
262	*FBgn0264979*	CG4267	Down-Regulation	*A.fumigatus*	24 Hours	-0.12	Adult	De Gregorio et al. 2002
				clean injury	45 min	-3.15	Plasmatocyte	Ramond et al. 2020
			Up-Regulation	*10 different bacteria*	-	0.8588896299	Adult	Troha et al. 2018
				E.coli, M.luteus	3 Hours	2.192	Adult male	De Gregorio et al. 2001
				ECC15	4 Hours	5.8	Gut	Buchon et al. 2009
								Chakrabarti et al. 2012
				ecdysone	-	6.859345857	Larval Hemocyte	Regan et al. 2013
				FHV	-	4.5	Adult	Go et al. 2006
				Gamasodes queenslandicus	-	-	Adult male	Benoit et al. 2020
				LPS and E. coli		5.13	mbn cell	Johansson et al. 2005
				Micrococcus luteus	-	1.14487	Adult male	Wei et al. 2018

				Pseudomonas entomophila	16 Hours	2.7	Gut	Chakrabarti et al. 2012
					4 Hours	3.2	Gut	Chakrabarti et al. 2012
263	*FBgn0265011*	Np	Down-Regulation	*S–W– vs S+W–*	24 Hours	-2.56430193	Adult	Higareda Alvear et al. 2021
264	*FBgn0265264*	CG17097	-	*Wolbachia*	-	1.083	spermathecae and seminal receptacles	Yuan et al. 2015
			Up-Regulation	*10 different bacteria*	-	1.844217379	Adult	Troha et al. 2018
				Aspergillus flavus	-	-	Adult	Ramirez-Camejo and Bayman 2020
				Wolbachia	-	2.629	spermathecae and seminal receptacles	Yuan et al. 2015
						2.813	spermathecae and seminal receptacles	Yuan et al. 2015
265	*FBgn0265267*	CG18258	Down-Regulation	*S–W– vs S+W–*	24 Hours	-2.081189227	Adult	Higareda Alvear et al. 2021
			Up-Regulation	*10 different bacteria*	-	1.517888747	Adult	Troha et al. 2018
266	*FBgn0283427*	FASN1	-	*Lipopolysaccharide*	-	-	Adult	Schlamp et al. 2021
				Wolbachia pipientis		-	Ovary	Christensen et al. 2016
			Down-Regulation	*E. coli and Micrococcus luteus*	3 Hours	0.3	Adult	Brun et al. 2006
				E.coli, M.luteus	3 Hours	-2.727	Adult male	De Gregorio et al. 2001
			Up-Regulation	*A.fumigatus*	24 Hours	0.016	Adult	De Gregorio et al. 2002
				Gamasodes queenslandicus	-	-	Adult male	Benoit et al. 2020
				Pseudomonas entomophila	4 Hours	1.0841	Gut	Soory and Ratnaparkhi 2022

267	*FBgn0284244*	l(2)k05911	Down-Regulation	*ECC15*	-	-2.7	larval Trachea	Gendrin et al. 2013
268	*FBgn0287184*	FASN3	Up-Regulation	*Gamasodes queenslandicus*	-	-	Adult male	Benoit et al. 2020